

# **Genes for sodium exclusion in wheat**

Caitlin Siobhan Byrt  
B. Sc (Hons) Plant Science

A dissertation submitted to the University of Adelaide  
in accordance with the requirements of  
the degree of PhD  
in the Faculty of Science,  
School of Agriculture, Food and Wine

October 2008

**Declaration**

This work contains no material which has been accepted for the award of any other degree or diploma in any university or other tertiary institution and, to the best of my knowledge and belief, contains no material previously published or written by another person except where due reference has been made in the text.

I give consent to this copy of my thesis when deposited in the University Library, being made available for loan and photocopying, subject to the provisions of the Copyright Act 1968.

I acknowledge that copyright of published works contained within this thesis as listed below resides with the copyright holders of those works.

Signed:.....Date:.....

## **Acknowledgements**

I would like to thank my supervisors, Rana Munns (CSIRO) and Mark Tester (University of Adelaide), for all their help, advice and support throughout my PhD, and for being fantastic supervisors. I would like to thank Richard James, Wolfgang Spielmeier, Shaobai Huang, Evans Lagudah, Matthew Gilliham and Steve Tyerman for their help and guidance.

I am very grateful to have had the opportunity to work at Plant Industry in the Crop Adaptation building with so many brilliant people and good role models. I am thankful for the support of friends both at CSIRO and ACPFG.

I would like to thank Paul and my family for their constant support throughout my PhD.

## **List of publications from this thesis**

### Journal publications

- Byrt CS, Platten JD, Spielmeier W, James RA, Lagudah ES, Dennis ES, Tester M, Munns R (2007) HKT1;5-like cation transporters linked to Na<sup>+</sup> exclusion loci in wheat, *Nax2* and *Kna1*. *Plant Physiology*. 143:1918-1928
- Byrt CS, Munns R (2008) Living with salinity. *New Phytologist* 179:903-905.

### Patents

- Byrt CS, James RA, Lagudah ES, Munns R, Platten JD, Spielmeier W (2008) Polynucleotides and methods for enhancing salinity tolerance in plants. Wipo Patent WO/2008/006169
- Byrt CS, Huang S, James RA, Lagudah ES, Munns R, Spielmeier W (2006) Salt tolerant plants. Australian provisional application No. 20069047 filed 31/9/06

### Conference posters

- Byrt CS, Platten JD, Spielmeier W, James RA, Lagudah ES, Dennis ES, Tester M, Munns R (2006) Is *Nax2* an HKT transporter? Gordon Research Conference, Salt and water stress in plants. Sept 3-7<sup>th</sup>, Oxford, UK.
- Byrt CS, Platten JD, Spielmeier W, James RA, Lagudah ES, Dennis ES, Tester M, Munns R (2007) Is *Nax2* an HKT transporter? 4<sup>th</sup> Annual ACPFG Research Symposium: The Genomics of Drought. 22-24 October, Adelaide, South Australia.
- Abbasov M, Byrt C, Spielmeier W, Street K, Shavrukov, Aliyev R, Tester M, Munns R (2008) Screening diploid wheats with various eco-graphic distributions for two salt tolerance genes. 5<sup>th</sup> International Crop Science Congress. April 13-18, ICC Jeju, Korea.

### Oral presentations

- Hare RA, James RA, Huang S, Byrt CS, Lagudah ES, Lindsay EP, Spielmeier W, Rathjen AJ, Munns R (2008) Breeding for salt tolerance in durum wheat. International durum wheat symposium: From Seed to Pasta, The Durum Wheat Chain. June 30 – July 3, Bologna, Italy.
- Byrt CS, James RA, Spielmeier W, Munns R, Gilliham M, Tester M (2008) Investigation of the function of a sodium transporter from wheat, HKT1;5. ComBio 2008, 22-25 September, Canberra, Australia.

## Table of contents

<b>Declaration</b> .....	2
<b>Acknowledgements</b> .....	3
<b>List of publications from this thesis</b> .....	4
<b>List of figures</b> .....	8
<b>List of tables</b> .....	9
<b>List of appendices</b> .....	9
<b>List of abbreviations</b> .....	11
<b>Abstract</b> .....	13
<b>Chapter 1: General introduction and literature review</b> .....	15
<b>1.1 Background on wheat and saline soils</b> .....	15
1.1.1 <i>Wheat production, globally and in Australia</i> .....	15
1.1.2 <i>Evolution and domestication of wheat</i> .....	15
1.1.3 <i>Growing cereals in saline soils</i> .....	16
<b>1.2 Wheat physiology, salt tolerance and the transport of Na<sup>+</sup> from soil to leaves</b> .....	18
1.2.1 <i>Salinity imposes an osmotic stress</i> .....	18
1.2.2 <i>Salinity imposes an ionic stress</i> .....	18
1.2.3 <i>Na<sup>+</sup> uptake into roots</i> .....	19
1.2.4 <i>Na<sup>+</sup> does not substitute for K<sup>+</sup></i> .....	20
1.2.5 <i>Na<sup>+</sup> transport in the xylem from root to shoot</i> .....	21
<b>1.3 Background and rationale for thesis</b> .....	23
1.3.1 <i>Genetic variation for Na<sup>+</sup> exclusion in wheat</i> .....	23
1.3.2 <i>Quantifying sodium exclusion in wheat</i> .....	23
1.3.3 <i>Aims and objectives</i> .....	25
<b>1.4 Thesis outline</b> .....	25
<b>Chapter 2: Mapping and cloning <i>Nax2</i>; a gene for sodium exclusion in wheat</b> .....	26
<b>2.1 Introduction</b> .....	26
<b>2.2 Materials and methods</b> .....	27
2.2.1 <i>Plant material</i> .....	27
2.2.2 <i>Phenotyping</i> .....	28
2.2.3 <i>Genotyping</i> .....	28
2.2.4 <i>Microsatellite markers</i> .....	29
2.2.5 <i>RFLP probe development</i> .....	29
2.2.6 <i>Isolation of <i>TaHKT1;5-D</i></i> .....	30
2.2.7 <i>Isolation of RNA, RT-PCR and isolation of <i>TmHKT1;5-A</i></i> .....	31
2.2.8 <i>Isolation of <i>HKT1;5</i> promoters from Bacterial Artificial Chromosomes</i> .....	32
<b>2.3 Results</b> .....	33
2.3.1 <i>Analysis of putative <i>Nax2</i> single gene lines</i> .....	33
2.3.2 <i>Genetics of <i>Nax2</i></i> .....	33
2.3.3 <i>Microsatellite markers on chromosome 5AL linked to <i>Nax2</i></i> .....	35
2.3.4 <i>Co-segregation of putative Na<sup>+</sup> transport gene, <i>HKT1;5</i>, with <i>Nax2</i></i> .....	37
2.3.5 <i>Wheat <i>HKT1;5</i> gene homologues</i> .....	39
2.3.6 <i><i>Nax2</i> is homoeologous to the major Na<sup>+</sup> exclusion locus in bread wheat, <i>Kna1</i></i> 41	
2.3.7 <i>Isolation of full length <i>HKT1;5</i> gene members</i> .....	43
2.3.8 <i>Expression of <i>HKT1;5</i></i> .....	45
2.3.9 <i>Isolation of wheat <i>HKT1;5</i> promoters from Bacterial Artificial Chromosomes</i> 45	
<b>2.4 Discussion</b> .....	47
2.4.1 <i>Mapping of <i>Nax2</i></i> .....	47

2.4.2	<i>Relationship of Nax2 to the major salt tolerance gene in hexaploid wheat, Kna1</i>	48
2.4.3	<i>Similarity of phenotype between sodium excluding genes in rice and wheat</i>	48
2.4.4	<i>Summary</i>	50
<b>Chapter 3: Diversity of two genes for sodium exclusion in diploid A genome wheat</b>		
<b>ancestors</b>		51
<b>3.1</b>	<b>Introduction</b>	51
3.1.1	<i>Allelic variation in HKT1;5 genes</i>	51
3.1.2	<i>Aims</i>	53
<b>3.2</b>	<b>Materials and Methods</b>	53
3.2.1	<i>Plant material</i>	53
3.2.2	<i>Phenotyping method</i>	54
3.2.3	<i>Marker development, PCR and RT-PCR</i>	54
3.2.4	<i>PCR fragment analysis</i>	55
<b>3.3</b>	<b>Results</b>	56
3.3.1	<i>Presence of Nax2 in diploid species</i>	56
3.3.2	<i>Leaf Na<sup>+</sup> concentrations in the diploid accessions</i>	59
3.3.3	<i>Linkage with Nax1 and interpretation</i>	60
3.3.4	<i>Expression of Nax1 and Nax2 may correlate with the Na<sup>+</sup> exclusion phenotype</i>	60
<b>3.4</b>	<b>Discussion</b>	63
3.4.1	<i>Trends within species and sub-species</i>	63
3.4.2	<i>Interpreting the results for different PCR markers</i>	63
3.4.3	<i>Expression of Nax1 and Nax2 correlates with Na<sup>+</sup> exclusion in T. monococcum</i>	65
3.4.4	<i>New genetic variation for Na<sup>+</sup> exclusion</i>	65
3.4.5	<i>Eco-graphic distribution of diploid accessions and Na<sup>+</sup> accumulation</i>	66
<b>Chapter 4: Transport properties of wheat HKT1;5 and related genes in Xenopus laevis</b>		
<b>oocytes</b>		67
<b>4.1</b>	<b>Introduction</b>	67
4.1.1	<i>Heterologous expression in Xenopus laevis oocytes and electrophysiology</i>	67
4.1.2	<i>The function of HKT-type transporters in Xenopus laevis oocytes</i>	68
4.1.3	<i>Heterologous expression of HKT1;5 in Xenopus laevis oocytes</i>	69
4.1.4	<i>Aims for this study</i>	69
<b>4.2</b>	<b>Materials and Methods</b>	70
4.2.1	<i>Building constructs for expression in Xenopus laevis oocytes</i>	70
4.2.2	<i>Transcription of RNA</i>	70
4.2.3	<i>Injection of cRNA into Xenopus laevis oocytes and electrophysiology</i>	71
4.2.4	<i>Total moles of Na<sup>+</sup> and K<sup>+</sup> per oocyte measured using a flame photometer</i>	72
<b>4.3</b>	<b>Results</b>	74
4.3.1	<i>Transcription of RNA</i>	74
4.3.2	<i>Measurement of currents in water-injected oocytes</i>	75
4.3.3	<i>Measurement of currents in AtHKT1;1 injected oocytes</i>	79
4.3.4	<i>Measurement of currents in OsHKT1;5 injected oocytes</i>	82
4.3.5	<i>Measurement of currents in OsHKT2;2 injected oocytes</i>	87
4.3.6	<i>Measurement of currents in TaHKT1;5-D injected oocytes</i>	91
4.3.7	<i>Total amount of Na<sup>+</sup> and K<sup>+</sup> extracted from oocytes expressing TaHKT1;5-D</i>	100
4.3.8	<i>Oocytes injected with TmHKT1;5-A cRNA did not exhibit the expected Na<sup>+</sup> transport activity</i>	102

4.3.9	<i>Potassium transport by HKTs</i> .....	106
<b>4.4</b>	<b>Discussion</b> .....	108
4.4.1	<i>Transcription of RNA encoding plant HKTs</i> .....	108
4.4.2	<i>Currents in water-injected oocytes</i> .....	108
4.4.3	<i>Currents in AtHKT1;1 and OsHKT1;5 injected oocytes</i> .....	108
4.4.4	<i>Absence of activity for Pokkali OsHKT1;5 and TmHKT1;5-A</i> .....	109
4.4.5	<i>Does HKT1;5 transport Na<sup>+</sup> only, or Na<sup>+</sup> and K<sup>+</sup> ?</i> .....	112
4.4.6	<i>Summary</i> .....	113
<b>Chapter 5:</b>	<b>RNA interference to induce silencing of TaHKT1;5-D</b> .....	114
<b>5.1</b>	<b>Introduction</b> .....	114
5.1.1	<i>RNA interference in plants</i> .....	114
5.1.2	<i>Transformation of wheat by particle bombardment</i> .....	117
5.1.3	<i>Aims</i> .....	117
<b>5.2</b>	<b>Materials and Methods</b> .....	118
5.2.1	<i>Plasmid preparation</i> .....	118
5.2.2	<i>Gene delivery by particle bombardment</i> .....	119
5.2.3	<i>Tissue culture and selection of transformants</i> .....	120
5.2.4	<i>Phenotyping T<sub>1</sub> plants</i> .....	120
5.2.5	<i>DNA extraction and PCR</i> .....	121
<b>5.3</b>	<b>Results</b> .....	122
5.3.1	<i>Transformation efficiency and contamination in tissue culture</i> .....	122
5.3.2	<i>Analysis of primary transgenic wheat plants</i> .....	123
5.3.3	<i>Analysis of the T<sub>1</sub> generation of putative transgenic wheat plants</i> .....	126
<b>5.4</b>	<b>Discussion</b> .....	138
<b>Chapter 6:</b>	<b>General Discussion</b> .....	140
<b>6.1</b>	<b>HKT1;5 homoeologues in wheat</b> .....	140
<b>6.2</b>	<b>Mapping of Nax2 and Kna1</b> .....	140
<b>6.3</b>	<b>The bread wheat HKT1;5 transports Na<sup>+</sup></b> .....	141
<b>6.4</b>	<b>Further questions and future directions</b> .....	142
<b>6.5</b>	<b>Improving the salinity tolerance of wheat and other crops</b> .....	145
<b>References</b>	.....	147
<b>Appendix</b>	.....	158

## List of figures

### Chapter 2:

Figure 2.1: Genotype of <i>Nax2</i> single gene lines .....	33
Figure 2.2: Segregation of the Na <sup>+</sup> exclusion gene, <i>Nax2</i> .....	34
Figure 2.3: Microsatellite markers linked to <i>Nax2</i> .....	36
Figure 2.4: Cosegregation of <i>HKT1;5</i> with <i>Nax2</i> .....	38
Figure 2.5: Chromosomal location of the <i>HKT1;5</i> fragments .....	40
Figure 2.6: Association of <i>HKT1;5</i> with <i>Kna1</i> .....	42
Figure 2.7: Gene structures of <i>TmHKT1;5-A</i> , <i>TaHKT1;5-D</i> and <i>OsHKT1;5</i> .....	44
Figure 2.8: Expression of <i>HKT1;5</i> in wheat analysed using RT-PCR .....	46

### Chapter 3:

Figure 3.1: Screening diploid accessions for <i>Nax2</i> with gene specific primers .....	58
Figure 3.2: Expression of <i>Nax1</i> and <i>Nax2</i> in selected diploid accessions .....	62
Figure 3.3: Wheat ancestors and wheat evolution .....	64

### Chapter 4:

Figure 4.1: RNA <i>in vitro</i> transcribed from pGEMHE .....	74
Figure 4.2: Currents over time in H <sub>2</sub> O injected oocytes exposed to a range of solutions with varying Na <sup>+</sup> and K <sup>+</sup> concentrations .....	76
Figure 4.3: Current-voltage curves for oocytes injected with water, in solutions with different cations and different Na <sup>+</sup> and K <sup>+</sup> concentrations .....	77
Figure 4.4: Current-voltage curves for oocytes injected with water, in solutions with 10 mM Na <sup>+</sup> and with different pH, calcium concentrations and channel blocking solutions .....	78
Figure 4.5: Currents over time in <i>AtHKT1;1</i> injected oocytes exposed to a range of solutions with varying Na <sup>+</sup> and K <sup>+</sup> concentrations .....	80
Figure 4.6: Current-voltage curves for <i>AtHKT1;1</i> expressing oocytes in solutions with different Na <sup>+</sup> and K <sup>+</sup> concentrations .....	81
Figure 4.7: Currents over time in <i>OsHKT1;5</i> (Nipponbare) injected oocytes exposed to a range of solutions with varying Na <sup>+</sup> and K <sup>+</sup> concentrations .....	83
Figure 4.8: Current-voltage curves for <i>OsHKT1;5</i> (Nipponbare) expressing oocytes in solutions with different Na <sup>+</sup> and K <sup>+</sup> concentrations .....	84
Figure 4.9: Current-voltage curves for oocytes expressing <i>OsHKT1;5</i> (Nipponbare), in solutions with various cations, different pH, and channel blocking solutions .....	85
Figure 4.10: Current-voltage curves for oocytes injected with cRNA products transcribed from pGEMHE containing the cDNA for <i>OsHKT1;5</i> (Pokkali) .....	86
Figure 4.11: Currents over time in <i>OsHKT2;2</i> injected oocytes exposed to a range of solutions with varying Na <sup>+</sup> and K <sup>+</sup> concentrations .....	88
Figure 4.12: Current-voltage curves for <i>OsHKT2;2</i> (Pokkali) expressing oocytes in solutions with different Na <sup>+</sup> and K <sup>+</sup> concentrations .....	89
Figure 4.13: Current-voltage curves for oocytes expressing <i>OsHKT2;2</i> (Pokkali), in solutions with various cations .....	90
Figure 4.14: Currents over time in <i>TaHKT1;5-D</i> injected oocytes exposed to a range of solutions with varying Na <sup>+</sup> and K <sup>+</sup> concentrations .....	93
Figure 4.15: Cation selectivity of oocytes injected with <i>TaHKT1;5-D</i> cRNA .....	94
Figure 4.16: Current-voltage curves for oocytes expressing <i>TaHKT1;5-D</i> in solutions with different Na <sup>+</sup> concentrations .....	95



Figure 4.17: Permeability of TaHKT1;5-D to Na <sup>+</sup> .....	96
Figure 4.18: Permeability of TaHKT1;5-D to K <sup>+</sup> .....	96
Figure 4.19: Current-voltage curves for TaHKT1;5 expressing oocytes in solutions with different Na <sup>+</sup> and K <sup>+</sup> concentrations .....	98
Figure 4.20: Current-voltage curves for oocytes expressing TaHKT1;5-D in solutions of 10 mM Na <sup>+</sup> and differing pH, Ca <sup>2+</sup> and channel blockers .....	99
Figure 4.21: K <sup>+</sup> /Na <sup>+</sup> ratio and total moles of Na <sup>+</sup> and K <sup>+</sup> extracted from oocytes expressing <i>TaHKT1;5</i> .....	101
Figure 4.22: Current-voltage curves for oocytes injected with cRNA products transcribed from pGEMHE containing the cDNA for <i>TmHKT1;5-A</i> .....	104
Figure 4.23: K <sup>+</sup> /Na <sup>+</sup> ratio and total moles of Na <sup>+</sup> and K <sup>+</sup> extracted from oocytes injected with different concentrations of <i>TmHKT1;5-A</i> <i>in vitro</i> -transcribed RNA products .....	105
Figure 4.24: Current-voltage curves for oocytes expressing different HKTs in solutions with 30 mM K <sup>+</sup> .....	107
Figure 4.25: Structural model of OsHKT1;5 .....	111

## Chapter 5:

Figure 5.1: A simplified diagram of the pSTARGATE vector for RNAi-induced gene silencing in monocotyledonous plants .....	116
Figure 5.2: Diagram of the fragments incorporated into the silencing construct in relation to the <i>TaHKT1;5-D</i> gene .....	119
Figure 5.3: Growth of calli in tissue culture and subsequent transfer to soil .....	124
Figure 5.4: Amplification by PCR of a fragment specific to the RNA interference constructs from DNA from putative transgenic plants .....	125
Figure 5.5: Putative transgenic T <sub>1</sub> plants growing in hydroponics .....	127
Figure 5.6: Leaf three Na <sup>+</sup> concentrations of Bob White non-transgenic individual plants (A) and transgenic plants segregating for the empty pSTARGATE vector (B) from four different tanks .....	129
Figure 5.7: Leaf three Na <sup>+</sup> concentration of putative transgenic plants compared to Bob White controls grown in Tank 1 (A) and Tank 2 (B) .....	132
Figure 5.8: Leaf three Na <sup>+</sup> concentration of putative transgenic plants compared to Bob White controls grown in Tank 3 (A) and Tank 4 (B) .....	133
Figure 5.9: K <sup>+</sup> /Na <sup>+</sup> ratio of leaf 3 from putative transgenic plants of interest, from the first screen, compared to control Bob White plants from the respective tank .....	134
Figure 5.10: Leaf three Na <sup>+</sup> concentrations (A) and K <sup>+</sup> to Na <sup>+</sup> ratio (B) of putative transgenic plants of interest, in the second screen, compared to Bob White controls .....	136
Figure 5.11: Amplification by PCR of a fragment specific to the RNA interference constructs from DNA from individual T <sub>1</sub> plants of the plants of interest .....	137

## List of tables

Table 3.1: Average leaf Na <sup>+</sup> concentrations in selected <i>Triticum</i> spp. ....	57
--	----

## List of appendices

Appendix Table 2.1: Agarose gel electrophoresis results from PCR with microsatellite markers on chromosome 5AL .....	158
Appendix Table 3.1: Accession numbers of diploid wheat material .....	160
Appendix Table 3.2: Key to <i>HKT1;5</i> B gene members from wheat .....	160

Appendix Figure 2.1: Wheat <i>HKT1;5</i> RFLP probe sequence (331 bp).....	161
Appendix Figure 2.2: Wheat <i>TaHKT1;5-D</i> full length genomic sequence showing introns (shaded) and exons (GenBank accession DQ646342) and predicted amino acid sequence...	163
Appendix Figure 2.3: Wheat <i>TmHKT1;5-A</i> full length genomic sequence showing introns (shaded) and exons (GenBank accession DQ646339) and predicted amino acid sequence...	165
Appendix Figure 2.4: Alignment of <i>TmHKT1;5-A</i> and <i>TaHKT1;5-D</i> genomic sequences ...	168
Appendix Figure 2.5: Alignment of predicted amino acid sequences for <i>TmHKT1;5-A</i> and <i>TaHKT1;5-D</i> .....	169
Appendix Figure 2.6: Alignment of predicted amino acid sequences for <i>TmHKT1;5-A</i> , <i>TaHKT1;5-D</i> and <i>OsHKT1;5</i> using CLUSTAL 2.0.3 multiple sequence alignment.....	170
Appendix Figure 2.7: <i>TmHKT1;5-A</i> promoter .....	171
Appendix Figure 2.8: <i>TaHKT1;5-D</i> promoter .....	172
Appendix Table 4.1: Replicates of oocytes used in various experiments .....	173

## List of abbreviations

ABARE	Australian Bureau of Agriculture and Resource Economics
ACPFPG	Australian Centre for Plant Functional Genomics
bp	base pair
cDNA	complementary DNA
CSIRO	Commonwealth Scientific and Industrial Research Organisation
cv.	cultivar
2,4-D	2,4-dichlorophenoxyacetic acid
DNA	deoxyribonucleic acid
EDTA	ethylenediaminetetraacetic acid
FAO	Food and Agriculture Organisation
GUS	$\beta$ -glucuronidase
HKT	High-affinity potassium ( $K^+$ ) transporter
kb	kilobase
kDa	kilodalton
LB	Luria-Bertani medium
mRNA	messenger RNA
NIL	near isogenic line
NLWRA	National Land and Water Resources Audit
PCR	polymerase chain reaction
PPM	Plant preservative mixture
QTL	quantitative trait loci
RFLP	restriction fragment length polymorphism
RNA	ribonucleic acid
RNAi	ribonucleic acid interference
RT-PCR	reverse-transcriptase polymerase chain reaction
SEM	standard error of the mean
spp.	species (plural)
ssp.	subspecies
TE	Tris-EDTA buffer
TRIS	tris(hydroxymethyl)methylamine
U	enzyme unit
USDA	United States Department of Agriculture

## Nomenclature

The current nomenclature for HKT transporters as described by Platten et al. (2006) and Huang et al. (2008)

New	Old	QTL
<i>AtHKT1;1</i>	<i>AtHKT1</i>	
<i>OsHKT1;5</i>	<i>OsHKT8</i>	<i>SKC1</i> (Ren et al., 2005)
<i>OsHKT2;1</i>	<i>OsHKT1</i>	
<i>TaHKT2;1</i>	<i>TaHKT1</i>	
<i>TmHKT1;4</i>	<i>TmHKT7</i>	<i>Nax1</i> (Huang et al., 2006)
<i>TmHKT1;5</i>	<i>TmHKT8</i>	<i>Nax2</i> (Byrt et al., 2007)
<i>TaHKT1;5</i>	<i>TaHKT8</i>	<i>Kna1</i> (Byrt et al., 2007)

## Abstract

Salinity stress limits the growth and productivity of agricultural crops in many regions of the world. Whole plant tolerance to soil salinity involves numerous processes in many different tissues and cell types. For many cereals, sensitivity to salinity is due to the accumulation of sodium ( $\text{Na}^+$ ) to toxic concentrations in the leaves. This thesis investigates a mechanism of control of  $\text{Na}^+$  accumulation in leaves of wheat.

Bread wheat excludes sodium from the leaves better than durum wheat. Bread wheat is hexaploid (AABBDD) whereas durum wheat is tetraploid (AABB). The D-genome in bread wheat carries a major locus for sodium exclusion, *Knal*, which may contribute to the differences in sodium exclusion between bread wheat and durum wheat.

An unusual durum wheat, Line 149, excludes sodium to a similar degree as bread wheat. Line 149 was derived from a cross between a *Triticum monococcum* (accession C68-101; AA) and a durum wheat (*T. turgidum* ssp. *durum* cv. Marrocos; AABB). Line 149 had been found to contain two major genes for sodium exclusion, named *Nax1* and *Nax2*, which appeared to retrieve sodium from the xylem sap in the roots and so prevent it reaching the leaves. Line 149 had been crossed with the durum wheat cv. Tamaroi, which accumulates high concentrations of  $\text{Na}^+$  in the leaves, and near-isogenic single-gene mapping populations had been developed for *Nax1* and *Nax2*. *Nax1* had been located on chromosome 2A. The objective of this thesis was to map *Nax2* and identify a candidate gene.

*Nax2* mapped to chromosome 5AL based on linkage to microsatellite markers. A high-affinity potassium ( $\text{K}^+$ ) transporter (HKT)-like gene, *HKT1;5* was considered as a candidate gene for *Nax2*, based on similarity of the phenotype to a rice orthologue. Sequence information from a wheat *HKT1;5*-like expressed sequence tag in the public database was used to develop a probe for use in Southern hybridisation. A *HKT1;5*-like fragment was identified in Line 149 and *T. monococcum* C68-101, but was absent in Tamaroi. The *HKT1;5*-like gene, named *TmHKT1;5-A*, co-segregated with *Nax2* in the *Nax2* single-gene mapping population. The *HKT1;5* probe identified three putative *HKT1;5*-like genes on the long arm of chromosome 4B, and one *HKT1;5*-like gene on the long arm of chromosome 4D, in Langdon (*T. turgidum* ssp. *durum*) substitution lines, and in Chinese Spring (*T. aestivum*) ditelomeric lines. No A-genome *HKT1;5* like gene was identified in Langdon or Chinese Spring.

The D-genome *HKT1;5* gene, named *TaHKT1;5-D*, was found to co-locate with *Knal*, the gene for sodium exclusion in bread wheat, in Chinese Spring chromosome 4D deletion lines. *Nax2* (*TmHKT1;5-A*) was found to be homoeologous with the gene for sodium exclusion in bread wheat, *Knal* (*TaHKT1;5-D*). *TmHKT1;5-A* and *TaHKT1;5-D*, and their

promoters, were 94% identical, and both were expressed in the roots of wheat plants. This is consistent with the genes being located in the stele of the roots and retrieving  $\text{Na}^+$  from the xylem sap as it flows towards the shoot, and so excluding  $\text{Na}^+$  from the leaves.

A marker for *TmHKT1;5-A* was developed to track this gene in durum wheat breeding programs. A study of the *HKT1;5* gene in diploid ancestors of wheat indicated that this gene is present in most *Triticum monococcum* accessions, some *T. boeoticum* accessions, but not present in any *T. urartu* accessions. *T. urartu* is the likely A genome ancestor of modern wheat. This may explain the absence of *HKT1;5* in the A genome of modern wheat.

The protein encoded by *TaHKT1;5-D* transported sodium when expressed in *Xenopus laevis* oocytes. The inward currents were specific to  $\text{Na}^+$ , but at particular mole fractions of  $\text{Na}^+$  and  $\text{K}^+$  outward currents were observed that were consistent with outward  $\text{K}^+$  transport. These data were consistent with the putative physiological function, of retrieving  $\text{Na}^+$  from the xylem sap as it flows to the leaves, and resulting in a net exchange with  $\text{K}^+$ .

A construct designed to silence the expression of *TaHKT1;5-D* was introduced to bread wheat cv. Bob White. Nineteen putative transgenic plants were developed. The leaf  $\text{Na}^+$  concentrations and genotype of the  $T_1$  individuals were assayed. The data from two of the transgenic plants indicated that *TaHKT1;5-D* may have been silenced and that this may have lead to the increase in  $\text{Na}^+$  accumulation in the leaves. However, this data is not conclusive at this time.

The information gained from this study will assist the introduction of the  $\text{Na}^+$  exclusion trait into current durum cultivars, which are poor at excluding  $\text{Na}^+$  and are salt sensitive. This information will also contribute to the body of knowledge of ion transport in plants and salinity tolerance in wheat.

## Chapter 1: General introduction and literature review

### 1.1 Background on wheat and saline soils

#### 1.1.1 Wheat production, globally and in Australia

Wheat is the most widely grown crop in the world (FAO, 2008). World wheat production in 2007 was 630 million tonnes and total wheat utilization was 632 million tonnes. This left the stock-to-use ratio at a historically low level, the lowest level since 1980 (ABARE, 2007; FAO, 2008).

In Australia approximately 12.4 million ha is planted to wheat yielding an average of 1.8 t/ha and producing approximately 22.5 million tonnes of grain (ABARE, 2007). Australia currently exports around 15 million tonnes of grain valued at about \$3.7 billion.

The world's population is increasing, and is expected to reach ten billion by the middle of the 21<sup>st</sup> century (Evans, 1998). Wheat constitutes one quarter of the world's food (Evans, 1998). Thus an increase in production of wheat is required to feed the growing population.

Increasing production of wheat calls for varieties of wheat with greater tolerance to hostile soil conditions and erratic precipitation. Of the abiotic stresses, salinity and drought cause the biggest crop losses (Vincor and Altman, 2005; Rengasamy, 2006). Subsoil constraints, such as salinity, play a large part in restricting the average wheat yield in Australia to 1.8 t ha<sup>-1</sup> (ABARE, 2007; Rengasamy, 2002). Over the next 20 years salinity will continue to limit crop production in Australia, and it is anticipated that salinity will cause a 1.5 percent decline in the value of agricultural profits (NLWRA, 2007). Therefore, to help achieve a sustainable increase in production of wheat, wheat varieties with greater tolerance to salinity are needed.

#### 1.1.2 Evolution and domestication of wheat

Wheat falls within the family Poaceae; tribe *Triticeae* and genus *Triticum*. Three to six million years ago an ancestral diploid goat grass species of wheat diverged into the ancestral species of *T. monococcum* ssp. *boeoticum* (A<sup>b</sup>A<sup>b</sup>), *T. urartu* (A<sup>u</sup>A<sup>u</sup>), an unknown species of *Aegilops* (BB) which was closely related to *Ae. speltoides*, and *Ae. tauschii* (DD). Subsequently, the A<sup>u</sup> and B genomes hybridized to give *T. turgidum* ssp. *dicoccoides* (wild emmer) (AABB).

Domestication of wheat began in the Fertile Crescent in the Middle East approximately 10 000 years ago (Heun et al., 1997). Domestication led to *T. monococcum*

*ssp. monococcum* (AA) (eikorn) and *T. turgidum ssp. dicoccum* (AABB) (emmer) and *T. spelta* (spelt; AABBDD) being cultivated. Subsequently, *T. turgidum ssp. dicoccum* (AABB) hybridized with *Ae. tauschii* (DD) to give *T. aestivum* (AABBDD).

Today the most common cultivated wheats are the hexaploid wheat *T. aestivum* (AABBDD) and tetraploid wheat *T. turgidum ssp. durum* (AABB). *T. aestivum* accounts for around 90% of global wheat production, and the grain is used for bread, noodles, cakes, biscuits and pastries, as well as animal feed. *T. turgidum ssp. durum* accounts for around 5% of global production, and the grain has a hard texture and is used for making pasta, couscous and bulgar. Wheat provides calories directly in the form of flour-based foods and indirectly as feed for animals which are a source of meat and dairy products.

### 1.1.3 Growing cereals in saline soils

Soil is described as saline when it has an electrical conductivity (ECe) of greater than 4 deciSiemens per metre (dS/m), equivalent to 40 mM NaCl, and an osmotic pressure of 0.2 MPa (USSL, 2008). This definition arises from the ECe (EC of the saturated paste extract) that will reduce the yield of most crop (USSL, 2008). Salinity can be caused by irrigation, or it can be found in dryland agriculture.

In the lower rainfall zones in Australia salt is present naturally in the soil. This type of salinity is referred to as subsoil or transient salinity (Rengasamy, 2002). Transient salinity is not associated with groundwater or rising water tables. The term ‘transient’ is used because the salt is leached below the root zone in the rainy season, but rises into the root zone in the dry season. In the high rainfall zones of Australia, soils can be affected by ‘dryland salinity’ due to rising water tables (Rengasamy, 2002). ‘Dryland salinity’ occurs as a result of land clearing for dryland agriculture. This leads to rising water tables which brings salt towards the surface of the soil. Major wheat growing areas in Australia are becoming more saline due to ‘dryland salinity’. ‘Dryland salinity’ currently threatens production from five million hectares of agricultural land in Australia, and by 2050 this is expected to treble (NLWRA, 2007; Rengasamy, 2006). Much of the area at risk is Australia’s most productive land, and corresponds with major wheat growing areas (Rengasamy, 2002).

A plant growing in saline soil is subject to two types of physiological stress; osmotic stress, as the presence of salt restricts water uptake, and a Na<sup>+</sup> specific stress as the concentration of Na<sup>+</sup> in the leaves increases and the Na<sup>+</sup> becomes toxic. Plant tolerance to these two types of stress involves different mechanisms; osmotic adjustment, and exclusion of Na<sup>+</sup> (Greenway and Munns, 1980; Tester and Davenport, 2003; Colmer et al., 2005).



The response of shoot growth to an increase in salinity occurs in two phases: a rapid response to the increase in external osmotic pressure (leading to decreased shoot growth), and a slower ionic response due to the accumulation of  $\text{Na}^+$  in leaves (leading to increased senescence of older leaves) (Munns and Tester, 2008). Ionic stress develops over time, and is due to a combination of ion accumulation in the shoot and an inability to tolerate the ions that have accumulated (Munns and Tester, 2008).

To achieve salinity tolerance, plants must limit the amount of salt reaching the xylem, control the transport of salt in the xylem throughout the plant, maintain the ionic and osmotic balance of cells, regulate leaf development and the onset of senescence, and minimize the sodium accumulation in the cytoplasm (Munns, 2005). The mechanisms involved are reviewed in the following section, 1.2.

Of the main cereals grown in Australia, barley (*Hordeum vulgare*) has high osmotic adjustment capability, in contrast to bread wheat which largely excludes sodium from the leaves. Barley can tolerate high leaf tissue concentrations of  $\text{Na}^+$  and  $\text{Cl}^-$  compared to wheat (Colmer et al., 2005; James et al., 2006b). When treated with salt, barley accumulates  $\text{Cl}^-$  in epidermal cells rather than mesophyll cells, and accumulates  $\text{K}^+$  in mesophyll cells rather than epidermal cells (James et al., 2006b). The high  $\text{Na}^+$  and the accompanying  $\text{Cl}^-$  in epidermal cells allows barley to osmotically adapt and to maintain turgor in the face of high soil salinities (Munns and Tester, 2008). Barley maintains photosynthetic capacity at high leaf  $\text{Na}^+$  levels by maintaining a high  $\text{K}^+$  and low  $\text{Na}^+$  concentration in the cytoplasm of mesophyll cells. Wild *Hordeum* species, such as *H. marinum*, with much greater exclusion of  $\text{Na}^+$  and  $\text{Cl}^-$  from the leaves than barley, are even better able to maintain tissue  $\text{K}^+$  concentrations and maintain growth in saline conditions (Garthwaite et al., 2005).

The main mechanism by which bread wheat maintains the  $\text{K}^+$  to  $\text{Na}^+$  ratio in the leaves is by exclusion of  $\text{Na}^+$  from the shoots. A candidate locus for  $\text{K}^+/\text{Na}^+$  discrimination is *Knal*, located on the long arm of chromosome 4D (Gorham et al., 1987). *Knal* was associated with a higher leaf  $\text{K}^+/\text{Na}^+$  ratio, and was attributed with providing bread wheat with its superior salinity tolerance over tetraploid wheats (Gorham et al., 1987).

In contrast to both barley and bread wheat, durum wheat is both poor at excluding sodium and poor at adjusting to the osmotic affect of salt in the soil solution

## **1.2 Wheat physiology, salt tolerance and the transport of Na<sup>+</sup> from soil to leaves**

### 1.2.1 Salinity imposes an osmotic stress

The osmotic effect of salinity on plants is caused by salt in the soil solution reducing the ability of the plant to take up water (Munns, 1993). The cellular and metabolic processes involved in the plant response to the osmotic effect of salt are similar to those processes involved in the plant response to drought. In dry or saline soil, chemical or hormonal signals from the roots are sent to the leaves, leading to reduced leaf growth (Westgate et al., 1996; Munns, 2005).

Several traits may improve the plant tolerance to the osmotic effect of salt. These include transpiration use efficiency, osmotic adjustment, and morphological or developmental patterns that conserve water and advance flowering date (Colmer et al., 2005).

Compatible solutes, or osmolytes, accumulate in plants in response to stress (Bohnert et al., 1999). The primary function of compatible solutes is to accumulate in the cytoplasm to balance salt in the vacuole, but they may also act as free-radical scavengers and help in membrane and or protein stabilization (Wang et al., 2003). Compatible solutes fall into three main groups; amino acids such as proline, quaternary amines such as glycine betaine, and sugars such as mannitol (Wang et al., 2003). Overexpression of compatible solutes in plants may improve tolerance to drought and salinity (Apse and Blumwald, 2002). In many halophytic plants the production of compatible solutes contributes to salt tolerance (Flowers and Colmer, 2008).

### 1.2.2 Salinity imposes an ionic stress

Ionic stress, or ion toxicity, occurs when Na<sup>+</sup> accumulates in the leaves to a concentration where the Na<sup>+</sup> causes injury to cells. An increase in the number of injured cells in transpiring leaves leads to leaf death. If new leaves are produced at a rate greater than that at which old leaves die, then there are enough photosynthesizing leaves for the plant to produce flowers and seeds, although in reduced numbers. However, if old leaves die faster than the new leaves develop, then the plant may not survive to produce seed (Munns, 1993).

The regulation of delivery of Na<sup>+</sup> to the shoot preventing accumulation of Na<sup>+</sup> in the leaves is referred to as Na<sup>+</sup> exclusion. Exclusion of Na<sup>+</sup> involves several steps; control of the initial entry of Na<sup>+</sup> into root epidermal and cortical cells, a balance between influx and efflux at the root epidermis, control of loading of Na<sup>+</sup> into the xylem, retrieval of Na<sup>+</sup> from the xylem before the shoot, allocation of Na<sup>+</sup> to particular parts of the shoot and control of storage of Na<sup>+</sup> (Tester and Davenport, 2003; Munns, 2002). For cereals, such as wheat, these

processes help to keep  $\text{Na}^+$  out of the transpiration stream so that it does not reach the leaves (Munns et al., 2006). However, in bread wheat sodium exclusion does not always correlate with salinity tolerance (Genc et al., 2007).

The transport proteins controlling these processes can be divided into three main classes: (1) Primary pumps: transporters directly energised by the hydrolysis of ATP. (2) Solute-coupled transporters: transport proteins that transport  $\text{Na}^+$  against a difference in electrochemical potential and are energized via coupling to the movement of another ion down its electrochemical potential difference and (3) ion channels: proteins that catalyze the rapid passive movement of  $\text{Na}^+$  and other solutes down their difference in electrochemical potential (Maathuis and Amtmann, 1999).

In wheat there is a strong correlation between  $\text{Na}^+$  exclusion and salt tolerance (Gorham et al., 1997; Dvorak et al., 1994; Munns and James, 2003). Discrimination between  $\text{Na}^+$  and  $\text{K}^+$  during transport from the roots to the shoots in bread wheat is associated with the *Kna1* locus on 4DL, and leads to less  $\text{Na}^+$  and more  $\text{K}^+$  in the leaves, which is important for salt tolerance (Dvorak et al., 1994).

### 1.2.3 $\text{Na}^+$ uptake into roots

The first barrier to the movement of ions into wheat roots is the root epidermal cells (Maathuis and Amtmann, 1999). This barrier enables most plants to exclude about 98% of the salt in the soil solution, allowing only 2% of the salt to enter the xylem (Munns et al., 2005).

Solutes may travel from the epidermis to the xylem either symplastically, by entering root cells and moving from cell to cell through plasmodesmata, or apoplastically, without traversing a single plasma membrane (White et al., 2002). In rice,  $\text{Na}^+$  moves through the root via both pathways (Garcia et al., 1997).

Non-selective cation channels (NSCC) are responsible for most of the  $\text{Na}^+$  that enters the root. The role of NSCCs in  $\text{Na}^+$  influx into wheat has been demonstrated through electrophysiological studies (Davenport and Tester, 2000). A 44 pS NSCC was described in wheat which is nonselective for monovalent cations and weakly voltage dependent (Davenport and Tester, 2000). The channel was partially sensitive to inhibition by  $\text{Ca}^{2+}$ ,  $\text{Mg}^{2+}$  and  $\text{Gd}^{3+}$ , and insensitive to many other inhibitors. The selectivity for  $\text{K}^+$  over  $\text{Na}^+$  was approximately 1.25; hence this NSCC is likely to catalyze toxic  $\text{Na}^+$  influx (Davenport and Tester, 2000). Gene families that are candidates for encoding NSCCs include cyclic nucleotide gated channels (CNGCs) and glutamate activated channels (GLRs) (Demidchik et al., 2002).

In glycophytes, such as wheat, there is evidence that net  $\text{Na}^+$  uptake is a result of efflux of excess  $\text{Na}^+$  as well as control of influx (Davenport et al., 1997; 2005). In a saline soil environment, the difference in electrical potential between the soil solution and epidermal root cells may be in the order of -150 mV. This electrical potential difference favours high rates of influx of cations into the root. However the high rates of unidirectional influx of  $\text{Na}^+$  into wheat roots do not correspond with the accumulation of  $\text{Na}^+$  in the plant, indicating that there must also be high rates of efflux back into the soil solution (Tester and Davenport, 2003). Efflux back in to the soil solution must be active, and  $\text{Na}^+/\text{H}^+$  antiporters in the plasma membrane of epidermal and cortical cells are likely to be responsible for the efflux of  $\text{Na}^+$  back into the soil solution. The high rates of  $\text{Na}^+$  efflux must impose an energetic burden on plants in saline conditions (Essah et al., 2003), but the quantitative significance of this in the overall plant energy budget is not certain.

#### 1.2.4 $\text{Na}^+$ does not substitute for $\text{K}^+$

High  $\text{Na}^+$  levels in the soil disrupt the uptake of other nutrients. Firstly, high salt concentration lowers the activity of Ca, with the potential to cause Ca deficiency or the influx of other cations through non-selective cation channels (Davenport et al., 1997; Tester and Davenport 2003; Husain et al. 2004). Secondly, when  $\text{Na}^+$  ions are in excess they will occupy the binding sites of transport proteins in the plasma membrane of root epidermal cells, such as  $\text{K}^+$ -selective channels. When  $\text{Na}^+$  occupies the binding sites of  $\text{K}^+$ -selective channels the  $\text{Na}^+$  ions may be transported into the cell instead of  $\text{K}^+$  ions.

When  $\text{Na}^+$  enters the transpiration stream it may not all flow up the xylem to the leaves. Some  $\text{Na}^+$  may be retrieved from the xylem before reaching the leaves. The transporters that may be responsible for this are reviewed in detail in the following section (1.2.5), as they are central to the work of this thesis.  $\text{Na}^+$  that does reach the leaves accumulates because  $\text{Na}^+$ , unlike other ions such as  $\text{K}^+$ , is not readily transported via the phloem. This minimizes its transport towards younger leaves or the apex, where it could concentrate to toxic levels, but also restricts its movement towards the roots.

$\text{Na}^+$  can be beneficial or toxic. Plants can use  $\text{Na}^+$  for osmotic adjustment, and in some enzymatic functions  $\text{Na}^+$  can be used instead of  $\text{K}^+$  when  $\text{K}^+$  is in limited supply (Tester and Davenport, 2003).

$\text{Na}^+$  can become toxic when it accumulates to high concentrations in the leaves. When the  $\text{Na}^+$  concentration in the cells exceeds the ability of the cells to compartmentalize the  $\text{Na}^+$  in the vacuole  $\text{Na}^+$  accumulates in the cytoplasm.  $\text{Na}^+$  ions compete with  $\text{K}^+$  for binding sites

essential for cellular function. The build up of  $\text{Na}^+$  in the cytoplasm results in replacement of  $\text{K}^+$  by  $\text{Na}^+$  in biochemical reactions and conformational changes causing inhibition of crucial enzymatic activity and loss of function of proteins (Maathuis and Amtmann, 1999).  $\text{K}^+$  is important in protein synthesis, and in activation of more than 50 known enzymes in plant metabolism (Tester and Davenport, 2003).  $\text{Na}^+$  cannot substitute for  $\text{K}^+$  in these metabolic processes, hence high  $\text{Na}^+:\text{K}^+$  ratios disrupt enzymatic processes in the cytoplasm, such as the accumulation of pyruvate (Tester and Davenport, 2003). Injury to plant cells may also be caused by build up of  $\text{Na}^+$  in the cell walls leading to dehydration of the cell (Munns et al., 2005).

Barley compartmentalizes salt in cell vacuoles to protect the cytoplasm from a build up of  $\text{Na}^+$  to toxic levels. An example of a transporter that could be involved in this process is *HvNHX1* or *HvNHX2* (Fukuda et al., 2004). Localized to the tonoplast, the *Arabidopsis thaliana* *NHX1* is a  $\text{Na}^+/\text{H}^+$  antiporter predicted to be involved in the control of vacuolar osmotic potential (Apse et al., 1999; Gaxiola et al., 1999; Qiu et al., 2004).

#### 1.2.5 $\text{Na}^+$ transport in the xylem from root to shoot

The concentration of  $\text{Na}^+$  in the xylem sap of a non-transpiring plant may be 10 mM  $\text{Na}^+$  (Munns, 1985) and the concentration of  $\text{Na}^+$  in the cytoplasm of root cells may be in the order of 10 – 30 mM  $\text{Na}^+$  (Tester and Davenport, 2003). In these circumstances, the energy difference across the plasma membrane would be approximately -100 mV inside parenchyma cells, relative to the xylem sap (Tester and Davenport, 2003). This negative potential difference does not favour the passive entry of  $\text{Na}^+$  into the xylem. As  $\text{Na}^+$  does get into the xylem, there is likely to be carriers actively transporting  $\text{Na}^+$  into the xylem.

For rapidly transpiring plants, circumstances may be different. If the cytosolic  $\text{Na}^+$  concentration in stellar cells was greater than 30 mM  $\text{Na}^+$ , and closer to 100 mM  $\text{Na}^+$ , and if the concentration of  $\text{Na}^+$  in the xylem was 1 – 2 mM  $\text{Na}^+$ , as found by Munns (1985), then the energy difference would favour passive leakage of  $\text{Na}^+$  into the xylem. In conditions where high salt has caused xylem parenchyma cells to become slightly depolarized, and the intracellular concentration of  $\text{Na}^+$  is much higher than the xylem concentration, then  $\text{Na}^+$  may enter the xylem passively via ion channels (Tester and Davenport, 2003). In a state where a 1:1 stoichiometry exists for  $\text{Na}^+:\text{H}^+$  exchange between the xylem and xylem parenchyma,  $\text{Na}^+/\text{H}^+$  antiporters may transport  $\text{Na}^+$  into the xylem due to the large pH difference between the cytosol and the xylem (Tester and Davenport, 2003). Or, if xylem pH changes or the

stoichiometry of the antiporter is different, then antiporters could act to pump  $\text{Na}^+$  out of the xylem solution (Tester and Davenport, 2003).

Mechanisms for loading or unloading  $\text{Na}^+$  from the xylem may involve  $\text{Na}^+/\text{H}^+$  antiporters, ion channels, or cation transporters such as those encoded by members of the *KUP/HAK* gene families (Davenport et al., 2005; Rus et al., 2004).

Recently, much progress has been made in identifying the proteins responsible for loading and unloading  $\text{Na}^+$  into the xylem, with High-affinity K<sup>+</sup> Transporters (HKT) implicated in the unloading process in several studies (Rus et al., 2004; Ren et al., 2005; Sunarpi et al., 2005; Horie et al., 2007). HKT transporters functioning in transport of  $\text{Na}^+$  in plants, and loading and unloading of  $\text{Na}^+$  into the xylem, has been documented in *Arabidopsis thaliana*, *Oryza sativa* and *Triticum* (Mäser et al., 2002a; Berthomieu et al., 2003; Garciadeblas et al., 2003; Rus et al., 2004; Haro et al., 2005; Ren et al., 2005; Sunarpi et al., 2005; Huang et al., 2006; Davenport et al., 2007; Horie et al., 2007). *AtHKT1;1* retrieves  $\text{Na}^+$  out of the xylem (Sunarpi et al., 2005; Davenport et al., 2007). *OsHKT1;5* retrieves  $\text{Na}^+$  out of the xylem (Ren et al., 2005). *OsHKT2;1* loads  $\text{Na}^+$  into the roots in  $\text{K}^+$  starved conditions (Horie et al., 2007), and *TaHKT2;1* is involved in low-affinity  $\text{Na}^+$  uptake in roots (Laurie et al., 2002; Gassmann et al., 1996; Wang et al., 1998).

HKT genes have been given a new nomenclature, and separated into two groups based on amino acid sequence (Platten et al., 2006). A glycine/serine residue in the first pore loop of the protein differs between group 1 and group 2 *HKT* genes (Mäser et al., 2002b).

Group 1 HKT genes have a serine in the first pore loop; this may make them more selective for  $\text{Na}^+$  (Horie et al., 2001; Mäser et al., 2002b; Garciadeblas et al., 2003; Platten et al., 2006). Group 1 HKT genes, such as *AtHKT1;1* (previous name *AtHKT1*) and *OsHKT1;5* (previous name *OsHKT8*), transport  $\text{Na}^+$  only, and may be involved in unloading of  $\text{Na}^+$  from the xylem (Garciadeblas et al., 2003; Uozumi et al., 2000; Ren et al., 2005; Sunarpi et al., 2005). In wheat, group 1 HKT genes are involved in  $\text{Na}^+$  transport, and may confer a phenotype of low leaf  $\text{Na}^+$  concentration in leaves (Huang et al., 2006).

For the group 2 genes there is no consensus on the mechanism of action, or whether the main function is to transport  $\text{Na}^+$  or  $\text{K}^+$  (Golldack et al., 2002; Haro et al., 2005; Horie et al., 2001; Rubio et al., 1995; Schachtman and Schroeder, 1994; Walker et al., 1996; Wang et al., 1998). Heterologous expression of *TaHKT2;1* (previous name *TaHKT1*) in yeast and *Xenopus laevis* oocytes indicated that this gene is likely to play a role in  $\text{Na}^+$  and  $\text{K}^+$  transport (Rubio et al., 1995; Mäser et al., 2002b). Rodriguez-Navarro and Rubio (2006) provide an explanation for the conflicting results for group 2 HKT genes. They suggest that in plants

some HKT messenger RNA transcripts have alternative initiations of translation, and in heterologous systems translation may not occur exactly as in plants, leading to expression of proteins with different kinetic properties. A physiologically relevant function for group 2 transporters might be to transport  $\text{Na}^+$  when there is a limited supply of  $\text{K}^+$  so that the plant may have a monovalent cation for use in osmotic adjustment in the vacuole (Rodríguez-Navarro and Rubio, 2006).

### **1.3 Background and rationale for thesis**

#### 1.3.1 Genetic variation for $\text{Na}^+$ exclusion in wheat

Modern durum cultivars do not exclude  $\text{Na}^+$  to the same extent as bread wheat; however a source of sodium exclusion in a novel durum wheat, Line 149, was described by Munns et al. (2000). Line 149 is derived from a cross between a *Triticum monococcum* L. (accession C68-101) (AA) and a durum cultivar Marrocos (AABB) (The, 1973). The *T. monococcum* is the donor of the sodium exclusion trait (James et al., 2006a). The sodium exclusion in Line 149 is conferred by two major genes (Munns et al., 2003), named *Nax1* and *Nax2* (for  $\text{Na}^+$  exclusion), inherited from the *T. monococcum*. Line 149 was crossed with the durum cultivar Tamaroi, and selected  $F_2$  lines were backcrossed into Tamaroi so that *Nax1* and *Nax2* were separated into two single gene  $BC_5F_2$  families (James et al., 2006a). *Nax1* was mapped on chromosome 2AL (Lindsay et al., 2004). *Nax1* is a putative  $\text{Na}^+$  transporter, a member of the HKT family, and present only in *T. monococcum*, not *T. turgidum* or *T. aestivum*. The candidate gene has been identified as *TmHKT7-A2* (Huang et al., 2006), and renamed *TmHKT1;4-A2* to conform with the new nomenclature (Huang et al., 2008). The *Nax1* gene confers a reduced rate of transport of  $\text{Na}^+$  from root to shoot, and retention of  $\text{Na}^+$  in the leaf sheath, thus giving a higher sheath to blade  $\text{Na}^+$  concentration ratio (James et al., 2006a). The second gene, *Nax2*, also confers a lower rate of transport of  $\text{Na}^+$  from root to shoot, and has a higher rate of  $\text{K}^+$  transport, resulting in enhanced  $\text{K}^+$  versus  $\text{Na}^+$  discrimination in the leaf (James et al., 2006a). It does not retain  $\text{Na}^+$  in the leaf sheath, and does not result in a high sheath to blade  $\text{Na}^+$  concentration, the distinguishing phenotype from *Nax1* (James et al., 2006a).

#### 1.3.2 Quantifying sodium exclusion in wheat

It is more reliable and feasible to screen for  $\text{Na}^+$  exclusion in wheat than screen for salt tolerance itself. This is because  $\text{Na}^+$  exclusion is subject to less environmental influence than growth rates, biomass or yield in saline soil (Munns et al., 2003). Screening for salt tolerance

at germination may be easy to measure, but it is not necessarily proportional to the salt tolerance of the seedling or adult plant (Almansouri et al., 2001).

The screen used by Munns et al. (2000) to identify genetic variation for sodium exclusion in durum wheat involves growing wheat in a hydroponic system. The hydroponic system is designed to flood and drain, avoiding the risk of water logging, which may be a problem in standard hydroponic systems. In this set up the roots of the wheat plants are supported; they grow in gravel inside individual pots with a mesh base. The mesh pots filled with gravel are flooded with nutrient solution every 30 min. This ensures that when the salinity treatment is imposed each plant is exposed to the same concentration of NaCl.

The NaCl treatment commences when the second leaf is half emerged. The emergence of the third leaf is recorded and 10 days after emergence the third leaf is harvested. The third leaf is dried, weighed, digested in nitric acid and the Na<sup>+</sup> concentration can be measured by atomic absorption spectrometry, flame photometer or inductively coupled plasma spectrometry. The Na<sup>+</sup> concentration is then related to the dry weight to give a measurement of  $\mu\text{mol of Na}^+$  per  $\text{gDW}^{-1}$  for each leaf. This measurement is used to compare the relative accumulation of Na<sup>+</sup> in the leaf between different lines.

It is important that each plant in the screen is at the same growth stage otherwise the accumulation of Na<sup>+</sup> will be confounded by the growth rate. It is necessary to maintain a Na<sup>+</sup> to Ca<sup>2+</sup> ratio of approximately 15 to 1 when the NaCl treatment is imposed, otherwise there is insufficient available Ca<sup>2+</sup> and the plants will suffer Ca<sup>2+</sup> deficiency.

This screening, or phenotyping, method is fast as it does not require plants to be grown to maturity to assess the leaf Na<sup>+</sup> exclusion, and makes it appropriate for using in genetic mapping. Genetic mapping involves the ascertainment of phenotype, such as Na<sup>+</sup> exclusion, in a genetically segregating population followed by association between the phenotype and genotype at marker loci spanning the entire genome (Jin et al., 2004).

The power of a genetic mapping study depends on the heritability of the trait. The realized heritability for the Na<sup>+</sup> accumulation trait in the Line 149/Tamaroi mapping population was 0.90 (Munns et al., 2003). This indicates that selection for low leaf Na<sup>+</sup> is feasible in this population. Molecular markers linked to the low Na<sup>+</sup> phenotype may be identified by testing markers that span the durum wheat genome in lines that are segregating for the low leaf Na<sup>+</sup> phenotype.



### 1.3.3 Aims and objectives

The aim of this study was to investigate the physiology and genetics of sodium exclusion in wheat. Specifically, the research described in this thesis explored the molecular basis of a gene for Na<sup>+</sup> exclusion identified in Line 149, *Nax2*. The aims were to:

- Identify the chromosomal location of *Nax2*
- Develop molecular markers for *Nax2*
- Identify a candidate gene for *Nax2*
- Clone the candidate gene for *Nax2*
- Characterize the candidate gene for *Nax2*

### **1.4 Thesis outline**

**Chapter 1** is a literature review on wheat, the impact of soil salinity, and the physiology, and molecular mechanisms of plant salt tolerance.

**Chapter 2** describes the identification of the chromosomal location of *Nax2* and *Kna1*, identification of *HKT1;5* as a candidate gene, the cloning of *HKT1;5* genes and their promoters, and the development of molecular markers.

**Chapter 3** investigates the allelic diversity of *HKT1;5* in ancestral diploid material.

**Chapter 4** describes a study of the transport properties of *HKT1;5* investigated by way of expression of *HKT1;5* in *Xenopus laevis* oocytes.

**Chapter 5** describes the development an RNA interference construct designed to knock-down the expression of *HKT1;5* and the transformation of wheat, by way of biolistics, to introduce the RNA interference construct.

**Chapter 6** summarizes the major findings of the previous chapters, discusses points of interest and describes future directions.

## Chapter 2: Mapping and cloning *Nax2*; a gene for sodium exclusion in wheat

### 2.1 Introduction

An increase in the salt tolerance of wheat is needed to sustain production in cropping regions affected by salinity. Exclusion of sodium is an important mechanism of salt tolerance, and a mechanism which may improve the salt tolerance of durum wheat (Munns et al., 2006; Tester and Davenport, 2003). Exclusion of  $\text{Na}^+$  from the leaves is due to a combination of low net  $\text{Na}^+$  uptake by cells in the root cortex, and the tight control of net loading of the xylem by xylem parenchyma cells in the stele (Tester and Davenport, 2003), and also in the base of the leaves (James et al., 2006a).

Significant variation in sodium exclusion exists within durum wheat (Munns et al., 2000). To fully exploit this variation to improve the salinity tolerance of modern wheat it is necessary to identify the molecular control of sodium exclusion. In bread wheat (ABD genomes)  $\text{Na}^+$  exclusion is linked with a locus on the D genome, *Kna1*, which results in low  $\text{Na}^+$  uptake and enhanced  $\text{K}^+/\text{Na}^+$  discrimination (Gorham et al., 1990). Durum wheat (AB genomes) lacks *Kna1*, accumulates more  $\text{Na}^+$  than bread wheat and is relatively intolerant of saline soils (Munns et al., 2000). However, a novel durum wheat, Line 149, has a greater ability to restrict  $\text{Na}^+$  accumulation in the shoot, resulting in greater  $\text{K}^+$  uptake and enhanced  $\text{K}^+$  to  $\text{Na}^+$  discrimination (Munns et al., 2000).

Line 149 contains two major genes for excluding  $\text{Na}^+$  from leaf blades, named *Nax1* and *Nax2* (James et al., 2006a). One of the two loci for sodium exclusion in line 149, *Nax1*, was mapped to chromosome 2AL. This QTL explained close to 40% of the phenotypic variation (Lindsay et al., 2004). A fine mapping approach identified a candidate gene, *TmHKT1;4-A2* (Huang et al., 2006). This knowledge has enabled the introduction of *Nax1* into durum wheat breeding programs. *Nax1* functions to remove  $\text{Na}^+$  from the xylem in the roots and the lower part of the shoot (James et al., 2006a).

*Nax2* also functions in removing  $\text{Na}^+$  from the xylem (James et al., 2006a). A compartmental loading experiment where  $^{22}\text{Na}^+$  was fed only to the lower part of the roots showed that lines with *Nax2* withdrew more of the total  $^{22}\text{Na}^+$  into the upper part of the root than lines without *Nax2* (James et al., 2006a). The rates of root unidirectional  $\text{Na}^+$  uptake were identical in the lines with and without *Nax2* indicating that differences in shoot uptake were due to the net rate of xylem loading in the root (James et al., 2006a).

The major Na<sup>+</sup> exclusion locus in bread wheat, *Kna1*, is located on the D genome, on the distal part of chromosome 4. The *Kna1* phenotype is similar to the *Nax2* phenotype: Na<sup>+</sup> exclusion from the leaves and discrimination of K<sup>+</sup> over Na<sup>+</sup> in leaves, but no difference in Na<sup>+</sup> concentrations in roots (Gorham et al., 1990). As there is no difference in Na<sup>+</sup> concentrations in the roots it is likely that *Kna1* controls net xylem loading rather than net Na<sup>+</sup> uptake (Gorham et al., 1990).

*Kna1* may be homoeologous to *Nax2*, the term homoeologous referring to a gene that used to be homologous in ancestral wheats before polyploidization of wheats and their related species. If so, one would expect that *Nax2* would be located in the group 4 chromosomes. During the evolution of wheat the distal part of chromosome 4A that is homoeologous to the distal part of chromosome 4D was translocated with chromosome 5A (Devos et al., 1995; Nelson et al., 1995). Therefore if *Kna1* is located on the distal part of chromosome 4D, and *Nax2* is homoeologous to *Kna1* then *Nax2* would be physically located on the distal end of chromosome 5AL.

*Kna1* has been transferred from *T. aestivum* to *T. turgidum* (from the D genome to the B genome) by homoeologous recombination (Dvořák and Gorham, 1992). *Kna1* has been mapped to the distal portion of the long arm of chromosome 4D, and five markers have been identified that are linked to *Kna1*, within 2.2cM (Dubcovsky et al., 1994; Dubcovsky et al., 1996; Luo et al., 1996). Despite the extensive mapping work towards isolating *Kna1*, no gene has been identified as a candidate for *Kna1*.

In this study, molecular markers spanning the durum wheat genome are tested in *Nax2* single gene BC<sub>5</sub>F<sub>2:3</sub> lines segregating for the low leaf Na<sup>+</sup> phenotype to try and identify markers linked to *Nax2*. In addition to mapping *Nax2*, this study explores whether *Nax2* is homoeologous to the major Na<sup>+</sup> exclusion gene in bread wheat, *Kna1*, and investigates a candidate gene for *Nax2* and *Kna1*.

## 2.2 Materials and methods

### 2.2.1 Plant material

Plant material for the mapping population was *Triticum turgidum* ssp. *durum* Line 149 (Munns et al., 2000) and the cultivar Tamaroi. Line 149 was derived from *Triticum monococcum* (C68-101) and the durum variety Marrocos (The, 1973). *T. monococcum* C68-101 is the putative donor of *Nax1* and *Nax2* (James et al., 2006a). Selected F<sub>2</sub> lines from the cross between Line 149 and Tamaroi were backcrossed into Tamaroi four times. A selected BC<sub>4</sub>F<sub>2</sub> individual that was heterozygous for *Nax1* but had a low leaf Na<sup>+</sup> concentration was

backcrossed once more into Tamaroi to produce a BC<sub>5</sub>F<sub>2</sub> family of 137 F<sub>2</sub> individuals containing *Nax2* but not *Nax1* (James et al., 2006a). This family containing the *Nax2* gene but not the *Nax1* gene formed the basis for this study.

Plant material for the Chinese Spring (CS) deletion line experiment included lines with the following Flow lengths: 0.09, 0.31, 0.38, 0.41, 0.46, 0.53, 0.56, 0.61, 0.70, 0.71, 0.86 and 1.00 (wild type CS) (Endo and Gill, 1996). Flow length refers to the remaining length of chromosome, equivalent to one minus the Fraction Length (Endo and Gill, 1996). The Selection Numbers for these lines are 4DL-249, 4DL-253, 4DL-250, 4DL-251, 4DL-247, 4DL-252, 4DL-256, 4DL254, 4DL-248, 4DL-255 and 4DL-257, respectively. Plant material for DNA extraction for Southern blot-hybridisation work included CS nulli-tetrasomic and deletion lines (Endo and Gill, 1996) and Langdon substitution lines. The Langdon substitution lines included 4D(4A) and 4D(4B), where chromosome 4D from CS had been substituted for chromosome 4A or 4B of Langdon respectively (Sears, 1954).

### 2.2.2 Phenotyping

Plants were grown in half strength Hoagland's solution in supported hydroponics in a method adapted from Munns et al. (2000). Salt treatment commenced when leaf two was half emerged. The NaCl concentration of the hydroponic solution was increased by 25 mM twice daily over three days to reach a final concentration of 150 mM. Supplemental calcium (Ca(NO<sub>3</sub>)<sub>2</sub>) was added to achieve a Na<sup>+</sup> to Ca<sup>2+</sup> ratio of 15:1. Leaf three was harvested after 10 days growing in salt and the Na<sup>+</sup> was extracted with nitric acid (0.5 M). The Na<sup>+</sup> concentration was measured using Inductively Coupled Plasma (ICP) analysis. Parental lines were replicated ten times. Based on the score of F<sub>2</sub> individuals nine plants from every family predicted to be homozygous low were tested and five plants were tested for every family predicted to be homozygous high or heterozygous. These numbers were based upon recommended population sizes required in biparental populations to obtain at least one target homozygous genotype in later generations for segregating loci (Bonnett et al., 2005).

### 2.2.3 Genotyping

Plants grown in salt tanks for phenotyping were transplanted into soil and allowed to grow for approximately four weeks prior to DNA extraction. A single plant was retained from each of the F<sub>2:3</sub> families. For families with a homozygous low Na<sup>+</sup> accumulation phenotype, the plant with the lowest leaf Na<sup>+</sup> concentration was used. The plant with the highest leaf Na<sup>+</sup> was used from families with a homozygous high Na<sup>+</sup> accumulation phenotype. For half of

those families with a heterozygous phenotype, the lowest of the low Na<sup>+</sup> accumulating plants was used, and for the other half of the families with a heterozygous phenotype, the highest of the high Na<sup>+</sup> accumulating plant was used. Leaf material from plants was harvested and DNA extracted as per Lagudah et al. (1991).

DNA was also extracted from 30 seed from BC<sub>4</sub>F<sub>2</sub> putative single gene *Nax2* lines, using a NucleoSpin Plant Kit (Macherey-Nagel, Duren, Germany) as per the manufacturers' instructions. To test for the absence of *Nax1* in the *Nax2* lines DNA from the 30 lines was tested by PCR with two markers linked to *Nax1*. The linked were *gwm312* and *gwm170* (Lindsay et al., 2004). PCR was conducted under standard conditions.

#### 2.2.4 Microsatellite markers

To establish the chromosomal location of *Nax2* in the durum Line 149 DNA from the parental lines, Tamaroi and Line 149, was screened with a total of 470 wheat microsatellite markers. Microsatellite markers were from Gatersleben in Germany (GWM), the French National Institute for Agricultural Research (GPW), Beltsville Agricultural Research Center (BARC) and GrainGenes (<http://wheat.pw.usda.gov>). Twenty-five markers were found to be polymorphic between Line 149 and Tamaroi, these were then tested on pooled DNA consisting of three samples of the single gene parent (n = 5 plants per sample), 15 markers were still polymorphic between the single gene *Nax2* parent and Tamaroi. These were tested on two samples each from the BC<sub>5</sub>F<sub>2:3</sub> lines with low leaf Na<sup>+</sup> and high leaf Na<sup>+</sup> (n = 10 plants per sample). Three wheat microsatellite markers on chromosome 5AL were linked to *Nax2*; *gwm291*, *gwm410* and *gpw2181* (Appendix Table 2.1). To confirm linkage of these markers with *Nax2*, the genotype of 19 BC<sub>5</sub>F<sub>2:3</sub> plants with a homozygous low Na<sup>+</sup> phenotype and 11 BC<sub>5</sub>F<sub>2:3</sub> plants with a homozygous high Na<sup>+</sup> phenotype were tested using the markers *gwm291*, *gwm410* and *gpw2181*. Linked markers, and an additional marker on chromosome 5AL developed by Jorge Dubcovsky (University of California, Davis, California), *Vrn2*(BM1) (Appendix Table 2.1), were then tested in each of the 137 BC<sub>5</sub>F<sub>2:3</sub> progeny.

#### 2.2.5 RFLP probe development

A search of the public database (Personal communication, Damien Platten, 2005) identified a wheat EST (CK193616) with strong homology, 86% nucleotide sequence identity, to the rice *SKC1* candidate gene (OSJNBb0022N24.16), subsequently named *OsHKT1;5* (Platten et al., 2006). The wheat EST was named *HKT1;5* as recommended by Platten et al. (2006). Primers designed internal to CK193616 were HKT1;5For01 (5'-

CATCACCGTCGAGGTTATCAG-3') and HKT1;5Rev01 (5'-TTGAGGTACTCGGCATA-3'). These primers were used to amplify a 332 base pair (bp) product from *T. monococcum* genomic DNA. The product was cloned into pGEMT-easy vector (Promega Corporation). To prepare an *TmHKT1;5* probe, the 332 bp fragment was amplified from the *HKT1;5* region from the plasmid DNA by PCR using primers HKT1;5For01 and HKT1;5Rev01. The PCR was conducted under standard conditions with the following cycling protocol: 95°C, 15 min; then 5 cycles at 94°C, 1 min; 55°C, 1 min; 72°C, 1 min 20 s; followed by 30 cycles of 94°C, 30 s; 55°C, 30 s; and finally 72°C, 2 min. After gel electrophoresis a band of the appropriate size (332 bp) was removed from the gel and purified using a QIAquick Gel Extraction Kit (Qiagen), using a microcentrifuge, according to the manufacturer's instructions. This fragment was radio-labelled with <sup>32</sup>P-CTP using the Megaprime DNA Labelling System (Amersham), according to the manufacturer's instructions. The probe was then purified through a column of G50 Sephadex beads equilibrated in Tris-EDTA.

DNA from the parental lines (Line 149 and Tamaroi), *T. monococcum* (AUS# 90382) and the BC<sub>5</sub>F<sub>2;3</sub> progeny were digested individually *Hind*III and/or *Eco*RV, *Nco*I, *Sac*I and/or *Xba*I. After gel electrophoresis, the gels were blotted onto a nitrocellulose membrane (Amersham Biosciences Hybond-N<sup>+</sup>) and hybridised with the *TmHKT1;5* probe. DNA samples from wheat nullisomic-tetrasomic lines and ditelomeric lines in a Chinese Spring background were also screened with the *TmHKT1;5* probe as described above (Endo and Gill, 1996).

#### 2.2.6 Isolation of *TaHKT1;5-D*

The Chinese Spring cDNA library was kindly supplied by Professor Timothy J. Close (University of California, Davis, California). The library was constructed from drought stressed root tissue from *Triticum aestivum* L. cv Chinese Spring, at full tillering, using the Uni-ZAP XR Vector System (Stratagene, US), which allows *in vivo* excision of the pBluescript II (SK-) Phagemid vector (Stratagene). The host cells were XL1-Blue-MRF (Stratagene). Approximately 120 000 clones of the mass excised phagemid library were plated and screened with the partial *TmHKT1;5* probe according to standard protocols (Sambrook, 1989). Eleven colonies hybridised to the probe. These were grown at 37°C overnight in Luria broth (Sambrook, 1989) and plasmid DNA was isolated using a Qiaspin miniprep kit<sup>®</sup> according to the manufacturer's instructions (Qiagen). Plasmid DNA was digested with *Eco*RI and *Xho*I to liberate the cloned inserts. The inserts were sequenced using T7 an SP6

universal primers (Invitrogen) using a BigDye® Terminator v3.1 Cycle Sequencing Kit (Applied Biosystems) as per the manufacturers instructions.

#### 2.2.7 Isolation of RNA, RT-PCR and isolation of *TmHKT1;5-A*

Plants were grown in hydroponic solution described in plant material. After two weeks plants were exposed to 50 mM NaCl. After 48 h leaf and root tissues were harvested separately and snap frozen in liquid nitrogen. RNA was extracted using TRIzol Reagent® (Invitrogen) as per the manufacturer's instructions. Reverse-transcriptase PCR to amplify *TmHKT1;5* was undertaken using primers that were external to the coding sequence named 5primeUTRFor (5'-AGAAGTCTCTACACAACCTTACAG-3') and 3primeUTRRev (5'-GATCATTGAGAAATATGCAGTCC-3') using a Qiagen® OneStep RT-PCR Kit as per the manufacturer's instructions. DNA fragments of the appropriate size were amplified from *T. monococcum* and Line 149. These fragments were cut out and purified using a Qiagen gel extraction kit® according to the manufacturer's instructions. The fragments were ligated into the pGEM-T Vector using the pGEM-T easy vector system 1 kit® (Promega).

Reverse-transcriptase PCR (RT-PCR) to observe presence or absence of expression of the *HKT1;5* A and D gene homoeologues was undertaken using A gene specific primers named ForA1 (5'-GAGTGGGGCTCCGACGGGCTGAA-3') and RevA1 (5'-CGTCAGGCGTCACCTGCCGGCCG-3') and D gene specific primers ForD1 (5'-GCTTGGCCATCTTCATCGCCGTG-3') and RevD1 (5'-GGCCACAGCTGTACCCGGTGCTG-3') using a Qiagen® OneStep RT-PCR Kit as per the manufacturer's instructions. The PCR was conducted under standard conditions with the following cycling protocol: 50°C, 20 min; 94°C, 15 min; then 35 cycles of 94°C, 30 s; 58°C, 30 s; 68°C, 1 min; and finally 72°C, 2 min. The forward and reverse primers in each primer set were designed in different exons so as to include an intron in between them. Therefore, products that amplified from trace DNA in the RNA samples differed in size from the products amplified from coding DNA. The expected product size for the A gene specific primers was 945 bp from genomic DNA and 445 bp from coding DNA. The expected product size for the D gene specific primers was 322 bp from genomic DNA and 147 bp from coding DNA. The control gene for the RT-PCR was a proton pump from wheat (GenBank accession no. AY543630); the following primers were used 5'-AACAAGACTGCTTTCACCAC-3' AND 5'-TCTCAGAGAGCTCACGGTAG-3' to amplify the control gene (Delhaize et al., 2004).

### 2.2.8 Isolation of *HKT1;5* promoters from Bacterial Artificial Chromosomes

A *Triticum monococcum* (DV92) Bacterial Artificial Chromosome (BAC) library filter (Lijavetzky et al., 1999) was purchased from Professor Jorge Dubcovsky (University of California, Davis, California) and screened with the *TmHKT1;5* probe (see 2.2.5 and 2.2.6) and 12 positive clones were ordered. Two BAC clones, with the strongest hybridization, (377C7 and 312C10) were grown on LB plates with 30µg/mL Chloramphenicol. A single colony was picked and grown in 2 mL LB with 30µg/mL Chloramphenicol at 37°C for 16 h. The 2 mL culture was then used to inoculate a 40 mL culture, which was grown in the same conditions. A *Triticum tauschii* BAC clone, from a diploid D genome BAC made from *Aegilops tauschii* (AUS18913) (Moulet et al., 1999), which the *TmHKT1;5* probe was previously found to hybridize (Evans Lagudah, personal communication, November 2006) was sourced from Evans Lagudah (CSIRO Plant Industry, Canberra, Australia). A 40 mL culture of the *T. tauschii* clone was grown in LB with 15 mg/mL tetracycline. The BAC DNA from each culture was then isolated using a BACMAX™ DNA Purification Kit (EPICENTRE, Cat. No. BMAX044) as per the manufacturers instructions.

A series of primers, based on the *TmHKT1;5-A* and *TaHKT1;5-D* genomic DNA sequences were used in sequencing reactions to sequence directly from the purified BAC DNA. These primers included 5'-CAGACAGAGAGTAGCTACATCTCG-3', 5'-CTACATCTCGCTCTAGCC-3', 5'-GCATGCATATCGATGGTCTG-3'. Sequencing was by means of a BigDye® Terminator v3.1 Cycle Sequencing Kit (Applied Biosystems) as per the manufacturers instructions. Promoters were amplified and cloned (methods as in 2.2.7) using the following primers; 5'-GCAGATGTTTCGCATACACTC-3' and 5'-CGCAGCTCACCAGCTCGG-5'.



## 2.3 Results

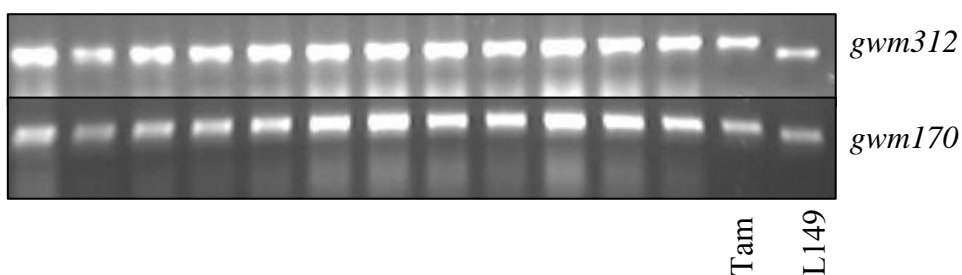
### 2.3.1 Analysis of putative *Nax2* single gene lines

The absence of *Nax1* in the single gene *Nax2* population was confirmed by PCR on 30 BC<sub>4</sub>F<sub>2</sub> *Nax2* lines using two markers closely linked to *Nax1*; *gwm312* and *gwm170* (Lindsay et al., 2004). Results for a selection of lines are shown in Figure 2.1.

### 2.3.2 Genetics of *Nax2*

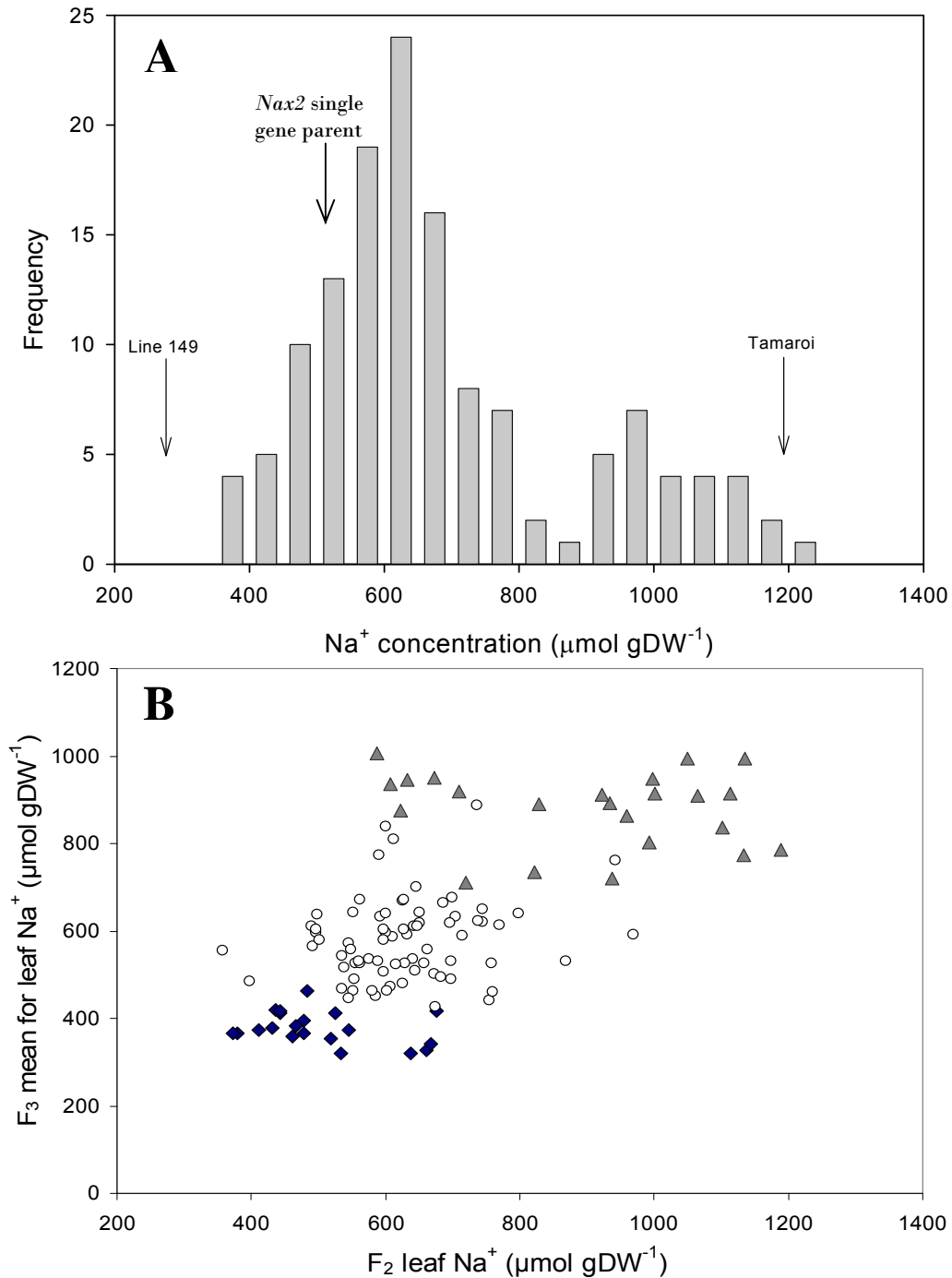
*Nax2* is responsible for a greater than 2-fold reduction in leaf Na<sup>+</sup>. The mean leaf Na<sup>+</sup> concentration of the BC<sub>4</sub>F<sub>2</sub> *Nax2* single gene parent was 473 ± 72 μmol g dry weight<sup>-1</sup> compared to Tamaroi, which had a mean leaf Na<sup>+</sup> concentration of 1,193 ± 48 μmol g dry weight<sup>-1</sup>.

*Nax2* is a single major gene. The frequency distribution of leaf Na<sup>+</sup> concentration from 137 BC<sub>5</sub>F<sub>2</sub> plants indicated that *Nax2* was dominant, segregating in a 3:1 (low:high leaf blade Na<sup>+</sup>) ratio (Figure 2.2A) (James et al., 2006a; Byrt et al., 2007). The segregation of the Na<sup>+</sup> exclusion trait was confirmed in the F<sub>2:3</sub> families (773 individuals). The F<sub>2:3</sub> families fitted the expected ratio for a single major gene (expected 94:31; observed 96:29;  $\chi^2 = 0.171$ ,  $P \geq 0.05$ ; Figure 2.2B). The mean leaf Na<sup>+</sup> of the *Nax2* single gene parent was 462 ± 23 μmol g dry weight<sup>-1</sup> in the F<sub>2:3</sub> generation, compared to 473 ± 72 μmol g dry weight<sup>-1</sup> in the F<sub>2</sub> generation.



### Figure 2.1: Genotype of *Nax2* single gene lines

The *Nax2* single gene BC<sub>4</sub>F<sub>2</sub> lines have Tamaroi (Tam), not Line149 (L149) chromatin for markers *gwm312* and *gwm170*, indicating that *Nax1* is absent in these lines.



**Figure 2.2: Segregation of the  $\text{Na}^+$  exclusion gene, *Nax2***

A. Frequency distribution for leaf three  $\text{Na}^+$  concentrations of the  $\text{BC}_5\text{F}_2$  lines in the single gene *Nax2* mapping population. Data from  $\text{BC}_5\text{F}_2$  is from James *et al.* (2006a), and data from  $\text{BC}_5\text{F}_{2:3}$  is from Byrt *et al.* (2007). Arrows indicate parental means ( $n=6$ ); Line 149:  $278 \pm 37$ , *Nax2* single gene parent:  $473 \pm 72$ , Tamaroi:  $1193 \pm 48$ .

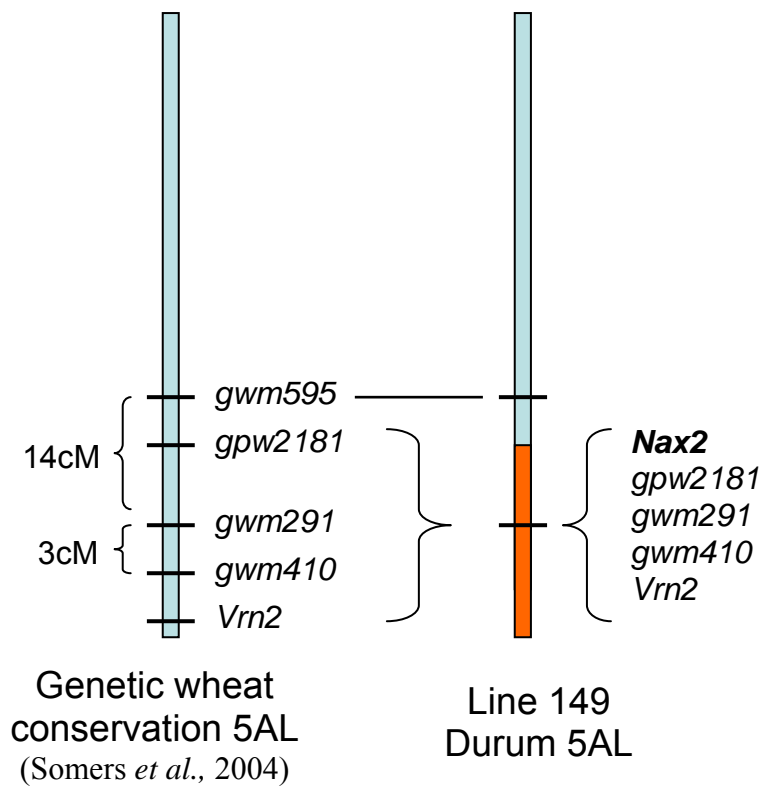
B. Relationship between the  $\text{F}_2$  and  $\text{F}_{2:3}$  progeny means for  $\text{Na}^+$  concentration of leaf three (Byrt *et al.*, 2007). Plants were grown at 150 mM NaCl for 10 days.  $\blacktriangle$  = homozygous lacking *Nax2*,  $\circ$  = heterozygous for *Nax2*,  $\blacklozenge$  = homozygous for *Nax2*.

### 2.3.3 Microsatellite markers on chromosome 5AL linked to *Nax2*

DNA from Line 149, Tamaroi, the single gene *Nax2* parent, and the BC<sub>5</sub>F<sub>2:3</sub> progeny were tested with microsatellite markers. Of the 470 markers tested, 15 markers were polymorphic for the single gene *Nax2* parent and Tamaroi, and three of these were dominant markers linked to *Nax2*; *gpw2181*, *gwm291* and *gwm410* (Appendix Table 2.1). These markers had been mapped previously to the distal end of chromosome 5AL (Roder et al., 1998). An additional co-dominant marker, *Vrn2*(BM1) was also linked to *Nax2* (Appendix Table 2.1). The linked markers were all located on chromosome 5AL indicating that *Nax2* is located on chromosome 5AL (Figure 2.3). The linkage between the four markers and *Nax2* in the BC<sub>5</sub>F<sub>2:3</sub> progeny was perfect. There was no evidence of recombination between any of the markers and or *Nax2*.

Four microsatellite markers on chromosome 5AL (Roder et al., 1998) were polymorphic between Line 149 and Tamaroi but not polymorphic between the single gene *Nax2* BC<sub>4</sub> parent and Tamaroi; *gwm595*, *gwm179*, *gwm126* and *barc232*. These markers were not retained in the BC<sub>4</sub> parent and therefore failed to segregate in the BC-derived family. This indicates that a recombination occurred between the *Nax2* gene and *gwm595* and the chromosomal region on 5AL proximal to *gpw2181* was replaced by Tamaroi during the process of five back crossing steps of transferring *Nax2* into Tamaroi (Figure 2.3). The complete linkage of *Nax2*, *Vrn2*, *gpw2181*, *gwm291* and *gwm410* in 137 BC<sub>4</sub>F<sub>2</sub> lines indicates a large non-recombining block from *T. monococcum* may have translocated to 5AL in the Tamaroi background (Figure 2.3). The region between *Vrn2* and the *BAmy* marker on the distal end of chromosome 5AL is 18 cM (Dubcovsky et al., 1996); therefore, the *T. monococcum* segment may be more than 30 cM long.

The major locus for sodium exclusion in bread wheat, *Kna1*, is located on the distal end of the long arm of chromosome 4D (4DL). If *Nax2* were homoeologous to *Kna1* then it would be expected that *Nax2* might be located on 4AL. However, in an ancestor of modern wheats chromosomes 4AL and 5AL exchanged short terminal segments (Liu et al., 1992). Therefore, although *Kna1* is on chromosome 4AL and *Nax2* is on chromosome 5AL, due to the reciprocal translocation between the distal end of 4AL and 5AL, *Nax2* does map to the location that we might expect to find a homoeologue of *Kna1*.



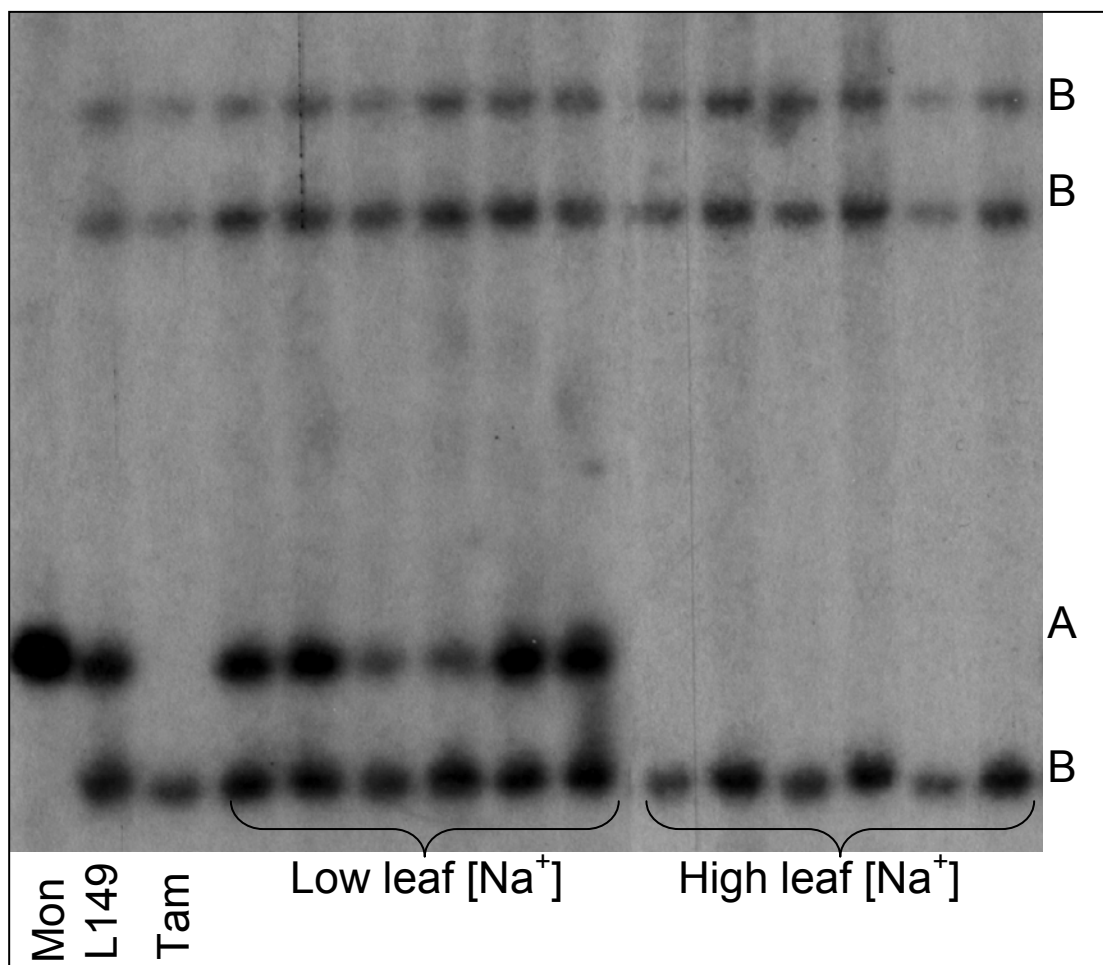
**Figure 2.3: Microsatellite markers linked to *Nax2***

Durum 5AL represents the fragment containing *Nax2* which introgressed from Line 149 (orange) into the Tamaroi background (blue) in the *Nax2* mapping population. Proximal to the introgression is *gwm595*. *Nax2* is linked to *gpw2181*, *gwm291*, *gwm410* and *Vrn2*. 5AL = chromosome 5AL; cM = centimorgans.

#### 2.3.4 Co-segregation of putative $\text{Na}^+$ transport gene, *HKT1;5*, with *Nax2*

Publicly available cation transporter sequences from rice were used to screen the GenBank database of wheat expressed sequence tags (ESTs) to identify putative cation transporters in wheat (Damien Platten, personal communication, April 2005). As part of this work, the protein sequence of *OsHKT1;5* (Ren et al., 2005) was used to search the wheat EST database. The search identified a single closely related partial wheat EST sequence (CK193616) (Damien Platten, personal communication, April 2005). This partial sequence (*TaHKT1;5*) shared 86% identity at the nucleotide level and contained parts of the corresponding sequences of exon 2 and exon 3 of *OsHKT1;5* (Ren et al., 2005).

A probe designed from the partial *HKT1;5* sequence (*HKT1;5* probe, see 2.2.5 and Appendix Figure 2.1) identified RFLP between parental lines. Polymorphism found between the parents, Line 149 and Tamaroi, was due to the presence of an additional fragment in Line 149 when compared to Tamaroi (Figure 2.4). The additional fragment in Line 149 cosegregated with the low  $\text{Na}^+$  accumulation phenotype in all of the 137  $\text{BC}_5\text{F}_2$  families tested. All of the lines in the mapping family verified as homozygous and heterozygous for *Nax2* had the additional fragment and those lines that were homozygous for the high leaf  $\text{Na}^+$  phenotype lacked the fragment (a selection is shown in Figure 2.4).



**Figure 2.4: Cosegregation of *HKT1;5* with *Nax2***

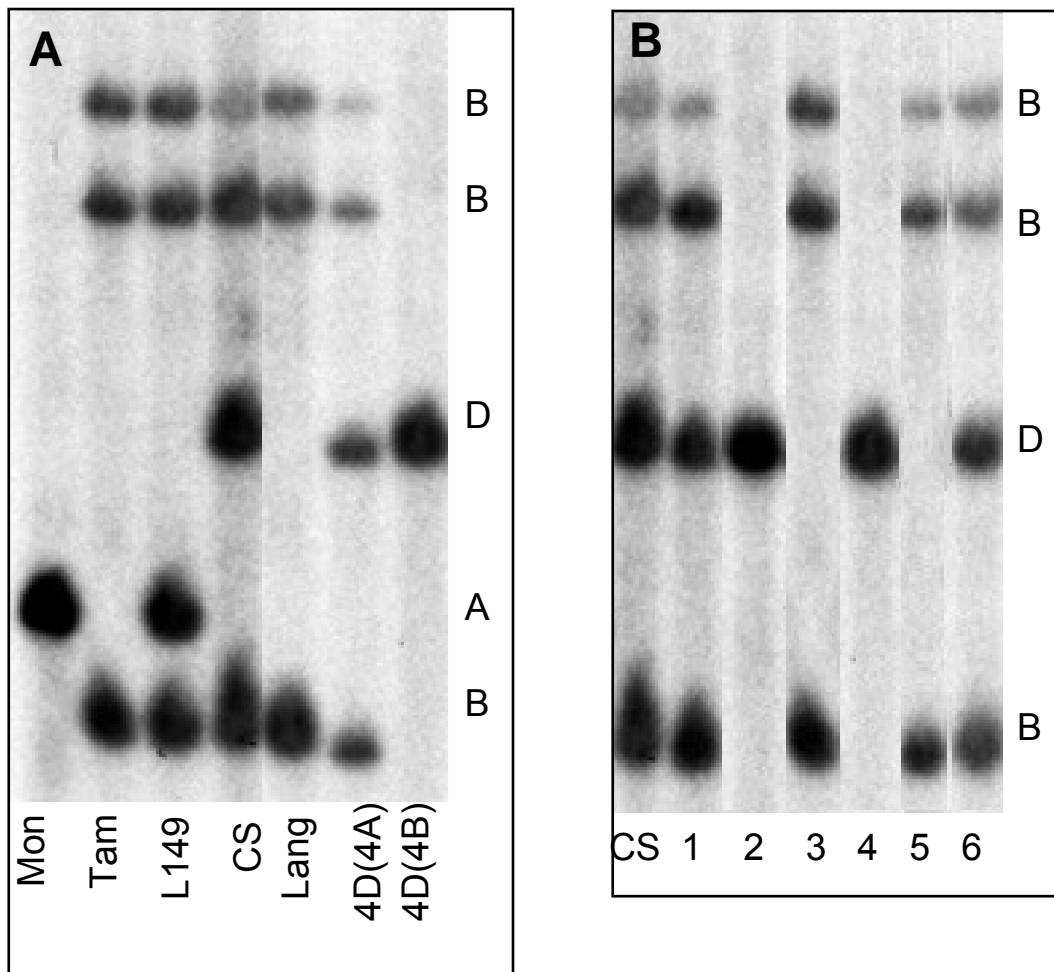
Southern blot hybridisation with the *HKT1;5* probe after *Hind*III digestion of DNA from *Triticum monococcum* (Mon), Line 149 (L149), Tamaroi (Tam), and plants from the *Nax2* BC<sub>5</sub>F<sub>3</sub> mapping population with high leaf three Na<sup>+</sup> concentrations, and low leaf three Na<sup>+</sup> concentrations. The genome origin of each band is shown on the right. In the *Nax2* mapping family the A genome band co-segregates with *Nax2* in all of the 137 families.

### 2.3.5 Wheat *HKT1;5* gene homologues

The *HKT1;5* probe hybridised to a single restriction fragment in DNA from the diploid *Triticum monococcum* L. (AA) (C68-101), the putative donor of salt tolerance in Line 149 (AABB) (The, 1973; James et al., 2006a). A fragment of the same size as the fragment in *T. monococcum* was present in Line 149 but not in Tamaroi. Three additional fragments were present in Line 149, these were of the same size as three fragments present in Tamaroi (Figure 2.4). The additional fragment in Line 149 co-segregated with *Nax2* (Figure 2.4). This result is consistent with the partial *HKT1;5* probe detecting a candidate gene for *Nax2* which was inherited from *T. monococcum*. Using a range of restriction enzymes, the *HKT1;5* probe always hybridised to at least two fragments in Tamaroi and three fragments in Line 149 (Data not shown). *HindIII* produced an additional fragment in both parents (Figure 2.4). This indicated that Tamaroi contained at least two *HKT1;5*-like genes, while Line 149 had the same two fragments plus one additional gene member and that was inherited from *T. monococcum*.

To further characterise the *HKT1;5* gene family in durum wheat, we analysed DNA from the durum cultivar Langdon carrying individual chromosome substitutions from Chinese Spring. The probe hybridised to at least two fragments in Langdon DNA producing an identical pattern to Tamaroi. Hybridisation of the partial *HKT1;5* probe to Chinese Spring DNA produced a pattern identical to that of Langdon and Tamaroi except for one additional chromosome 4D fragment. Langdon with chromosome 4A substituted by 4D of Chinese Spring retained all three fragments and gained an additional fragment from chromosome 4D of Chinese Spring. The Langdon substitution line with chromosome 4B replaced by chromosome 4D of Chinese Spring had lost all three Langdon fragments but retained the 4D fragment from Chinese Spring (Figure 2.5A). These results indicate that all *HKT1;5* hybridising fragments in Langdon and Tamaroi are located on chromosome 4B and that Line 149 inherited an additional A genome member from *T. monococcum*.

Analysis of nulli-tetrasomic Chinese Spring lines of homoeologous group 4 confirmed that *HKT1;5* fragments were located either on chromosome 4B or 4D (Figure 2.5B). DNA hybridisation of the partial *HKT1;5* probe to ditelosomic lines of Chinese Spring positioned these genes on the long arm of chromosome 4B (at least two members) and the long arm of chromosome 4D (at least one member) (Figure 2.5B).



**Figure 2.5: Chromosomal location of the *HKT1;5* fragments**

Southern blot hybridisation with the *HKT1;5* probe after *HindIII* restriction digest

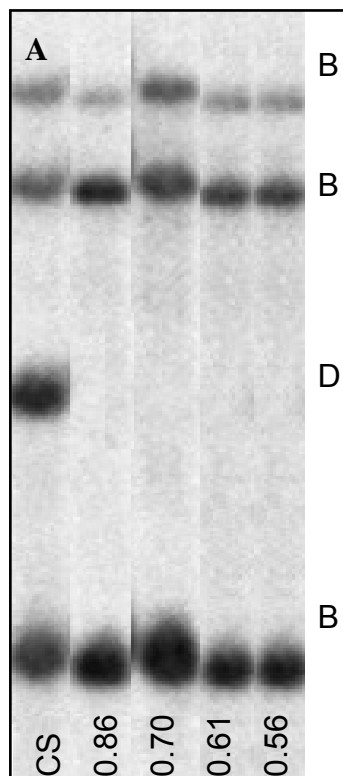
A. DNA from *T. monococcum* (Mon), Tamaroi (Tam), Line 149 (L149), Chinese Spring (CS), Langdon (Lang) and Langdon substitution lines 4D(4A) and 4D(4B). The genome locations of the *HKT1;5* gene members, and the approximate sizes (kilo base pairs) of the fragments are shown on the right.

B. DNA from Chinese Spring (CS); Chinese Spring chromosome arm deletion lines for chromosome 4B: N4AT4B (1), m4BT4A (2), N4DT4B (3); and Chinese Spring ditelomeric lines Dt4BS (4), Dt4DS (5) and Dt4DL (6); [(N = nullitetrasonic (no copies); T = tetrasomic (four copies); m = monosomic (one copy); Dt = ditelomeric (for Dt4BS the long arm of 4B is missing and the short arm of 4B is present)]. The genome locations of the *HKT1;5* gene members are shown on the right.

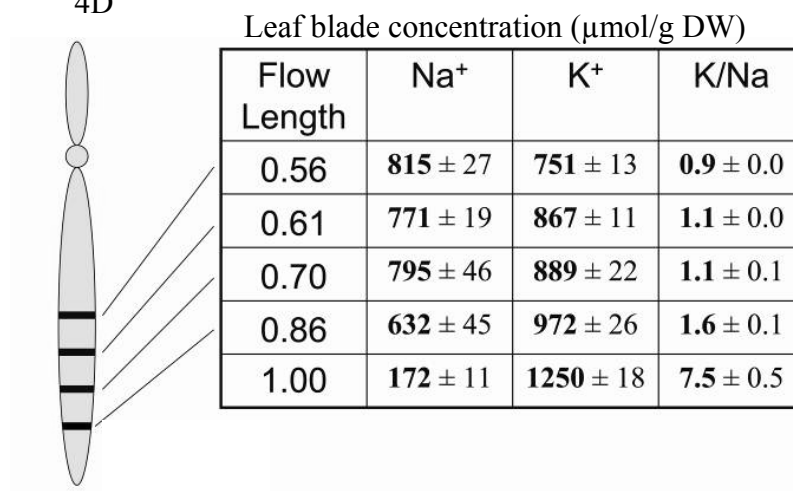


### 2.3.6 *Nax2* is homoeologous to the major $\text{Na}^+$ exclusion locus in bread wheat, *Kna1*

To study the relationship of *Kna1* to the *TaHKT1;5-D* gene member, we probed DNA from Chinese Spring and a series of telomeric deletion lines generated from chromosome 4DL in Chinese Spring (Endo and Gill, 1996). The *HKT1;5* gene member on chromosome 4DL was absent in the terminal deletion line Flow length (remaining length) 0.86 (Selection number 4DL-257) with approximately 14% of the chromosome arm deleted (Figure 2.6A). The 4DL fragment was also missing in other lines with progressively larger terminal deletions (Figure 2.6A). The loss of the *TaHKT1;5-D* gene member corresponded to an increase in average  $\text{Na}^+$  concentrations in the leaf blade of the deletion lines compared with the euploid salt tolerant Chinese Spring, and a decrease in the  $\text{K}^+$  to  $\text{Na}^+$  ratio from 7.5 to 1.2 (Figure 2.6B).



**B** Chromosome  
4D



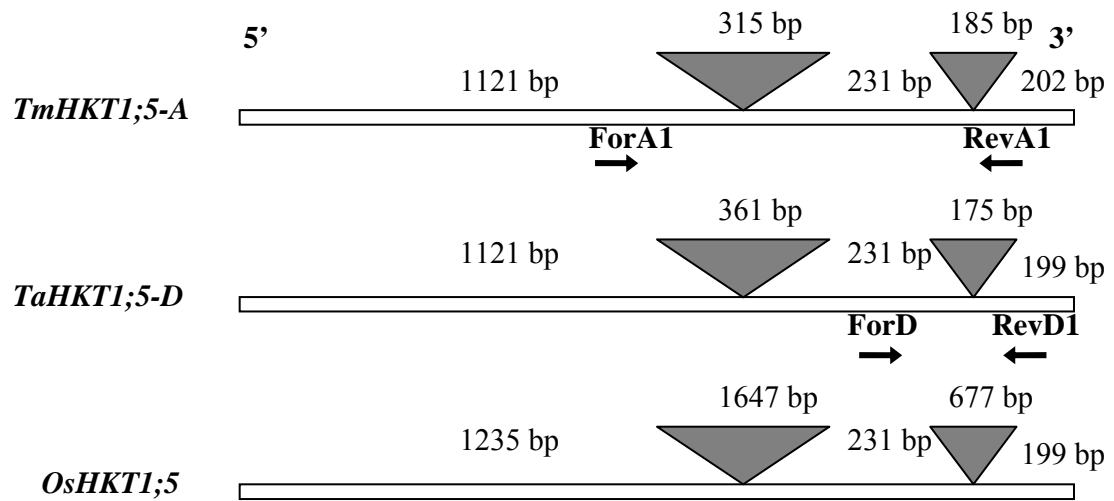
**Figure 2.6: Association of *HKT1;5* with *Knal***

A. Southern blot hybridisation with *HKT1;5* probe after *HindIII* restriction digest of DNA from Chinese Spring (CS) and Chinese Spring chromosome deletion lines 0.86, 0.70, 0.61, and 0.56. The *TaHKT1;5-D* gene member maps to the most distal deletion bin. The genome location of the *TaHKT1;5* gene members are shown on the right.

B. Chinese Spring and Chinese Spring chromosome deletion lines were grown in salt tanks (see Materials and Methods). Flow length describes remaining fraction of chromosome 4DL. *Knal* maps to the same location (Dubcovsky et al., 1996) as *TaHKT1;5-D*. Leaf blade Na<sup>+</sup> and K<sup>+</sup> concentrations were recorded after leaf three had grown for ten days in 50 mM NaCl.

### 2.3.7 Isolation of full length *HKT1;5* gene members

The partial *HKT1;5* probe was used to screen a cDNA library from root tissue of Chinese Spring. Several positive phagemid clones were isolated and when sequenced revealed identical DNA sequences with insert size varying between 812 bp and 1741 bp. The cDNA sequences were identical to genomic sequence derived from a BAC clone that was previously isolated from a BAC library made from the diploid D genome progenitor species *Aegilops tauschii* Coss. (Evans Lagudah, personal communication May 2005) suggesting that the cDNA sequence isolated from Chinese Spring was derived from the D genome. The *TaHKT1;5-D* sequence is included in Appendix Figure 2.2. The cDNA was predicted to encode a full length gene based on the comparison of its predicted amino acid sequence to *OsHKT1;5 (SKC1)* in rice. Reverse-transcriptase PCR with primers designed from the 5' and 3' untranslated regions of *TaHKT1;5-D* amplified the corresponding A gene member, *TmHKT1;5-A*, from *T. monococcum* and Line 149. The *TmHKT1;5-A* sequence is included in Appendix 2.3, and an alignment of the genomic sequences of *TmHKT1;5-A* and *TaHKT1;5-D* is included in Appendix Figure 2.4. The predicted open reading frame (ORF) of *TmHKT1;5-A* is 1554 bp and the predicted ORF of *TaHKT1;5-D* is 1551 bp. *OsHKT1;5*, *TmHKT1;5-A* and *TaHKT1;5-D* each have two introns. The predicted amino acid sequence of *TmHKT1;5-A* and *TaHKT1;5-D* shared 94% identity (Appendix Figure 2.5) and were closely related to the rice Na<sup>+</sup> transporter *OsHKT1;5* (66% identity) (Appendix Figure 2.6). The intron and exon structure of the *TmHKT1;5-A*, *TaHKT1;5-D* and *OsHKT1;5* genes are shown in Figure 2.7.



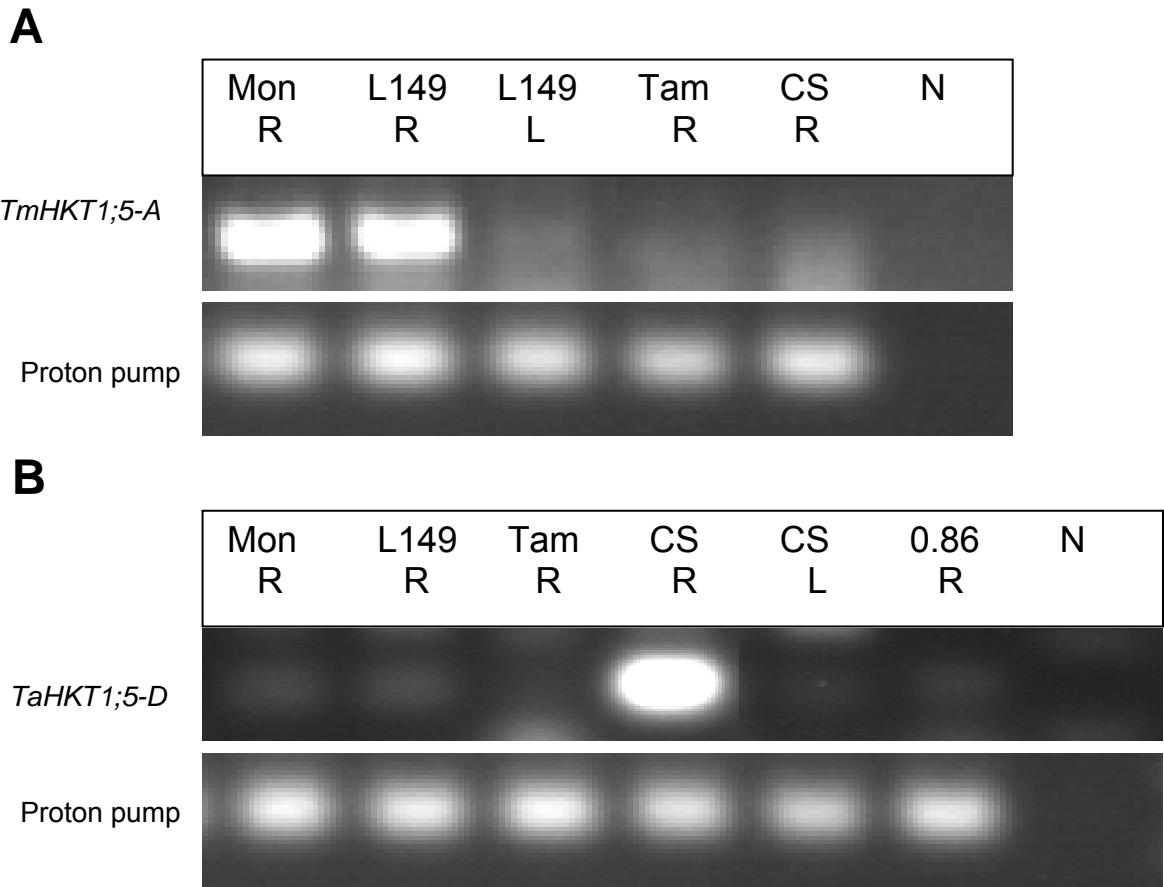
**Figure 2.7: Gene structures of *TmHKT1;5-A*, *TaHKT1;5-D* and *OsHKT1;5***  
 The grey triangles represent the intron regions of the gene. *TmHKT1;5-A* and *TaHKT1;5-D* share 94% identity with each other and 66% identity with the rice Na<sup>+</sup> transporter *OsHKT1;5*. The arrows indicate the primers designed for gene expression analysis (Figure 2.8).

### 2.3.8 Expression of *HKT1;5*

Reverse-transcriptase PCR with specific primers for A and D genome members was used to analyze the expression of the *HKT1;5* A and D gene members in *T. monococcum*, Line 149, Tamaroi and Chinese Spring. *TmHKT1;5-A* was expressed in the roots of *T. monococcum* and Line 149, but not in the shoots (Figure 2.8A). *HKT1;5-A* was not expressed in Tamaroi or Chinese Spring. The *TaHKT1;5-D* gene member was expressed in Chinese Spring roots but not shoots (Figure 2.8B). The *TaHKT1;5-D* gene member was not expressed in the Chinese Spring deletion line missing the distal 14% of chromosome 4DL (0.86) (Figure 2.8B). The expression results for the *HKT1;5-D* gene member are consistent with the mapping results indicating that *HKT1;5-D* is missing from the Chinese Spring deletion line 0.86 and is therefore positioned in the same region as *Kna1*.

### 2.3.9 Isolation of wheat *HKT1;5* promoters from Bacterial Artificial Chromosomes

Wheat *HKT1;5* promoters from the A (Appendix Figure 2.7) and D (Appendix Figure 2.8) genomes were sequenced from *T. monococcum* and *T. tauschii* BAC libraries respectively, their nucleotide sequences share 93% identity. The 5' region between the neighboring gene and the start codon of *HKT1;5* on the D genome is 1027 bp. The 5' region between the neighboring gene and the start codon of *HKT1;5* on the A genome is 1048 bp.



**Figure 2.8: Expression of *HKT1;5* in wheat analysed using RT-PCR**

A. Expression of *TmHKT1;5-A*. A product of the expected size (442 bp) was observed for the *T. monococcum* and Line 149 root samples. B. Expression of *TaHKT1;5-D*. A product of the expected size (147 bp) was observed for the Chinese Spring root sample. Mon = *T. monococcum*; L149 = Line 149; Tam = Tamaroi; CS = Chinese Spring; 0.86 = Chinese Spring deletion line missing the distal 14% of chromosome 4DL; N = no template control; R = root tissue; L = leaf tissue. Plants were grown in hydroponic solution for two weeks before addition of 50 mM NaCl, tissue was harvested 48 h after addition of NaCl. Primers for a proton pump (Delhaize et al., 2004) was used as a control.

## 2.4 Discussion

### 2.4.1 Mapping of *Nax2*

The segregation of low:high leaf blade  $\text{Na}^+$  concentration in  $\text{BC}_5\text{F}_2$  plants in a 3:1 ratio showed that *Nax2* is a single dominant gene (Figure 2.2). *Nax2* is located on the distal part of chromosome 5AL (Figure 2.3). The *HKT1;5* gene member on the A genome mapped to the same region as *Nax2*, and co-segregated with *Nax2*.

HKT genes were considered to be the best candidates for *Nax2* based on the role of other HKT transporters in higher plants. *TmHKT1;4-A2* cosegregates with *Nax1*, which confers  $\text{Na}^+$  exclusion from leaves in wheat (Huang et al., 2006), *AtHKT1;1* confers  $\text{Na}^+$  exclusion from leaves in *Arabidopsis* (Uozumi et al., 2000; Sunarpi et al., 2005), and *OsHKT1;5* (*SKC1*) confers  $\text{Na}^+$  exclusion from leaves in rice (Ren et al., 2005).

There are up to five *HKT1;5* genes in wheat, a partial wheat *HKT1;5* probe detected one gene member on the D genome, two or three on the B genome, and one gene member on the A genome derived from *T. monococcum* (C68-101). The predicted amino acid identity between the wheat *HKT1;5-A* and *HKT1;5-D* gene members is 94%. The most closely related gene in rice, *OsHKT1;5*, shares 66% identity (75% positives) with the predicted wheat *HKT1;5* sequences.

No synteny was found between the location of the wheat *HKT1;5* genes and the location of the rice *OsHKT1;5* genes. *OsHKT1;5* is located on chromosome 1S of rice (Lin et al., 2004; Ren et al., 2005). This region is syntenous to chromosome 3 in wheat (Sorrells et al., 2003), however, *TmHKT1;5-A* is located on chromosome 5AL and *TaHKT1;5-D* is located on chromosome 4DL.

There may be a second gene in the *Nax2* region having an effect on leaf  $\text{Na}^+$ , but it would have to be closely linked, as every time that the *HKT1;5-A* gene member is lost, leaf  $\text{Na}^+$  increases significantly. This has been demonstrated in the *Nax2* mapping population (Figure 2.4), and when *HKT1;5-A* was transferred into other genetic backgrounds including bread wheat (Rana Munns and Richard James, personal communication, 2006; Munns et al., 2008). In moderately saline field conditions Tamaroi had an average leaf  $\text{Na}^+$  concentration of  $125 \mu\text{mol gDW}^{-1}$  whereas  $\text{BC}_4\text{F}_2$ -derived lines with *HKT1;5-A* had an average leaf  $\text{Na}^+$  concentration of  $25 \mu\text{mol gDW}^{-1}$ , a five fold difference (Ray Hare and Rana Munns, personal communication, 2006). In a completely different field environment with the same lines *HKT1;5* conferred a 2 fold reduction in leaf  $\text{Na}^+$  concentration (Anthony Rathjen and Rana Munns, personal communication, 2006).

Overall, in field and glasshouse experiments, all the lines with the *HKT1;5-A* gene had at least twofold lower leaf  $\text{Na}^+$  than all those without the *HKT1;5-A* gene. When transferred into the bread wheat Westonia, which already contains the  $\text{Na}^+$  exclusion locus *Kna1* on the D genome, *HKT1;5-A* reduced leaf  $\text{Na}^+$  by a further 25% (Munns et al., 2008).

#### 2.4.2 Relationship of *Nax2* to the major salt tolerance gene in hexaploid wheat, *Kna1*

The *HKT1;5-A* genome member, which is the candidate for *Nax2*, is physically located on the distal part of chromosome 5AL, which ancestrally corresponds to the distal part of chromosome 4AL. *Kna1* maps to the distal region of chromosome 4DL of wheat (Dubcovsky et al., 1996) raising the possibility that *Nax2* and *Kna1* are homoeologous genes located on ancestral group 4 chromosomes. The *TaHKT1;5-D* genome member maps to the distal 14% of chromosome 4DL in hexaploid bread wheat (Figure 2.6A) coinciding with the map location of *Kna1* (Dubcovsky et al., 1996). The locus for *Kna1* on chromosome 4DL is homoeologous to the location for *Nax2* on chromosome 5AL and the *TaHKT1;5-D* genome member may be *Kna1*. Further dissection of the region in 5A<sup>m</sup>L containing *Nax2* and the region in 4DL containing *Kna1*, with common markers, is needed to determine whether these two genes are true orthologues.

The loss of the region containing the *TaHKT1;5-D* gene member from Chinese Spring deletion lines corresponded to an increase in average  $\text{Na}^+$  concentrations in the leaf blade and a six fold decrease in the  $\text{K}^+$  to  $\text{Na}^+$  ratio from 7.5 to 1.2 (Figure 2.6B), when plants were grown at 50mM NaCl. These results are consistent with our hypothesis that the *HKT1;5* probe detects not only a candidate gene for *Nax2* in durum wheat, but also a candidate gene for *Kna1* in hexaploid bread wheat and that both genes are located in homoeologous regions of the wheat genome. These results are also consistent with other data on the effect of *Kna1* on leaf  $\text{K}^+$  and  $\text{Na}^+$  concentrations. When the *Kna1* region was transferred from the bread wheat, Chinese Spring, into the durum wheat cultivar, Langdon, lines with *Kna1* had a greater leaf  $\text{K}^+$  to  $\text{Na}^+$  ratio (Dvořák and Gorham, 1992). Lines of Langdon containing the *Kna1* region had a leaf  $\text{K}^+$  to  $\text{Na}^+$  ratio approximately eight times higher than those without *Kna1* when plants were grown at 50 mM, and six times higher when grown at 150 mM NaCl (Gorham et al., 1987; Gorham et al., 1990).

#### 2.4.3 Similarity of phenotype between sodium excluding genes in rice and wheat

There are five phenotypic characteristics in common between *Nax2*, *Kna1* and *SKC1*:  
(i) low  $\text{Na}^+$  concentration in the leaves; (ii) enhanced discrimination of  $\text{K}^+$  over  $\text{Na}^+$  in



transport from the roots to the shoots; (iii) regulation of the  $K^+$  to  $Na^+$  ratio in the leaves; (iv) no effect on root  $Na^+$  concentration; and (v) no effect on the sheath to blade  $Na^+$  ratio (Davenport et al., 2005; Gorham et al., 1990; James et al., 2006a; Ren et al., 2005). *Nax1*, which cosegregates with *Triticum monococcum HKT1;4-A2*, has a distinctive mechanism that differs from *Nax2*, *Kna1* and *SKC1*. The characteristic of *Nax1* is a high sheath to blade  $Na^+$  concentration ratio. *Nax1* confers low leaf blade  $Na^+$  and high leaf blade  $K^+$  to  $Na^+$  ratio by unloading  $Na^+$  in the leaf sheath and displacing  $K^+$  in the leaf blade (James et al., 2006a). In the Tamaroi background,  $BC_5F_2$  lines with *Nax1* (*HKT1;4-A2*) have a four fold lower leaf  $Na^+$  concentration than lines without *Nax1* (Huang et al., 2006).

The mechanism behind the common phenotype for the *Nax2*, *SKC1* and *Kna1* genes may be unloading of  $Na^+$  from the xylem. We know that *Nax2* unloads  $Na^+$  from the xylem as experiments with  $^{22}Na^+$  showed that the rate of unloading of  $Na^+$  from the xylem was double that in lines with *Nax2* than in those without (James et al., 2006a). *SKC1* in rice also unloads  $Na^+$  from the xylem (Ren et al., 2005). Under salt stress the shoots and the xylem sap of near-isogenic lines with *SKC1* contained more  $K^+$  and less  $Na^+$  than those without *SKC1* (Ren et al., 2005). There is also indirect evidence that *Kna1* may unload  $Na^+$  from the xylem. One is the observation that there is no difference in the  $Na^+$  concentration in the roots of lines with and without *Kna1* (Gorham, 1990), and the other is that the membrane potential-dependent uptake of  $Na^+$  was no different in vesicles from hexaploid wheat (cv. Troy), which has *Kna1*, and tetraploid wheat (cv. Langdon), which does not have *Kna1* (Allen et al., 1995). Gorham et al. (1997) suggested that this observation of Allen et al (1995) would be expected if *Kna1* acts specifically on xylem loading.

A single *HKT* gene may be sufficient to explain the *Nax2* or *Kna1* phenotypes. The *Nax1* gene in wheat, and the *SKC1* gene in rice, are both *HKT* genes, and they both have a strong affect on the leaf  $K^+$  to  $Na^+$  ratio, and  $Na^+$  concentration. Wheat lines with *Nax1* (*TmHKT1;4-A2*) have a four times greater leaf  $K^+$  to  $Na^+$  ratio, and four times less leaf  $Na^+$  than lines without *Nax1* (Huang et al., 2006; James et al., 2006a). Transformed rice lines with *SKC1* (*OsHKT1;5*) have a 2.5 times greater leaf  $K^+$  to  $Na^+$  ratio, and two times less leaf  $Na^+$  than transformed lines without *SKC1* (Ren et al., 2005). Wheat lines with *Nax2* have a 3.6 times greater leaf  $K^+$  to  $Na^+$  ratio, and approximately 2.5 times less leaf  $Na^+$ , than lines without *Nax2*. One *HKT1;5-A* gene could account for these differences. Likewise, for *Kna1*, one *HKT1;5-D* gene may account for the six times greater leaf  $K^+$  to  $Na^+$  ratio, and the four times less leaf  $Na^+$  in Chinese Spring compared to the Chinese Spring deletion lines lacking *Kna1*.

#### 2.4.4 Summary

The data presented support the hypothesis that *TmHKT1;5-A* is a candidate for *Nax2*, *TaHKT1;5-D* is a candidate for *Kna1*, and the data suggest that *Nax2* may be a homoeologue of *Kna1*.

## Chapter 3: Diversity of two genes for sodium exclusion in diploid A genome wheat ancestors

### 3.1 Introduction

*Nax1* (*TmHKT1;4-A2*) and *Nax2* (*TmHKT1;5-A*) are two genes that retrieve  $\text{Na}^+$  from the xylem as it flows from roots to leaf blades, thereby conferring a phenotype of low leaf  $\text{Na}^+$ , which is a beneficial trait for salinity tolerance (James et al., 2006). *Nax1* and *Nax2* were identified in durum wheat, Line 149 (*Triticum turgidum* subsp. *durum* [Desf.]), and are absent in modern durum and bread wheat (Huang et al., 2006; Byrt et al., 2007). Line 149 is the result of crosses made between *Triticum monococcum* (C68-101) and the durum variety Marrocos (The, 1973), in the process of transferring a rust resistance gene, *Sr21*, into bread wheat. *T. monococcum* (C68-101) was found to contain both *Nax1* and *Nax2* (Huang et al., 2006; Byrt et al., 2007). As *Nax1* and *Sr21* are both located on chromosome 2AL, the presence of *Nax1* can be thus explained. However, it is difficult to explain the co-presence of *Nax2*, as *Nax2* is located on chromosome 5AL. The absence of the sodium exclusion genes in modern wheat is interesting in relation to the evolution of polyploidy wheat. This prompted investigation of the origin and diversity of *Nax1* and *Nax2* in diploid wheat.

#### 3.1.1 Allelic variation in *HKT1;5* genes

In rice and *Arabidopsis*, allelic variation in *HKT* genes (*OsHKT1;5* and *AtHKT1;1*) may confer significant differences in leaf  $\text{Na}^+$  accumulation (Ren et al., 2005, Rus et al., 2006). In rice, six nucleotide substitutions in the coding region of *OsHKT1;5* differ between the tolerant allele, from Nona Bokra, and the sensitive allele, from Koshihikari, leading to four amino acid residues differing (Ren et al., 2005). Under salt stress Koshihikari had almost double the leaf  $\text{Na}^+$  concentration of near isogenic lines with the Nona Bokra *SKC1* (*OsHKT1;5*) allele. Changes in the coding region, rather than differences in the promoter, are likely to account for the functional variation in the two alleles (Ren et al., 2005). The data that support this include a genetic complementation test, where the Nona Bokra promoter and open reading frame was transferred into a sensitive line and recovered the *SKC1* phenotype, and an observation that there was little difference in the expression patterns for the different *OsHKT1;5* alleles (Ren et al., 2005).

In *Arabidopsis*, allelic variation in the promoter of *AtHKT1;1*, rather than the coding region, may account for functional differences between *AtHKT1;1* from Columbia-0 and two natural variants, Tsu-1 and Ts-1 (Rus et al., 2006). The *AtHKT1;1* alleles from Tsu-1 and Ts-

1 are associated with differences in leaf  $\text{Na}^+$ . Sequence differences included 19 single nucleotide polymorphisms in the coding region leading to seven different amino acid residues which may be responsible for the differences in leaf  $\text{Na}^+$  (Rus et al., 2006). A deletion in a tandem repeat sequence in the promoter may also be responsible for the difference in leaf  $\text{Na}^+$  as there was reduced expression of *AtHKT1;1* in the roots (Rus et al., 2006). Curiously, the Tsu-1 allele, linked to higher leaf  $\text{Na}^+$ , was also linked to salt tolerance. Salt tolerance was determined by calculating the percentage of plants that were found to be dead three to seven weeks after the one-month-old plants in pots were watered with 100 mM NaCl (Ren et al., 2006). The loss of function mutant, *Athkt1;1*, accumulated more  $\text{Na}^+$  in the leaves than wild type (Columbia-0) and was more NaCl sensitive (Rus et al., 2004). However, as Rus et al. (2006) note, a second gene that influences NaCl tolerance may be segregating with *AtHKT1;1* in the Tsu-1 population.

In modern wheat the A-genome *HKT1;5* gene appears to be absent. In isogenic BC<sub>5</sub>F<sub>2;3</sub> lines from a cross between Line 149 and the durum cultivar Tamaroi, the difference in leaf  $\text{Na}^+$  between lines with and without *Nax2* was determined by the presence or absence of the *HKT1;5-A* gene (Figure 2.4). There was a single *HKT1;5* gene member on the A genome of families containing *Nax2* that was absent in those without *Nax2*. This gene member was found in *T. monococcum* (C68-101; Figure 2.4), and had apparently been introgressed into Line 149 by crossing *T. monococcum* with the durum cultivar Marrocos (The, 1973). There was no homologue of *HKT1;5* on the A genome of Marrocos or Tamaroi, or in the durum cultivar Langdon, or the bread wheat Chinese Spring (Figure 2.5A). Recent work has shown that *HKT1;5-A* was absent in all the modern wheat varieties tested, including six Australian durum varieties, as well as Langdon, and 19 Australian bread wheat varieties, as well as Chinese Spring (Richard James, personal communication, 2008). This indicates that it is very likely that the *HKT1;5* gene was not present in the A genome diploid ancestor that gave rise to modern wheat. In contrast, the *HKT1;5-D* allele isolated from Chinese Spring has the same open reading frame as the *HKT1;5-D* gene members isolated from three *Triticum tauschii* accessions (Evans Lagudah, personal communication, 2006).

### 3.1.2 Aims

The objective of this work was to conduct an extensive screen of diverse genetic material to look for allelic variation for the candidate gene for *Nax2*, *TmHKT1;5-A*, in the diploid wheat ancestors *T. urartu*, *T. monococcum* ssp. *boeoticum* and *T. monococcum* ssp. *monococcum*. As this material was likely to also have *Nax1*, *TmHKT1;4-A2* (Huang et al., 2006), it was necessary for the interpretation of the phenotype, to screen for *Nax1* as well.

A total of 196 diploid wheat genotypes of diverse origin were screened for leaf Na<sup>+</sup> exclusion and screened with markers for the *Nax2* gene, as well as testing of the expression of the *Nax2* gene. This work was conducted in collaboration with visiting student, Mehraj Abbasov of the Azerbaijan National Academy of Sciences Genetic Resources Institute and Dr Yuri Shavrukov of the Australian Centre for Plant Functional Genomics. The purpose of the screen was to test how widespread the occurrence of *Nax2* was in A-genome wheat species, and whether the absence of *Nax2* in polyploidy wheat could be explained by its absence in *T. urartu*, thought to give rise to modern wheat. The other purpose of the screen was to identify wheat genotypes with the following attributes:

1. Low leaf Na<sup>+</sup> and neither *Nax1* or *Nax2*, indicating the presence of additional genes for Na<sup>+</sup> exclusion
2. Material with *Nax1* or *Nax2* and significantly lower leaf Na<sup>+</sup> exclusion than the control (*T. monococcum* C68-101), indicating possible allelic variation in *Nax1* or *Nax2* conferring greater leaf Na<sup>+</sup> exclusion

## 3.2 Materials and Methods

### 3.2.1 Plant material

Diploid wheat seed from the Middle East and Central Asia was provided courtesy of Dr Kenneth Street (ICARDA, Aleppo, Syrian Arab Republic). The seed included 31 *T. monococcum* ssp. *monococcum* accessions, 78 *T. monococcum* ssp. *boeoticum* accessions, and 87 *T. urartu* accessions (Appendix Table 3.1). Information about the locations from which the seed was collected was also provided, the locations included Albania, Armenia, Bulgaria, Georgia, Greece, Iran, Iraq, Italy, Jordan, Lebanon, Marrakesh, Romania, Serbia, Syria, Turkey and Ukraine.

### 3.2.2 Phenotyping method

Screening for the accumulation of Na<sup>+</sup> in the leaves under saline conditions (150 mM NaCl) was undertaken by Mehraj Abbasov using a method similar to the method described in section 2.2.2 with the following exceptions; a flame photometer was used to measure Na<sup>+</sup> concentrations, rather than ICP, as described by Shavrukov et al. (2006), and the supported hydroponic system was as described by Shavrukov et al. (2006).

### 3.2.3 Marker development, PCR and RT-PCR

The genomic sequence of *TmHKT1;5-A* was aligned with the *TaHKT1;5-D* genomic sequence to identify single nucleotide polymorphisms and other polymorphism that may be useful in the design for markers specific to *Nax2*. A primer was designed on an additional three nucleotides present in the A gene member and absent in the D gene member. The additional base pairs 'TGA' are 1938 bp into the A gene genomic sequence. Where there is 'CCC' encoding a proline in the D sequence, there is 'CCTGAC' encoding a proline and an additional Aspartic acid residue in the A sequence. The primers for the *Nax2* marker, ForA1 (5'-GAGTGGGGCTCCGACGGGCTGAA-3') and RevA1 (5'-CGTCAGGCGTCACCTGCCGGCCG-3'), also used in RT-PCR as described in section 2.2.7, are diagnostic of the presence of *TmHKT1;5-A* in all breeding material tested (Dan Mullan, durum wheat breeder, personal communication, January 2008).

An additional marker for *Nax2* was developed and tested. The primers for this additional marker are called 5Start (5'-TAGAAATGGGTTCTTTGCATGTC-'3) and 3Stop (5'GCATGGAGGATAATATAACCTAG'3). These primers amplify the entire genomic sequence of *TmHKT1;5-A* (2054 bp). In tetraploid or hexaploid backgrounds these primers also amplify the B and D genome *HKT1;5* gene members as they are homologous to the D genome sequence and very similar to the B genome sequences (Appendix Table 3.2); however, this was not a problem in the diploid A genome material as the B and D genomes are not present.

DNA extraction, RNA extraction, and Reverse Transcriptase-PCR methods were as described in Chapter 2. The ForA1, RevA1 and 5Start, 3Stop primers were used for PCR under standard conditions to screen for *Nax2* in DNA from the diploid accessions. These same primers were also used in RT-PCR to assay the expression of *Nax2*. The RT-PCR conditions are described in the methods of Chapter 2, section 2.2.7.

The marker used to screen for *Nax1*, *gwm312* was identified by Lindsay et al. (2004). The *gwm312* marker was used to screen for *Nax1* because a gene-specific marker for *Nax1*

was not available due to the high sequence similarity between *TmHKT1;4-A1* and *TmHKT1;4-A2* (Huang et al., 2006). RT-PCR conditions and primers for analysis of expression of *Nax1* are described by Huang et al. (2006). The glyceraldehyde-3-phosphate dehydrogenase (GAP) gene (Burton et al., 2004) was used as a control in RT-PCR.

#### 3.2.4 PCR fragment analysis

Primers for *gwm312* (Lindsay et al., 2004; Huang et al., 2006) were developed with M13 tags by Dr Shaobai Huang according to the method described by Rampling et al. (2001), and PCR was otherwise standard. Fragment analysis was undertaken by Mehraj Abbasov and John To on an Applied Biosystems 3130XL Genetic Analyzer and analyzed using GeneMapper® Software v4.0 as per manufacturers' instructions.

The *gwm312* marker used to screen for *Nax1* is a microsatellite marker that is distal to *Nax1* and located within approximately 1.2 cM of *Nax1* (Lindsay et al., 2004; Huang et al., 2006). In the population used to map *Nax1* the product size of the *gwm312* marker was 199 bp in Accession 149 and 236 bp in Tamaroi (Shaobai Huang, personal communication, December 2006).

### 3.3 Results

#### 3.3.1 Presence of *Nax2* in diploid species

*Nax2* was present in almost all *T. monococcum* ssp. *monococcum* accessions, and most ssp. *boeoticum* accessions, but was absent in all *T. urartu* accessions (Table 3.1). Assessment of the presence or absence of *Nax2* was based on the consensus of two *Nax2* gene specific markers. One of the two gene specific markers amplifies the whole open reading frame (ORF = 2054 bp; primers 5Start and 3Stop), the other marker (primers ForA1 and RevA1) amplifies a 945 bp fragment spanning the first intron. Both of these markers were deemed to be diagnostic for *Nax2* in diploid A-genome accessions, as hybridization to the B-genome *HKT1;5* genes would not be a problem. Only the latter marker was diagnostic for *Nax2* in diploid, tetraploid and hexaploid material as it was designed on a section of sequence unique to *TmHKT1;5-A* so that it would not amplify from the *HKT1;5* genes on the B-genome (see section 3.2.3).

Interestingly the two markers did not always agree on the presence or absence of *Nax2*. An example is presented in Figure 3.1 (lane 8) where the ForA1 and RevA1 primer product (Figure 3.1 A) was consistent with the presence of *Nax2* yet there was no product for the 5Start and 3Stop primers (Figure 3.1 B). These results were repeated in a second experiment. The *T. boeoticum* accession in question (ID. 44906) had low leaf  $\text{Na}^+$  ( $35.6 \mu\text{mol g}^{-1}$  DW). It is possible that the 5Start and 3Stop primers did not amplify due to sequence variation at one or both of the priming sites.

The *T. boeoticum* accession (ID. 44866) with both *Nax1* and *Nax2*, and the highest leaf  $\text{Na}^+$  of the *T. boeoticum* accessions containing both *Nax1* and *Nax2* ( $75.7 \mu\text{mol g}^{-1}$  DW), also had conflicting results for the two primer sets for *Nax2*. Again, the ForA1 and RevA1 primers indicated the presence of *Nax2* yet there was no product for the 5Start and 3Stop primers. There may be sequence variation at one or both of the priming sites.



**Table 3.1: Average leaf Na<sup>+</sup> concentrations in selected *Triticum* spp.**

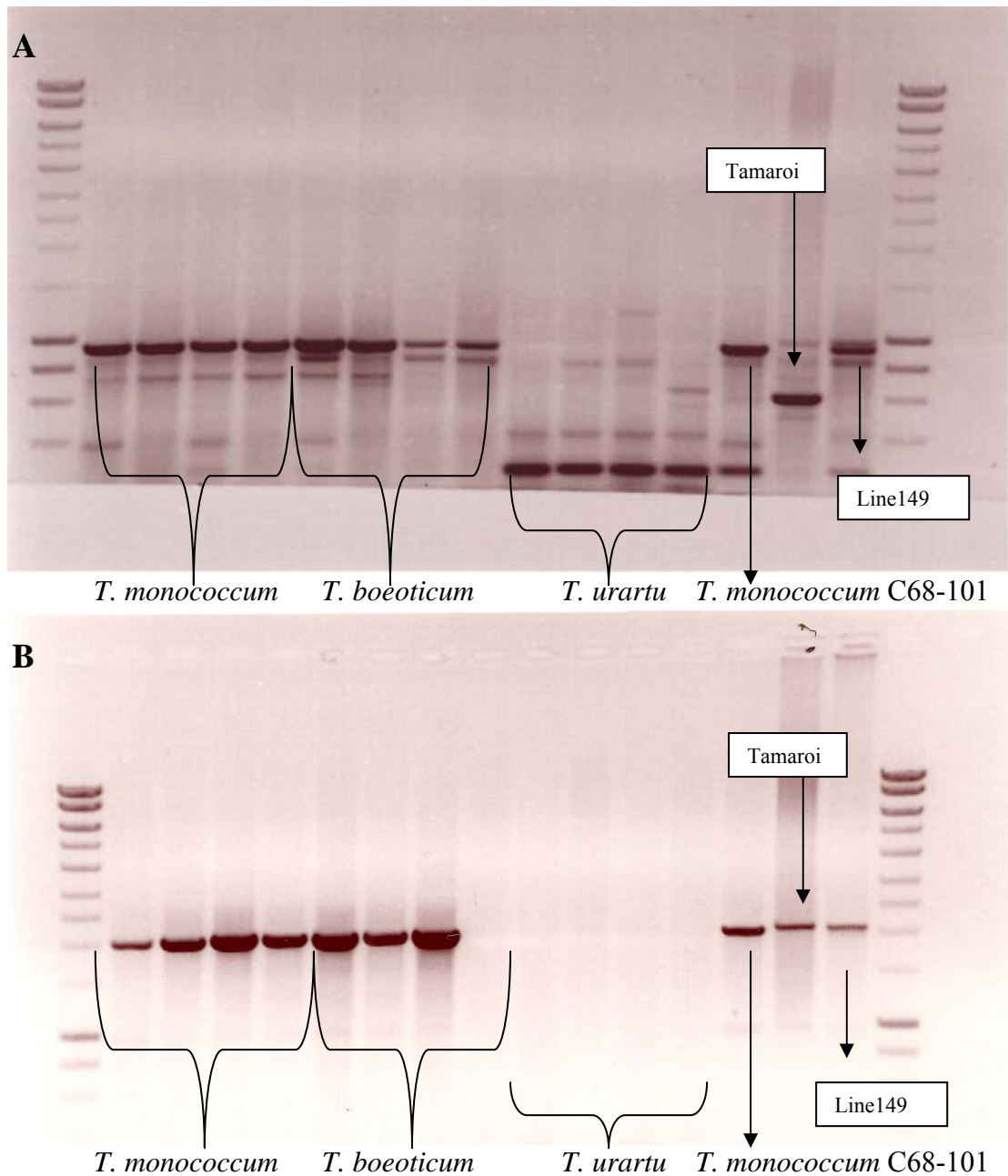
Leaf Na<sup>+</sup> concentrations of control germplasm (A). Leaf Na<sup>+</sup> concentrations in *T. monococcum* ssp. *monococcum*, *T. monococcum* ssp. *boeoticum*, and *T. urartu*, separated by presence or absence of *Nax1* (note that  $\pm Nax1$  indicates presence or absence of the *gwm312* marker) and *Nax2* (B). Plants were grown in hydroponics, leaf three was harvested and the sodium concentration measured, after growing for 10 days in a solution with 150 mM NaCl. n = 6. The average and standard error is of the mean of all accessions in each category. Accessions with inconsistent results for the genotyping were not included.

**A.**

Control germplasm	Av. leaf Na <sup>+</sup> ( $\mu\text{mol g}^{-1}$ DW)
Tamaroi	154 $\pm$ 3
Line 149	40 $\pm$ 16
<i>T. monococcum</i> (C68-101)	31 $\pm$ 16

**B.**

<i>T. monococcum</i> ssp. <i>monococcum</i>	No. accessions (28)	Av. leaf Na <sup>+</sup> ( $\mu\text{mol g}^{-1}$ DW) 56 $\pm$ 7 (range 16 – 175)
+ <i>Nax2</i> , + <i>Nax1</i>	24	53 $\pm$ 5
+ <i>Nax2</i> , - <i>Nax1</i>	3	19 $\pm$ 5
- <i>Nax2</i> , - <i>Nax1</i>	1	175 $\pm$ 22
<i>T. monococcum</i> ssp. <i>boeoticum</i>	No. accessions (69)	Av. leaf Na <sup>+</sup> ( $\mu\text{mol g}^{-1}$ DW) 44 $\pm$ 4 (range 8 – 182)
+ <i>Nax2</i> , + <i>Nax1</i>	15	35 $\pm$ 6
+ <i>Nax2</i> , - <i>Nax1</i>	44	42 $\pm$ 4
- <i>Nax2</i> , + <i>Nax1</i>	1	72 $\pm$ 22
- <i>Nax2</i> , - <i>Nax1</i>	7	70 $\pm$ 21 (15-182)
<i>T. urartu</i>	No. accessions (87)	Av. leaf Na <sup>+</sup> ( $\mu\text{mol g}^{-1}$ DW) 66 $\pm$ 4 (range 15 – 251)
- <i>Nax2</i> , + <i>Nax1</i>	2	94 $\pm$ 37
- <i>Nax2</i> , - <i>Nax1</i>	85	66 $\pm$ 4 (15-251)



**Figure 3.1: Screening diploid accessions for *Nax2* with gene specific primers**

A. Agarose gel electrophoresis of products of PCR with primers ForA1 and RevA1. Expected product size for *Nax2* is 945 bp. These primers are specific to the A gene *HKT1;5* hence there is no product from Tamaroi. B. Agarose gel electrophoresis of products of PCR with primers 5Start and 3Stop. Expected product size is 2054 bp. These primers will amplify the A and B gene members of *HKT1;5*, hence there is a product from Tamaroi which lacks an A genome *HKT1;5*, but contains three B genome *HKT1;5* genes. The ladder is 1Kb<sup>+</sup>.

### 3.3.2 Leaf Na<sup>+</sup> concentrations in the diploid accessions

The leaf Na<sup>+</sup> concentrations of the control germplasm included in the screen of the diploid accessions was as expected from previous studies (Chapter 2 and James et al., 2006a). Tamaroi had a leaf Na<sup>+</sup> concentration approximately four times that of Line 149, and *T. monococcum* (C68-101) had a leaf Na<sup>+</sup> concentration similar to Line 149 (Table 3.1 A).

The average leaf Na<sup>+</sup> of all of the *T. monococcum* ssp. *monococcum* accessions was 56 ± 7 µmol g<sup>-1</sup> DW, the average leaf Na<sup>+</sup> of all of the *T. monococcum* ssp. *boeoticum* accessions was 44 ± 4 µmol g<sup>-1</sup> DW, and the average leaf Na<sup>+</sup> of the *T. urartu* accessions was 66 ± 4 µmol g<sup>-1</sup> DW.

Of the 31 ssp. *monococcum* accessions, 24 accessions had both *Nax1* and *Nax2*. The average leaf Na<sup>+</sup> concentration of these accessions was 53 ± 5 µmol g<sup>-1</sup> DW. Only a single accession lacked *Nax2*, this accession also lacked *Nax1*, and it had a high leaf Na<sup>+</sup> concentration, 175 ± 22 µmol g<sup>-1</sup> DW. Three ssp. *monococcum* accessions lacked *Nax1*, according to the data for the *gwm312* marker, and these accessions had low leaf Na<sup>+</sup>, with an average leaf Na<sup>+</sup> concentration of 19 ± 5 µmol g<sup>-1</sup> DW. This indicates that *Nax2* can confer a phenotype of low leaf Na<sup>+</sup> on its own.

For the ssp. *boeoticum* accessions, 15 of 78 accessions were confirmed as having both *Nax1* and *Nax2*. The leaf Na<sup>+</sup> of those accessions, with both *Nax1* and *Nax2*, ranged between 8 and 76 µmol g<sup>-1</sup> DW and the average was 35 ± 6 µmol g<sup>-1</sup> DW. The number of accessions with *Nax2* and not *Nax1* was 44. These accessions had an average leaf Na<sup>+</sup> of 42 ± 4 µmol g<sup>-1</sup> DW, and a range of 10 to 148 µmol g<sup>-1</sup> DW. One accession had only *Nax1*; the leaf Na<sup>+</sup> concentration of this accession was 72 ± 22 µmol g<sup>-1</sup> DW. Seven *T. boeoticums* were confirmed as having neither *Nax1* nor *Nax2*, the average leaf Na<sup>+</sup> of these accessions was 70 ± 21 µmol g<sup>-1</sup> DW, ranging from 15 to 182 µmol g<sup>-1</sup> DW.

No *T. urartu* accessions had *Nax2*, and only two accessions had *Nax1*. The leaf Na<sup>+</sup> concentrations of the accessions with *Nax1* were 57 ± 17 and 131 ± 35 µmol g<sup>-1</sup> DW. The average leaf Na<sup>+</sup> concentration of the other *T. urartu* accessions was 66 ± 4 µmol g<sup>-1</sup> DW.

The diploid wheat with the lowest leaf Na<sup>+</sup> concentration was a *boeoticum* accession from the Kayseri province of Turkey (ID 44821). This accession had a leaf Na<sup>+</sup> concentration of 8 ± 1 µmol g<sup>-1</sup> DW. The accession with the highest leaf Na<sup>+</sup> concentration was a *T. urartu* from Aleppo, Syria (ID 117911). This accession had a leaf Na<sup>+</sup> concentration of 251 ± 123 µmol g<sup>-1</sup> DW, the accession with the second highest leaf Na<sup>+</sup> was also a *T. urartu* accession from the same location (ig 110753), it had a leaf Na<sup>+</sup> concentration of 235 ± 24 µmol g<sup>-1</sup> DW.

The maximum leaf Na<sup>+</sup> concentrations in the ssp. *boeoticum* accessions and ssp. *monococcum* accession were in the order of 180 μmol g<sup>-1</sup> DW.

Seed from three countries were recorded as having been collected from areas with saline soils, these countries were Armenia, Iran and Jordan, and the average leaf Na<sup>+</sup> concentrations of accessions from these countries were 37 ± 5, 44 ± 4, and 57 ± 9 μmol g<sup>-1</sup> DW, respectively. In comparison, the average of all accessions tested was 56 ± 3 μmol g<sup>-1</sup> DW.

Accessions with leaf Na<sup>+</sup> concentrations of less than 20 μmol g<sup>-1</sup> DW were regarded as having very low leaf Na<sup>+</sup>. There were 14 accessions with very low leaf Na<sup>+</sup> concentrations, these accessions were collected from Armenia (2), Albania (1), Greece (1), Iran (1), Jordan (1), Lebanon (2), Ukraine (1) and Turkey (5).

Accessions with leaf Na<sup>+</sup> concentrations greater than 100 μmol g<sup>-1</sup> DW were regarded as having high leaf Na<sup>+</sup> concentrations. There were 18 accessions with high leaf Na<sup>+</sup> concentrations, these accessions were collected from Bulgaria (1), Iran (1), Jordan (1), Serbia (1), Syria (7) and Turkey (7).

### 3.3.3 Linkage with *Nax1* and interpretation

The *gwm312* marker was used to check the presence or absence of *Nax1* alleles in the diploid accessions. A product size of 199 bp for the *gwm312* marker indicates the presence of a *Nax1* allele and a product size of 236 bp indicates the absence of a *Nax1* allele. Of the diploid accessions, 24 *monococcum*, 16 *boeoticum* and two *T. urartu* accessions had product sizes of 199 bp, these accessions were regarded as having *Nax1*. In the diverse diploid accessions variation in the product size for the *gwm312* marker was observed. For example; two *monococcum* accessions and eight *boeoticum* accessions gave product sizes of 197 bp, a *monococcum* accession from Turkey had a product size of 209 bp, a *monococcum* accession from Serbia had a product size of 232 bp, and *boeoticum* accessions from Syria, Lebanon and Greece had product sizes of 226, 224 and 201 bp respectively. Accessions with products sizes differing from 199 bp were considered as lacking *Nax1*.

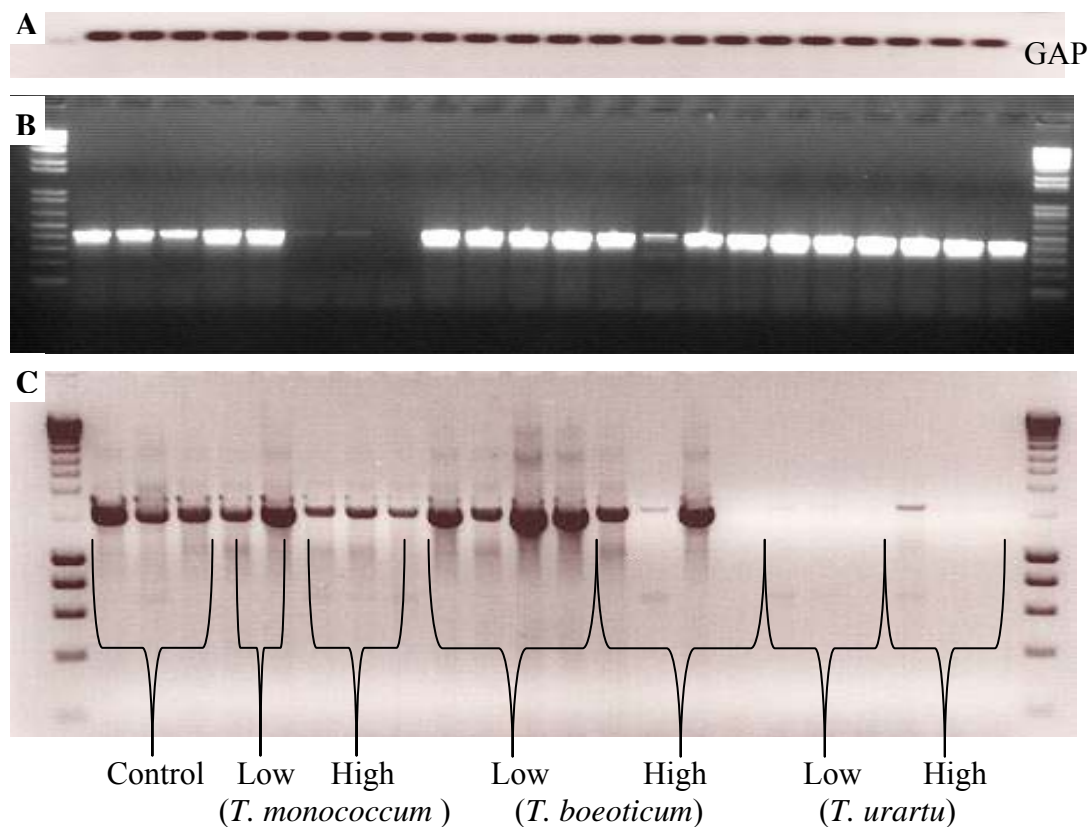
### 3.3.4 Expression of *Nax1* and *Nax2* may correlate with the Na<sup>+</sup> exclusion phenotype

The expression of *Nax2* was lower in the selected *T. monococcum* accessions with high leaf Na<sup>+</sup> compared those accessions selected with lower leaf Na<sup>+</sup> (Figure 3.2). In some *T. boeoticum* accessions which had *Nax2*, as diagnosed by PCR, no expression of *Nax2* was

observed. Faint expression of a putative *HKT1;5*-like gene was observed in one of the *T. urartu* accessions that did not have *Nax2*.

The expression of *Nax1* was almost absent in the *T. monococcum* accessions selected for having high leaf Na<sup>+</sup> compared to those accessions selected with low leaf Na<sup>+</sup> (Figure 3.2). One of the *T. boeoticum* accessions with high leaf Na<sup>+</sup> had low expression of *Nax1* but for the other accessions there was no difference in the expression of *Nax1* between those accessions with low leaf Na<sup>+</sup> and those accessions with high leaf Na<sup>+</sup>.

A fragment was amplified from all *T. urartu* accessions in the screen for expression of *Nax1*, but this cannot be due to *Nax1* as it is not present in these *T. urartu* accessions, hence there must be a *HKT1;4*-like gene with sequence similarity in *T. urartu* and the primers must be amplifying from this gene of similar sequence. A *HKT1;4-A1* gene has been described on the A-genome of bread wheat (Huang et al., 2008). This gene does not confer the *Nax1* (*TmHKT1;4-A2*) phenotype, but has a similar sequence to *TmHKT1;4-A2* (Huang et al., 2008). Therefore, the primers used to assay the expression of *Nax1* may be hybridizing to a *HKT1;4-A1* gene in *T. urartu*. It is likely that the *Nax1* primers are only diagnostic of the expression of *Nax1* in the *T. monococcum* accessions and not the *T. urartu* accessions.



**Figure 3.2: Expression of *Nax1* and *Nax2* in selected diploid accessions**

Selected accessions with ‘Low’ and ‘High’ leaf Na<sup>+</sup> concentration, from each diploid species and subspecies, were tested for the expression of *Nax1* and *Nax2*. The three control lanes represent *T. monococcum* (C68101), Line 149 and a second lane with C68101. The ladder is 1Kb<sup>+</sup>. A. Reverse transcriptase PCR for the glyceraldehyde-3-phosphate dehydrogenase (GAP) gene was used to check the loading for each lane. B. Expression of *Nax1* was assayed using primers designed by Huang et al. (2006). C. Expression of *Nax2* was assayed using the 5Start and 3Stop primers which amplify the entire coding sequence (1554 bp) of *TmHKT1;5-A*.

### 3.4 Discussion

#### 3.4.1 Trends within species and sub-species

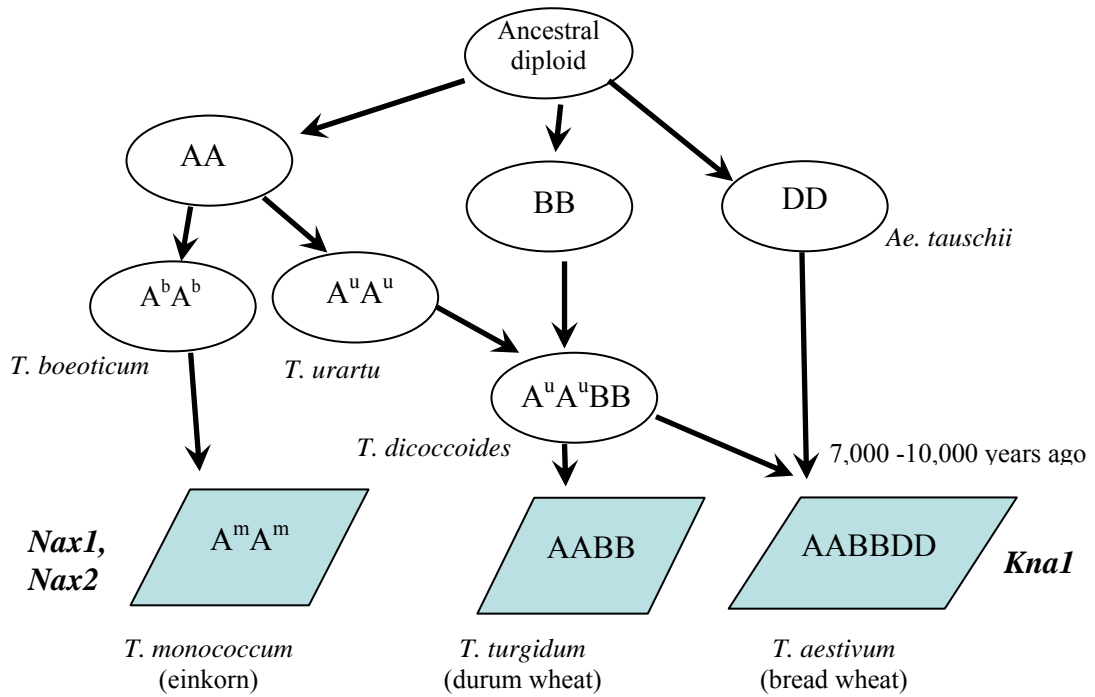
*Nax2* was present in almost all *T. monococcum* ssp. *monococcum*, and most ssp. *boeoticum* accessions but was absent in almost all *T. urartu* accessions. *Nax1* was present in most *T. monococcum* ssp. *monococcum*, but *Nax1* was present in less than half of the *T. monococcum* ssp. *boeoticum* accessions tested and *Nax1* may only be present in two of 87 *T. urartu* accessions. This is consistent with previous studies that suggest that *T. urartu* is the ancestor of the A genome in modern wheat (Dvořák et al., 1993; Dvořák et al., 1998), as both *T. urartu* and modern wheat generally lack *Nax1* and *Nax2* (Figure 3.3).

Accumulation of Na<sup>+</sup> in *T. monococcum* ssp. *monococcum* and ssp. *boeoticum* is generally lower when *Nax1* and *Nax2* are present, although there are several exceptional accessions where this is not the case. Allelic variation may explain some of these differences, alternatively there may be other genes influencing leaf Na<sup>+</sup> in these accessions. It is clear that other genes, not *Nax1* (*TmHKT1;4-A2*) or *Nax2* (*TmHKT1;5-A*), control leaf Na<sup>+</sup> accumulation in *T. urartu*.

#### 3.4.2 Interpreting the results for different PCR markers

Results for the two different gene specific *Nax2* markers, based on different parts of the *TmHKT1;5-A* open reading frame, were contradictory in some for the diploid accessions. This is likely to be due to sequence variation within the A gene *HKT1;5* open reading frame. There may be a relationship between specific allelic variation in *HKT1;5-A* gene members and the leaf Na<sup>+</sup> accumulation in the diploid accessions but to ascertain whether this is the case it is necessary to sequence the open reading frame from a number of the *HKT1;5* alleles from low and high Na<sup>+</sup> accumulating accessions. Future work may involve cloning and sequencing of *HKT1;5* alleles from a selection of accessions with particularly low or particularly high leaf Na<sup>+</sup> concentrations to test this theory.

The *gwm312* marker is used to screen for *Nax1* in breeding accessions (Rana Munns and Richard James, personal communication). It is deemed, at 1.2 cM distance from *Nax1*, to be close enough as to be reliably diagnostic of the presence of *Nax1*. However, it is possible that amongst this diverse diploid material the relationship between *Nax1* and *gwm312* may differ. Unfortunately, a gene specific marker for *Nax1* was not available to test this theory. Future work may involve checking whether the relationship between *Nax1* and *gwm312* holds in this diverse material using Southern Hybridization.



**Figure 3.3: Wheat ancestors and wheat evolution**

Wheat ancestors and wheat evolution in relation to modern wheat and the occurrence of  $\text{Na}^+$  exclusion genes, *Nax1*, *Nax2* and *Kna1*. Adapted from Huang et al. (2008). Bread wheat (*Triticum aestivum* L., AABBDD) originated from hybridization of three diploid species, *T. urartu* (A genome) (Dvořák et al., 1988), an unknown B genome which is closely related to *Ae. speltoides*, and *Ae. tauschii* (D genome).



### 3.4.3 Expression of *Nax1* and *Nax2* correlates with $\text{Na}^+$ exclusion in *T. monococcum*

In *T. monococcum* ssp. *monococcum* there may be a correlation between expression of *Nax1* and *Nax2* and  $\text{Na}^+$  exclusion. This correlation was not observed in *T. monococcum* ssp. *boeoticum* or *T. urartu* accessions (Figure 3.2). In two of the four *T. monococcum* ssp. *boeoticum* accessions selected with high leaf  $\text{Na}^+$  concentration the PCR screen indicated the presence of *Nax2* yet the expression analysis indicated that *Nax2* was not expressed, or not highly expressed.

Neither *Nax1* nor *Nax2* is present in the selected *T. urartu* accessions, yet products were observed for *Nax1* from every accession (Figure 3.2). The candidate gene for *Nax1* is *TmHKT1;4-A2*, and two related genes, *TaHKT1;4-A1* and *TaHKT1;4-A2* have been identified in Chinese Spring (Huang et al., 2006), that do not confer the *Nax1* phenotype, therefore it is likely that a related gene may be present in *T. urartu* which does not confer the *Nax1* phenotype. *Nax1* unloads  $\text{Na}^+$  from the xylem, and partitions  $\text{Na}^+$  into the leaf sheath, and partitioning of  $\text{Na}^+$  into the leaf sheath has not been observed, or at least described, in modern wheat. It is likely that the primers used in RT-PCR are not specific to *Nax1* in the *T. urartu* background.

For one *T. urartu* accession a very faint product was observed for the *Nax2* primers. This product may have amplified from a different gene of similar sequence. The RT-PCR results were otherwise consistent with the PCR results for *Nax2* in the *T. urartu* accessions.

### 3.4.4 New genetic variation for $\text{Na}^+$ exclusion

Allelic variants of the single *Arabidopsis HKT* gene (*AtHKT1;1*) have been found to have differing effects on leaf  $\text{Na}^+$  accumulation (Rus et al., 2006). It is likely that allelic variation for the nine genes in the *HKT* gene family in monocotyledonous plants, such as wheat, can also be exploited to improve the salinity tolerance of crops plants. Novel *HKT* alleles may be identified in wild relatives of wheat, such as those diploid wheat accessions screened in this project, or other diploid species such as *Aegilops* species (Colmer et al., 2006), which may confer greater tolerance to salinity than the alleles already identified. An additional benefit of studying *HKT* genes in cereals is that the research can be directly applied to the improvement of crop plants.

The marker screen indicated that the Turkey *boeoticum* with the lowest leaf  $\text{Na}^+$  had both the *Nax1* and *Nax2* genes. This accession accumulated one quarter of the  $\text{Na}^+$  as the original *Nax1* and *Nax2* donor accession (*T. monococcum* C68101). It is possible that the *Nax1* and *Nax2* alleles in this low  $\text{Na}^+$  accumulating *boeoticum* differ from those of *T.*

*monococcum* (C68101). Cloning and sequencing of *Nax1* and *Nax2* from this *boeoticum* accession is needed to test this hypothesis. Alternatively there may be other genes in this *boeoticum* accession contributing to the very low leaf Na<sup>+</sup> accumulation.

In each of the species, and subspecies, accessions were identified with significantly lower leaf Na<sup>+</sup> than the original 'C68101' *monococcum* accession. This indicates that there may be useful genetic variation for Na<sup>+</sup> exclusion in each species and subspecies. The material screened may provide new traits for improving the salinity tolerance of wheat and new or variant *HKT* alleles.

#### 3.4.5 *Eco-geographic distribution of diploid accessions and Na<sup>+</sup> accumulation*

Dr Kenneth Street (ICARDA, Aleppo, Syrian Arab Republic) collected the seed. Dr Street suggested that seed collected from Armenia, Iran and Jordan, may have come from saline sites. Unfortunately more detailed information about the salinity at the sites of collection was not available. There was much variation in the leaf Na<sup>+</sup> concentration of the accessions from these countries indicating that they could not be generalised as having particularly low or particularly high leaf Na<sup>+</sup> concentrations. There was no obvious trend between accessions with particularly low or particularly high leaf Na<sup>+</sup> and the origins of those accessions. Salinity is likely to vary greatly within small regional areas; therefore significantly more detailed information about the salinity at sites of collection is needed to test whether *Nax1* and *Nax2* are better represented or better conserved in accessions from saline as compared to non-saline areas.

## Chapter 4: Transport properties of wheat HKT1;5 and related genes in *Xenopus laevis* oocytes

### 4.1 Introduction

#### 4.1.1 Heterologous expression in *Xenopus laevis* oocytes and electrophysiology

The egg, or oocyte, from the South African clawed frog, *Xenopus laevis*, is commonly used as a functional expression system for plant membrane proteins (Theodoulou and Miller, 1995). *In vitro* transcribed and capped RNA encoding the protein is microinjected into the cytoplasm of the oocyte and over the following days the activity of the encoded protein is measured. The effect of the plant membrane protein on the electrical properties of the oocyte is measured by placing a voltage electrode and a current electrode, hollow glass pipettes approximately 1  $\mu\text{m}$  in diameter filled with electrolyte, into the membrane of the oocyte (oocyte diameter approximately 1 mm). The electrodes are connected to an amplifier, and a data acquisition system, creating an electrical circuit and allowing the direct observation and recording of the electrical activity of the cell.

To study the current-voltage relationships of membrane proteins, current is injected to the oocyte to maintain a particular voltage. The amplifier measures the membrane potential and feeds a signal into a feedback amplifier which determines how much current is injected to keep the voltage clamped at a particular command potential. The feedback circuit passes current into the cell to produce a current equal and opposite to the ionic current. The ionic current crossing the cell's membrane is thus measured at the given voltage.

As the oocyte, electrodes and amplifier form an electrical circuit Ohm's Law can be applied (Eqn 1):

$$I = V/R \quad (1)$$

where  $I$  is the current (amperes),  $V$  is the potential difference (volts), and  $R$  is the resistance (ohms).

The membrane of the oocyte expressing the protein of interest behaves as a resistor. Injection of current through the membrane, or resistor, moves the membrane to a particular voltage. The slope of the relationship between current and voltage is a measure of the conductance ( $G = 1/R$ ) of a particular ion through the protein of interest.

The intercept of the current-voltage relationship, where the current changes from positive to negative, is the reversal potential. The reversal potential can be used to calculate the electrical potential of the cell membrane with respect to one type of ion using the Nernst Equation (Eqn 2):

$$E_{\text{rev}} = (RT/zF) \ln(C_o/C_i) \quad (2)$$

where  $E_{\text{rev}}$  is the reversal potential,  $R$  is the gas constant ( $8.31 \text{ J}\cdot\text{K}^{-1}$ ),  $T$  is the absolute temperature (Kelvin),  $z$  is the ion charge,  $F$  is the Faraday constant ( $9.65 \times 10^4 \text{ Coulombs mol}^{-1}$ ),  $C_i$  is the internal activity of the ion and  $C_o$  is the external activity of the ion. Therefore, at  $25^\circ\text{C}$   $RT/zF = 58 \text{ mV}/z$ .

The electrical potential across the cell membrane that exactly opposes the net movement of a particular ion through the membrane is called the Nernst potential for that ion. The magnitude of the Nernst potential is determined by the ratio of the concentrations of that specific ion on the two sides of the membrane. The greater the ratio, the greater the tendency for the ion to move in one direction, and therefore the greater the Nernst potential required to prevent the movement.

The ratio of permeability of a protein to different ions is calculated using the Goldman-Hodgkin-Katz equation (Eqn 3). Each ion makes a contribution to the membrane potential that depends upon both its concentration and permeability.

$$E_{\text{rev}} = (RT/zF) \ln((P_K K_o + P_{Na} Na_o)/(P_K K_i + P_{Na} Na_i)) \quad (3)$$

written for  $\text{Na}^+$  and  $\text{K}^+$  where  $P_K$  is the permeability of potassium and  $P_{Na}$  is the permeability of sodium.

#### 4.1.2 The function of HKT-type transporters in *Xenopus laevis* oocytes

The relationship between the function of HKT transporters in *Xenopus* oocytes and their function *in planta* is not clear. HKT transporters were originally thought to be  $\text{K}^+$ - $\text{H}^+$  symporters (Schachtman and Schroeder, 1994). It was then suggested that they co-transported  $\text{Na}^+$  and  $\text{K}^+$  (Rubio et al., 1995), but later that they functioned as high-affinity  $\text{Na}^+$  transporters (Rodriguez-Navarro and Rubio, 2006). The confusion has been exacerbated by observations that the same cDNA inserted into different constructs resulted in alternative initiations of translation, and gave different proteins with different kinetic functions when expressed in *Xenopus* oocytes (Haro et al., 2005).

The confusion is partially clarified by dividing HKT-type transporters into two groups based on introns size and on a glycine/serine substitution (See Chapter 1, section 1.2.5; Platten et al., 2006). Group 2 transporters may function as  $\text{Na}^+/\text{K}^+$  symporters when expressed in *Xenopus laevis* oocytes, as for TaHKT2;1 (Rubio et al., 1995), or as  $\text{Na}^+$  specific transporters, as for OsHKT2;1, which may be involved in nutritional  $\text{Na}^+$  uptake in  $\text{K}^+$  starved conditions in rice (Horie et al., 2007). Group 1 transporters, such as AtHKT1;1 and OsHKT1;5 function as  $\text{Na}^+$ -selective transporters when expressed in *Xenopus* oocytes, and *in*

*planta* these transporters are likely to control shoot  $\text{Na}^+$  and  $\text{K}^+$  by withdrawing  $\text{Na}^+$  from the xylem into xylem parenchyma (Uozumi et al., 2000; Ren et al., 2005; Davenport et al., 2007).

#### 4.1.3 Heterologous expression of *HKT1;5* in *Xenopus laevis* oocytes

The candidate gene for *Nax2* is *TmHKT1;5-A*, and the candidate gene for *Kna1* is *TaHKT1;5-D* (Byrt et al., 2007). These genes share 94% identity and are 66% identical to the rice  $\text{Na}^+$  transporter *OsHKT1;5*, which is the candidate for *SKC1* (Ren et al., 2005).

*Nax2*, *Kna1* and *SKC1* each confer a phenotype of  $\text{K}^+$  to  $\text{Na}^+$  discrimination from root to shoot, leading to higher leaf  $\text{K}^+$  concentration and lower leaf  $\text{Na}^+$  concentration (See Chapter 2 section 2.3.2). *Nax2* was shown to be involved in retrieval of  $\text{Na}^+$  from the xylem in a compartmental loading experiment where upper and lower roots were separated; the lower roots fed  $^{22}\text{Na}^+$ , and the labeling in the upper roots measured (James et al., 2006a). This experiment compared homozygous  $\text{BC}_5\text{F}_3$  lines with and without *Nax2* and demonstrated that *Nax2* was involved in withdrawing  $^{22}\text{Na}^+$  into the upper parts of the root leading to a 4-fold higher  $^{22}\text{Na}^+$  content in the leaves of the lines without *Nax2* compared to the lines with *Nax2* (James et al., 2006a). Chromosome deletion lines with *Kna1* had 6 times greater leaf  $\text{K}^+$  to  $\text{Na}^+$  ratio and four times less leaf  $\text{Na}^+$  than the deletion lines lacking the fragment containing *Kna1* (Byrt et al., 2007), indicating that *Kna1* may also retrieve  $\text{Na}^+$  from the xylem. This is consistent with Gorham et al.'s (1990) finding that lines with and without *Kna1* had the same concentration of  $\text{Na}^+$  in the roots, but lower  $\text{Na}^+$  in the leaves of lines with *Kna1*, and concluding that *Kna1* influenced net loading of  $\text{Na}^+$  into the xylem.

Transgenic rice lines with *SKC1* (*OsHKT1;5*) had a 2.5 times greater leaf  $\text{K}^+$  to  $\text{Na}^+$  ratio, and 2-times less sodium than transformed lines without *SKC1* (Ren et al., 2005). It is therefore reasonable to suggest that *OsHKT1;5* is a  $\text{Na}^+$  transporter involved in retrieval of  $\text{Na}^+$  from the xylem in rice, and that the homologous genes in wheat, *TaHKT1;5-D* and *TmHKT1;5-A*, which confer phenotypes very similar to that of *OsHKT1;5*, may also encode  $\text{Na}^+$  transporters involved in retrieval of  $\text{Na}^+$  from the xylem.

#### 4.1.4 Aims for this study

In this study, a *Xenopus laevis* oocyte expression system was used to test whether *TmHKT1;5-A* and *TaHKT1;5-D* are  $\text{Na}^+$  transporters. We compared the activity of the wheat *HKT1;5* transporters with the activity of *AtHKT1;1*, *OsHKT1;5* as *OsHKT2;1*, as these transporters have been studied previously (Uozumi et al., 2000; Horie et al., 2001; Ren et al., 2005). Data is collected with the aim of addressing the following questions:

1. Do the wheat HKT1;5 transporters conduct Na<sup>+</sup>?
2. Are the wheat HKT1;5 transporters permeable to other ions?
3. Are the transport properties of the wheat HKT1;5 transporters affected by pH, external calcium, or channel blockers?
4. How do the transport properties of the wheat HKT1;5 transporters compare to other known HKT-type transporters including OsHKT1;5, OsHKT2;2 and AtHKT1;1?

## 4.2 Materials and Methods

### 4.2.1 Building constructs for expression in *Xenopus laevis* oocytes

For construction of the oocyte expression plasmids the *TmHKT1;5-A* (1554 bp) and *TaHKT1;5-D* (1551 bp) cDNAs were cloned into the Gateway® entry vector pCR®8/GW/TOPO® using the Invitrogen TOPO TA Cloning Kit as per the manufacturers instructions. Plasmid DNA was sequenced to check the orientation of the cDNA. Dr Darren Plett (ACPFPG) kindly provided a pCR®8/GW/TOPO® vector containing the cDNA for *Arabidopsis thaliana* *Lansberg erecta*. *AtHKT1;1* (1521 bp), and Dr Olivier Cotsaftis (ACPFPG) kindly provided pCR®8/GW/TOPO® vectors containing the Pokkali *OsHKT1;5* (1668 bp) cDNA, the Nipponbare *OsHKT1;5* (1662 bp) cDNA and the Pokkali *OsHKT2;2* (1593 bp) cDNA. Each respective cDNA was transferred to a Gateway® enabled pGEMHE vector (Supplied by the Membrane Transporter Expression Facility (MTEF) at the University of Adelaide) via an LR recombination reaction as per the manufacturers' instructions. Purified plasmid DNA of pGEMHE containing each of the respective sequences was then sequenced to ensure presence and correct orientation of the cDNA inserts.

### 4.2.2 Transcription of RNA

Plasmid DNA of pGEMHE with each of the cDNAs of interest was linearised with the following enzymes; the *AtHKT1;1* plasmid was linearised with *SphI* (in NEB buffer 2), both the Pokkali and Nipponbare *OsHKT1;5* plasmids, the *OsHKT2;2* plasmid, and the *TaHKT1;5* and *TmHKT1;5* plasmids were linearised with *XbaI* (Surecut Buffer H), approximately 2 µg of DNA was digested for each plasmid, at 37°C for 12 h. Restriction enzymes and their respective recommended buffers were from New England BioLabs, reaction conditions as recommended by the manufacturer ([www.neb.com](http://www.neb.com)). Restriction enzymes were chosen that did not cut within the coding sequence of each respective gene of interest but did cut once in the pGEMHE plasmid, as close to the terminator of the cDNA sequence as possible. This was

to try and prevent the transcription of large molecules from the linearised plasmid. Linearised reactions were terminated and cleaned up as per the instructions in the mMACHINE mMACHINE® High Yield Capped RNA Transcription Kit Instruction Manual (Ambion Inc., Austin, Tex. USA). Linearised plasmid DNA was checked on a gel.

RNA was transcribed with T7 RNA polymerase from 1 µg of the linearised pGEMHE plasmid DNA using the mMACHINE mMACHINE Capped Transcription Reaction Assembly protocol (Ambion Inc., Austin, Tex. USA), with a 2 hr incubation step to achieve maximum yield. DNase treatment was as recommended in the protocol. The phenol:chloroform extraction and isopropanol precipitation method for recovery of the RNA was as described in the manual. cRNA quality (amount and presence of full-length transcript) was checked by loading a denatured cDNA sample on an agarose gel and the concentration checked on a NanoDrop spectrophotometer 1000 (Thermo Scientific). cRNA was diluted to 1 µg/µL with sterile autoclaved Milli-Q (Millipore) purified H<sub>2</sub>O and stored at -80°C.

#### 4.2.3 *Injection of cRNA into Xenopus laevis oocytes and electrophysiology*

This work utilized the Membrane Transporter Expression Facility (MTEF) at the University of Adelaide, which is supported by BioInnovation SA and the Australian Research Council. *Xenopus laevis* oocytes were supplied by the MTEF and the *Xenopus* frog colony is maintained by the University of Adelaide Animal Housing Facilities.

Oocytes were prepared as described by Zhou et al. (2007) and kept in modified Barth's solution (96mM NaCl, 2 mM KCl, 5 mM MgCl<sub>2</sub>, 5mM HEPES/KOH pH 7.6) containing 0.5 mM CaCl<sub>2</sub>, 2.5 mL per 50 mL horse serum (H-1270; Sigma, St Louis, MO, USA), 50 µg mL<sup>-1</sup> tetracyclin (Sigma) and 0.5 mL per 50 mL of penicillin-streptomycin (P4333, 10 000 units penicillin and 10 mg streptomycin per milliliter, Sigma) at 18°C. Solutions were changed daily.

Oocytes of uniform size (1 mm diameter) and colouring were injected at the border between animal and vegetal poles on the animal side with approximately 23 ng of cRNA in 46 nL of nuclease-free water per oocyte using a Nanoinject II microinjector (Drummond Scientific Company, Australia). In other experiments higher concentrations of cRNA, as specified, were injected in the same volume of water. Electrophysiological measurements were made 1-3 d after the injection with a two-microelectrode voltage and patch clamp amplifier (GeneClamp 500; Axon Instruments) together with a Digidata 1322A data acquisition system interface (Axon Instruments) using 0.5 to 1 MΩ pipettes filled with 3M KCl.

Membrane currents were measured in standard solution that contained 6 mM MgCl<sub>2</sub>, 1.8 mM CaCl<sub>2</sub>, 10 mM 2-(N-morpholino)-ethanesulfonic acid (MES) adjusted to pH 6.5 with TRIS base (Trizma® base, Sigma-Aldrich) for the standard solution or L-Glutamic acid for solutions where the pH was less than 6.5. Osmolarities were adjusted with mannitol to 240-260 mosmol/kg using a vapor pressure osmometer (Wescor 5500, Wescor). Bath solutions were modified with Na<sup>+</sup> glutamate, K<sup>+</sup> glutamate, LiOH, RbCl, CsCl, TRIS glutamate, triethanolamine (TEA), gadolinium or flufenamate, as specified. Free ion activities were calculated using Visual MINTEQ (Version 2.53) (Gustafsson, 2003). All experiments were performed at room temperature (20-22 °C).

Voltage-pulse protocols, data acquisition and analysis were performed with the pClamp 9.0 program suite (Axon Instruments, CA, USA). The filter frequency was set to 1 kHz; the acquisition time of data points was in the range of 2-10 ms depending on the voltage protocols.

For continuous trace data, the membrane potential was clamped at -120 mV, and data were collected continuously as various solutions were run through the bath.

To collect data for current-voltage relationships, ramp commands were constructed in pCLAMP. The membrane potential was increased in 20 mV steps from -140 mV (or just -120 mV in some experiments) through to 40 mV. Each voltage was held for ~5 s followed by ~4 s at 0 mV. A break, where no voltage was injected, was included in between each step-increase in membrane potential. For reasons of clarity, error bars were not displayed on all of the graphs generated from the current-voltage data. To give an indication of the error, the standard errors of the means (SEM) are included in Figure 4.15 and Figure 4.16. As can be seen in these two figures, the errors were so small in magnitude that the error bars were usually hidden by the symbols representing each data point. Each voltage was held for 5 seconds; however, the current-voltage data was calculated based on the average value for current obtained during a representative 1.5 seconds of injection of the specific voltage. Experimental replication is included in Appendix Table 4.1.

#### 4.2.4 *Total moles of Na<sup>+</sup> and K<sup>+</sup> per oocyte measured using a flame photometer*

Oocytes were harvested three days after injection of cRNA. Oocytes were kept in modified Barth's solution (which contains 96 mM Na<sup>+</sup> and 2 mM K<sup>+</sup>, see section 4.2.3) with horse serum and antibiotics (Zhou et al., 2007) at 18°C, and solutions were changed daily. At harvest oocytes were washed three times for 10 s in 1 mL of autoclaved Milli-Q (Millipore) purified H<sub>2</sub>O to wash off any Barth's solution. Three oocytes per sample were homogenized in



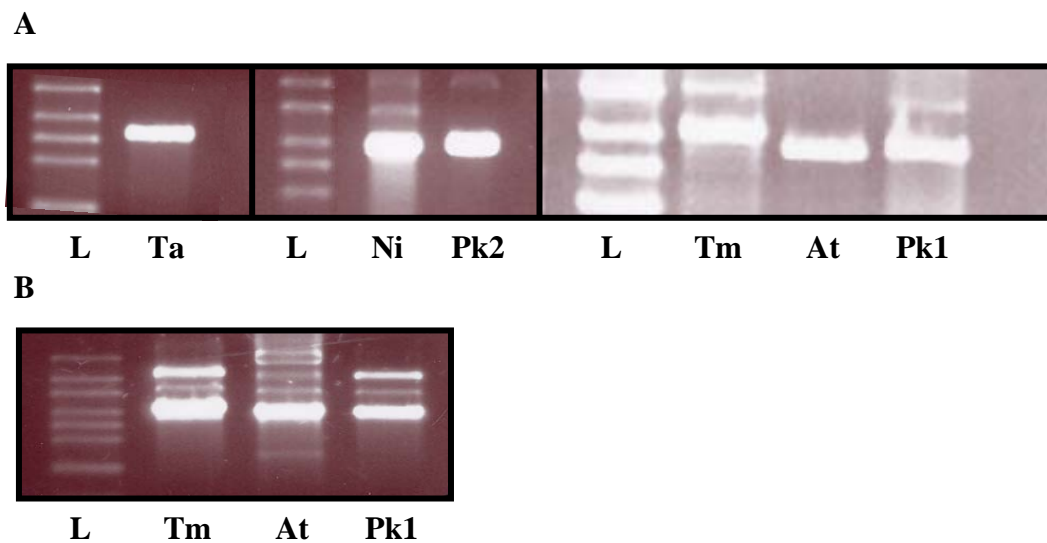
1 mL of 1% nitric acid and incubated at 75°C for 1 h. Samples were then mixed and 0.5 mL was diluted with a further 1.5 mL of 1% nitric acid. Total moles of Na<sup>+</sup> and K<sup>+</sup> were measured using a flame photometer (M410, Corning, Palo Alto, CA) (Essah et al., 2003). Solutions of 0.1 mM NaCl and 0.1 mM KCl were used to calibrate the flame photometer as per the manufacturer's instructions.

### 4.3 Results

#### 4.3.1 Transcription of RNA

Strong bands of the expected product sizes were transcribed from linearized pGEMHE vector DNA containing the coding sequences of the genes of interest; *TaHKT1;5-D* (1551 bp); Nipponbare *OsHKT1;5* (1665 bp); Pokkali *OsHKT2;2* (1593 bp); *TmHKT1;5-A* (1554 bp); *AtHKT1;1* (1521 bp) and Pokkali *OsHKT1;5* (1665 bp) (Figure 4.1 A).

Additional bands of larger sizes were observed for *TmHKT1;5-A* and Pokkali *OsHKT1;5*, there was also very faint bands of larger sizes in the Nipponbare *OsHKT1;5* and Pokkali *OsHKT2;2* lanes. The RNA transcription reaction was repeated and the additional bands were again observed, faint bands were also observed in the *AtHKT1;1* sample (Figure 4.1 B). Larger bands may be additional unwanted transcribed products. It was anticipated that the RNA product sizes may not correspond exactly to the ladder as despite the denaturing process the RNA may have folded into a secondary structure affecting the rate of movement through the agarose gel, this may also explain the differing product sizes.



**Figure 4.1: RNA *in vitro* transcribed from pGEMHE**

A. RNA products transcribed from the coding sequences of *TaHKT1;5-D* (Ta) (1551 bp); Nipponbare *OsHKT1;5* (1665 bp) (Ni); Pokkali *OsHKT2;2* (1593 bp) (Pk2); *TmHKT1;5-A* (1554 bp) (Tm); *AtHKT1;1* (1521 bp) (At); and Pokkali *OsHKT1;5* (1665 bp) (Pk1). B. Repeat of transcription of *TmHKT1;5-A* (1554 bp) (Tm); *AtHKT1;1* (1521 bp) (At); and Pokkali *OsHKT1;5* (1665 bp) (Pk1). L = 1Kb ladder.

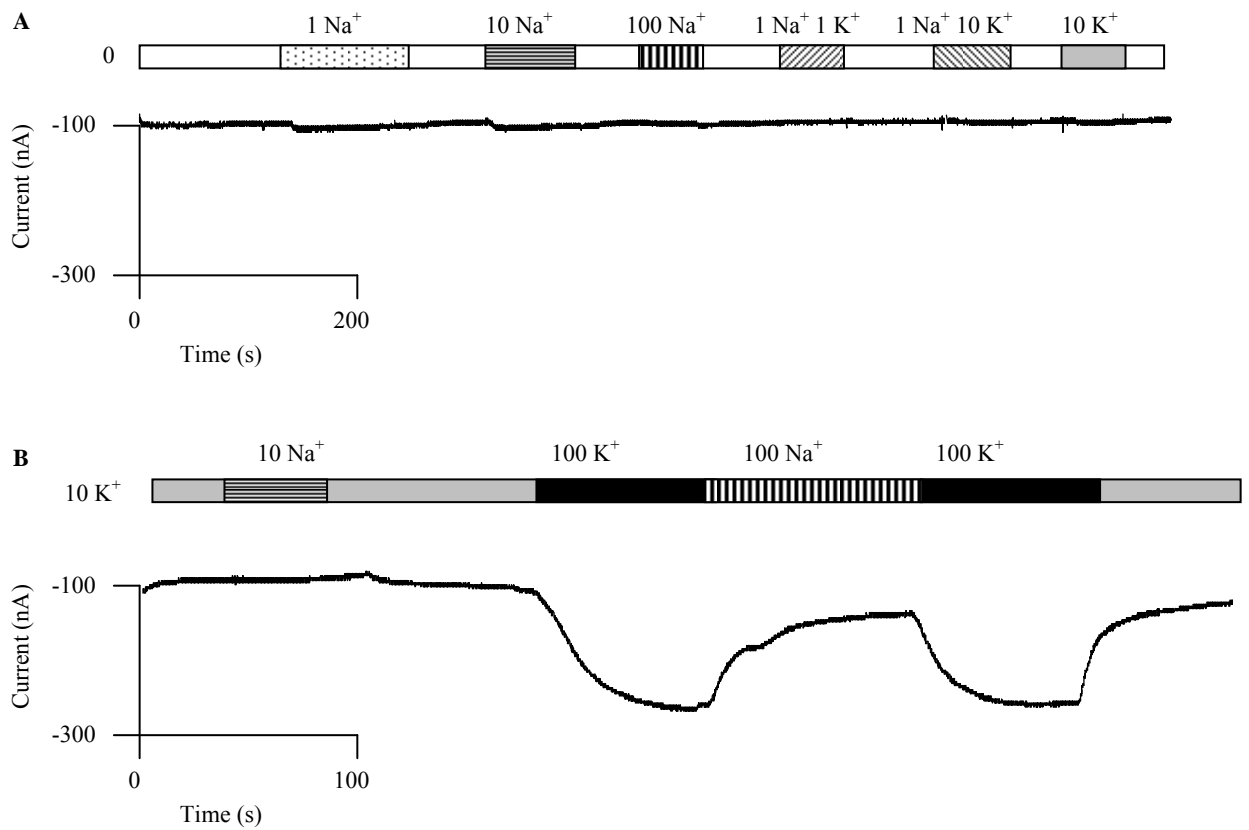
#### 4.3.2 *Measurement of currents in water-injected oocytes*

Water-injected control oocytes were included in all experiments. There was no significant change in conductance observed in response to increasing concentrations of exogenous  $\text{Na}^+$  (Figure 4.2 A). The only significant conductance observed for water injected oocytes was in response to external solutions with a concentration of 100 mM  $\text{K}^+$  (Figure 4.2 B). This endogenous conductance did not consistently occur, and was only observed on a couple of occasions, and only in response to very negative membrane potentials of around  $-120$  mV.

No significant conductance was observed in water injected oocytes at various membrane potentials when exposed to various bath solutions (Figure 4.3 and Figure 4.4). Small endogenous conductance was observed at very negative membrane potentials ( $\leq 120$  mV) when oocytes were exposed to 100 mM  $\text{K}^+$ , 100 mM CsCl and 100 mM RbCl (Figure 4.3 A). The conductance in most solutions, including 100 mM  $\text{Na}^+$  and 100 mM  $\text{K}^+$ , was approximately 1  $\mu\text{S}$ . The maximum conductance was observed when the oocytes were in the solution with  $\text{Rb}^+$ , in this solution the conductance was  $\sim 2$   $\mu\text{S}$ . Varying the concentration of  $\text{Na}^+$  or  $\text{K}^+$  or both  $\text{Na}^+$  and  $\text{K}^+$  in the bath solution did not induce currents in water injected oocytes (Figure 4.3 B and C).

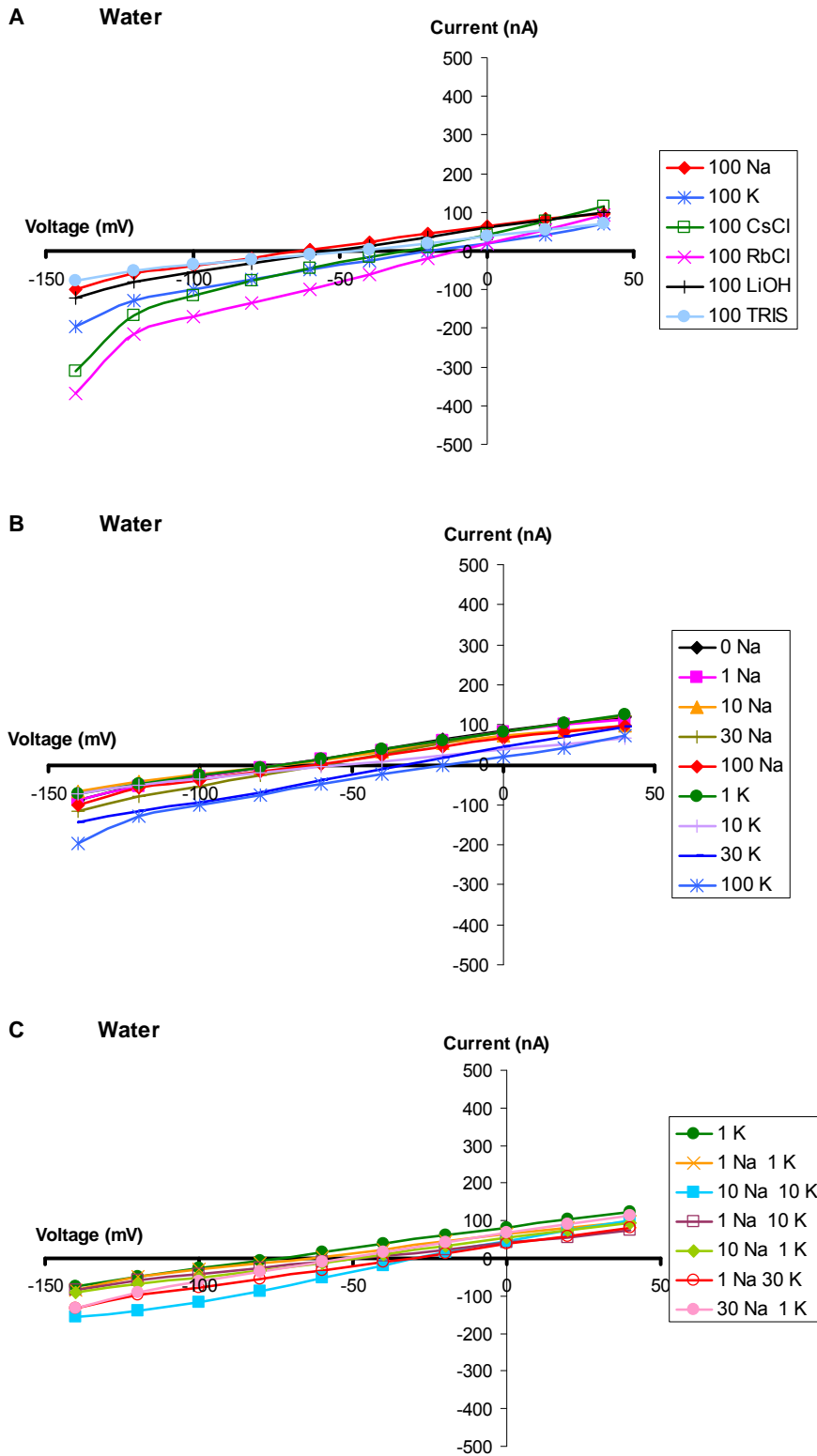
If the oocytes were transporting  $\text{Na}^+$  or  $\text{K}^+$ , in response to increased external concentrations of  $\text{Na}^+$  or  $\text{K}^+$ , then the slope of the current-voltage relationship would increase with increasing external  $\text{Na}^+$  or  $\text{K}^+$ . When the external  $\text{Na}^+$  and/or  $\text{K}^+$  concentration was increased there was no change in the slope of the current-voltage relationship (Figure 4.3 B and C) indicating that there was no significant transport of  $\text{Na}^+$  or  $\text{K}^+$  into or out of the water-injected oocytes.

No significant currents were observed for water injected oocytes in 10 mM  $\text{Na}^+$  when the pH was altered, or when the calcium concentration was altered (Figure 4.4). The conductance of water-injected oocytes in the presence of 10 mM  $\text{Na}^+$  did not decrease when channel blockers (flufenamate and gadolinium) were present (Figure 4.4).



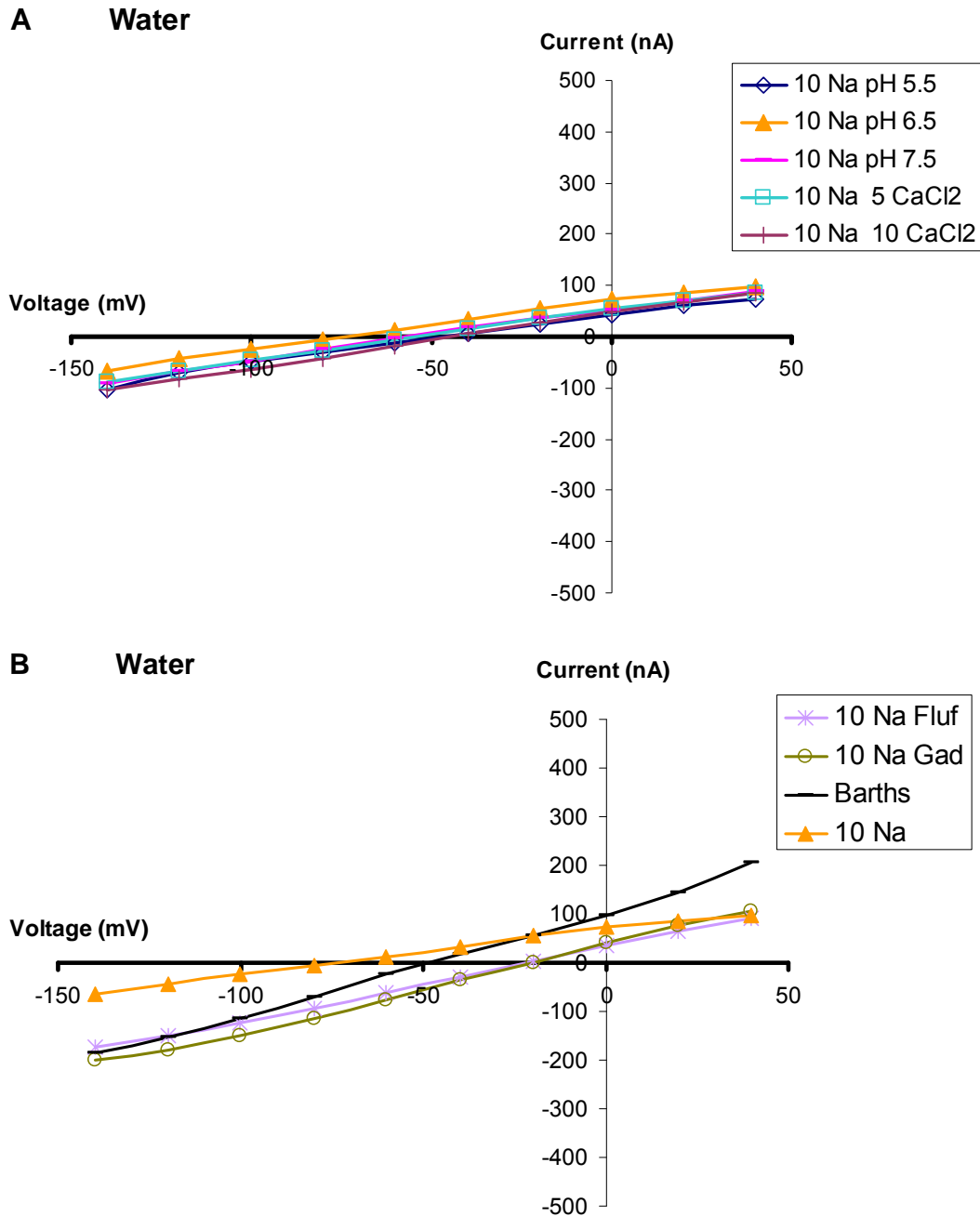
**Figure 4.2: Currents over time in H<sub>2</sub>O injected oocytes exposed to a range of solutions with varying Na<sup>+</sup> and K<sup>+</sup> concentrations**

A. No currents were observed in response to varying Na<sup>+</sup> concentrations. B. Small endogenous inward currents were observed in response to 100 mM K<sup>+</sup>. The membrane potential was held at -120 mV. Units for Na<sup>+</sup> and K<sup>+</sup> concentrations are in mM. 0 refers to the standard solution (See 4.2.3).



**Figure 4.3: Current-voltage curves for oocytes injected with water, in solutions with different cations and different Na<sup>+</sup> and K<sup>+</sup> concentrations**

Oocytes were exposed to solutions with different salts (A), and solutions with different Na<sup>+</sup> (glutamate) concentrations, or K<sup>+</sup> (glutamate) concentrations (B), and different combinations of Na<sup>+</sup> and K<sup>+</sup> (glutamate) concentrations (C). Concentrations are in mM. Numbers of oocytes are listed in Appendix Table 4.1.



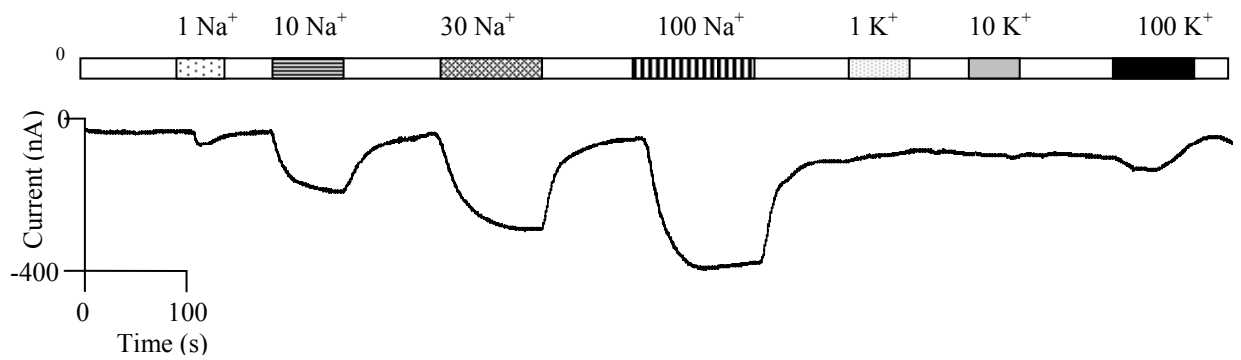
**Figure 4.4: Current-voltage curves for oocytes injected with water, in solutions with 10 mM Na<sup>+</sup> and with different pH, calcium concentrations and channel blocking solutions** Oocytes were exposed to solutions with 10 mM Na<sup>+</sup> and solutions with 10 mM Na<sup>+</sup> and different pH and calcium concentrations (A); and solutions with 10 mM Na<sup>+</sup> and different channel blockers (Fluf = 0.1 mM Flufenamate, Gad = 0.1 mM Gadolinium, (B); Na = Na<sup>+</sup> (glutamate); concentrations are in mM. Numbers of oocytes are listed in Appendix Table 4.1.

#### 4.3.3 Measurement of currents in *AtHKT1;1* injected oocytes

When the membrane potential of the oocytes was held at  $-120$  mV *AtHKT1;1* transported  $\text{Na}^+$ , but not  $\text{K}^+$  (Figure 4.5). The conductance of *AtHKT1;1* significantly increased with increasing external  $\text{Na}^+$ , consistent with *AtHKT1;1* transporting  $\text{Na}^+$  into the oocyte when the membrane potential was negative (approximately  $-100$  mV; Figure 4.5 and 4.6). The small currents induced by  $100$  mM  $\text{K}^+$  (Figure 4.5 and 4.6 A) may be endogenous, as similar currents were observed in water injected oocytes exposed to  $100$  mM  $\text{K}^+$  (Figure 4.2 B). In response to increasing external  $\text{K}^+$  there was a small increase in conductance and the  $E_{\text{rev}}$  moved positive (Figure 4.6 A).

In  $1$  or  $10$  mM  $\text{Na}^+$ , the conductance of *AtHKT1;1* was approximately  $2$   $\mu\text{S}$ . The conductance of  $\text{Na}^+$  by *AtHKT1;1* in the presence of  $30$  mM  $\text{Na}^+$  ( $6$   $\mu\text{S}$ ) and in the presence of  $100$  mM  $\text{Na}^+$  ( $5$   $\mu\text{S}$ ) was similar, indicating that the transporter was saturated in the presence of approximately  $30$  mM  $\text{Na}^+$  (Figure 4.6 A). A 10-fold increase in the external  $\text{Na}^+$  activity, from approximately  $0.8$  to  $8$  mM  $\text{Na}^+$ , leads to a positive shift in the  $E_{\text{rev}}$ , from approximately  $-55$  to  $-40$  mV. When the external  $\text{Na}^+$  activity increased from approximately  $8$  to  $80$  mM  $\text{Na}^+$ , the  $E_{\text{rev}}$  shifted from approximately  $-40$  to  $-20$  mV.

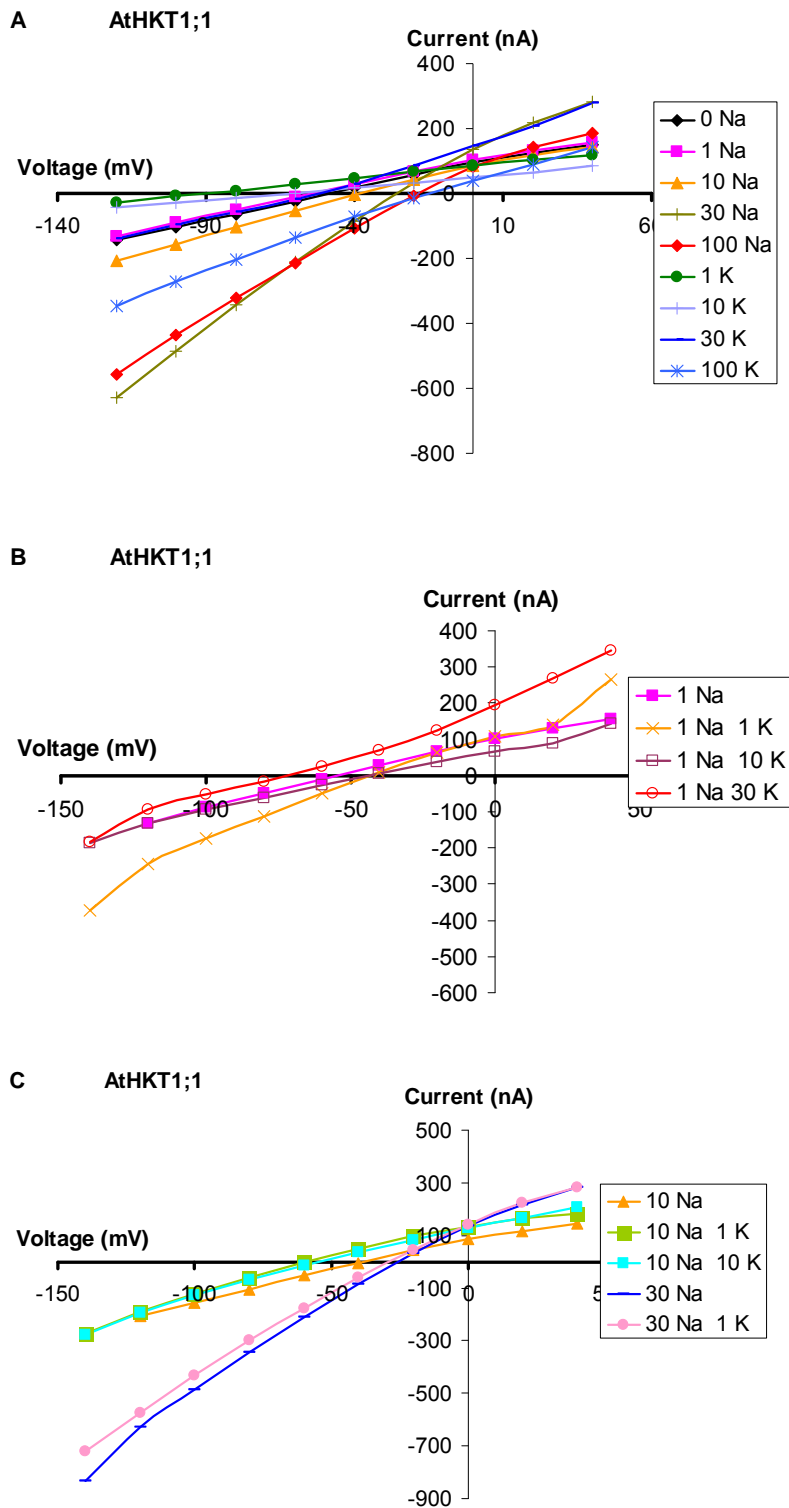
Conductance of  $\text{Na}^+$  by oocytes expressing *AtHKT1;1* in a solution with  $1$  mM  $\text{K}^+$  and  $1$  mM  $\text{Na}^+$  was slightly greater than in a solution with just  $1$  mM  $\text{Na}^+$ , but the conductance in solutions with  $1$  mM  $\text{Na}^+$  and either  $10$  or  $30$  mM  $\text{K}^+$  was not significantly different to the conductance in  $1$  mM  $\text{Na}^+$  (Figure 4.6 B). The presence of  $\text{K}^+$  in the external solution did not significantly change the conductance of  $\text{Na}^+$  when the concentration of  $\text{Na}^+$  in the external solution was  $10$  or  $30$  mM (Figure 4.6 C). The conductance of  $\text{Na}^+$  by *AtHKT1;1* expressing oocytes in  $10$  mM  $\text{Na}^+$  was similar to the conductance in a solution containing both  $10$  mM  $\text{Na}^+$  and either  $1$  mM  $\text{K}^+$  or  $10$  mM  $\text{K}^+$  (Figure 4.6 C). Similarly, the conductance of *AtHKT1;1* expressing oocytes in  $30$  mM  $\text{Na}^+$  was not significantly different to the conductance in a solution with both  $30$  mM  $\text{Na}^+$  and  $1$  mM  $\text{K}^+$  (Figure 4.6 C). These data indicated that the conductance of *AtHKT1;1* was not altered by the presence of  $\text{K}^+$  in the external solution.



**Figure 4.5: Currents over time in *AtHKT1;1* injected oocytes exposed to a range of solutions with varying  $\text{Na}^+$  and  $\text{K}^+$  concentrations**

Currents were observed in response to varying  $\text{Na}^+$  concentrations, but not  $\text{K}^+$ , other than a small endogenous current for 100 mM  $\text{K}^+$ . The membrane potential was held at  $-120$  mV. Units for  $\text{Na}^+$  and  $\text{K}^+$  concentrations are in mM. 0 refers to the standard solution (See 4.2.3).





**Figure 4.6: Current-voltage curves for AtHKT1;1 expressing oocytes in solutions with different Na<sup>+</sup> and K<sup>+</sup> concentrations**

Oocytes were exposed to solutions with different Na<sup>+</sup> (glutamate) concentrations, or K<sup>+</sup> (glutamate) concentrations (A), and different combinations of Na<sup>+</sup> and K<sup>+</sup> (glutamate) concentrations (B) and (C). Na is Na<sup>+</sup>; K is K<sup>+</sup>; units are mM. Numbers of oocytes are listed in Appendix Table 4.1.

#### 4.3.4 Measurement of currents in *OsHKT1;5* injected oocytes

*OsHKT1;5* exhibited selectivity for  $\text{Na}^+$  rather than  $\text{K}^+$  (Figure 4.7), with the exception of concentrations of approximately 30 mM  $\text{K}^+$  (Figure 4.8 B). The currents induced by 100 mM  $\text{K}^+$  (Figure 4.7) may be endogenous, as similar currents were observed in water injected oocytes exposed to 100 mM  $\text{K}^+$  (Figure 4.2 B).

The conductance of  $\text{Na}^+$  by *OsHKT1;5* did not increase significantly with increasing  $\text{Na}^+$  activity in the external solution (Figure 4.8 A). The conductance of *OsHKT1;5* was  $\sim 7 \mu\text{S}$  in 1 and 100 mM  $\text{Na}^+$ , and  $\sim 6 \mu\text{S}$  in 10 and 30 mM  $\text{Na}^+$ .

As the  $\text{Na}^+$  activity in the external solution was increased from 0.8 to 8 to 80 mM  $\text{Na}^+$ , the  $E_{\text{rev}}$  became less negative, shifting from  $-80$  to  $-50$  to  $-10$  mV, respectively (Figure 4.8 A). This was consistent with previous data for *OsHKT1;5* where an increase in the external  $\text{Na}^+$  concentration from  $\sim 0.3$  mM to  $\sim 10$  mM lead to only a small increase in conductance for the Nona Bokra allele, and no difference in conductance for the weaker Koshihikari allele (Figure 4g and h; Ren et al., 2005). In the data presented by Ren et al. (2005) the  $\sim 10$ -fold increase in external  $\text{Na}^+$  activity lead to a positive shift in  $E_{\text{rev}}$  from approximately  $-62$  to  $-31$  mV.

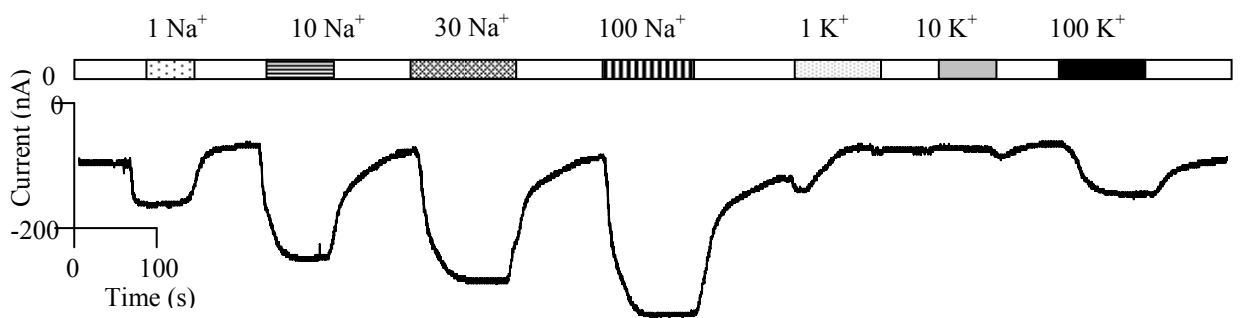
*OsHKT1;5* expressing oocytes did not exhibit significant conductance of  $\text{K}^+$  when the  $\text{K}^+$  concentration in the external solution was 1 or 10 mM  $\text{K}^+$  ( $E_{\text{rev}} \approx -100$  mV), but there was significant conductance when the external solution contained 30 mM  $\text{K}^+$ , and the  $E_{\text{rev}}$  was more positive at this higher  $\text{K}^+$  concentration ( $\approx -87$  mV; Figure 4.8 A).

The conductance of *OsHKT1;5* in solutions with 1 mM  $\text{Na}^+$  was similar to the conductance in 1 mM  $\text{Na}^+$  and 10 mM  $\text{K}^+$ , with the former having a slightly more positive  $E_{\text{rev}}$  ( $-75$  mV) than the latter ( $-85$  mV) (Figure 4.8 B). However, in 1 mM  $\text{Na}^+$  the presence of either 1 mM  $\text{K}^+$  or 30 mM  $\text{K}^+$  in the solution lead to a decrease in conductance and a less negative  $E_{\text{rev}}$  ( $-65$  and  $-45$  mV, respectively).

There was less conductance of *OsHKT1;5* in the solution with 10 mM  $\text{Na}^+$  and 1 mM  $\text{K}^+$  than in the solution with just 10 mM  $\text{Na}^+$ , but there was greater conductance in the solution with 10 mM  $\text{Na}^+$  and 10 mM  $\text{K}^+$  than in the solution with just 10 mM  $\text{Na}^+$ , although the  $E_{\text{rev}}$  did not differ in the solution with 10 mM  $\text{Na}^+$  and 10 mM  $\text{K}^+$  compared to the solution with just 10 mM  $\text{Na}^+$  (Figure 4.8 C). There was slightly more conductance in a solution with 30 mM  $\text{Na}^+$  and 1 mM  $\text{K}^+$  than in a solution with just 30 mM  $\text{Na}^+$ , and the  $E_{\text{rev}}$  in 30 mM  $\text{Na}^+$  and 1 mM  $\text{K}^+$  ( $-30$  mV) was more positive than for just 30 mM external  $\text{Na}^+$  ( $-40$  mV).

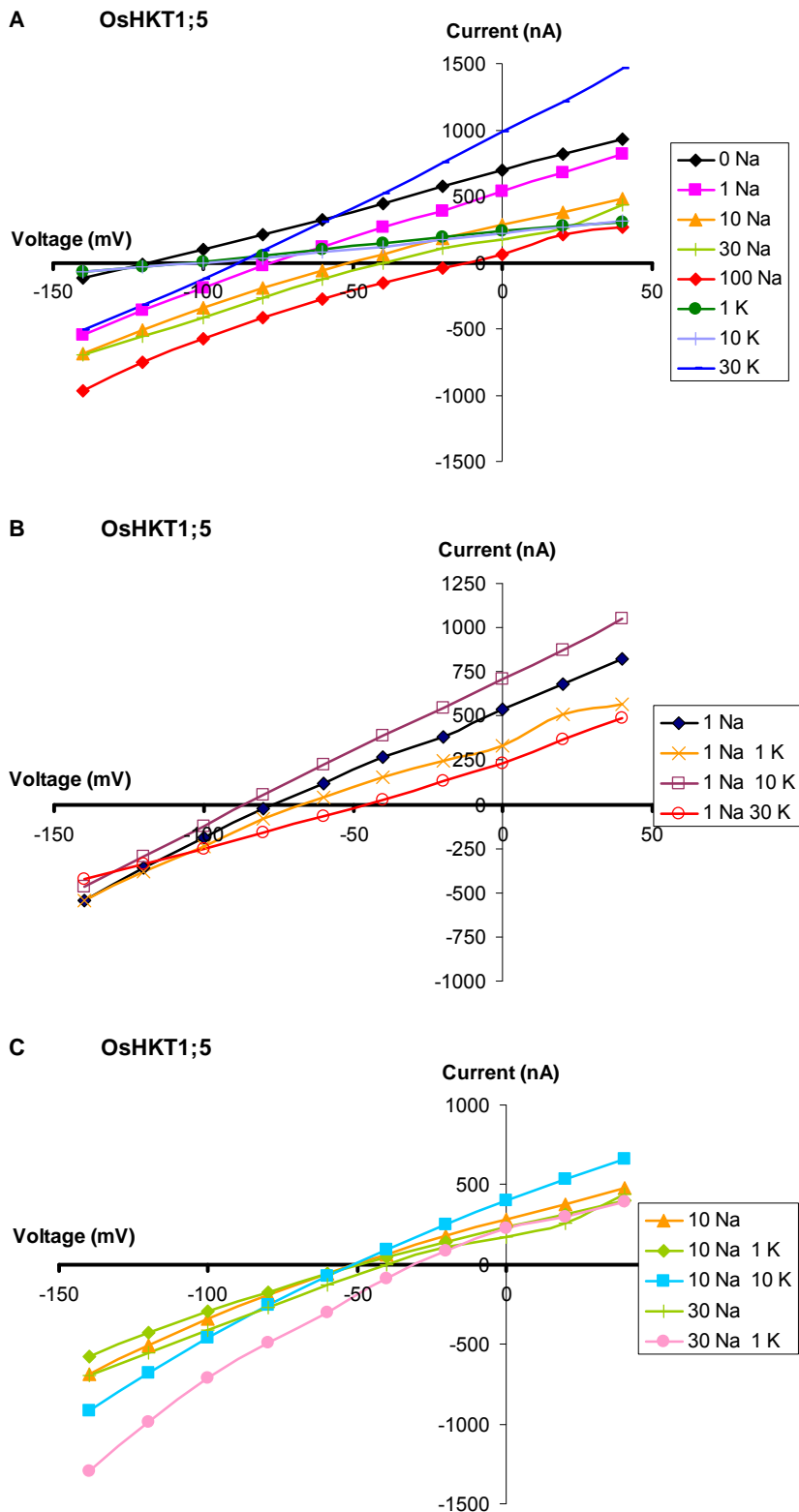
OsHKT1;5 was selective for Na<sup>+</sup> over other ions (Figure 4.9 A). However, there may have been a small amount of conductance of Cs<sup>+</sup> and Rb<sup>+</sup>. Varying the pH and calcium, and adding channel blockers, did not significantly affect the conductance of Na<sup>+</sup> observed for OsHKT1;5 in the presence of 10 mM Na<sup>+</sup> (Figure 4.9 B).

Surprisingly, no significant conductance was observed for oocytes injected with Pokkali OsHKT1;5 capped RNA (Figure 4.10), even though the Pokkali HKT1;5 and Nipponbare HKT1;5 amino acid sequences are 98% identical. The conductance in 100 mM K<sup>+</sup> (Figure 4.10) may be due to an endogenous transporter, as similar currents were observed in water injected oocytes exposed to 100 mM K<sup>+</sup> (Figure 4.2 B).



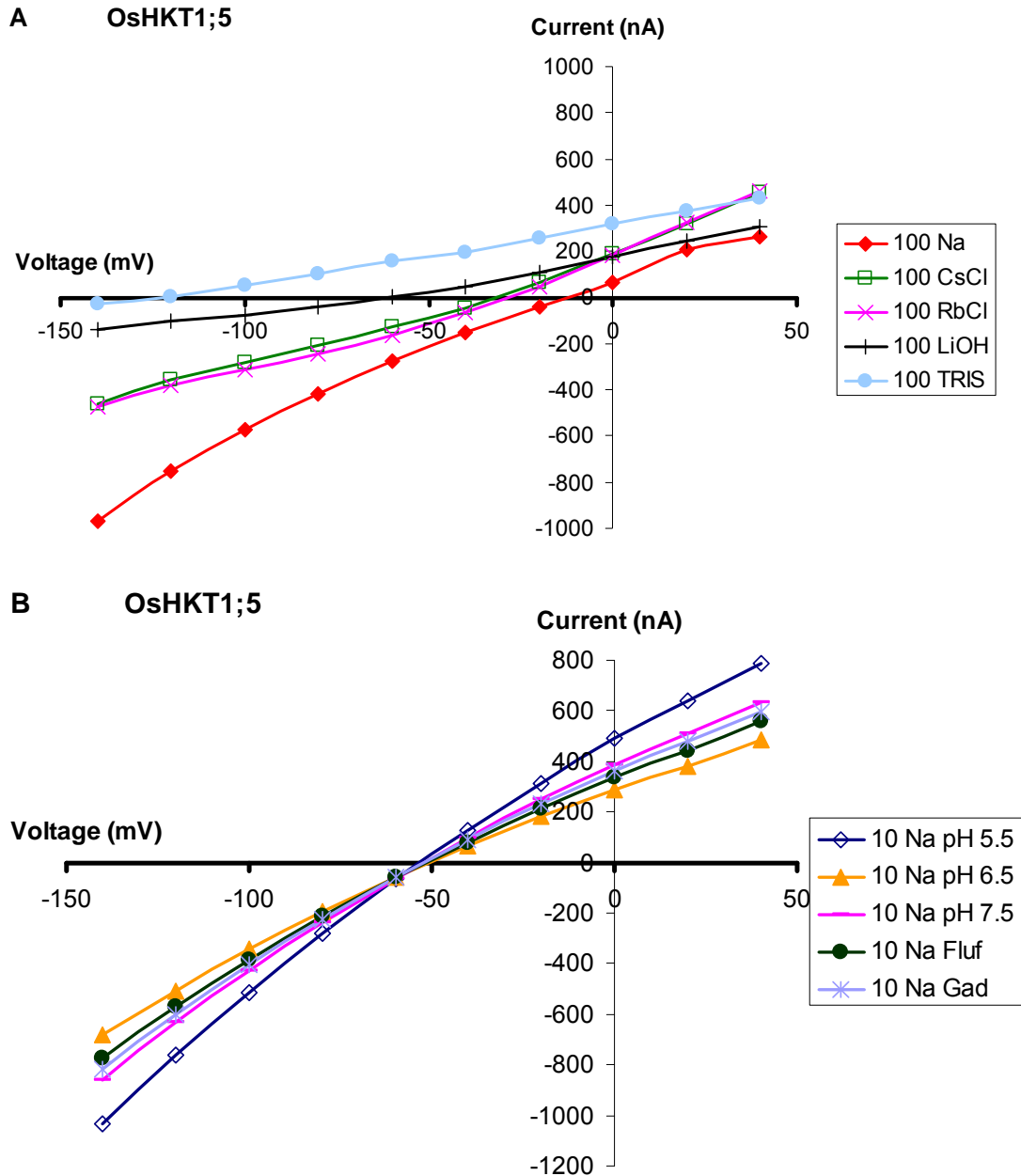
**Figure 4.7: Currents over time in *OsHKT1;5* (Nipponbare) injected oocytes exposed to a range of solutions with varying Na<sup>+</sup> and K<sup>+</sup> concentrations**

Currents were observed in response to varying Na<sup>+</sup> concentrations, but not K<sup>+</sup>, other than a small endogenous current for 100 mM K<sup>+</sup>. The membrane potential was held at -120 mV. Units for Na<sup>+</sup> and K<sup>+</sup> concentrations are in mM. 0 refers to the standard solution (See 4.2.3).

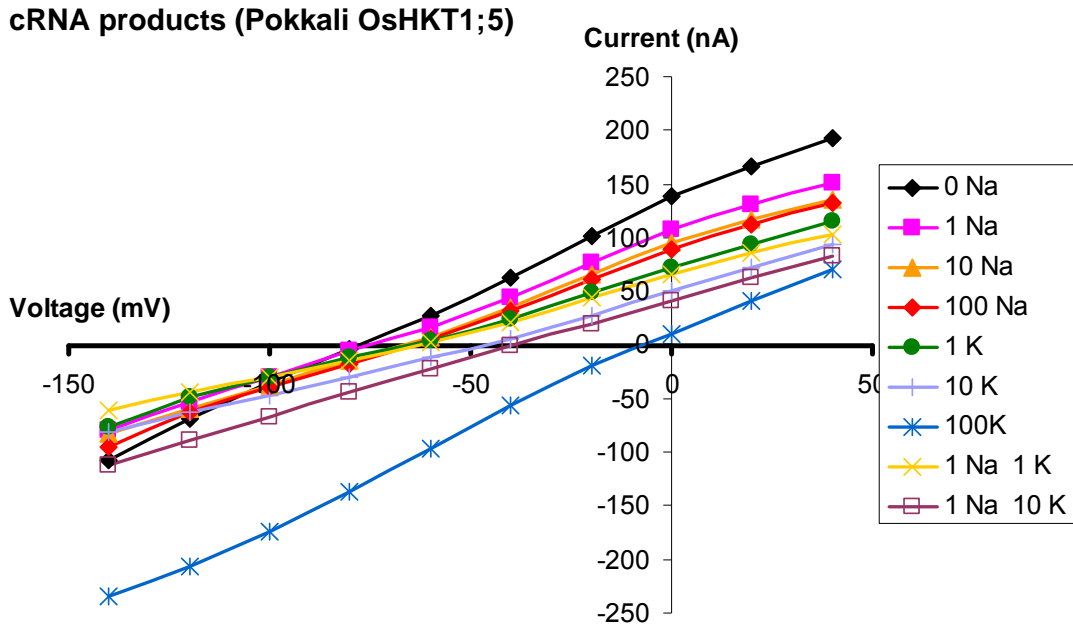


**Figure 4.8: Current-voltage curves for OsHKT1;5 (Nipponbare) expressing oocytes in solutions with different  $\text{Na}^+$  and  $\text{K}^+$  concentrations**

Oocytes were exposed to solutions with different  $\text{Na}^+$  (glutamate) concentrations, or  $\text{K}^+$  (glutamate) concentrations (A), and different combinations of  $\text{Na}^+$  and  $\text{K}^+$  (glutamate) concentrations (B) and (C). Na is  $\text{Na}^+$ ; K is  $\text{K}^+$ ; units are mM. Numbers of oocytes are listed in Appendix Table 4.1.



**Figure 4.9: Current-voltage curves for oocytes expressing OsHKT1;5 (Nipponbare), in solutions with various cations, different pH, and channel blocking solutions**  
 Oocytes were exposed to solutions with different cations (A) and different pH and channel blockers (B) Large inward currents were observed in the presence of 100 mM Na<sup>+</sup>. (G) is glutamate; Na is Na<sup>+</sup>; K is K<sup>+</sup>; TRIS is Trizma® base; 100 is 100 mM; Fluf = 0.1 mM Flufenamate; Gad = 0.1 mM Gadolinium; Na = Na<sup>+</sup> (glutamate); K = K<sup>+</sup> (glutamate) concentrations in mM. Numbers of oocytes are listed in Appendix Table 4.1.



**Figure 4.10: Current-voltage curves for oocytes injected with cRNA products transcribed from pGEMHE containing the cDNA for *OsHKT1;5* (Pokkali)**

The currents observed for 100 mM  $K^+$  may be endogenous. No other significant currents were observed for solutions with various  $Na^+$  and  $K^+$  concentrations. Na is  $Na^+$  (glutamate); K is  $K^+$  (glutamate); concentration in mM. Numbers of oocytes are listed in Appendix Table 4.1.

#### 4.3.5 Measurement of currents in *OsHKT2;2* injected oocytes

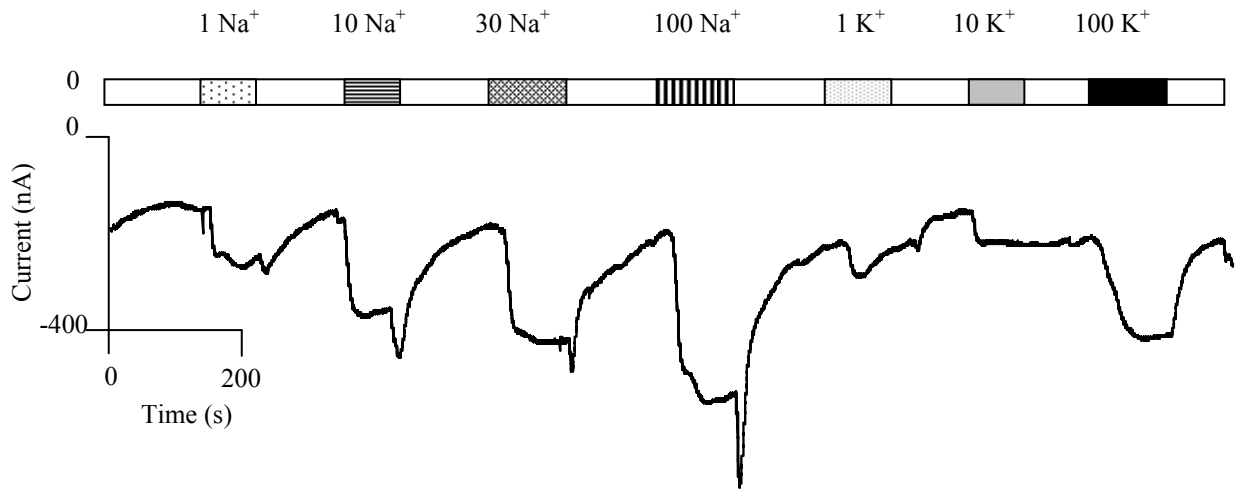
*OsHKT2;2* behaved as a  $\text{Na}^+$  and  $\text{K}^+$  coupled transporter, which is consistent with previous literature (Horie et al., 2001). At negative membrane potentials ( $-120$  mV) conductance of  $\text{Na}^+$  and  $\text{K}^+$  was observed when either  $\text{Na}^+$  or  $\text{K}^+$  was present in the external solution (Figure 4.11). Increasing concentrations of  $\text{Na}^+$  and  $\text{K}^+$  in the external solution lead to positive shifts in the  $E_{\text{rev}}$  (Figure 4.12 A and B).

The conductance of  $\text{Na}^+$  was greater when the concentration of  $\text{Na}^+$  in the external solution was 1 or 10 mM (17 and 16  $\mu\text{S}$ , respectively), compared to higher concentrations of 30 or 100 mM  $\text{Na}^+$  (11 and 12  $\mu\text{S}$ , respectively; Figure 4.12 A). In solutions containing only  $\text{K}^+$ , the greatest conductance was at concentrations of 1 mM and 30 mM  $\text{K}^+$  (9 and 10  $\mu\text{S}$ , respectively), and at 10 mM  $\text{K}^+$  the conductance was significantly lower ( $\sim 5$   $\mu\text{S}$ ; Figure 4.12 B).

Greater conductance was observed for *OsHKT2;2* ( $\sim 11$   $\mu\text{S}$ ; Figure 4.12 A and B) in the modified Barth's solutions (0 mM  $\text{Na}^+$  and 0 mM  $\text{K}^+$ ), than for water ( $\sim 1$   $\mu\text{S}$ ; Figure 4.3 B) or *AtHKT1;1* ( $\sim 2$   $\mu\text{S}$ ; Figure 4.6 A) injected oocytes.

In solutions with both  $\text{Na}^+$  and  $\text{K}^+$ , increasing the concentration of  $\text{Na}^+$  and  $\text{K}^+$  lead to positive shifts in the reversal potential. The greatest conductance observed for *OsHKT2;2* expressing oocytes was in a solution of 30 mM  $\text{Na}^+$  and 1 mM  $\text{K}^+$  ( $\sim 22$   $\mu\text{S}$ ). Similar conductance was observed for *OsHKT2;2* in a solution of 10 mM  $\text{Na}^+$  and 1 mM  $\text{K}^+$  ( $\sim 21$   $\mu\text{S}$ ). Conductance was high ( $\sim 18$   $\mu\text{S}$ ) in a solution of 10 mM  $\text{Na}^+$  and 10 mM  $\text{K}^+$  and the  $E_{\text{rev}}$  observed for this solution ( $-25$  mV) was more positive than the  $E_{\text{rev}}$  for other solutions. In comparison, the  $E_{\text{rev}}$  in a solution of 10 mM  $\text{Na}^+$  was approximately  $-75$  mV.

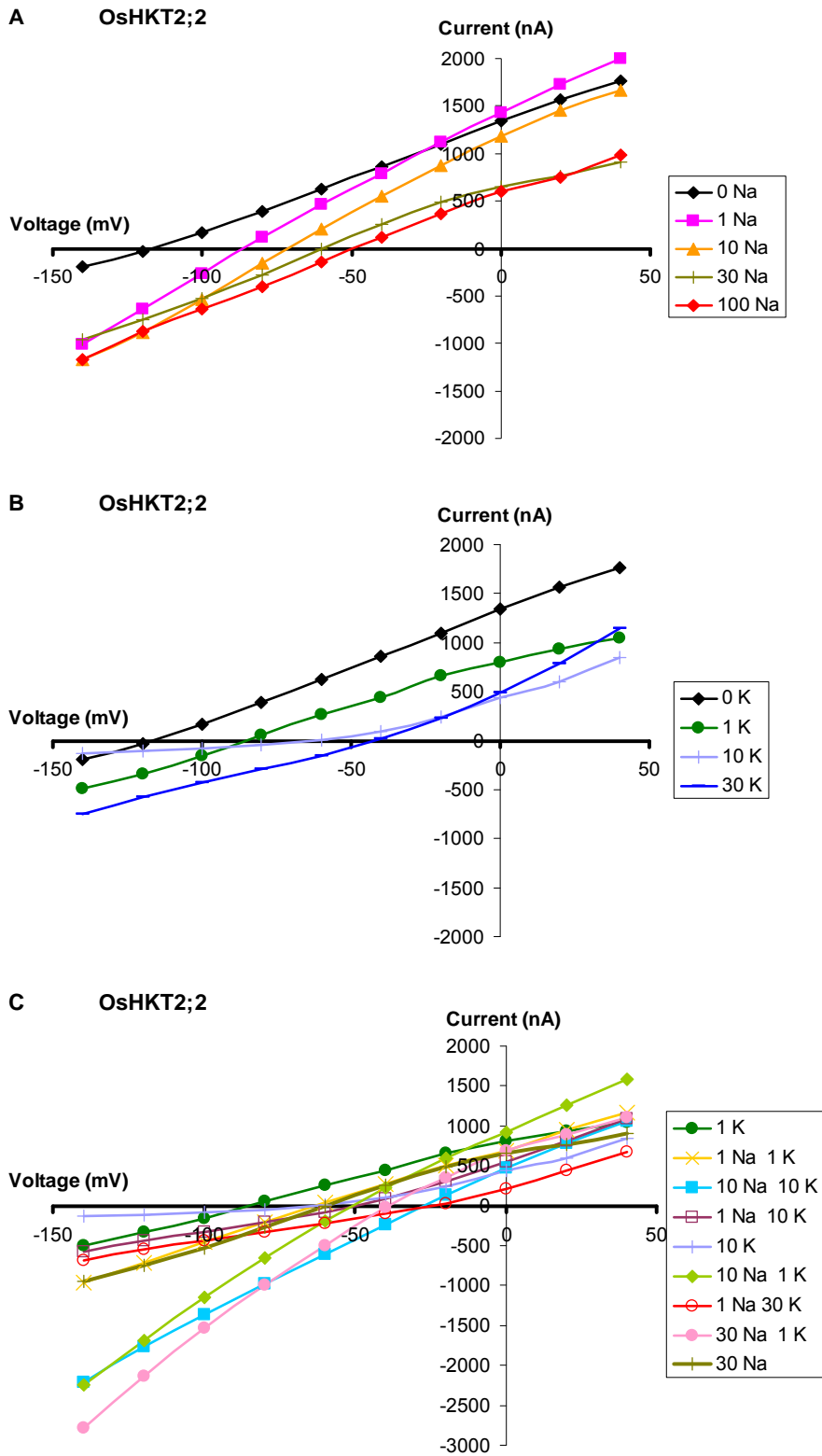
*OsHKT2;2* expressing oocytes were more permeable to other cations such as  $\text{Cs}^+$ ,  $\text{Rb}^+$ , and  $\text{Li}^+$ , and a solution with TRIS (Figure 4.13) than *OsHKT1;5* expressing oocytes (Figure 4.9 A).



**Figure 4.11: Currents over time in *OsHKT2;2* injected oocytes exposed to a range of solutions with varying Na<sup>+</sup> and K<sup>+</sup> concentrations**

Currents were observed in response to varying Na<sup>+</sup> concentrations, but not K<sup>+</sup>, other than a small endogenous current for 100 mM K<sup>+</sup>. The membrane potential was held at -120 mV. Units for Na<sup>+</sup> and K<sup>+</sup> concentrations are in mM. 0 refers to the standard solution (See 4.2.3).

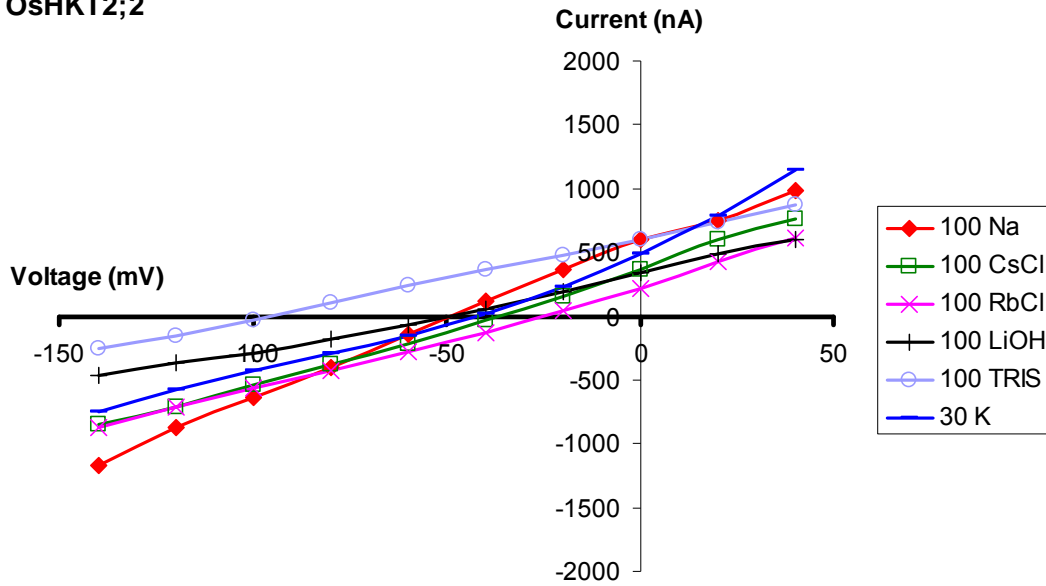




**Figure 4.12: Current-voltage curves for OsHKT2;2 (Pokkali) expressing oocytes in solutions with different Na<sup>+</sup> and K<sup>+</sup> concentrations**

Oocytes were exposed to solutions with different Na<sup>+</sup> (glutamate) concentrations (A), or K<sup>+</sup> (glutamate) concentrations (B), and different combinations of Na<sup>+</sup> and K<sup>+</sup> (glutamate) concentrations (C). Na is Na<sup>+</sup>; K is K<sup>+</sup>; units are mM. Numbers of oocytes are listed in Appendix Table 4.1.

## OsHKT2;2



**Figure 4.13: Current-voltage curves for oocytes expressing OsHKT2;2 (Pokkali), in solutions with various cations**

Oocytes were exposed to solutions with different cations. Large inward currents were observed in the presence of 100 mM Na<sup>+</sup>, OsHKT2;2 also showed permeability to Cs, Rb and K. (G) is glutamate; Na is Na<sup>+</sup>; K is K<sup>+</sup>; concentrations are in mM; Numbers of oocytes are listed in Appendix Table 4.1.

#### 4.3.6 Measurement of currents in TaHKT1;5-D injected oocytes

The wheat TaHKT1;5-D, like the rice HKT1;5, exhibited Na<sup>+</sup>-specific inward currents at negative membrane potentials when expressed in *Xenopus* oocytes (Figure 4.14).

Greater conductance of Na<sup>+</sup> was observed for TaHKT1;5 expressing oocytes than for any of the other transporters tested when exposed to bath solutions containing either 30 or 100 mM Na<sup>+</sup> (14 and 24  $\mu$ S, respectively). However, the relative amount of the different proteins in the plasma membrane was not tested and the amount of protein influences this data.

At 1 mM Na<sup>+</sup>, TaHKT1;5 and OsHKT1;5 had similar conductance of Na<sup>+</sup> ( $\sim$ 7  $\mu$ S) and at 10 mM Na<sup>+</sup> OsHKT1;5 ( $\sim$ 6  $\mu$ S) had greater conductance of Na<sup>+</sup> than TaHKT1;5 ( $\sim$ 4  $\mu$ S).

TaHKT1;5 was highly selective for Na<sup>+</sup> and not other cations in the external solution (Oocytes were exposed to external solutions with 100 mM concentrations of K<sup>+</sup>, Cs<sup>+</sup>, Li<sup>+</sup>, Rb<sup>+</sup> and TRIS) (Figure 4.15).

The slope of the current-voltage curves (Figure 4.16) were used to calculate conductance, and plotted against increasing Na<sup>+</sup> activity (Figure 4.17). Conductance of TaHKT1;5 increased with increasing Na<sup>+</sup> activity and at the highest Na<sup>+</sup> concentration tested, equivalent to  $\sim$ 80 mM Na<sup>+</sup> activity, TaHKT1;5 may not have been saturated (Figure 4.17).

As the external Na<sup>+</sup> concentration increased 10-fold from  $\sim$ 0.8 mM to 8 mM, or 8 mM to 80 mM, the  $E_{rev}$  became approximately +50 mV more positive (Figure 4.16).

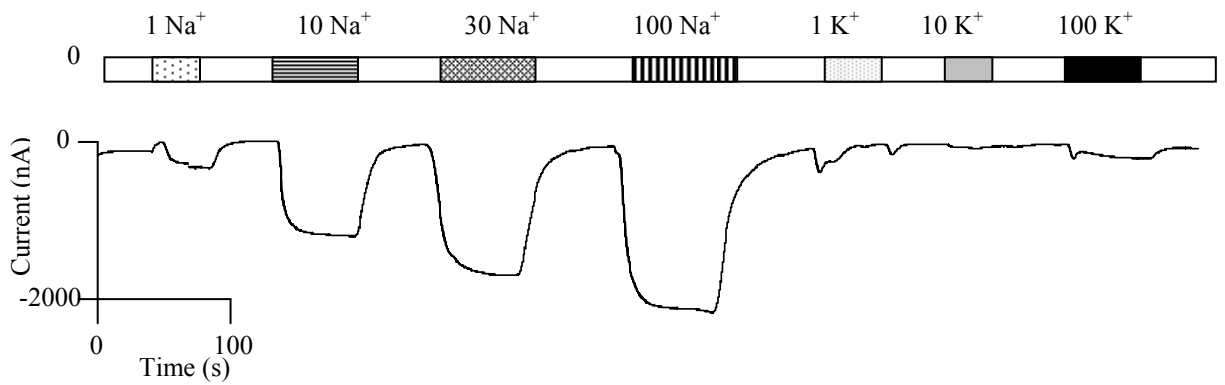
The permeability of TaHKT1;5 to K<sup>+</sup> was also plotted. Surprisingly, as TaHKT1;5 was predicted to be a Na<sup>+</sup> transporter, there was significant conductance ( $\sim$ 12  $\mu$ S) in solutions with K<sup>+</sup> activities of  $\sim$ 30 mM (Figure 4.18). The conductance of TaHKT1;5 in solutions with 1, 10 and 100 mM K<sup>+</sup> was 3, 5 and 2  $\mu$ S, respectively. The conductance of AtHKT1;1 in solutions with K<sup>+</sup> concentrations of 1, 10, 30 and 100, was 1, 1, 3 and 3, and the conductance of OsHKT1;5 in solutions with K<sup>+</sup> concentrations of 1, 10 and 30 was 2, 2 and 11. Therefore, the 1;5-type transporters both exhibited significantly greater conductance at 30 mM K<sup>+</sup> than the group 1;1-type transporter, even greater than the 2;2-type transporter which had a conductance of 10  $\mu$ S in 30 mM K<sup>+</sup> (the conductance of OsHKT2;2 in solutions with 1 and 10 mM K<sup>+</sup> was 9 and 5  $\mu$ S, respectively).

In solutions with 1 mM Na<sup>+</sup> and varying K<sup>+</sup> concentrations, the greatest conductance for TaHKT1;5 was for 1 mM Na<sup>+</sup> with 30 mM K<sup>+</sup> ( $\sim$ 14  $\mu$ S; Figure 4.19 A). For 1 mM Na<sup>+</sup> and 1 mM K<sup>+</sup> the conductance was  $\sim$ 12  $\mu$ S and for 1 mM Na<sup>+</sup> with 10 mM K<sup>+</sup> the conductance was  $\sim$ 5  $\mu$ S. In a solution with 10 mM Na<sup>+</sup> and 1 mM K<sup>+</sup> the conductance was  $\sim$ 13  $\mu$ S, and in a solution with 10 mM Na<sup>+</sup> and 10 mM K<sup>+</sup> the conductance was much lower, at  $\sim$ 6  $\mu$ S (Figure 4.19 B), but the conductance in both these solutions was greater than the

conductance in just 10 mM Na<sup>+</sup>, which was ~4 μS. The conductance of TaHKT1;5 in a solution of 30 mM Na<sup>+</sup> with 1 mM K<sup>+</sup> (~20 μS), was much greater than the conductance in just 30 mM Na<sup>+</sup> (~14 μS; Figure 4.19 C). These data indicate that, in general, there was greater conductance in solutions with both Na<sup>+</sup> and K<sup>+</sup> than in solutions with just Na<sup>+</sup>.

As the concentration of K<sup>+</sup> in the external solution increased 10-fold, from ~1 mM to ~10 mM, the  $E_{rev}$  became more negative, shifting from -105 mV to -123 mV. A further 10-fold increase external K<sup>+</sup> concentration, from ~10 mM to ~100 mM, lead to a positive shift in  $E_{rev}$ , from -123 mV to -70 mV (Figure 4.19 A).

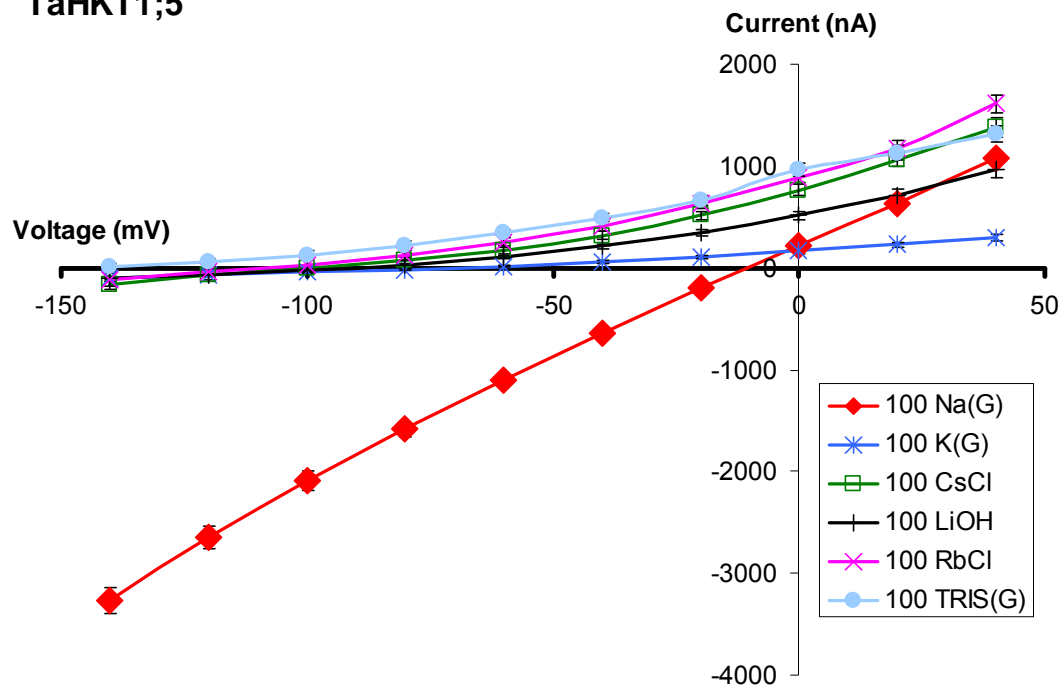
The conductance of TaHKT1;5 in a solution with 10 mM Na<sup>+</sup> did not change significantly when the pH was changed between 5.5, 6.5 or 7.5 (Figure 4.20 A). Nor did the conductance change significantly when the calcium concentration of the solution was increased from 2 to 5 to 10 mM, except for small changes at positive membrane potentials, which may be endogenous (Figure 4.20 B). Conductance of TaHKT1;5 in 10 mM Na<sup>+</sup> was not reduced by the addition of channel blocking solutions, gadolinium or flufenamate (Figure 4.20 C). These data are consistent with TaHKT1;5 being a Na<sup>+</sup> transporter, not a channel, and indicates that TaHKT1;5 functions independently of pH and Ca<sup>2+</sup> concentration.



**Figure 4.14: Currents over time in *TaHKT1;5-D* injected oocytes exposed to a range of solutions with varying  $\text{Na}^+$  and  $\text{K}^+$  concentrations**

Currents were observed in response to varying  $\text{Na}^+$  concentrations, but not  $\text{K}^+$ , other than a small endogenous current for 100 mM  $\text{K}^+$ . The membrane potential was held at -120 mV. Units for  $\text{Na}^+$  and  $\text{K}^+$  concentrations are in mM. 0 refers to the standard solution (See 4.2.3).

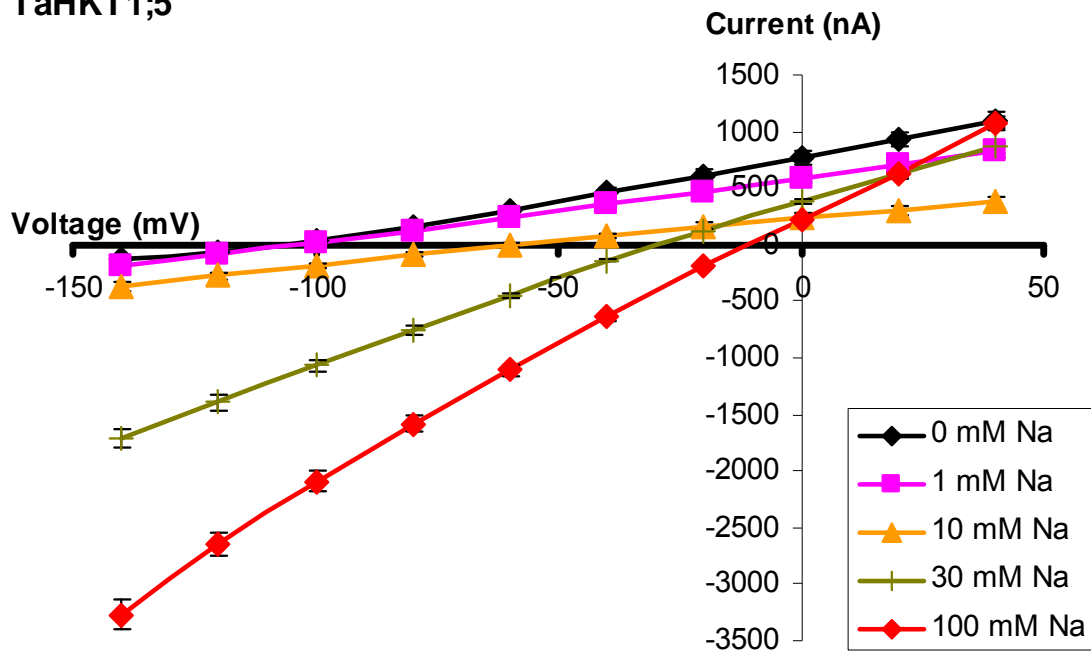
## TaHKT1;5



**Figure 4.15: Cation selectivity of oocytes injected with *TaHKT1;5-D* cRNA.**

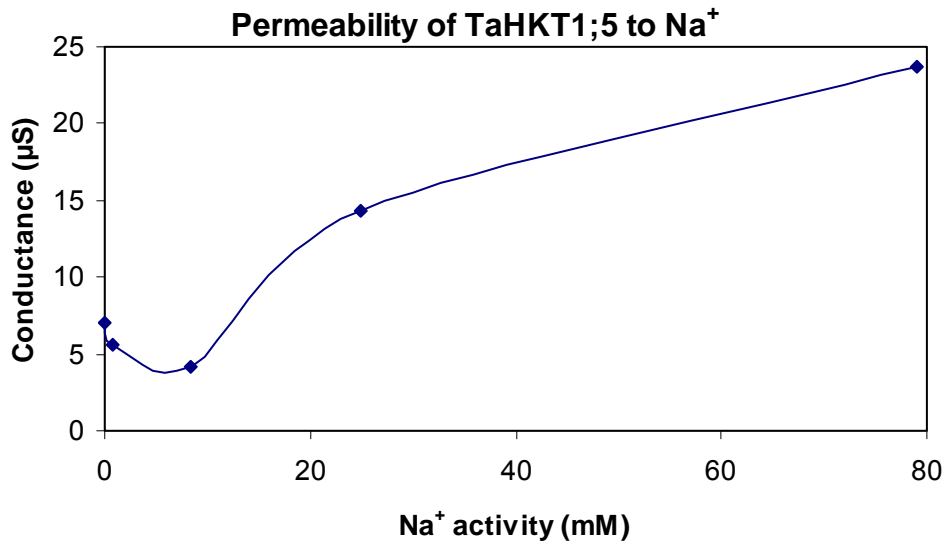
Oocytes were exposed to solutions with different salts. Large inward currents were observed in the presence of 100 mM  $\text{Na}^+$ . (G) is glutamate; Na is  $\text{Na}^+$ ; K is  $\text{K}^+$ ; concentrations are in mM. Error bars display SEM. Numbers of oocytes are listed in Appendix Table 4.1.

## TaHKT1;5

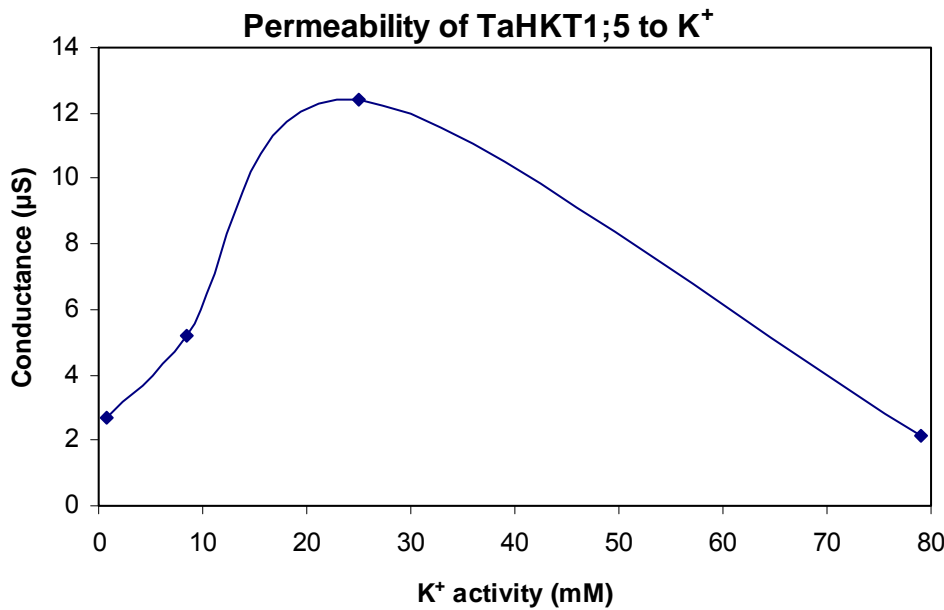


**Figure 4.16: Current-voltage curves for oocytes expressing TaHKT1;5-D in solutions with different Na<sup>+</sup> concentrations**

Oocytes were exposed to solutions with different Na<sup>+</sup> (glutamate) concentrations. The magnitude of inward currents increased with increasing Na<sup>+</sup> concentration. Na is Na<sup>+</sup>. Error bars display SEM. Numbers of oocytes are listed in Appendix Table 4.1.

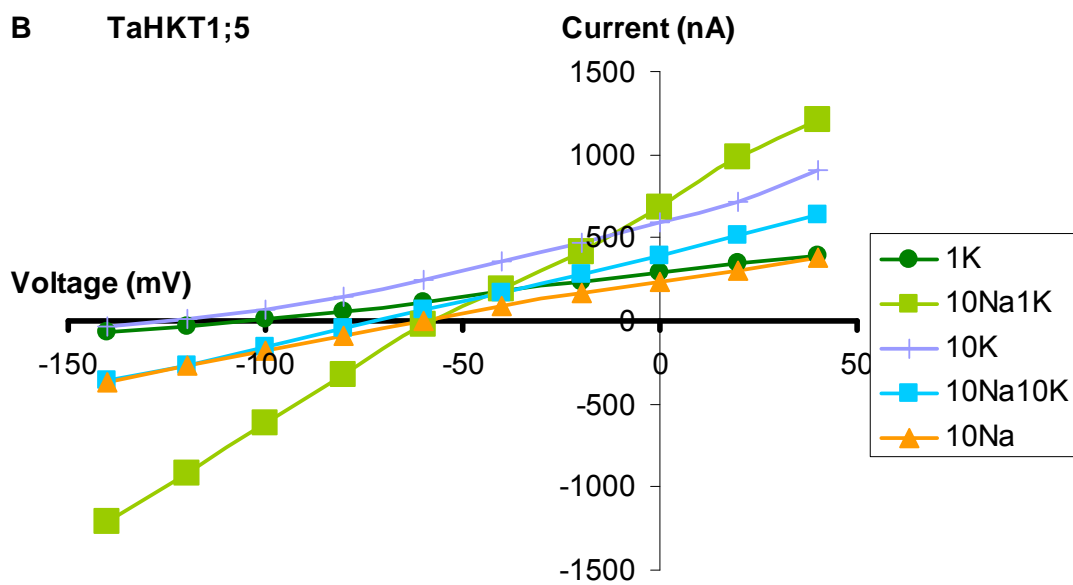
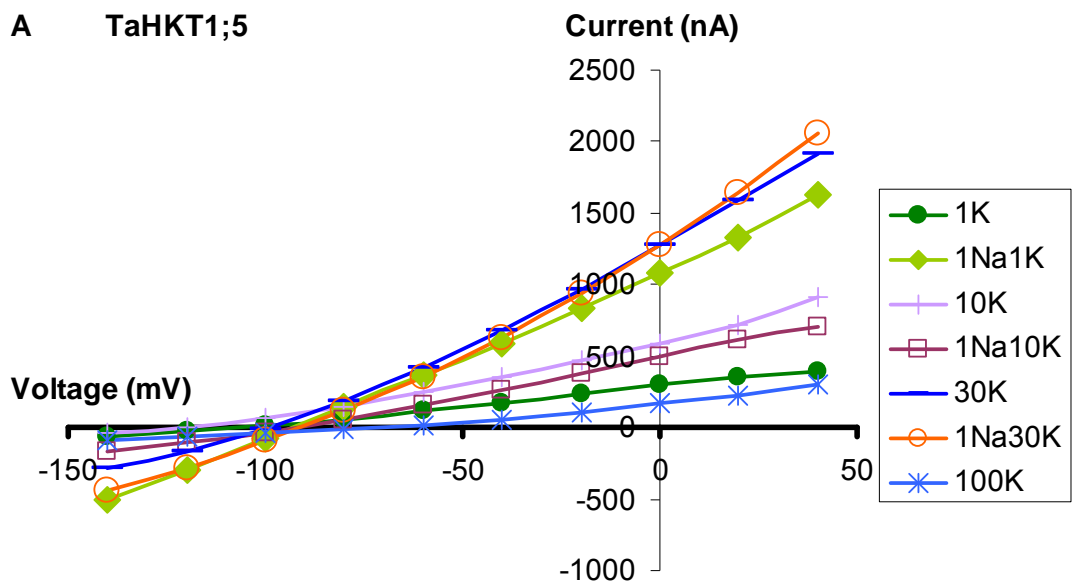


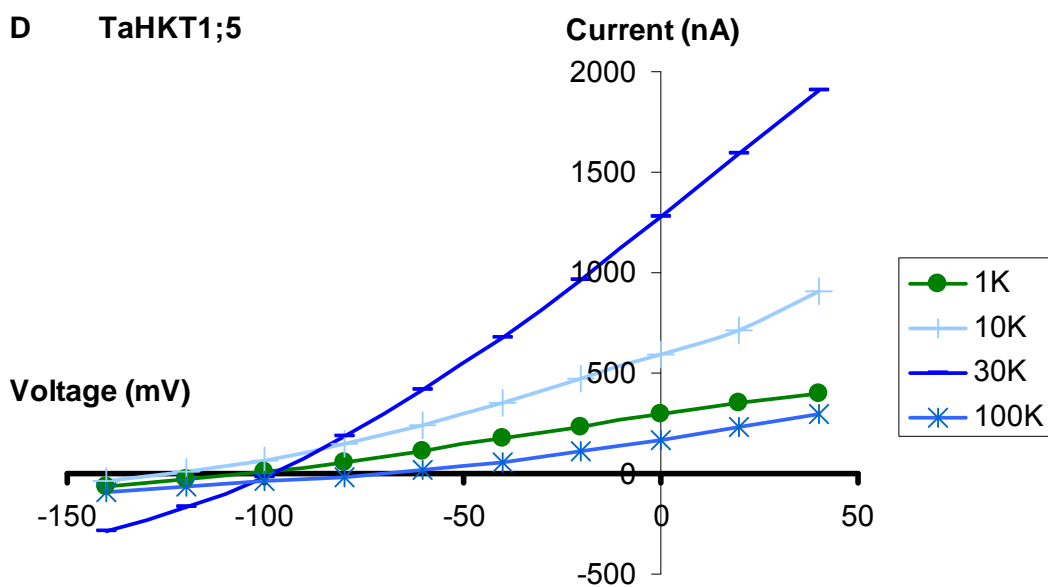
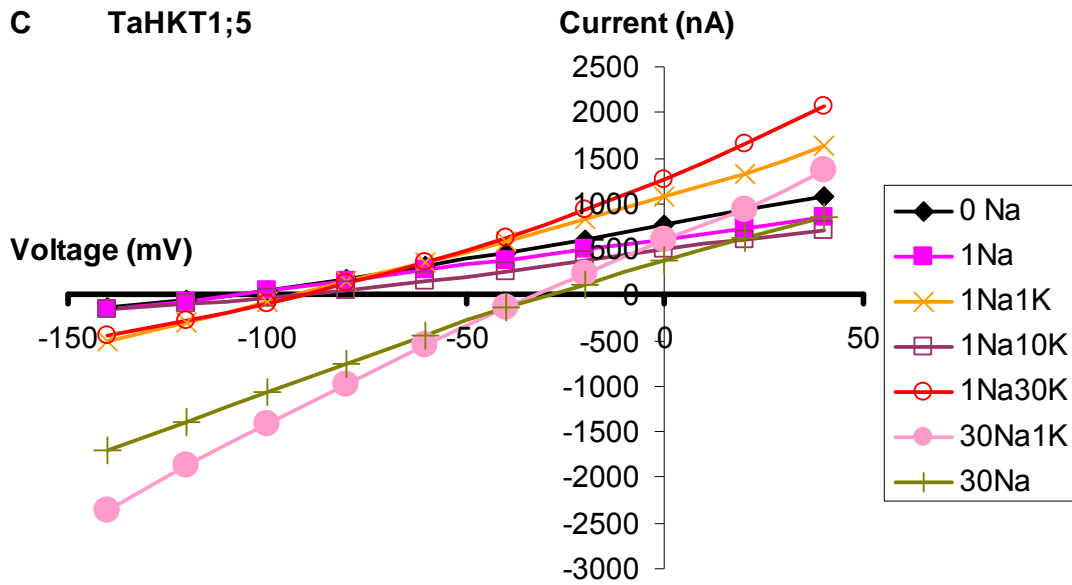
**Figure 4.17: Permeability of TaHKT1;5-D to Na<sup>+</sup>**  
 Conductance is in microsiemens (µS) of Na<sup>+</sup> by TaHKT1;5 in solutions of differing Na<sup>+</sup> activity when expressed in *Xenopus laevis* oocytes (n = 13). TaHKT1;5 is not saturated at 80 mM Na<sup>+</sup>.



**Figure 4.18: Permeability of TaHKT1;5-D to K<sup>+</sup>**  
 Conductance is in microsiemens (µS) of K<sup>+</sup> by TaHKT1;5 in solutions of differing K<sup>+</sup> activity when expressed in *Xenopus laevis* oocytes (n = 6). TaHKT1;5 conducts K<sup>+</sup> when the K<sup>+</sup> concentration in the external solution is approximately 30 mM but there is negligible conductance at lower and higher K<sup>+</sup> concentrations.

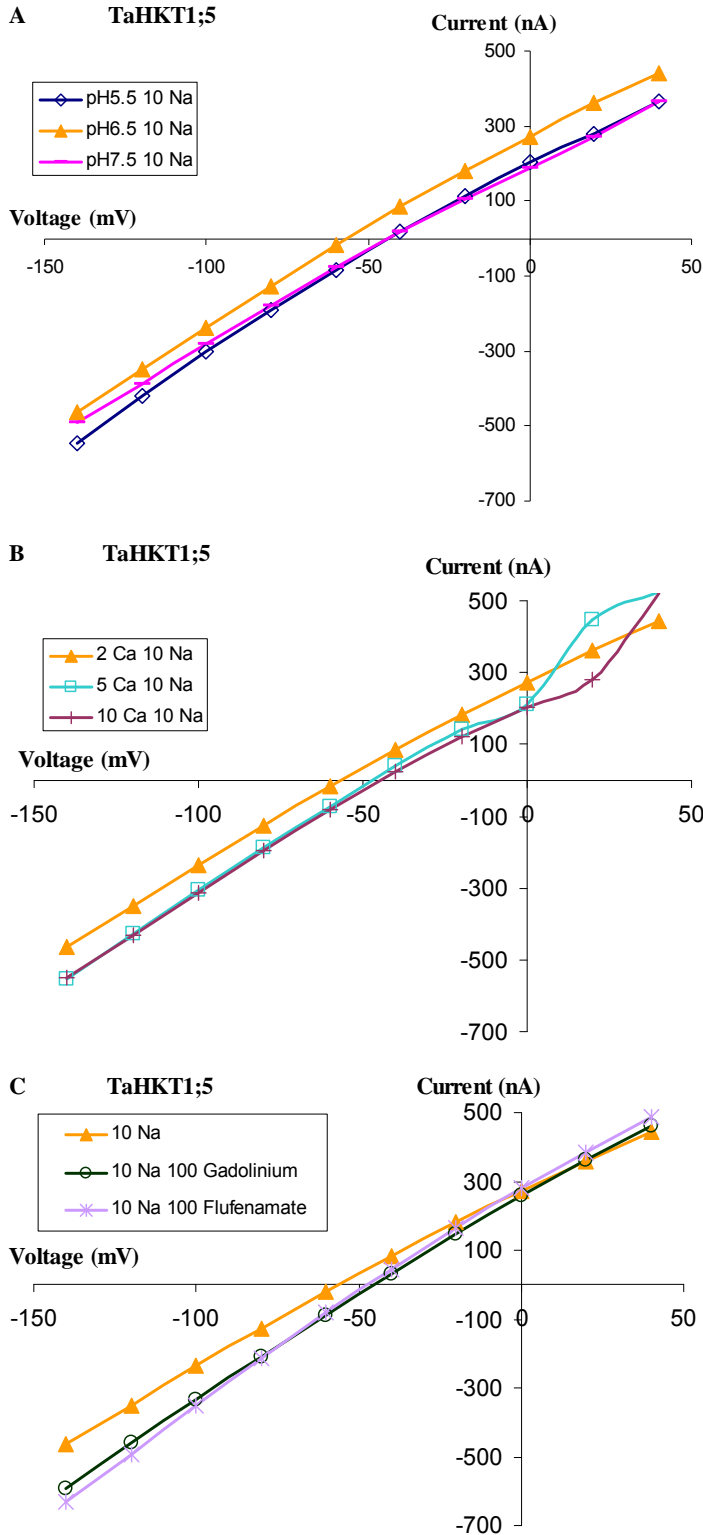






**Figure 4.19: Current-voltage curves for TaHKT1;5 expressing oocytes in solutions with different Na<sup>+</sup> and K<sup>+</sup> concentrations**

Oocytes were exposed to solutions with different combinations of Na<sup>+</sup> (glutamate) and K<sup>+</sup> (glutamate) concentrations. Various K<sup>+</sup> concentrations with and without 1 mM K<sup>+</sup> are compared (A). Solutions with 10 mM Na<sup>+</sup> with varying concentrations of K<sup>+</sup> are compared (B). Solutions with 1 or 30 mM and varying K<sup>+</sup> concentrations are compared (C). Solutions with no Na<sup>+</sup>, but increasing concentrations of K<sup>+</sup> are compared (D). Na is Na<sup>+</sup>; K is K<sup>+</sup>; units are mM. Numbers of oocytes are listed in Appendix Table 4.1.

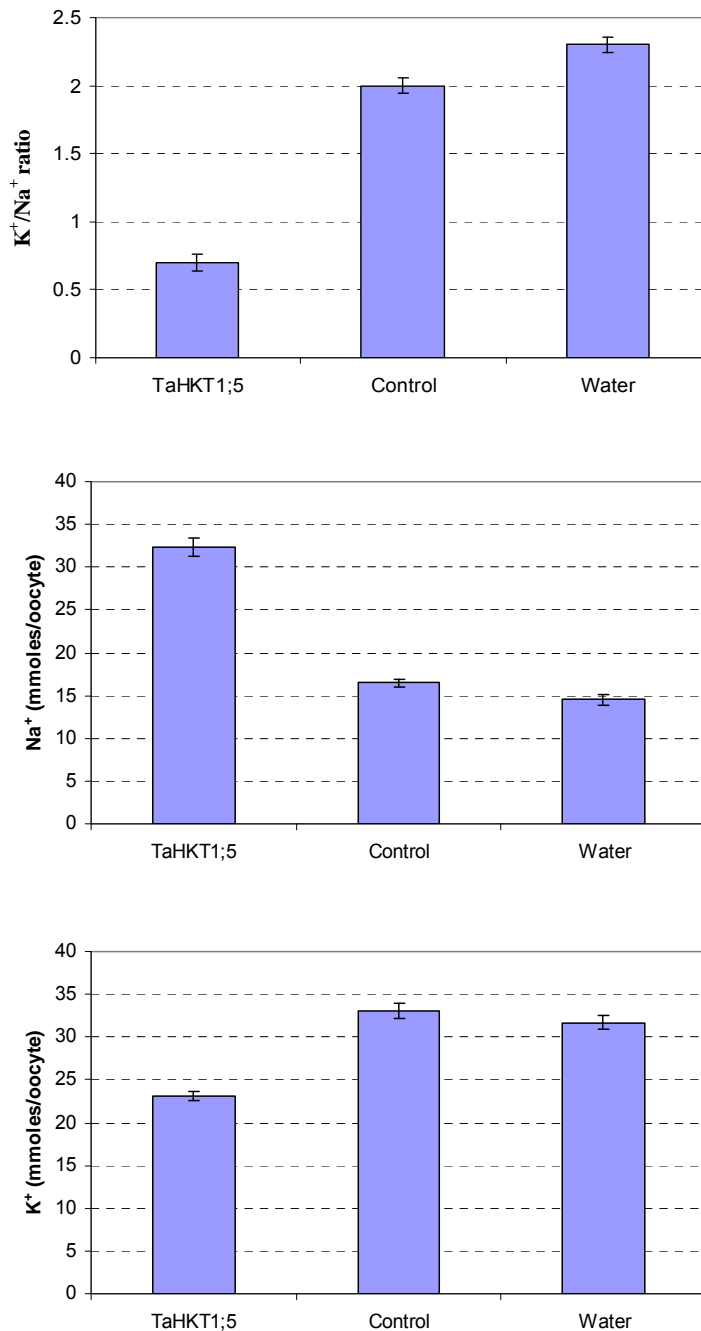


**Figure 4.20: Current-voltage curves for oocytes expressing TaHKT1;5-D in solutions of 10 mM Na<sup>+</sup> and differing pH, Ca<sup>2+</sup> and channel blockers**

Oocytes were exposed to solutions with 10 mM Na<sup>+</sup> (glutamate) concentrations and differing pH (A), CaCl<sub>2</sub> concentrations (B) and two different channel blockers (Gadolinium and Flufenamate) (C). Na is Na<sup>+</sup>. Numbers of oocytes are listed in Appendix Table 4.1.

#### 4.3.7 Total amount of $\text{Na}^+$ and $\text{K}^+$ extracted from oocytes expressing *TaHKT1;5-D*

Oocytes expressing *TaHKT1;5* had a lower  $\text{K}^+$  to  $\text{Na}^+$  ratio, double the moles of  $\text{Na}^+$ , and approximately two thirds the moles of  $\text{K}^+$  of water injected and uninjected oocytes (Figure 4.21). These data are consistent with *TaHKT1;5* facilitating the transport of  $\text{Na}^+$  into the oocyte. It is not clear from this data whether the lower moles of  $\text{K}^+$  from the *TaHKT1;5* expressing oocytes were due to *TaHKT1;5* facilitating the transport of  $\text{K}^+$  out of the oocytes, or whether endogenous proteins were transporting  $\text{K}^+$  out of the oocyte to counter the influx of  $\text{Na}^+$ .



**Figure 4.21: K<sup>+</sup>/Na<sup>+</sup> ratio and total moles of Na<sup>+</sup> and K<sup>+</sup> extracted from oocytes expressing *TaHKT1;5***

The K<sup>+</sup>/Na<sup>+</sup> ratio, and the total moles of Na<sup>+</sup> and K<sup>+</sup> extracted from *TaHKT1;5* expressing oocytes (n = 10) were compared to control oocytes (control refers to oocytes that have not been injected, n = 8) and water injected oocytes (water refers to oocytes injected with nuclease-free water, n = 11). Moles of Na<sup>+</sup> and K<sup>+</sup> extracted from 3 oocytes/sample were measured on a flame photometer after 3 days in modified Barth's solution, which containing 96 mM Na<sup>+</sup> (see materials and methods).

#### 4.3.8 Oocytes injected with *TmHKTI;5-A* cRNA did not exhibit the expected $\text{Na}^+$ transport activity

The current-voltage data recorded for oocytes injected with *TmHKTI;5-A* cRNA, when exposed to various solutions containing either  $\text{Na}^+$  or  $\text{K}^+$  (Figure 4.22 A) or both  $\text{Na}^+$  and  $\text{K}^+$  (Figure 4.22 B), were not significantly different to the current-voltage data recorded for water-injected oocytes in each of the respective solutions (Figure 4.3 B and C). For both water and *TmHKTI;5-A* injected oocytes a conductance of  $\sim 1 \mu\text{S}$  was recorded in solutions with various concentrations of  $\text{Na}^+$  and/or  $\text{K}^+$ .

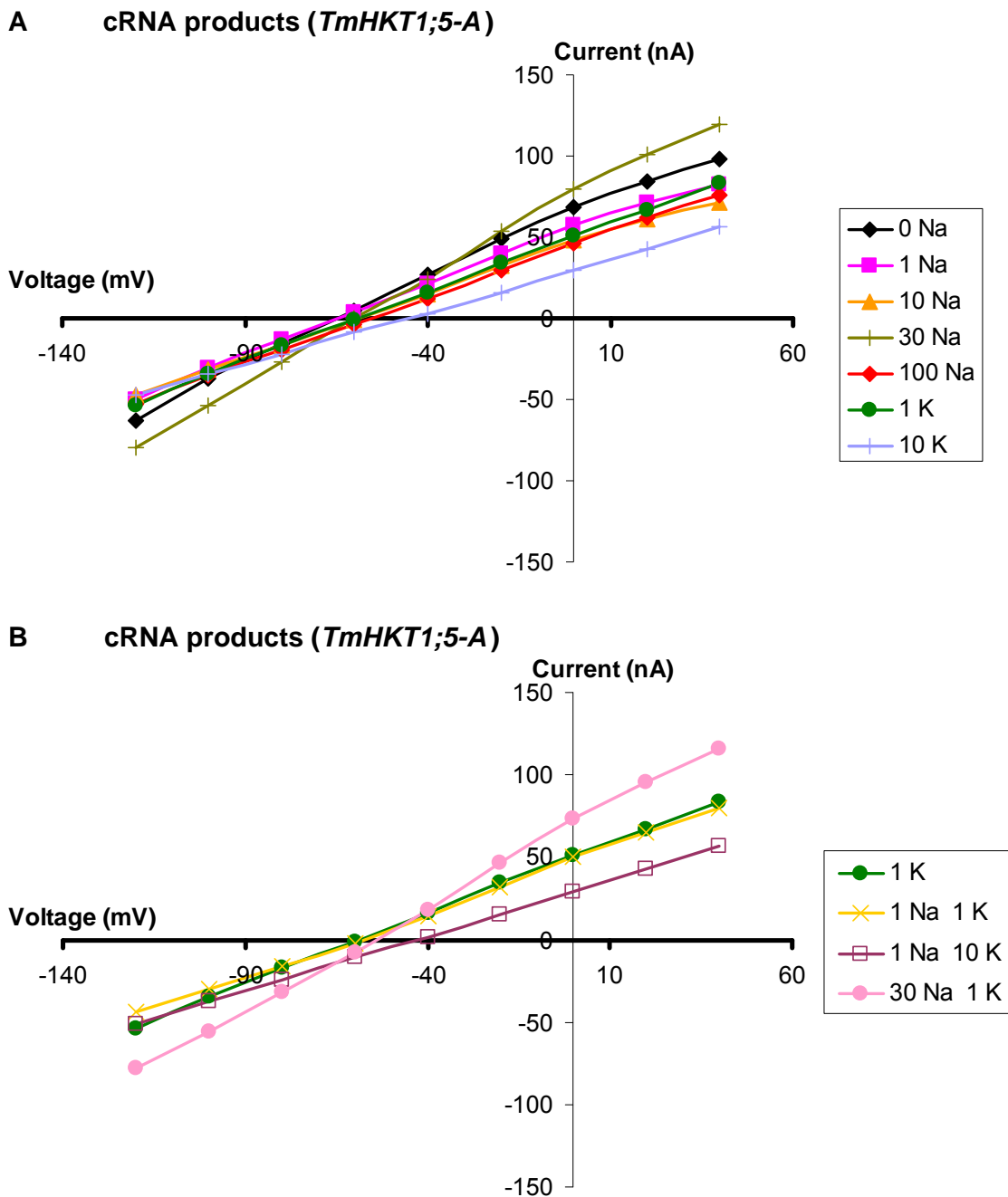
To check whether the *TmHKTI;5-A* cRNA might encode an electroneutral transporter, a possible explanation for the lack of currents, the total moles of  $\text{Na}^+$  and  $\text{K}^+$  of *TmHKTI;5-A* injected oocytes were compared to water injected oocytes and uninjected oocytes. The total moles of  $\text{Na}^+$  and  $\text{K}^+$  extracted from *TaHKTI;5-D* expressing oocytes was significantly different than water injected and uninjected oocytes (Figure 4.17), but there were no significant differences between *TmHKTI;5-A* cRNA injected oocytes and water injected or uninjected oocytes (Figure 4.23).

It may be that run off of the contaminating product in the *TmHKTI;5-A* cRNA sample lead to a lower concentration of the desired cRNA product, and the quantity of cRNA injected may affect conductance (Very et al., 1995). It might be anticipated that increasing the amount of cRNA injected would lead to greater conductance, so a greater quantity of *TmHKTI;5-A* cRNA was injected into oocytes to explore whether a greater concentration of cRNA would affect the transport properties of the oocyte.

The oocytes injected with concentrated cRNA product had slightly lower  $\text{K}^+$  to  $\text{Na}^+$  ratio, slightly more  $\text{Na}^+$  and slightly less  $\text{K}^+$ , but the difference was not significant and differences of similar magnitude were observed between water injected and uninjected oocytes. The  $\text{K}^+/\text{Na}^+$  ratio of uninjected oocytes, and oocytes injected with concentrated *TmHKTI;5* cRNA products was identical, and slightly lower than the  $\text{K}^+/\text{Na}^+$  of oocytes injected with water or dilute *TmHKTI;5* cRNA products, but the differences were not significant (Figure 4.23 A).

The total moles of  $\text{Na}^+$  extracted from oocytes injected with *TmHKTI;5* cRNA products was slightly higher than that of uninjected and water injected oocytes, but again the differences were not significant (Figure 4.23 B). The total moles of  $\text{K}^+$  extracted from oocytes injected with concentrated *TmHKTI;5* cRNA products was less than that of oocytes injected with dilute *TmHKTI;5* cRNA, and slightly less than uninjected oocytes, but it was greater than water injected oocytes (Figure 4.23 C). It is puzzling that the total moles of  $\text{K}^+$  extracted

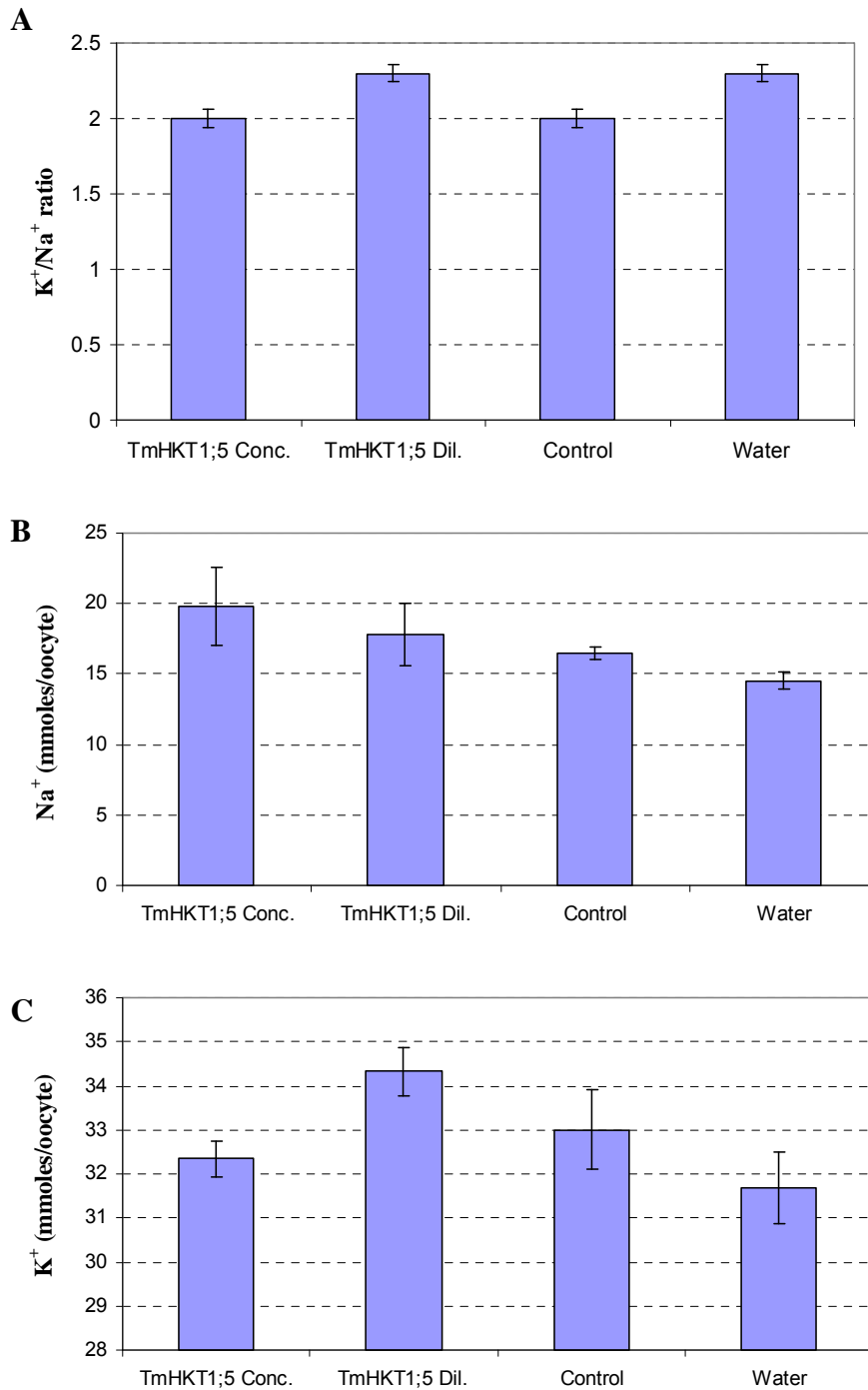
from oocytes injected with dilute *TmHKT1;5* cRNA products was greater than the total moles of  $K^+$  extracted from water injected oocytes. Had the uninjected oocytes not been included in this experiment then these data may have mistakenly been interpreted as significant.



**Figure 4.22: Current-voltage curves for oocytes injected with cRNA products transcribed from pGEMHE containing the cDNA for *TmHKT1;5-A***

Oocytes were exposed to solutions with various  $\text{Na}^+$  or  $\text{K}^+$  concentrations (A) ( $n \geq 8$ ), or various combinations of  $\text{Na}^+$  and  $\text{K}^+$  (B). Na is  $\text{Na}^+$  (glutamate); K is  $\text{K}^+$  (glutamate); concentration in mM. Numbers of oocytes are listed in Appendix Table 4.1.





**Figure 4.23:  $K^+/Na^+$  ratio and total moles of  $Na^+$  and  $K^+$  extracted from oocytes injected with different concentrations of *TmHKT1;5-A* in vitro-transcribed RNA products**  
 Conc. = concentrated RNA injected (46 ng) (n = 7). Dil. = dilute RNA injected (23 ng) (n = 9). Control refers to oocytes that have not been injected (n = 8). Water refers to oocytes injected with water (n = 11). Each sample (n) included 3 oocytes. Moles of  $Na^+$  and  $K^+$  were measured by Flame Photometer after 3 days in Calcium Ringers containing 96 mM  $Na^+$ .

#### 4.3.9 Potassium transport by HKTs

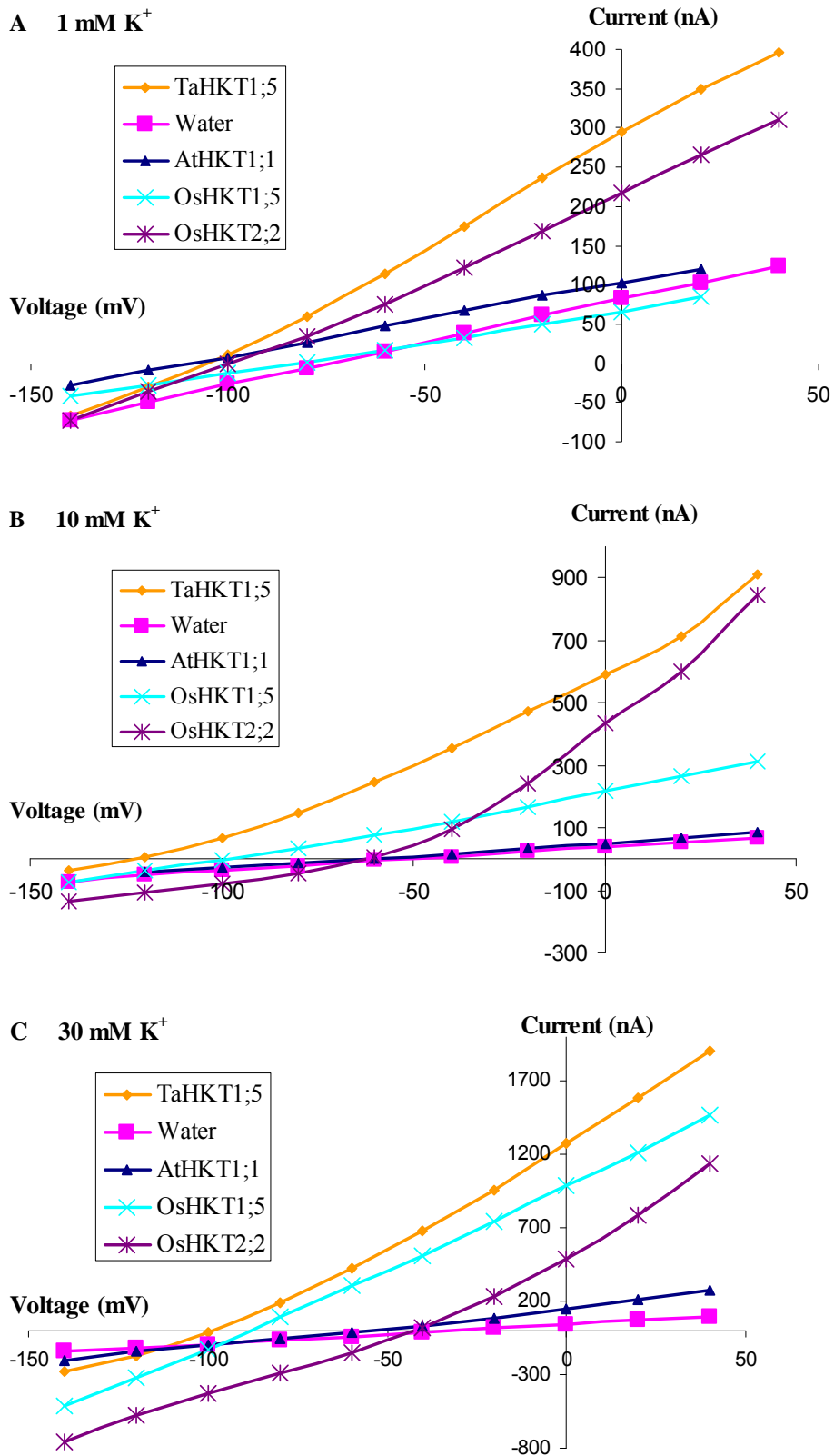
In the presence of an external solution containing 1 mM K<sup>+</sup>, the  $E_{rev}$  for water injected oocytes was -75 mV, the  $E_{rev}$  for each of the HKT-expressing oocytes was more negative than the  $E_{rev}$  of the water injected oocytes, OsHKT1;5 was -80 mV, OsHKT2;2 was -100, TaHKT1;5 was -105 and AtHKT1;1 was -110 mV (Figure 4.24 A).

In the presence of an external solution containing 10 mM K<sup>+</sup>, the  $E_{rev}$  for water injected oocytes was -55 mV, the  $E_{rev}$  for each of the HKT-expressing oocytes was again more negative than the  $E_{rev}$  of the water injected oocytes, OsHKT2;2 was -62, AtHKT1;1 was -62 mV, OsHKT1;5 was -100 mV and TaHKT1;5 was -123 (Figure 4.24 B).

Therefore, in response to a 10-fold increase in Na<sup>+</sup> activity, the  $E_{rev}$  of TaHKT1;5 and OsHKT1;5 became ~20 mV more negative, where as the  $E_{rev}$  of the water injected oocytes became ~20 mV more positive, the  $E_{rev}$  of AtHKT1;1 became ~48 mV more positive and the  $E_{rev}$  of OsHKT2;2 became ~38 mV more positive.

In 30 mM K<sup>+</sup>, TaHKT1;5 again had the most negative  $E_{rev}$  (-100 mV), followed by OsHKT1;5 (-87 mV). The  $E_{rev}$  of AtHKT1;1 (-53 mV), and OsHKT2;2 (-42 mV), were still more negative than the  $E_{rev}$  of water injected oocytes (-33 mV; Figure 4.24 C).

In the presence of an external solution containing 30 mM K<sup>+</sup>, TaHKT1;5 had a similar conductance (~12  $\mu$ S), to OsHKT1;5 (~11  $\mu$ S) and OsHKT2;2 (~10  $\mu$ S), and AtHKT1;1 had a much lower conductance (~3  $\mu$ S), although the conductance for AtHKT1;1 was still greater than the conductance for water injected oocytes (~1  $\mu$ S; Figure 4.24 C). In the presence of an external solution containing 1 or 10 mM K<sup>+</sup>, TaHKT1;5 and OsHKT2;2 had significantly greater conductance than AtHKT1;1 and OsHKT1;5 (Figure 4.24 A and B).



**Figure 4.24: Current-voltage curves for oocytes expressing different HKTs in solutions with 30 mM K<sup>+</sup>**

Oocytes were exposed to solutions with 1 mM K<sup>+</sup> (A), 10 mM K<sup>+</sup> (B) and 30 mM K<sup>+</sup> (C). K<sup>+</sup> is potassium glutamate. Numbers of oocytes are listed in Appendix Table 4.1.

## 4.4 Discussion

### 4.4.1 Transcription of RNA encoding plant HKTs

The contaminating bands in the *in vitro* RNA transcription may be due to incomplete digestion of the plasmid DNA, despite overnight digestion. Alternatively some other contaminant may be present such as left over plasmid DNA, despite a DNase treatment step. Problems with unwanted production of significant amounts of long, template-sized RNA transcripts from vector DNA have been described in the literature (Schenborn and Mierendorf, 1985; Hartje et al., 2000). In future work a step to blunt the ends of the linearised plasmid DNA could be undertaken to test if this prevents the occurrence of contaminating bands.

### 4.4.2 Currents in water-injected oocytes

Endogenous currents in water-injected oocytes were observed occasionally in some, but not all, experiments in response to an external solution containing 100 mM K<sup>+</sup> (Figure 4.2 B). Endogenous inward currents have been observed previously, in solutions containing K<sup>+</sup>, when oocyte membrane potentials were negative (Véry et al., 1995). Endogenous currents may also be activated by hyperpolarizing pulses which may activate Ca<sup>2+</sup>-sensitive and Ca<sup>2+</sup>-insensitive currents in *Xenopus* oocytes (Schachtman et al., 1992; Kowdley et al., 1994).

### 4.4.3 Currents in *AtHKT1;1* and *OsHKT1;5* injected oocytes

Data indicating that *OsHKT1;5* and *AtHKT1;1* transported Na<sup>+</sup> into the oocyte when the membrane potential was negative was consistent with previous studies (Uozumi et al., 2000; Ren et al., 2005). However, data for *OsHKT1;5* when both Na<sup>+</sup> and K<sup>+</sup> were present in the external solution, and when specific concentrations of K<sup>+</sup>, such as 10 mM and 30 mM K<sup>+</sup>, were present in the solution, indicated that *OsHKT1;5* may not be a Na<sup>+</sup>-specific transporter. This conflicts with the proposed function for *OsHKT1;5* suggested by Ren et al., (2005), and conflicts with the hypothesis that group 1 HKT-type proteins transport Na<sup>+</sup> only (Platten et al., 2006). However, these observations may be specific to the *in vitro* conditions and may not be relevant to *in planta* protein activity.

The addition of 10 mM K<sup>+</sup> to a solution of 10 mM Na<sup>+</sup> and the addition of 1 mM K<sup>+</sup> to a solution of 30 mM Na<sup>+</sup> lead to much greater conductance for *OsHKT1;5* than observed for just 10 mM Na<sup>+</sup> or 30 mM Na<sup>+</sup>, respectively (Figure 4.8 B). There were also much greater conductance for solutions of 1 mM Na<sup>+</sup> when 1 or 10 mM K<sup>+</sup> were present (Figure 4.8 B), and significant conductance was observed for *OsHKT1;5* expressing oocytes when the external solution contained 30 mM K<sup>+</sup> compared to the conductance in solutions with various

concentrations of Na<sup>+</sup> (Figure 4.8 A). It is possible that this may be due to efflux of K<sup>+</sup> through OsHKT1;5 but it is also possible that the presence of K<sup>+</sup> changes the transport properties of the protein without K<sup>+</sup> necessarily being transported. There was insufficient information to make a conclusion as to whether the conductance recorded for OsHKT1;5 in solutions containing K<sup>+</sup> was due to the transport of K<sup>+</sup>.

It was expected that the conductance and  $E_{rev}$  for AtHKT1;1 would remain constant when the concentration of external K<sup>+</sup> changed, as this had been described previously (figure 4C, Uozumi et al., 2000). In ~1 and ~10 mM external K<sup>+</sup> the conductance for AtHKT1;1 was not significantly different to that of water injected oocytes (~1  $\mu$ S), but in ~30 and ~100 mM external K<sup>+</sup> the conductance was greater, at ~3  $\mu$ S (Figure 4.6 A). However, in the previous study the maximum concentration of K<sup>+</sup> tested was 10 mM (Uozumi et al., 2000). In response to increases in external K<sup>+</sup> concentration the  $E_{rev}$  for AtHKT1;1 expressing oocytes became more positive, shifting from -90 mV in ~1 mM K<sup>+</sup> to -60 mV in ~10 mM K<sup>+</sup>. This was not consistent with previous data where the  $E_{rev}$  did not change when the external K<sup>+</sup> concentration was increased from 1 to 10 mM (Uozumi et al., 2000).

#### 4.4.4 Absence of activity for Pokkali OsHKT1;5 and TmHKT1;5-A

No currents were observed in oocytes injected with *TmHKT1;5-A* or Pokkali *OsHKT1;5* cRNA (Figure 4.22 and 4.10). The absence of activity for Pokkali *OsHKT1;5*, and *TmHKT1;5-A* was puzzling, as the Nipponbare *OsHKT1;5*, and *TaHKT1;5-D*, transporters actively transported Na<sup>+</sup> and the amino acid identities between these two *Oryza sativa* and two *Triticum* proteins are 98% and 94%, respectively.

There are many reasons why the injection of cRNA into an oocyte may not lead to changes in conductance. The oocyte may not translate the protein encoded by the cRNA, or the oocyte may not process the translated product properly. The protein may not be folded correctly, or the protein may not be targeted to the plasma membrane. The absence of activity for Pokkali *OsHKT1;5* cRNA injected oocytes, and *TmHKT1;5-A* cRNA injected oocytes, may have been for any of these reasons, in addition to the obvious option that a non-functional protein is encoded by this gene.

Alternatively, the absence of activity may have been because the Pokkali *OsHKT1;5* and *TmHKT1;5-A* cRNA products had contaminating bands of sizes larger than expected (Figure 4.1). However, the *AtHKT1;1* cRNA sample had products of larger than expected sizes (Figure 4.1 B), and oocytes injected with these cRNA samples exhibited transport properties consistent with those described in the literature (Uozumi et al., 2000), and the

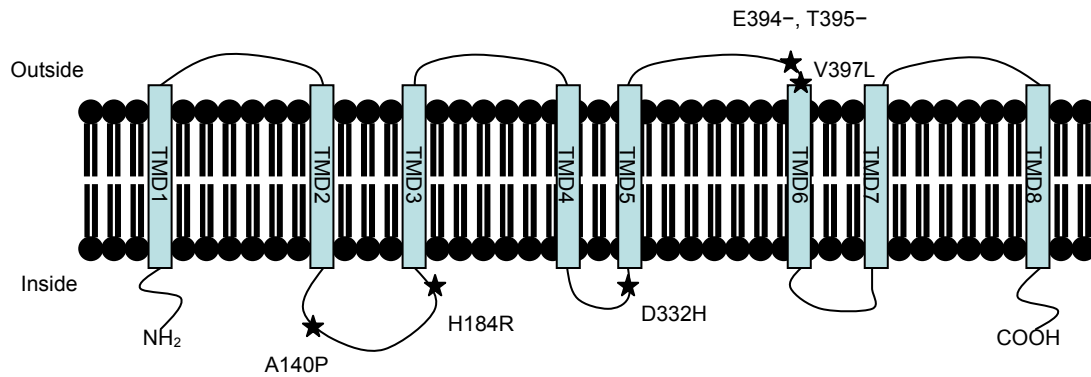
Nipponbare OsHKT1;5 exhibited activity consistent with previous results for OsHKT1;5 (compare Figure 4.7 with Ren et al., 2005), despite the Nipponbare OsHKT1;5 cRNA sample having faint larger bands (Figure 4.1).

Four amino acids differed between OsHKT1;5 alleles from Nona Bokra and Koshihikari (Ren et al., 2005). These may or may not explain the difference in flux between the two alleles; the Nona Bokra allele being more active than the Koshihikari allele. These four differing amino acids were A140P, H184R, D332H and V395L, in Nona Bokra and Koshihikari respectively. Two of these are conservative substitutions (H184R and V395L), and another is in a poorly conserved region (A140P), but the fourth (D332H) is a possible candidate for conferring the increased flux for the Nona Bokra allele.

Seven amino acids (AAs) differ between the Pokkali and Nipponbare OsHKT1;5 alleles (Olivier Coftsaftis, personal communication, July 2007). Of these seven, four substitutions (A140P, H184R, D332H, V397L) are similar, or the same as those between Nona Bokra and Koshihikari, with the Pokkali allele being more like the Nona Bokra allele and the Nipponbare allele being more like the Koshihikari allele, for these specific residues (Figure 4.25). There is another substitution where an alanine is present in the Nipponbare allele, at amino acid number 406, where there is a valine in the Nona Bokra, Koshihikari and Pokkali alleles, but this substitution is conservative. Therefore, the only outstanding difference in the Pokkali allele sequence is two additional amino acids, glutamine (E) and threonine (T) (at 394 and 395; Figure 4.25). As the Nona Bokra, Koshihikari and Nipponbare OsHKT1;5 transporters have all been found to be active in the *Xenopus* oocyte expression system, and we found that the Pokkali OsHKT1;5 was not, it leads to the question as to whether these two additional amino acids in the Pokkali OsHKT1;5 allele are the reason that this transporter did not exhibit activity in the oocyte expression system.

In total there are 24 amino acids that differ between TaHKT1;5-D and TmHKT1;5-A. Sixteen of these are in poorly conserved regions. A further four are conservative substitutions. This leaves T69M, R331N and W407C differing between TaHKT1;5-D and TmHKT1;5-A, respectively, and an additional aspartic acid residue (471) in TmHKT1;5-A. Any, all, or none of these substitutions may be the reason that TmHKT1;5-A was not active, and TaHKT1;5-D was active, in the *Xenopus* expression system. It could be that the additional aspartic acid in TmHKT1;5-A, not present in TaHKT1;5-D, is the reason that the TmHKT1;5-A transporter was not active, similar to that which was proposed as a reason that the Pokkali OsHKT1;5 allele was not active. However, the additional aspartic acid residue (471) in TmHKT1;5-A is in a different region of the protein to the additional glutamine and threonine residues in

Pokkali OsHKT1;5 (394 and 395). Still, it is curious that these two particularly divergent alleles, Pokkali OsHKT1;5 and TmHKT1;5-A, were the only two transporters that were not active in the *Xenopus* oocyte expression system.



**Figure 4.25: Structural model of OsHKT1;5**

A model adapted from figure 2 from Ren et al. (2005) showing the likely structure of OsHKT1;5 based on predicted hydrophobicity. TMD = trans-membrane domain. Stars indicate positions of residue substitutions of interest between Pokkali and Nipponbare alleles.

#### 4.4.5 Does HKT1;5 transport $\text{Na}^+$ only, or $\text{Na}^+$ and $\text{K}^+$ ?

In the presence of large concentrations (100 mM) of  $\text{K}^+$ ,  $\text{Cs}^+$ ,  $\text{Li}^+$ ,  $\text{Rb}^+$  or TRIS, no significant conductance was observed for TaHKT1;5 expressing oocytes (Figure 4.15). Conductance observed for TaHKT1;5-D expressing oocytes in bath solutions containing  $\text{Na}^+$  indicate that TaHKT1;5-D transports  $\text{Na}^+$  (Figures 4.14 and 4.16). The conductance, in response to the presence of external  $\text{Na}^+$ , generally increased relative to increasing  $\text{Na}^+$  activity in the external solution (with the exception of 10 mM  $\text{Na}^+$ , Figure 4.16), and the transporter may not have been saturated, even in bath solutions containing 100 mM  $\text{Na}^+$  (Figure 4.17).

A 10-fold increase in the external  $\text{Na}^+$  activity lead to an increase in the  $E_{\text{rev}}$  of approximately +50 for TaHKT1;5-D expressing oocytes (Figure 4.16), this is close to the Nernst potential for  $\text{Na}^+$ , which is approximately +55 mV.

The conductance of  $\text{Na}^+$  was not affected by external pH, calcium or channel blockers (Figure 4.20). In recordings of currents over time for TaHKT1;5-D expressing oocytes, in bath solutions with 1 mM  $\text{K}^+$ , 10 mM  $\text{K}^+$ , or 100 mM  $\text{K}^+$ , there appeared to be no conductance of  $\text{K}^+$  (Figure 4.19 A). From these data, one might suggest that TaHKT1;5-D is a  $\text{Na}^+$ -specific transporter, but further experiments indicated otherwise.

Conductance observed for TaHKT1;5-D expressing oocytes in bath solutions with 1 mM  $\text{Na}^+$  and 1 mM  $\text{K}^+$  was double the conductance observed for these oocytes in bath solutions with only 1 mM  $\text{Na}^+$  (Figure 4.19 C). Similarly, conductance in solutions with 10 mM  $\text{Na}^+$  and 1 mM  $\text{K}^+$  was more than three times the conductance in just 10 mM  $\text{Na}^+$  (Figure 4.19 B). Conductance in solutions of 30 mM  $\text{Na}^+$  and 1 mM  $\text{K}^+$  was 1.4 times greater than the conductance in just 30 mM  $\text{Na}^+$  (Figure 4.19 C). Therefore, the addition of 1 mM  $\text{K}^+$ , to bath solutions containing  $\text{Na}^+$ , is somehow increasing the conductance of TaHKT1;5-D expressing oocytes.

This is not exactly the case for greater  $\text{K}^+$  concentrations. Adding 10 mM  $\text{K}^+$  to a 1 mM  $\text{Na}^+$  solution more than halved the conductance. Adding 30 mM  $\text{K}^+$  to a 1 mM  $\text{Na}^+$  solution did not affect the conductance (Figure 4.19 C). Adding 10 mM  $\text{K}^+$  to a 10 mM  $\text{Na}^+$  solution increased the conductance slightly (6  $\mu\text{S}$ ) compared to 10 mM  $\text{Na}^+$  (4  $\mu\text{S}$ ; Figure 4.19 B). These data indicated that the TaHKT1;5-D transporter is not impervious to the presence of  $\text{K}^+$  in the bath solution and that transport properties change in response to changes in the external concentration of  $\text{K}^+$ . Unfortunately, these data alone do not indicate whether TaHKT1;5-D actually transports  $\text{K}^+$  or whether TaHKT1;5-D simply transports more  $\text{Na}^+$  in the presence of 1 mM  $\text{K}^+$ .



The large conductance observed for TaHKT1;5-D expressing oocytes, in the presence of 10 and 30 mM  $K^+$  was puzzling. This may indicate that TaHKT1;5-D both influxes  $Na^+$  and effluxes  $K^+$ . TaHKT1;5-D expressing oocytes had double the moles of  $Na^+$  and approximately one third less moles of  $K^+$  than control oocytes (Figure 4.21). However, one cannot interpret whether the differences in total moles of  $Na^+$  and  $K^+$  support the idea that TaHKT1;5-D is effluxing  $K^+$  as these differences could be due to endogenous oocyte channels or transporters dumping  $K^+$  to try and maintain charge and osmotic balance in response to the artificially high quantity of  $Na^+$  due to the activity of TaHKT1;5-D. Hence it can only be concluded that further work is needed to determine if TaHKT1;5-D transports  $K^+$ .

It may be that at specific concentrations of external  $K^+$ , such as 30 mM, there was an anomalous mole fraction effect stimulating these currents. Maybe there is a  $K^+$  and  $Ca^{2+}$  interaction, at particular  $K^+$  concentrations only, allowing permeation of  $Ca^{2+}$  leading to an  $Ca^{2+}$  activated  $Cl^-$  channel taking in  $Cl^-$ , leading to these currents. One could check this by eliminating extra-cellular  $Ca^{2+}$  or extra-cellular  $Cl^-$  to see if the current disappears, or adding a  $Cl^-$  channel blocker such as flufenamic acid or nilflumic acid. Alternatively to check whether the currents really were due to  $K^+$  efflux, one could check the theoretical reversal potential of  $K^+$  (and  $Cl^-$ ), and the reversal potential of this current through the protein. This is done by flicking to different voltages whilst the current is active and finding the specific voltage, at which the current is activated, and then collecting the tail current data and plotting this against the voltage to determine the specific ion that is moving and leading to the current. It was puzzling that significant conductance in the presence of external  $K^+$  was observed for both TaHKT1;5 and OsHKT1;5 but not AtHKT1;1, and that it made TaHKT1;5 and OsHKT1;5 seem as though they had properties more like the group 2 transporter, OsHKT2;2, than the group 1 transporter, AtHKT1;1 (Figure 4.24).

#### 4.4.6 Summary

In the presence of external  $Na^+$ , at negative membrane potentials, TaHKT1;5 facilitated the transport of  $Na^+$  into the oocytes. In addition to transporting  $Na^+$ , TaHKT1;5 may conduct  $K^+$ , but TaHKT1;5 was not permeable to other cations ( $Cs^+$ ,  $Li^+$ ,  $Rb^+$  or TRIS). The transport properties of HKT1;5 were not significantly affected by changes in external pH, external  $Ca^{2+}$  or channel blockers. The transport properties of the wheat HKT1;5 were similar to those of the rice HKT1;5.

## Chapter 5: RNA interference to induce silencing of *TaHKT1;5-D*

### 5.1 Introduction

The *Knal* gene on chromosome 4D confers, on hexaploid wheat, a phenotype of low leaf  $\text{Na}^+$  and a high leaf  $\text{K}^+$  to  $\text{Na}^+$  ratio. Chinese Spring substitution lines lacking chromosome 4D had lower  $\text{K}^+$  to  $\text{Na}^+$  ratios than the substitution lines with chromosome 4D (Gorham et al., 1987). Langdon substitution lines with and without the *Knal* region were different in their leaf  $\text{K}^+$  to  $\text{Na}^+$  ratio (Dvorak and Gorham, 1992). Lines with *Knal* had leaf  $\text{K}^+$  to  $\text{Na}^+$  ratios six to eight times higher than those without *Knal* (Dvořák and Gorham, 1992).

*Knal* and the *TaHKT1;5-D* gene co-locate to the distal end of chromosome 4DL on the D genome of bread wheat, so *TaHKT1;5-D* was therefore a candidate gene for *Knal* (See Chapter 2). Loss of the region containing *TaHKT1;5-D* in Chinese Spring deletion lines corresponded to an increase in average  $\text{Na}^+$  concentrations in the leaf blade and a six fold decrease in the  $\text{K}^+$  to  $\text{Na}^+$  ratio from 7.5 to 1.2 (Figure 2.6). However, this is a large region, comprising the distal 14% of chromosome 4DL, and it may contain other genes involved in controlling  $\text{Na}^+$  and or  $\text{K}^+$  transport. *In planta* proof of function is required to test whether *TaHKT1;5-D* confers the phenotype of leaf  $\text{K}^+$  to  $\text{Na}^+$  discrimination attributed to *Knal*.

#### 5.1.1 RNA interference in plants

RNA interference (RNAi) is a post-transcriptional gene-silencing technology that can be used to investigate gene function in plants. RNAi, induced by the introduction of an antisense or hairpin construct, takes advantage of a sequence-specific RNA degradation mechanism inherent in plants. Constructs are designed to form double-stranded RNA products homologous in sequence to the targeted gene. Double-stranded products are detected by the plant genome as abnormal and are cleaved by dicer-like enzymes into short and long small interfering RNAs (Hamilton and Baulcombe, 1999). In association with an RNA-induced silencing complex, small interfering RNAs direct the cleavage of endogenous mRNA transcripts. The small interfering RNAs, usually 21-26 bp, trigger systemic silencing, and may also lead to methylation of homologous DNA (Hamilton et al., 2002; Fu et al., 2007).

A recent review of the use of RNAi for functional gene analysis in wheat by Fu et al. (2007) highlighted the following successful attempts to silence specific genes with important functions: silencing of *vernalisation 2* (*VRN2*) mRNA levels to 40% leading to a 40 day acceleration of flowering (Yan et al., 2004); silencing of *vernalisation 1* (*VRN1*) mRNA to 19% delaying flowering by 2 weeks (Loukoianov et al., 2005); reduction of seed amylase by

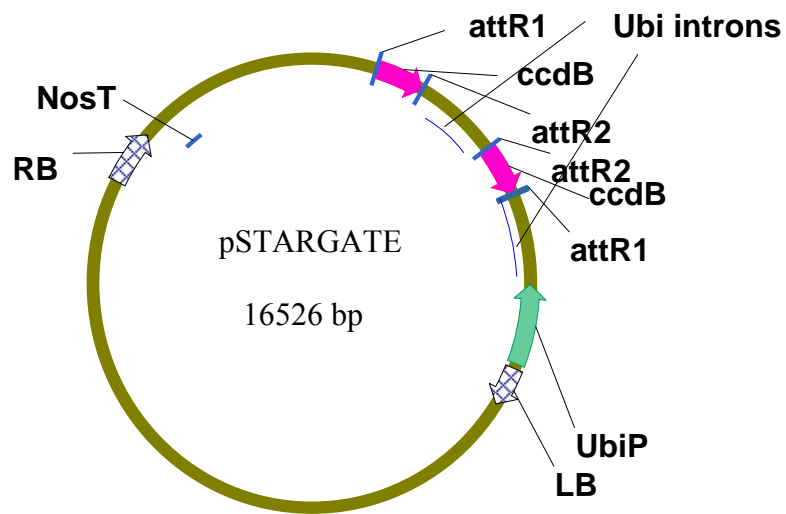
RNAi-induced reduction of *granule-bound starch synthase (GBSSI)* transcripts (Li et al., 2005); and silencing the *phytoene desaturase (PDS)* gene transcripts to around 10% and 50% of control levels, leading to albino and streaked leaf phenotypes respectively (Travella et al., 2006).

Research into the control of the degree of silencing induced by RNAi is still in its infancy. Five important observations relevant to RNAi in wheat include:

- Homozygous transgenic plants tend to have a stronger reduction of the target transcripts, accumulate more small interfering RNA, and have a greater change in phenotype than the heterozygous plants, suggesting a dosage effect of RNAi (Travella et al., 2006; Fu et al., 2007)
- Inclusion of intron or spacer sequences in hairpin constructs enhances silencing, possibly by aligning the complementary arms of the hairpin (Smith et al., 2000)
- Variation in intron size and sequence has been shown to influence the silencing phenotype (Smith et al., 2000; Hirai et al., 2007)
- RNAi can equally reduce the transcript levels of all three homoeologous genes on the three genomes in hexaploid wheat (Travella et al., 2006)
- RNAi may lead to silencing of non-target genes (Van Houdt et al., 2003)

Further research is required to characterize the relationships between various silencing constructs, their impact on different gene families and the degree of silencing that is achieved.

A comparison of different constructs and their relative efficiency of post-transcriptional gene silencing was made by Smith et al. (2000). This group developed a construct for RNAi-induced silencing in monocotyledonous plants called pSTARLING, which is a modification of pHELLSGATE (Wesley et al., 2001). pHELLSGATE has the cauliflower mosaic virus 35S promoter for driving expression in dicotyledonous plants whereas pSTARLING contains the maize ubiquitin promoter and introns (Christensen et al., 1996; Rooke et al., 2000), for driving expression in monocotyledonous plants (Figure 5.1). pSTARLING was later modified to be compatible with the Gateway<sup>TM</sup> recombination system (Invitrogen) and renamed pSTARGATE (<http://www.pi.csiro.au/rnai/vectors.htm>). The pSTARLING vector was successfully used to silence two MADS-box genes *BMI* and *BM10* in barley (Trevaskis et al., 2006). It was suggested that intron-hairpin-RNA constructs, such as pSTARGATE, should be efficient at inducing post-translational gene silencing for a wide range of genes in a variety of circumstances. This makes pSTARGATE an ideal construct for the silencing of the putative plasma membrane Na<sup>+</sup> transporter, *TaHKT1;5-D*.



**Figure 5.1: A simplified diagram of the pSTARGATE vector for RNAi-induced gene silencing in monocotyledonous plants**

The pSTARGATE vector contains the maize ubiquitin promoter (UbiP) to promote expression of the fragment in monocotyledonous plants. Fragments for insertion recombine with the two sections between sites labeled attR1 and attR2. In between the fragments are ubiquitin introns (Ubi introns). The ccdB gene encodes a cytotoxic protein which prevents growth of phages if fragments have not recombined away. RB, right border; LB, left border; NosT, terminator.

### 5.1.2 Transformation of wheat by particle bombardment

Particle bombardment, or biolistics, of regenerable tissue cultures is the most widely-used system for the transformation of cereals. The procedure was devised by Sanford et al. (1987). It involves precipitating DNA onto gold particles which are then delivered at high velocity into target plant tissue by means of a burst of gas such as helium.

Other methods of plant transformation include *Agrobacterium*-mediated transformation, electroporation, and polyethylene glycol (PEG)-mediated transformation of protoplasts, but for these methods there has been limited success for transformation of wheat and the regeneration frequency remains low. One of the major problems in the transformation of wheat and other crop plants is the need to regenerate transformed cells via tissue culture. This is because there is significant variability for callus induction between genotypes, plant regeneration is very sensitive to the composition of the tissue culture medium, and it is often found, for unknown reasons, that a low percentage of calli retain totipotency and regenerate (Sears and Deckard, 1982). There have been some reports of successful regeneration of stably transformed wheat plants using *Agrobacterium*-mediated methods with transformation efficiencies of around 2 to 5 % (Shewry and Jones, 2005; Jones et al., 2005). However, transformation efficiencies of up to 60% have been documented using biolistics (Pellegrineschi et al., 2002).

Genetic transformation technology provides a powerful research tool to study gene function in plants. Here this technology is employed to study the *in planta* function of *TaHKT1;5-D*.

### 5.1.3 Aims

The aim was to test whether reduction of the expression of *TaHKT1;5-D* (corresponding to Accession No. DQ646342), by post-transcriptional gene silencing of its mRNA, resulted in loss of the *Knal* phenotype. Two RNAi constructs designed to reduce the expression of *TaHKT1;5-D* were developed and introduced into bread wheat (*Triticum aestivum* cv. Bob White). T<sub>1</sub> seed from transgenic plants was used in an experiment to test whether there was a difference in leaf Na<sup>+</sup> concentration between plants that contain each of the RNAi constructs and those in which the RNAi construct has segregated away. The purpose of screening the T<sub>1</sub> material was to identify lines with a phenotype of interest which might later be characterised further, both in terms of phenotype, and in terms of genotype, in the T<sub>2</sub> generation.

## 5.2 Materials and Methods

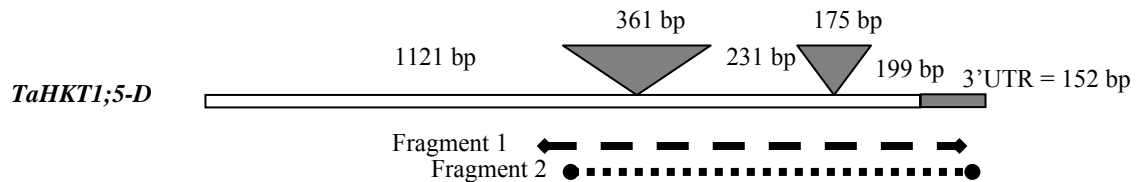
### 5.2.1 Plasmid preparation

The fragments of *TaHKT1;5-D* used in the constructs were amplified by PCR under standard conditions. Fragment 1 consisted of 600 bp and started at nucleotide 1082, while fragment 2 consisted of 559 bp and started at nucleotide 1096 (Figure 5.2). Both fragments included the region at the 3' end of the cDNA, as this was the region where the *TaHKT1;5-D* allele was least similar to the *TaHKT1;5-B* genome alleles. However, because of the high degree of identity even in this region, it was expected that the B genome alleles (Appendix Table 3.2) might also be down-regulated to some extent in the transgenic wheat plants. It is also possible that these segments may trigger silencing of other *HKT*-like genes with similar sequence.

The two fragments were amplified from pBluescript II vector containing the full coding DNA sequence for *TaHKT1;5-D* (see Chapter 2 section 2.2.6). Fragment 1 was amplified using primers *rnaiF1* (5'-CACCCCGTGTCTCGGCCCTCGTGGTGC-3') and *rnaiR1* (5'-TTGATATGCATGCAGTGATTGAGG-3'). Fragment 2 was amplified using primers *rnaiF2* (5'-CACCCCTCGTGGTGCTCTATGTGGTCATG-3') and *rnaiR2* (5'-TCGGCATAATGGAAATATGTTTCAG-3'). The products were amplified in a reaction with *Pfu* DNA Polymerase and *Pfu* Buffer (Fermentas, US), according to the manufacturers instructions, with the following cycling protocol: 95°C, 3 min; then 40 cycles of 95°C, 30 sec; 55°C, 30 sec; 72°C, 3 min; followed by a final extension step of 72°C for 10 mins. Products were checked on an agarose gel for the correct sizes and then 1 µL of the product was used in a Topo Cloning reaction (Invitrogen, Australia).

Fragments 1 and 2 were ligated individually into pENTR-D-TOPO (Invitrogen) as per the manufacturers instructions, and transformed into *Escherichia coli* (DH5α) via electroporation. Transformation suspensions were spread on Luria Bertani (LB) agar plates with 50 µg mL<sup>-1</sup> Kanamycin. Purified plasmid pENTR-D-TOPO DNA containing each of the fragments was sequenced to confirm the insert, and then used in a Gateway Recombinase reaction as per the manufacturers instructions (Invitrogen) to transfer the insert into Gateway-enabled pSTARGATE (provided by Dr Peter Waterhouse, CSIRO Plant Industry, Canberra, Australia). In both cases, this resulted in the insertion of two copies of the insert, one in sense orientation and the other in antisense orientation, under the control of a single ubiquitin promoter. When transcribed from the promoter, the chimeric DNA constructs are designed so as to express a self-complementary RNA where the sense and antisense sequences can hybridize to form a hairpin RNA having a 600bp, or 559bp duplex region, for fragment 1 and

fragment 2, respectively. Plasmid DNA of pSTARGATE with each of the fragments present was purified, concentrated to 1 µg/uL), and referred to as pSTARGATE RNA insert 1 and pSTARGATE RNA insert 2.



**Figure 5.2: Diagram of the fragments incorporated into the silencing construct in relation to the *TaHKT1;5-D* gene**

Fragment 1 is 600 bp and starts at nucleotide 1082. Fragment 2 is 559 bp and starts at nucleotide 1096.

### 5.2.2 Gene delivery by particle bombardment

Seed of *Triticum aestivum* L. cv. Bob White were harvested 12 days after anthesis. Seed were washed in 70% ethanol made up with sterile water, followed by washing for 15 mins in 20% NaOCl (Bleach, White King, Australia), followed by ten washes in sterile water. In sterile conditions, scutella were isolated and only those of approximately 1 mm in length were kept. Plasmid DNA of pSTARGATE RNA insert 1, pSTARGATE RNA insert 2 or pSTARGATE without inserts were co-bombarded with a marker gene construct (pNEO1 plasmid DNA, kindly provided by Terese Richardson, CSIRO) with the *nptII* gene (encoding neomycin phosphotransferase which confers resistance to the antibiotic geneticin) into immature wheat scutella of approximately 1 mm in length via biolistics techniques according to Pellegrineschi et al. (2002). Approximately 30 scutella at a time were aligned in the centre of a plate containing Murashige and Skoog (MS) osmotic basal salt medium (Murashige and Skoog, 1962). Approximately 2.5 µg of NPTII DNA and 3.5 µg of pSTARGATE plasmid DNA were precipitated onto gold particles (0.6 micron in size) which had been separated by placement in a sonicator for 1 min. Precipitation involved vortexing in the presence of 50 µL

of 2.5M CaCl<sub>2</sub> and 20 µL of 0.1M Spermidine and incubation on ice for 5 m followed by a wash in 100% EtOH.

For each bombardment 10 µL of microparticle (DNA-coated gold) was placed onto a sterile macrocarrier (Biorad Labs, USA). Bombardments were conducted at a distance of 5 cm from the stopping plate using an Bio-Rad PDS-1000/He microprojectile gun with 900 psi (equivalent to 6.985 kPa). After bombardment the plates with the scutella were wrapped in foil to keep them in the dark at 25°C.

### 5.2.3 *Tissue culture and selection of transformants*

The day following bombardment the scutella were placed on MS medium (Murashige and Skoog, 1962) containing 2.5 mg dichlorophenoxyacetic acid (2,4-D)/L, 30g sucrose/L, and 8 g Bacto-Agar for somatic embryo induction. Calli were kept on this medium, in the dark, for two weeks. All subsequent cultures were maintained with 12 h light and 25°C. Actively growing calli from the scutella were transferred every 2 weeks, onto fresh MS regeneration medium without (2,4-D)/L but containing Geneticin Selective Antibiotic Liquid (Invitrogen) (50 µg/L) as selective agent (to select for cells transformed with the *nptII* selectable marker gene) and those that survived and grew were maintained until roots had grown and a few leaves had grown. Healthy green plants were then transferred to soil mixture in peat cups in a mist chamber and then at leaf 5 or 6 stage transferred into pots, grown to maturity and T<sub>1</sub> seed was harvested. Approximately 30 scutella (cv. Bob White) were isolated and grown in tissue culture without selection for use as a control, of these; four plants were maintained for use as a control in subsequent experiments.

### 5.2.4 *Phenotyping T<sub>1</sub> plants*

Phenotyping the leaf Na<sup>+</sup> concentration of T<sub>1</sub> plants was by a method similar to the method described in Chapter 2 (section 2.2.2). Seed germinated on Petri dishes on approximately 25<sup>th</sup> February 2007, and seed was planted in gravel pots in tanks on the following day. Plants were grown in half strength Hoagland's solution in supported hydroponics in a method adapted from Munns et al. (2000). Plants were grown in natural light with 16 h days and the temperature in the glass house was 17°C during the day and 9°C at night. Salt treatment commenced when leaf two was half emerged (6<sup>th</sup> March 2007). The NaCl concentration of the hydroponic solution was increased by 25 mM twice daily over two days to reach a final concentration of 100 mM. Supplemental calcium (Ca(NO<sub>3</sub>)<sub>2</sub>) was added to achieve a Na<sup>+</sup> to Ca<sup>2+</sup> ratio of 15:1. Leaf three was harvested after 10 days growing in salt



(commencing on 15<sup>th</sup> March 2007), the leaf was dried and the dry weight was recorded, and the Na<sup>+</sup> and K<sup>+</sup> was extracted with nitric acid (0.5 M). The Na<sup>+</sup> and K<sup>+</sup> concentration was measured using Inductively Coupled Plasma (ICP) analysis. Four to six seed from each plant of interest were tested. The phenotyping screen was then repeated on additional seed from two of the plants of interest and controls, and the concentration of NaCl in the hydroponic growth solution was increased to 150 mM in the second screen.

#### 5.2.5 DNA extraction and PCR

Leaf tissue from a selection of primary transgenic plants, selected T<sub>1</sub> plants of interest, and control Bob White plants, was harvested and ~250 mg of tissue was homogenized under liquid nitrogen. DNA was extracted using the reagents supplied in a NucleoSpin Plant L Kit (Macherey-Nagel, Germany), by the protocol recommended by the manufacturer for DNA isolation from plant tissue.

PCR to check the quality of the DNA samples was conducted by amplifying a control gene, *Actin*, from the DNA samples using the following primers actinF (5'-GGCACACTGGTGTCATGG-3') and actinR (5'-CTCCATGTCATCCCAGTT-3') (Provided courtesy of Dr Linda Tabe, CSIRO Plant Industry). The PCR was conducted under standard conditions with the following cycling protocol: 95°C, 15 min; then 30 cycles of 95°C, 1 min; 60°C, 1 min; 72°C, 1 min. The expected product size was 134 bp. PCR to check the presence of the RNAi constructs was conducted under standard conditions and the same cycling protocol, but using the following primers; FD4 (5'-GCTTGGCCATCTTCATCGCCGTG-3') and RD1 (5'-GGCCACAGCTGTACCCGGTGCTG-3'). These primers amplify a 147 bp product from the coding DNA sequence present in the RNAi construct. As these primers cross a 175 bp introns, the product amplified from Bob White DNA is distinguishable from the product amplified from the cDNA as the genomic DNA product is of a larger size, 322 bp.

## 5.3 Results

### 5.3.1 Transformation efficiency and contamination in tissue culture

Of the 1000 embryos that were bombarded via biolistics, approximately 400 were co-bombarded with the pSTARGATE insert 1 construct and pNEO1, 400 were co-bombarded with the pSTARGATE insert 2 construct and pNEO1, and a further 200 were co-bombarded with the standard pSTARGATE construct with no insert and pNEO1. Biolistics events were conducted on five separate occasions on the following dates in 2007: 24<sup>th</sup> January; 5<sup>th</sup>, 12<sup>th</sup> and 26<sup>th</sup> of February; and the 6<sup>th</sup> of March.

Contamination of the scutella became a problem during the February transformation experiments. The contamination was a cream-coloured bacterial growth around the embryo, occurring two to three days after isolation, when calli were on callus induction media (Figure 5.3 A). Infected scutella died. The source of the contamination was thought to be endogenous to the plant tissues, as opposed to a lack of sterile technique, as the origin of the infection seemed to be the scutella and the infection then spread out on the media plates from the scutella. Bacteria may have been introduced to the embryos via thrips as the contamination corresponded with an outbreak of thrips in the stock material. If the bacteria were inside the seed then the steps to surface sterilization the seed would not kill the bacteria. Of 1000 embryos bombarded via biolistics approximately 500 embryos were lost to this specific contamination. No other contamination problems occurred after the thrip outbreak was controlled by pesticide spraying in the glasshouses.

Embryos that were isolated from seed which had been collected from stock material prior to the thrip outbreak, and after the thrip outbreak had been controlled, developed in tissue culture as expected. The calli grew and become green (Figure 5.3 B). As expected, the majority of the calli died, as the pNEO1 plasmid DNA containing the *nptII* gene for resistance was not expected to integrate into the genome of every single scutella. Some plants were resistant to the Geneticin in the growth media, these continued to grow and produce roots and leaves (Figure 5.3 C), and eventually resembled plants (Figure 5.3 D). The resistant plants were transferred to a mist chamber (Figure 5.3 E), and most of these grew to look increasingly like a wheat plant, and those that looked healthy were transferred to pots (Figure 5.3 F) and grown to maturity. Three plants died in the mist chamber.

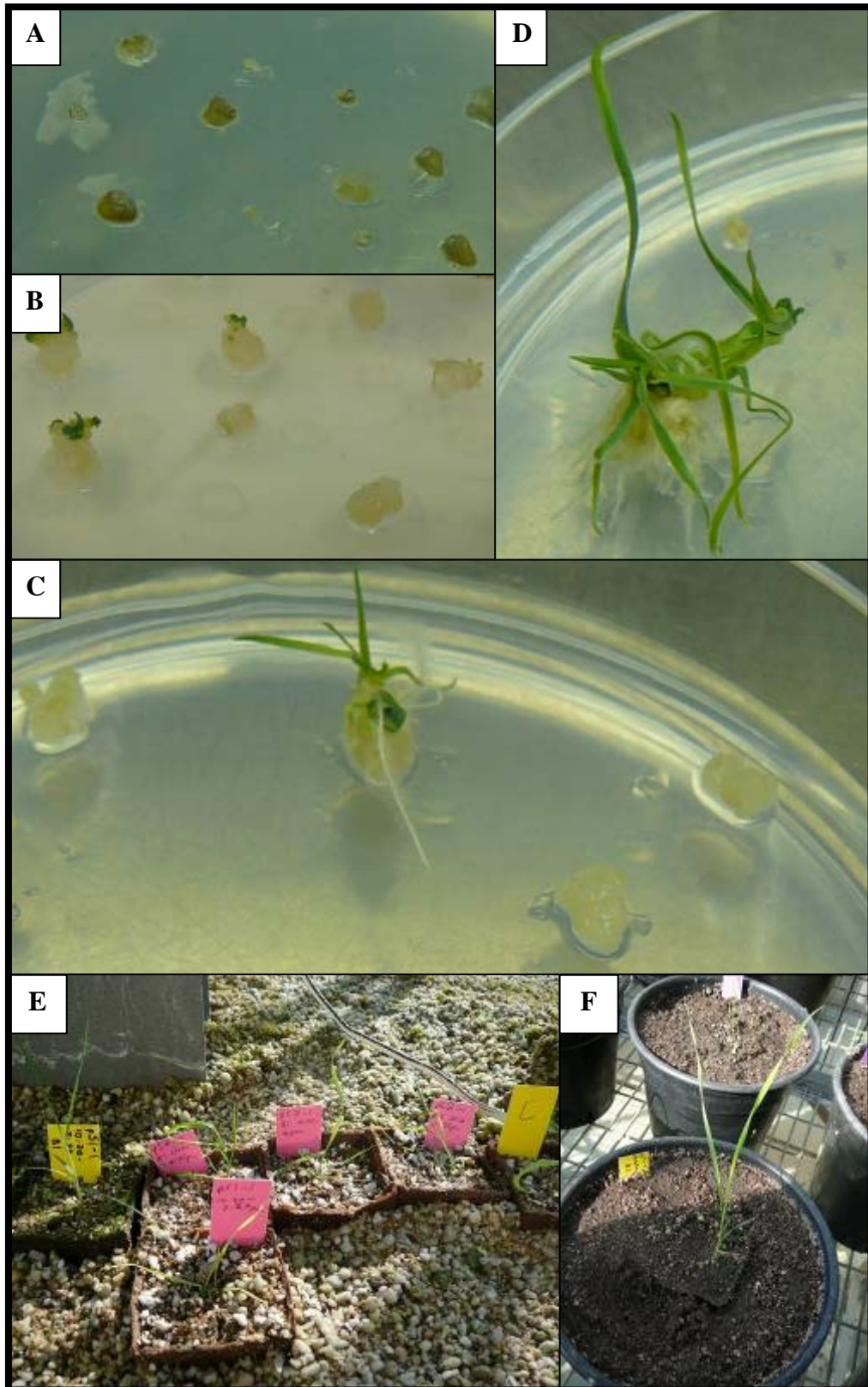
As 500 embryos were lost to contamination and did not survive tissue culture the transformation efficiency was calculated based on 500 embryos. A total of twenty independent transgenic plants survived selection on Geneticin and grew to maturity. These consisted of a single plant transformed with pSTARGATE construct with no insert, six plants

transformed with pSTARGATE containing fragment 1, and 13 plants transformed with pSTARGATE containing fragment 2. This equates to a transformation efficiency of 4%.

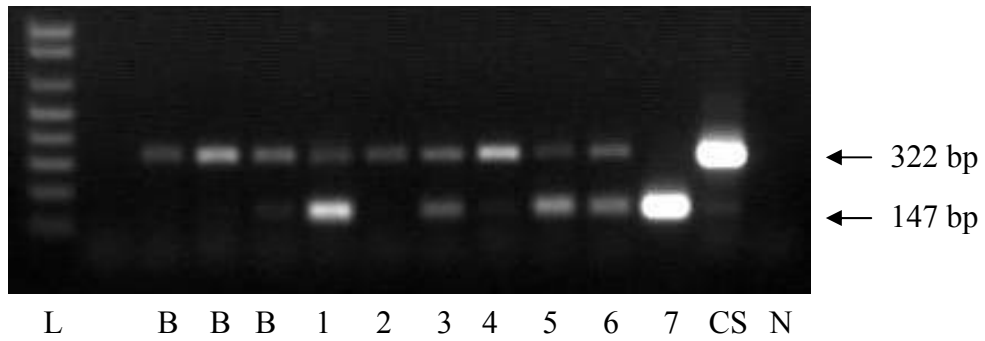
The single transgenic plant that survived tissue culture which had the empty pSTARGATE vector was referred to as 'c'. The six putative transgenic plants generated which had pSTARGATE containing fragment 1 were named 1s01, 1s02, 1s03, 1s04, 1s05 and 1s06. The 13 putative transgenic plants generated which had pSTARGATE containing fragment 2 were named 2s01, 2s02, 2s03, 2s04, 2s05, 2s06, 2s07, 2s08, 2s09, 2s10, 2s11, 2s12 and 2s13. Therefore, the prefix 1 or 2 indicates whether the plants were transformed with the RNAi construct with fragment 1 or 2, respectively. Four Bob White plants which had been through tissue culture that were not transgenic, and did not grown on media with geneticin, were maintained as controls, these are referred to as b1, b2, b3 and b4.

### *5.3.2 Analysis of primary transgenic wheat plants*

Genomic DNA was extracted from seven putative transgenic plants, these plants were the first plants to survive selection on Geneticin, and produce enough leaf biomass that a leaf could be harvested without compromising the survival of the plants. Primers specific to the coding sequence of the gene of interest (FD4 and RD1) were used in a PCR to check the presence of the insert in these plants. Five of the seven plants tested positive for the presence one or other of the RNAi constructs (1s06, 1s01, 2s05, 2s01 and 2s10, Figure 5.4). For two of the primary putative-transgenic plants, 1s04 and 1s05, the PCR data indicated that the RNAi construct was not present.



**Figure 5.3: Growth of calli in tissue culture and subsequent transfer to soil**  
Bacterial contamination killed half of the 1000 scutella bombarded (A). Of the ~500 scutella that did not become infected, some grew into calli and turned green (B). Some calli grew roots and leaves on selective media (C). Calli that grew into healthy plants (D) were transferred to a mist chamber (E) with constant humidity, and of these, only the healthy plants were transferred to pots (F) and grown to maturity.



**Figure 5.4: Amplification by PCR of a fragment specific to the RNA interference constructs from DNA from putative transgenic plants**

L = 1Kb<sup>+</sup> ladder; B = Bob White control (not transgenic) plants; 1 = 1s06 (fragment 1); 2 = 1s04 (fragment 1); 3 = 1s01 (fragment 1); 4 = 1s05 (fragment 1); 5 = 2s05 (fragment 2); 6 = 2s01 (fragment 2); 7 = 2s10 (fragment 2); CS = Chinese Spring (control). N = no template control. A product of 322 bp indicates amplification from genomic DNA. A product size of 147 bp indicates amplification from either of the two RNA interference constructs.

### 5.3.3 *Analysis of the T<sub>1</sub> generation of putative transgenic wheat plants*

The leaf Na<sup>+</sup> concentration of the putative transgenic wheat plants was tested and compared to the leaf Na<sup>+</sup> concentration four individual progeny from one of four non-transgenic Bob White plants which had been through tissue culture, but not grown on selective media. For one single plant (1s06), the seed did not germinate in time to be included in the screen.

Plants were grown in hydroponics with 50 mM NaCl in the growth solution (Figure 5.5). The mild NaCl concentration of 50 mM rather than a higher concentration was chosen because it was not known how well the transgenic plants would tolerate saline conditions. In addition to seed from the four non-transgenic Bob White controls, seed from the single putative-transgenic plant that survived tissue culture, which had been bombarded with the empty pSTARGATE vector, was also included in the screen. The T<sub>1</sub> putative transgenic plants, and controls, were grown in four different hydroponic tanks in a glasshouse, therefore, the leaf Na<sup>+</sup> data for the plants in each tank was compared to the controls from the same tank as conditions might have varied between tanks.

#### *Plant growth habit*

The growth habit of the T<sub>1</sub> putative transgenic plants predicted to contain the RNAi constructs appeared normal, and leaf emergence of all individuals occurred within a three day period, hence the timing of development stages was reasonably well aligned (Figure 5.5). However, the growth habit of the progeny of the single plant containing the empty pSTARGATE vector was not normal. These plants grew slower than the majority of the other plants, and the third leaf of these lines did not emerge until approximately two days after the majority of the other plants had produced leaf three, despite germinating at approximately the same time.



**Figure 5.5: Putative transgenic  $T_1$  plants growing in hydroponics**

Approximately 7 days after germination (3<sup>rd</sup> March 2007) leaf two had emerged on most plants, photo (A). On the 6<sup>th</sup> of March the salt treatment commenced (50 mM NaCl). Harvest of leaf three began on the 15<sup>th</sup> of March and photo (B) was taken on the 17<sup>th</sup> of March.

### Leaf three Na<sup>+</sup> concentrations of control plants

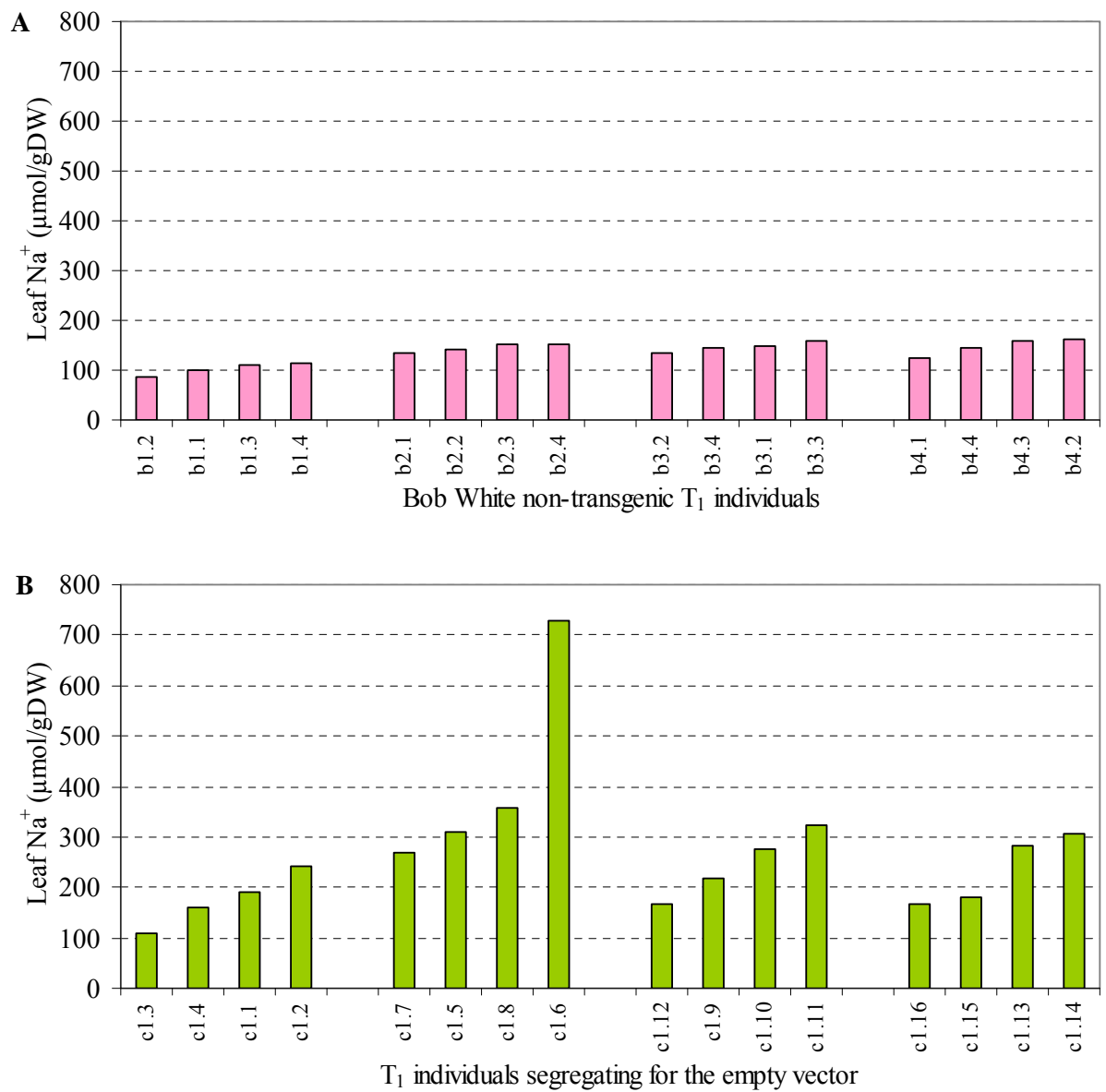
The leaf Na<sup>+</sup> concentration of the control plants from each tank were compared first to assess the background variation between the tanks (Figure 5.6). The plants with the prefix b1, b2, b3 and b4 are from tanks 1, 2, 3 and 4, respectively (Figure 5.6 A). Likewise, plants with the prefix c1, c2, c3 and c4 are from tanks 1, 2, 3 and 4, respectively (Figure 5.6 B).

The average leaf Na<sup>+</sup> of all of the non-transgenic Bob White plants, across all of the tanks, was  $135 \pm 6$   $\mu\text{mol/gDW}$  ( $n = 16$ ). The plants from tank 1 had the lowest range of leaf Na<sup>+</sup> concentrations (87 to 114  $\mu\text{mol/gDW}$ ;  $n = 4$ ), whereas the plants from tanks 2, 3 and 4 had similar ranges (between 123 and 163  $\mu\text{mol/gDW}$ ;  $n = 4$ ), indicating that the Na<sup>+</sup> in the hydroponic solution in tank 1 may have been less concentrated than in the other tanks, or more likely that there may have been less transpiration from tank 1, which could be due to less light, less airflow or a lower temperature in that part of the growth room. Likewise the four c1 individuals from tank 1 had lower leaf Na<sup>+</sup> concentrations than the T<sub>1</sub> individuals from the same primary transgenic plant that were grown in the other tanks.

The majority of the T<sub>1</sub> individuals from the single transgenic plant that was transformed with the empty pSTARGATE vector (denoted 'c') had higher leaf Na<sup>+</sup> than the Bob White non-transgenic controls. The c1 individuals from tank 1 ranged from 108 to 243  $\mu\text{mol/gDW}$ , and the plants from the other three tanks ranged from 168 to 728  $\mu\text{mol/gDW}$ . The average leaf Na<sup>+</sup> of all the individuals from the empty pSTARGATE plant was  $226 \pm 35$   $\mu\text{mol/gDW}$  ( $n = 16$ ).

The slow growth rate of the individuals segregating for the empty pSTARGATE vector may explain why many of the individuals had higher leaf Na<sup>+</sup> concentrations than the control Bob White individuals (Figure 5.5 A), because slow growth leads to greater accumulation of Na<sup>+</sup> in the leaves. As the control Bob White plants had also been through tissue culture and did not exhibit delayed growth it was not likely that the delayed growth of the T<sub>1</sub> individuals segregating for the empty pSTARGATE vector was due to the parent plant growing in tissue culture.





**Figure 5.6: Leaf three Na<sup>+</sup> concentrations of Bob White non-transgenic individual plants (A) and transgenic plants segregating for the empty pSTARGATE vector (B) from four different tanks**

Leaf three was grown for 10 days in a solution containing 50 mM NaCl.

Analysis of the phenotype of T<sub>1</sub> individuals from each transgenic plant

All five T<sub>1</sub> plants tested against Bob White controls in tank 1 had individuals that had higher leaf Na<sup>+</sup> than the Bob White non-transgenic control replicates (Figure 5.7 A).

As it was expected that the RNAi fragment would be segregating in the T<sub>1</sub> individuals, variation in the leaf Na<sup>+</sup> concentration in the progeny of the primary transgenic plants was expected. By extension, it was likely that the plants of greatest interest would be plants where within the T<sub>1</sub> individuals there were plants with Na<sup>+</sup> concentrations similar to that of Bob White non-transgenic controls as well as plants with significantly higher leaf Na<sup>+</sup>, maybe two to three times that of the Bob White non-transgenic controls, as this is what would be expected in individuals segregating for a construct silencing the *Kn1* gene.

Hence, the plant of greatest interest in tank 1, was 1s02. The varying leaf Na<sup>+</sup> concentrations of the individuals of 1s02 (Figure 5.7 A) could possibly be explained by segregation of the silencing construct, whereby the plant with low leaf Na<sup>+</sup>, similar to the leaf Na<sup>+</sup> concentrations of the controls, might be a null plant, the two plants with high leaf Na<sup>+</sup> might be homozygous for the RNAi construct, and the plant with intermediate Na<sup>+</sup> might be heterozygous for the RNAi construct.

Of the other plants in tank 1, plant 1s01 had an individual progeny with approximately double the leaf Na<sup>+</sup> concentration of the Bob White controls, although there was less variation within individuals than for 1s02. Plants 2s01, 2s02 and 2s03 had individuals that had leaf Na<sup>+</sup> concentrations around 1.5 times that of the Bob White controls, but again, there was not significant variation between individuals from these plants (Figure 5.7 A).

Of the plants in tank 2, the individuals of one plant, 2s04, had the same or lower leaf Na<sup>+</sup> than the Bob White controls (Figure 5.7 B). Three plants had individuals with leaf Na<sup>+</sup> concentrations around 1.5 times that of the controls (1s02, 1s04 and 2s06). Individuals from plant 2s05 were not significantly different to the controls. Therefore, none of the plants in tank 2 stood out as having a phenotype of interest as there was not significant variation within the individuals of each plant (Figure 5.7 B).

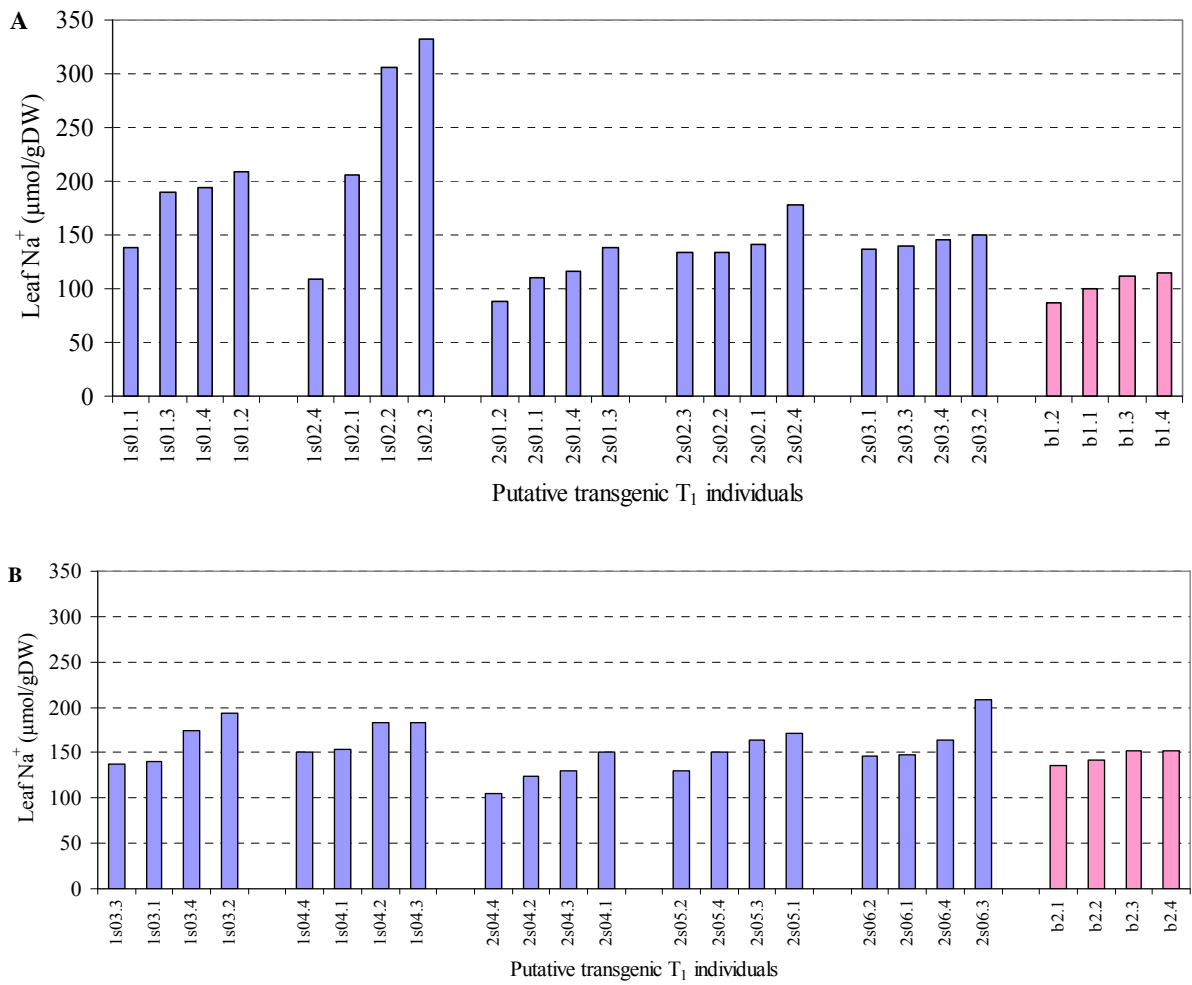
Similarly, in tank 3, none of the plants represented (1s05, 2s07, 2s08, 2s09 and 2s10) stood out as having progeny with significantly higher leaf Na<sup>+</sup> than the controls, as well as having significant variation within the individuals (Figure 5.8 A).

The individual progeny of two of the plants represented in tank 4 (2s12 and 2s13), were not significantly different from the Bob White controls for leaf Na<sup>+</sup> (Figure 5.8 B). The progeny of the third plant grown in tank 4, plant 2s11, did have both significantly higher leaf

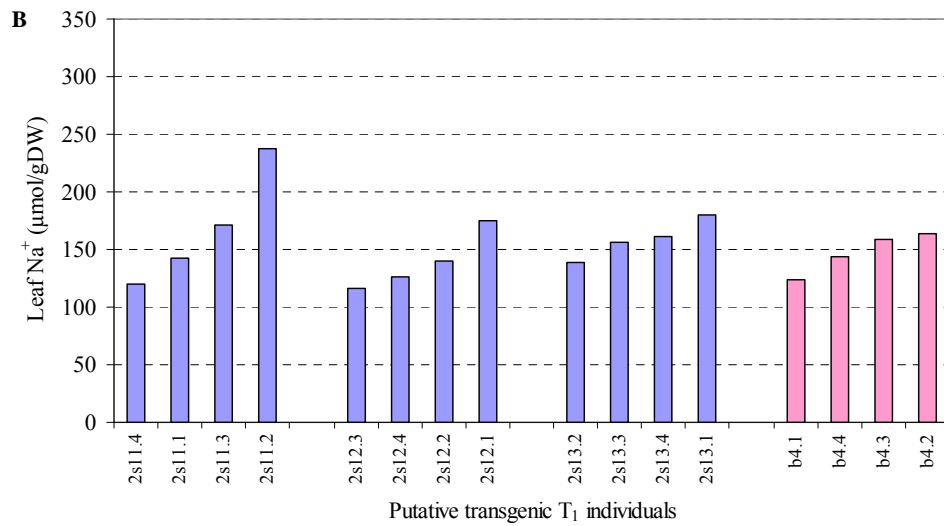
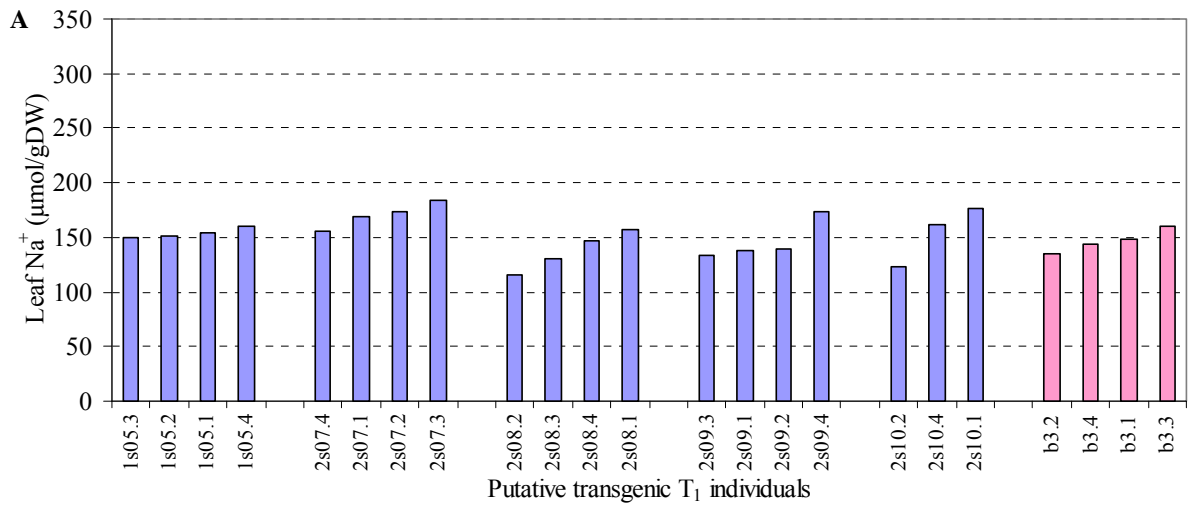
Na<sup>+</sup> than the controls, in one of the individuals, as well as individuals with similar leaf Na<sup>+</sup> concentrations as the controls, hence, this plant was of interest.

*Putative transgenic plants of interest*

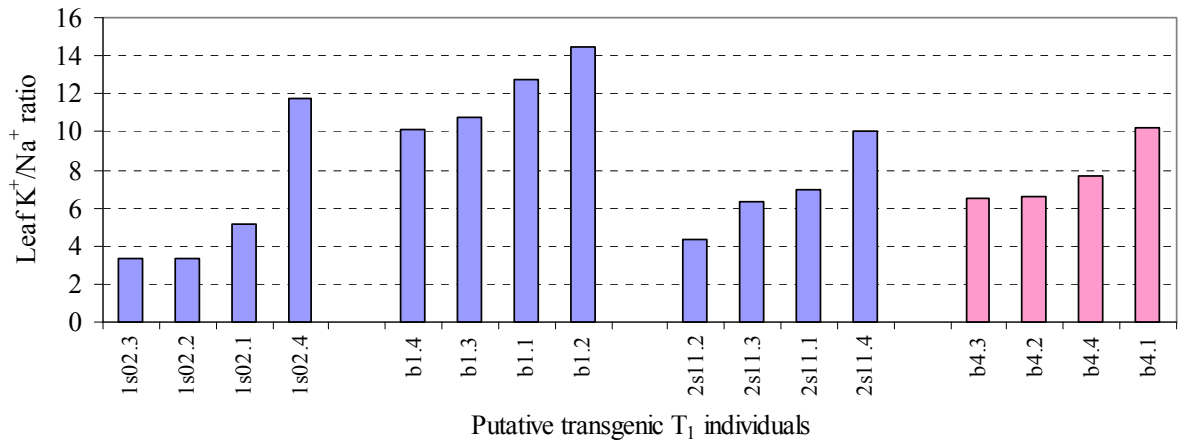
The K<sup>+</sup> to Na<sup>+</sup> ratios of leaf three of the individuals of the two plants of most interest (1s02 and 2s11), are shown in Figure 5.9. The K<sup>+</sup> to Na<sup>+</sup> ratio of the 1s02 plant with the highest leaf Na<sup>+</sup> concentration and the lowest K<sup>+</sup> to Na<sup>+</sup> ratio was 3.4 (1s02.3). The 1s02 plant with the lowest leaf Na<sup>+</sup> concentration and the highest K<sup>+</sup> to Na<sup>+</sup> ratio (1s02.4) had a ratio of approximately 12, which was similar to the K<sup>+</sup> to Na<sup>+</sup> ratio of the Bob White control plants in tank 1, which ranged from 10 to 14. The K<sup>+</sup> to Na<sup>+</sup> ratio of the 2s11 plant with the highest leaf Na<sup>+</sup> and the lowest K<sup>+</sup> to Na<sup>+</sup> ratio (2s11.2) was 4.3, and the 2s11 plant with the lowest leaf Na<sup>+</sup> and the highest K<sup>+</sup> to Na<sup>+</sup> ratio (2s11.4) had a ratio of 10, similar to the K<sup>+</sup> to Na<sup>+</sup> ratio of the Bob White control plants from tank 4, which ranged from approximately 6.5 to 10. The 1s02 plant with the highest leaf Na<sup>+</sup> (1s02.3; 333 μmol/gDW), had three times the leaf Na<sup>+</sup> of the 1s02 plant with the lowest leaf Na<sup>+</sup> (1s02.4; 108 μmol/gDW), and the 2s11 plant with the highest leaf Na<sup>+</sup> ratio (2s11.2; 238 μmol/gDW), had a leaf Na<sup>+</sup> ratio approximately double that of the 2s11 plant with the lowest leaf Na<sup>+</sup> ratio (2s11.4; 120 μmol/gDW). The 1s02 plant with the highest K<sup>+</sup> to Na<sup>+</sup> ratio (1s02.4; ratio 11.7), had a ratio 3.4 times greater than the plant with the lowest ratio (1s02.3; ratio 3.4), and the 2s11 plant with the highest K<sup>+</sup> to Na<sup>+</sup> ratio (2s11.4; ratio 10.0), had a ratio 2.3 times greater than the plant with the lowest ratio (2s11.2; ratio 4.3).



**Figure 5.7: Leaf three Na<sup>+</sup> concentration of putative transgenic plants compared to Bob White controls grown in Tank 1 (A) and Tank 2 (B)**  
 Leaf three was grown for 10 days in a solution containing 50 mM NaCl.



**Figure 5.8: Leaf three Na<sup>+</sup> concentration of putative transgenic plants compared to Bob White controls grown in Tank 3 (A) and Tank 4 (B)**  
 Leaf three was grown for 10 days in a solution containing 50 mM NaCl.



**Figure 5.9: K<sup>+</sup>/Na<sup>+</sup> ratio of leaf 3 from putative transgenic plants of interest, from the first screen, compared to control Bob White plants from the respective tank**  
 Leaf three was grown for 10 days in a solution containing 50 mM NaCl.

### Re-screen of the plants of interest

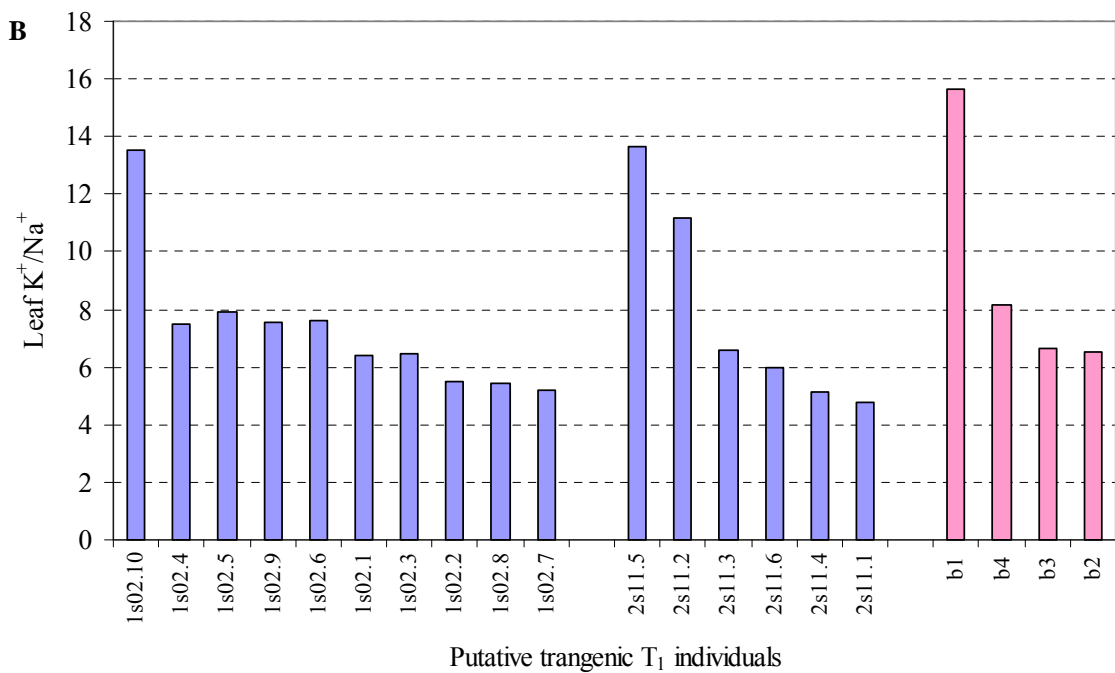
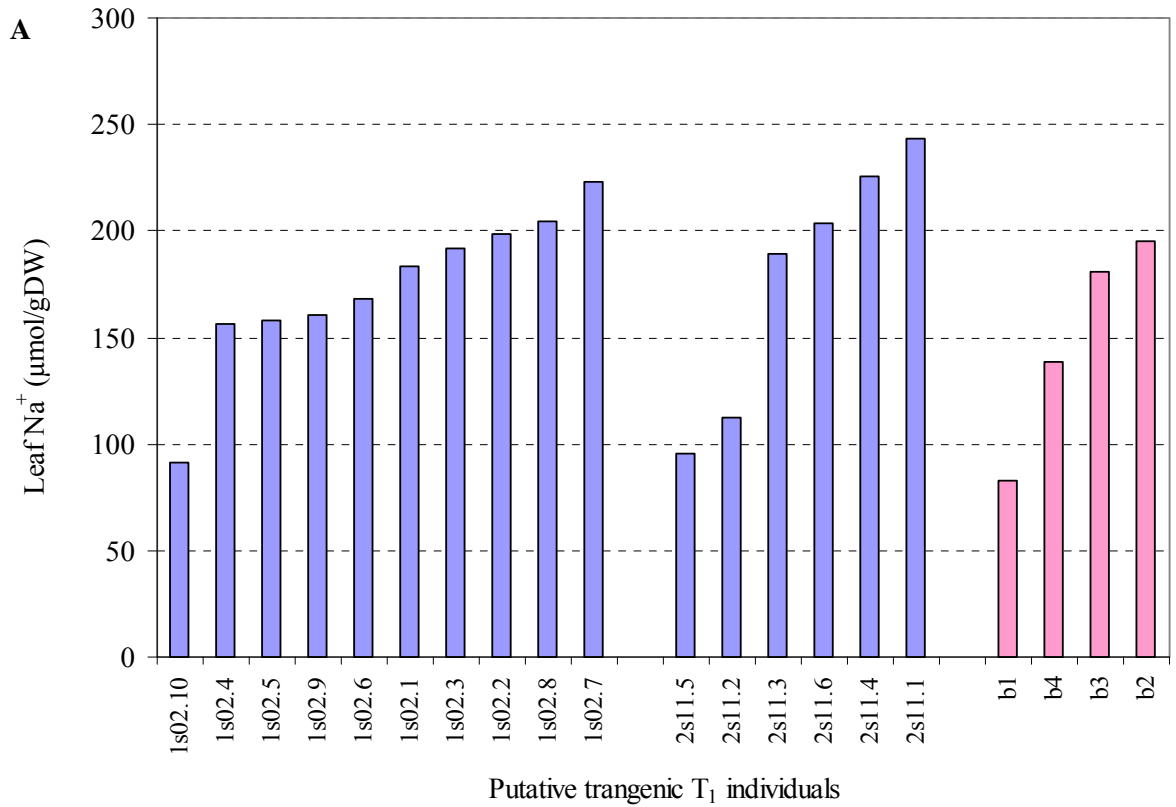
The phenotype screen was repeated for the two plants with the most interesting phenotypes (1s02 and 2s11), this time with a salt concentration of 150 mM in the hydroponic growth solution.

In the second screen, significant variation in the leaf Na<sup>+</sup> concentrations (Figure 5.10 A) and the K<sup>+</sup> to Na<sup>+</sup> ratios (Figure 5.10 B) of the individual plants for plants 1s02 and 2s11 were again observed. However, there was greater variation in the leaf Na<sup>+</sup> concentrations of the Bob White individuals in the second screen than in the first screen. As the variation in the controls was considered to be background variation, influenced by growth conditions, because the variation in the control plants was high, this meant that the variation in the transgenic plants was not regarded as being as significant as it may have, had the background variation been lower.

The average leaf Na<sup>+</sup> of the Bob White controls in the second screen was  $149 \pm 25$   $\mu\text{mol/gDW}$  ( $n = 4$ ) (compared to an average of  $135 \pm 6$   $\mu\text{mol/gDW}$ ,  $n = 16$ , in the first screen), and the range was 83 to 195  $\mu\text{mol/gDW}$ . The 1s02 individuals had leaf Na<sup>+</sup> concentrations ranging from 91 to 223  $\mu\text{mol/gDW}$  (compared to 109 to 332  $\mu\text{mol/gDW}$  in the first screen). The 2s11 individuals had leaf Na<sup>+</sup> concentrations varying from 95 to 243  $\mu\text{mol/gDW}$  (compared to 119 to 237  $\mu\text{mol/gDW}$  in the first screen).

The transgenic plants with the highest leaf Na<sup>+</sup> concentrations (223 and 243  $\mu\text{mol/gDW}$  for 1s02.7 and 2s11.1, respectively), had leaf Na<sup>+</sup> concentrations approximately 1.5 times greater than the average of the Bob White plants (149  $\mu\text{mol/gDW}$ ,  $n = 4$ ).

The K<sup>+</sup> to Na<sup>+</sup> ratio of these transgenic plants (1s02.7 and 2s11.1) was approximately five, whereas the average K<sup>+</sup> to Na<sup>+</sup> of the Bob White control plants was nearly double, at approximately nine (Figure 5.10 B). The 1s02 plant with the lowest K<sup>+</sup> to Na<sup>+</sup> ratio (1s02.7), had a K<sup>+</sup> to Na<sup>+</sup> ratio of 5.2, which is less than half of the K<sup>+</sup> to Na<sup>+</sup> ratio of the plant with the highest K<sup>+</sup> to Na<sup>+</sup> ratio (1s02.10), which had a ratio of 13.5. The 2s11 plant with the lowest K<sup>+</sup> to Na<sup>+</sup> ratio (2s11.1), had a K<sup>+</sup> to Na<sup>+</sup> ratio of 4.8, which is approximately one-third of the K<sup>+</sup> to Na<sup>+</sup> ratio of the plant with the highest K<sup>+</sup> to Na<sup>+</sup> ratio (2s11.5), which had a ratio of 13.6.



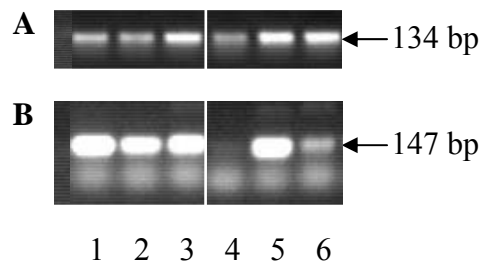
**Figure 5.10: Leaf three  $\text{Na}^+$  concentrations (A) and  $\text{K}^+$  to  $\text{Na}^+$  ratio (B) of putative transgenic plants of interest, in the second screen, compared to Bob White controls** Leaf three was grown for 10 days in a solution containing 150 mM NaCl.



Genotype of the plants of interest

Genomic DNA was extracted from six of the individual plants of the two plants of interest from screen two. These included the two individuals with the lowest leaf  $K^+$  to  $Na^+$  ratio from each plant, and the individual with the highest  $K^+$  to  $Na^+$  ratio from each plant. The DNA samples were checked by PCR with primers for the actin gene (Figure 5.11 A), and then primers specific to the coding sequence of the gene of interest (FD4 and RD1) were used in a PCR to check the presence of the insert in these plants (Figure 5.11 B).

For the 1s02 individuals, the PCR data indicated that the RNAi transgene was present in every individual tested (Figure 5.11 B). Whereas, for the 2s11 individuals, the PCR data indicated that the RNAi transgene was absent in the individual with the high  $K^+$  to  $Na^+$  ratio, and low leaf  $Na^+$ , and the RNAi transgene was present in the two individuals with the low  $K^+$  to  $Na^+$  ratio, and high leaf  $Na^+$  ratio (Figure 5.11 B).



**Figure 5.11: Amplification by PCR of a fragment specific to the RNA interference constructs from DNA from individual  $T_1$  plants of the plants of interest**

Primers designed to amplify a 134 bp from the actin gene were used as a control to check the DNA samples (A). A product size of 147 bp, amplified using the FD4 and RD1 primers, was diagnostic of the presence or absence of the RNAi construct. 1 = 1S02.10; 2 = 1S02.8; 3 = 1S02.7; 4 = 2S11.5; 5 = 2S11.4; 6 = 2S11.1.

## 5.4 Discussion

Previously, transgenic wheat plants with ubiquitin promoter-reporter constructs have exhibited GUS activity that was deemed to be influenced by the genomic site of integration of the transgene in the genome (Barro et al., 1997; Rooke et al., 2000). In regard to the present study, there was no reason to expect that the sites of integration of the transgene in the genome would not be completely random. Certainly, the biolistic method used to introduce the transgene fragments does not include a way to control the site of integration of the transgene fragment. It was, therefore, anticipated that of all of the transgenic plants developed, the presence of the transgene would not necessarily lead to the predicted phenotype of significantly higher leaf  $\text{Na}^+$  in every plant. This was expected because the site of integration of the transgene fragment in any given plant may or may not be suitable for induction of significant expression of the RNAi fragment and so may not lead to significant accumulation of the RNAi fragment in the appropriate plant tissue, this being the specific cells in the root where the native *TaHKT1;5-D* gene member is expressed.

There was also no way to ensure that the site of integration would not disrupt a different gene in the genome and lead to an altered phenotype due to the disruption of the random gene. An undesirable site of integration of the transgene, such as in the middle of an important gene, is a possible explanation for the phenotype of slow growth observed in the single plant containing the empty pSTARGATE vector. It is possible that in this plant the transgene landed in a location that disrupted a gene which is involved in plant growth and or development. The slow growth phenotype of this plant was the most likely explanation for the observation that some of the  $T_1$  plants from this primary transgenic plant had very high leaf  $\text{Na}^+$  concentration, as slow growth leads to greater accumulation of  $\text{Na}^+$  in leaf tissues. However, the possibility that the pSTARGATE vector itself was influencing the leaf  $\text{Na}^+$  concentration could not be eliminated. Future work may include comparing the genotype of the plants segregating for the empty pSTARGATE vector to check whether the segregation of the construct correlates in any way with the leaf  $\text{Na}^+$  phenotype.

Previous studies have described the difference in leaf  $\text{K}^+$  to  $\text{Na}^+$  ratio between lines with and without the most distal fragment of the long arm of chromosome 4D, where *Kna1* is located (Dvořák and Gorham, 1992). Recombinant lines with *Kna1* had  $\text{K}^+$  to  $\text{Na}^+$  ratios six to eight times greater than lines without *Kna1* (Dvořák and Gorham, 1992). In Chapter 2, linkage between *TaHKT1;5-D* and the *Kna1* locus was described. Loss of the region containing *TaHKT1;5-D* and *Kna1* lead to almost a four-fold increase in leaf  $\text{Na}^+$ , and a six-fold decrease in the leaf  $\text{K}^+$  to  $\text{Na}^+$  ratio. In the most interesting plants studied, the leaf  $\text{Na}^+$

concentration was two or three times greater in the high Na<sup>+</sup> individuals than the low Na<sup>+</sup> individuals, and the K<sup>+</sup> to Na<sup>+</sup> ratio was two to three times lower. Therefore, the difference between the leaf Na<sup>+</sup> and leaf K<sup>+</sup> to Na<sup>+</sup> ratio within the transgenic plants is smaller than the difference between the chromosome 4D deletion lines with and without the distal 14% of the long arm of chromosome 4D containing *TaHKT1;5-D* and *Kna1* (Chapter 2). However, transgenic rice lines with and without the *SKC1* gene for shoot K<sup>+</sup> concentration, for which *OsHKT1;5* is the candidate gene (Ren et al., 2005), had half the leaf Na<sup>+</sup> and 2.5 times greater leaf K<sup>+</sup> to Na<sup>+</sup> ratios, respectively (Ren et al., 2005). Therefore, if *TaHKT1;5-D* was in fact silenced in the transgenic wheat plants, then the two to three-fold difference in leaf Na<sup>+</sup> and K<sup>+</sup> to Na<sup>+</sup> observed would be similar to the difference in leaf Na<sup>+</sup> and K<sup>+</sup> to Na<sup>+</sup> in the rice lines with and without *OsHKT1;5*, which was approximately a two and a half fold difference.

There was significant variation observed in the control Bob White plants, particularly those grown in the second screen for leaf Na<sup>+</sup> accumulation. This made it difficult to assess whether the variation in leaf Na<sup>+</sup> and leaf K<sup>+</sup> to Na<sup>+</sup> ratio in the transgenic plants was simply due to the conditions of the experiment or whether the variation was due to the effects of gene silencing. To test whether the variation in leaf Na<sup>+</sup>, and K<sup>+</sup> to Na<sup>+</sup> ratios in the individuals of the transgenic wheat plants are due to the growth conditions, or even due to disruption of an alternative gene due to the integration of the transgene, versus whether the variation is due to the silencing of *TaHKT1;5-D*, it would be necessary to test whether the level of *TaHKT1;5-D* messenger RNA is significantly lower in those plants with higher leaf Na<sup>+</sup> and lower K<sup>+</sup> to Na<sup>+</sup> ratios. This is the next step required. Regrettably time limitations did not allow this step to be included in this study.

The other remaining important data needed is the transgene copy number in each of the plants, and/or individuals, of interest. This should be done by Southern-blot hybridisation with the *HKT1;5* probe (Chapter 2). For plant 1s02 in particular, there may be multiple insertions of the transgene, and this may explain why the transgene was present in both plants with the low leaf Na<sup>+</sup> and high K<sup>+</sup> to Na<sup>+</sup> ratios as well as those with high leaf Na<sup>+</sup> and low K<sup>+</sup> to Na<sup>+</sup> ratios (Figure 5.11 B). The PCR data for plant 2s11 was promising; the data indicated that the segregation of the RNAi transgene corresponded with the expected phenotype in the three individuals tested. However, further work is required to confirm these data. Future work should also test the T<sub>2</sub> generation of the plants of interest for leaf Na<sup>+</sup> and K<sup>+</sup> accumulation in saline conditions, identifying the copy-number of the transgene in each individual, and quantifying the messenger RNA levels of *TaHKT1;5-D* in each plant of interest.

## Chapter 6: General Discussion

### 6.1 *HKT1;5* homoeologues in wheat

This body of work, by way of a combination of both mapping and candidate gene approaches, identified *HKT1;5* as a candidate for both *Kna1* and the novel locus in durum wheat for Na<sup>+</sup> exclusion, *Nax2*. *Nax2* from durum wheat Line 149, like *Kna1* from bread wheat, confers a phenotype of high K<sup>+</sup> to Na<sup>+</sup> concentration ratio in the leaves.

The isolation of *TmHKT1;5-A*, and development of markers to track *TmHKT1;5-A*, has enabled breeders to select for this gene in a breeding program to improve the salinity tolerance of durum wheat and bread wheat (Munns et al., 2008).

As a result of the isolation of *TmHKT1;5-A* and *TaHKT1;5-D*, it is now possible to study the function of these genes to better understand how they are having a major affect on leaf Na<sup>+</sup> accumulation. No quantitative trait loci in wheat, other than *Kna1* (*TaHKT1;5-D*) (Gorham et al., 1990; Dvořák and Gorham, 1992), *Nax1* (*TmHKT1;4-A2*) (Huang et al., 2006) and *Nax2* (*TmHKT1;5-A*) (Byrt et al., 2007), have been shown to confer such a strong Na<sup>+</sup> excluding phenotype, hence these genes are a valuable resource.

The discovery that *TmHKT1;5-A*, on the long arm of chromosome 5AL, and *TaHKT1;5-D*, on the long arm of chromosome 4DL, are homoeologous, has significant repercussions for our understanding of the evolution of the A genome from diploid to tetraploid wheats. These data are consistent with data indicating that in an ancestor of modern wheat, chromosomes 4AL and 5AL exchanged short terminal segments (Liu et al., 1992). Data was described (Chapter 3) that indicated that *Nax2* came from and is present in most *T. monococcum* subspecies and is absent in *T. urartu* and modern wheat - this data also is consistent with previous data indicating that the ancestor of the A genome of modern wheat is *Triticum urartu* (not *Triticum monococcum*) (Dvořák and Zhang, 1990).

### 6.2 Mapping of *Nax2* and *Kna1*

*Nax2* was located on the long arm of chromosome 5AL, distal to the marker *gwm595*, and a candidate gene *TmHKT1;5*, was identified (Chapter 2). However, a marker on the distal side of *Nax2* was not identified, and no recombination between the four markers that were linked to *Nax2* was observed in the 137 BC<sub>3</sub>F<sub>2</sub> lines tested. In contrast, for *Nax1* (*TmHKT1;4-A2*) on chromosome 2AL flanking markers, ‘*HAK15*’ and ‘*E*’, were identified at distances of 0.24 cM and 0.12 cM, proximal and distal to *Nax1*, respectively (Huang et al., 2006). For that study, Huang et al. (2006) generated a high-resolution mapping family by screening 864

BC<sub>5</sub>F<sub>2</sub> lines, and of these lines there were 22 F<sub>2</sub> lines that contained recombination events between the original flanking markers (*gwm312* and *HAK11*).

It is possible that by screening additional lines for the *Nax2* mapping family, flanking markers and recombinant lines may be identified and the *Nax2* region narrowed. However, it is also possible that in this region the *T. monococcum* and Tamaroi chromatin is particularly divergent and does not recombine freely. Poor recombination between homologous chromosomes of wheat and *T. monococcum* has been described previously (Dubcovsky et al., 1995). Screening of the phenotype and genotype of more F<sub>2</sub> lines is needed to explore whether recombination, between chromosome 5A of *T. monococcum* and Tamaroi, is limited.

The chromosomal region on the long arm of chromosome 4D in which *Kna1* and the candidate gene, *TaHKT1;5-D*, were located, equates to the distal 14% of the chromosome. This region, like the *Nax2* region, is large, and in both the *Nax2* and *Kna1* regions there may be other genes within the region that influence leaf Na<sup>+</sup> and leaf K<sup>+</sup> to Na<sup>+</sup> ratio.

### **6.3 The bread wheat HKT1;5 transports Na<sup>+</sup>**

The HKT1;5 on the D genome of bread wheat, TaHKT1;5-D, like the rice OsHKT1;5, behaved as a Na<sup>+</sup> transporter, when expressed in *Xenopus laevis* oocytes (Chapter 4). Previous data, describing the difference in net loading of <sup>22</sup>Na<sup>+</sup> into the xylem in near isogenic lines with and without *TmHKT1;5-A*, indicate that *TmHKT1;5-A* may be unloading Na<sup>+</sup> from the xylem in the roots (James et al., 2006a; Byrt et al., 2007). Likewise, *OsHKT1;5* was proposed to unload Na<sup>+</sup> from the xylem in the roots (Ren et al., 2005).

If TaHKT1;5-D was localized to the plasma membrane of xylem parenchyma cells in the roots, and exhibited transport properties in xylem parenchyma cells similar to the transport properties observed in *Xenopus laevis* oocytes, this being transport of Na<sup>+</sup> into the cell, then this might lower the Na<sup>+</sup> concentration of Na<sup>+</sup> in the xylem and lead to a phenotype of low leaf Na<sup>+</sup> in the leaves. It was puzzling that TmHKT1;5-A did not exhibit transport activity when putatively expressed in *Xenopus laevis* oocytes, but further work is required to confirm this observation. The high conductance of TaHKT1;5-D and OsHKT1;5 in the presence of external K<sup>+</sup> was also puzzling. These data may be consistent with this transporter permitting an exchange of Na<sup>+</sup> and K<sup>+</sup>, but further work with radioactive tracers is required to test this theory, as it is not possible to determine the ion responsible for the net outward currents from the data collected in this study.

## 6.4 Further questions and future directions

There are many other remaining questions about *HKT* transporters and whole plant management of  $\text{Na}^+$  transport, such as:

- (1) Is *TaHKT1;5-D*, alone, conferring the *Kna1* phenotype?

The transgenic plant material developed in this project, namely wheat lines where an RNA interference construct has been introduced to silence expression of the native *TaHKT1;5-D* gene (Chapter 5), should be a valuable resource to help in testing whether *TaHKT1;5-D* is conferring the *Kna1* phenotype. Preliminary data, indicating that segregation of the silencing construct in the  $T_1$  material may correlate with a 2.5 fold difference in leaf  $\text{K}^+$  to  $\text{Na}^+$  ratio, is promising. The next step is testing the leaf  $\text{K}^+$  to  $\text{Na}^+$  ratio, and the expression of *TaHKT1;5-D*, in the  $T_2$  plants.

- (2) In what cell types and tissues are *HKT* genes expressed?

The *TmHKT1;5-A* and *TaHKT1;5-D* promoters were isolated, and found to be 94% identical (Chapter 2). These promoters could be used to develop *HKT* promoter:GUS fusion constructs for transformation of barley, and or *HKT* promoter:gene fusion constructs. Barley lines expressing these transgenes could be used to assess where *HKT1;5* is expressed, and assess the differences in  $\text{Na}^+$  concentrations in specific cell types as influenced by the presence or absence of *HKT* genes. Tissue sections of the transgenic material could be examined by X-ray microanalysis to study which cell types have altered  $\text{Na}^+$  concentrations. Further to these experiments, one could introduce promoter:GUS fusion constructs, driven by *TmHKT1;4-A2* (Huang et al., 2006), *TmHKT1;5-A* and *TaHKT1;5-D* promoters, into barley, and observe GUS expression to identify the cell types in which *HKT1;4* is expressed, in contrast to where *HKT1;5* is expressed. This may help us to understand which cell types are important for unloading  $\text{Na}^+$  from the xylem, a trait conferred by both *HKT1;4* and *HKT1;5*, in contrast to which cell types may be involved in partitioning  $\text{Na}^+$  into the sheath, a phenotype specific to *HKT1;4* (James et al., 2006a).

- (3) Are HKT proteins localized to the plasma membrane?

An understanding of the location in which HKT proteins are functioning is needed, as this may assist in conceiving of ways to manipulate HKT proteins to influence where  $\text{Na}^+$  accumulates in plants. Experiments such as immunolocalization of the HKT1;5 protein, using microscopy and plant tissue sections exposed to a gold-labelled HKT1;5 antibody, may help to answer this question.

- (4) What transcription factors regulate the expression of *HKT* genes?

A yeast one-hybrid method could be used to try and identify the transcription factors that regulate expression of *HKT*s. The transcription factors may then be mapped and isolated and one could test to see if the expression patterns overlap those of the *HKT* genes, and whether these genes map to regions of the genome harbouring salinity tolerance loci.

(5) What is the range of ion transport properties of HKT proteins?

Characterisation of the diverse diploid wheat material, and identification of lines with greater  $\text{Na}^+$  exclusion than our current material (Chapter 3), may contribute to the future cloning of new *HKT* genes or alleles which may have a greater conductance of  $\text{Na}^+$ , or higher expression, and may be a valuable resource for breeding wheat with greater salinity tolerance. It may be found that different HKT proteins have vastly different levels of conductance of  $\text{Na}^+$  and some may transport other ions. It would also be interesting to screen a range of halophytic species (Colmer et al., 2006; Flowers and Colmer, 2008), by Southern-blot hybridization using a probe based on a conserved fragment of an HKT gene, and compare any sequence differences with species closely related to each of the halophytic species, that are not salt tolerant. This work may identify additional novel HKT proteins and/or novel controls of the level or site of expression of the *HKT* genes.

The current hypothesis on the function of group 1 HKT-type transporters is that they are involved in retrieval of  $\text{Na}^+$  from the xylem into xylem parenchyma, thereby reducing the amount of  $\text{Na}^+$  reaching the leaves, and leading to lower leaf  $\text{Na}^+$  concentrations (Ren et al., 2005; Davenport et al., 2007). Removal of  $\text{Na}^+$  from the xylem would contribute to a higher  $\text{K}^+$  to  $\text{Na}^+$  ratio in the xylem, leading to a higher  $\text{K}^+$  to  $\text{Na}^+$  ratio in the leaves. Loading of the phloem has been suggested (Berthomieu et al., 2003; Horie et al., 2007), but there is no quantitative evidence for significant retranslocation (James et al., 2006a; Davenport et al., 2007).

In many monocotyledonous plants, such as wheat, barley and rice, there are eight or nine *HKT* genes (Huang *et al.*, 2008). In *Arabidopsis*, which is a dicotyledonous plant, there is only a single *HKT* gene, and relative to cereals *Arabidopsis* is not good at excluding sodium. To best manipulate *HKT* genes and improve the salinity tolerance of crop plants, we need to study the function of each of the different HKT proteins.

*HKT* genes are somehow involved in loading and/or unloading of  $\text{Na}^+$  into the xylem (Davenport *et al.*, 2007; James *et al.*, 2006a), and in cereals *HKT* genes are also involved in partitioning  $\text{Na}^+$  into the sheath (James *et al.*, 2006a; Huang *et al.*, 2006). However, it is likely that these preliminary studies illustrate just the tip of the iceberg in terms of the involvement of *HKT* genes in the management of cations in plants. For example, a recent study of

OsHKT2;1 found that this protein is the central transporter for nutritional uptake of Na<sup>+</sup> into rice roots in K<sup>+</sup> starved conditions (Horie *et al.*, 2007). HKT genes are likely to play a crucial role in transport of Na<sup>+</sup> and K<sup>+</sup> in many different tissue types and to many different ends. The accumulation of Na<sup>+</sup> in the cytoplasm of plant cells is toxic, but Na<sup>+</sup> also has roles in moving osmotic potential more negative, which helps plants retain water and maintain turgor, and it may be found that *HKT* genes also function in these important processes.

(6) What other transporters are necessary for HKT function?

Other genes are needed to control Na<sup>+</sup> accumulation, particularly in the epidermal and cortical cells of roots, to limit the uptake from the soil into the root. The *HKT1;5* genes are probably located within the stele and control the net uptake of Na<sup>+</sup> into the xylem, however, other genes are equally, if not more, important in restricting Na<sup>+</sup> entry into the root at the root-soil interface. To most effectively manipulate *HKT* genes in plants towards improving the control of Na<sup>+</sup> transport, we need to know what other genes are important. To study this, one could transform *athkt1* null lines with a T-DNA insert, or alternatively mutate *athkt1* null lines, via neutron bombardment or ethylmethanesulfonate (EMS), and then screen the mutants. Most lines would be salt-sensitive, because they lack the AtHKT1 protein, and therefore, accumulate Na<sup>+</sup> in the leaves to concentrations that are toxic. If a mutation occurs in a gene involved in, for example, influx of sodium in epidermal cells in the root, then these plants may survive longer on highly saline media. Surviving plants could be recovered and a TILLING (Targeting Induced Local Lesions in Genomes) array used to identify the fragment of chromosome in which the mutation has occurred (Till *et al.*, 2003). The mutant line could then be crossed with the mother line to develop a population for mapping of the locus of the gene. This technique was used by Rus *et al.* (2001) with a *sos3-1* mutant to demonstrate that *AtHKT1* is involved in controlling Na<sup>+</sup> entry into plant roots. As the full genome of *Arabidopsis* is sequenced one could identify the exact gene that has been mutated. This might help in the discovery of gene families other than *HKT* genes that are involved in the control of Na<sup>+</sup> transport in plants. This work could also lead to the identification of additional processes of control of ion transport in plants.

(7) What physical structure do HKT proteins have?

Purification and crystallization of HKT proteins may pre-emanate solving of the 3D structure of the HKT protein. Knowledge of the 3D structure of the HKT protein may help us to understand how HKT proteins transport cations, how they sit in cell membranes, what amino acid mutations may make them more or less selective for different ions, and how they transport Na<sup>+</sup> and or K<sup>+</sup>.



## 6.5 Improving the salinity tolerance of wheat and other crops

As salt accumulates inside plants, it becomes toxic. The primary mechanism most plants employ to avoid this is to minimise the  $\text{Na}^+$  accumulating in the tissues, especially the shoot, as  $\text{Na}^+$  toxicity inside the plant is likely to be most damaging in photosynthesising tissue. Limiting the amount of  $\text{Na}^+$  reaching photosynthesising tissue is an effective strategy to increase tolerance to salinity (Munns, 2005).

In wheat, the decrease in leaf  $\text{K}^+$  concentration with increasing salinity tends to be proportional to the increase in leaf  $\text{Na}^+$  concentration with increasing salinity (Gorham et al., 1990; Munns et al., 2004), indicating that many wheat varieties cannot maintain leaf  $\text{K}^+$  with increasing intake of  $\text{Na}^+$  into the plant. Therefore, breeding and selection for a HKT group 1-type gene that effectively removes  $\text{Na}^+$  from the xylem, particularly when xylem  $\text{Na}^+$  concentration is high, may improve the capacity of wheat lines to maintain leaf  $\text{K}^+$  concentration, and  $\text{K}^+$  to  $\text{Na}^+$  ratio, in saline soils. Both the *TmHKT1;4-A2* (Huang et al., 2006) and *TmHKT1;5-A* (Byrt et al., 2007) genes were isolated from the A genome of *T. monococcum* ssp. *monococcum*, and as neither of these genes have been observed in modern wheat they offer new sources of  $\text{Na}^+$  exclusion for improving the salinity tolerance of cereals.

Another strategy for improving the  $\text{K}^+$  to  $\text{Na}^+$  discrimination may be simultaneously breeding and selecting for a combination of both a group 1 HKT-type transporter, and an outward-rectifying  $\text{K}^+$  channel such as SKOR (Roberts and Tester, 1995; Gaymard et al., 1998), as long as the particular SKOR was highly selective for  $\text{K}^+$  and did not allow leakage of  $\text{Na}^+$  into the xylem in highly saline conditions.

Future directions involving this strategy require significant work in gene discovery and protein characterization, or protein engineering. Ancestral wheat accessions from saline areas (Chapter 3), and halophytic grass species (Colmer et al., 2006; Flowers and Colmer, 2008), may be a source of novel *HKT* and *SKOR* alleles that are not present in modern wheat. Cloning of many *HKT* and *SKOR* alleles from wheat and halophytic grasses, and characterization of the cation selectivity and transport properties of the respective proteins by expression in *Xenopus laevis* oocytes, may help to identify alleles that may be of use in wheat breeding. Studies of the relationship between amino acid sequence and transport properties for many HKT and SKOR proteins would assist with better prediction of protein function from simply the analysis of amino acid sequence.

A better understanding of how amino acid sequence influences transport properties, in combination with promoter studies to select promoters which drive gene expression in specific plant tissues, may one day enable the engineering of promoter gene combinations that

can be introduced into wheat which are highly effective in controlling the uptake and transport of  $\text{Na}^+$ .

## References

- ABARE (2007) Australian commodities June quarter **14**(2):266-408 ISSN 1321-7844  
[http://www.abareconomics.com/interactive/ac\\_june07/htm/wheat.htm](http://www.abareconomics.com/interactive/ac_june07/htm/wheat.htm) and  
[http://www.abareconomics.com/interactive/cr\\_june07/excel/cr\\_table1.xls](http://www.abareconomics.com/interactive/cr_june07/excel/cr_table1.xls)
- Allen GJ, Wyn Jones RG, Leigh RA (1995) Sodium transport measured in plasma membrane vesicles isolated from wheat genotypes with differing K<sup>+</sup>/Na<sup>+</sup> discrimination traits. *Plant, Cell Environ.* **18**:105-115
- Almansouri M, Kinet J-M, Lutts s (2001) Effect of salt and osmotic stresses on germination in durum wheat (*Triticum durum* Desf). *Plant Soil* **231**:243-254
- Apse MP, Aharon GS, Snedden WA, Blumwald E (1999) Salt tolerance conferred by overexpression of a vacuolar Na<sup>+</sup>/H<sup>+</sup> antiport in *Arabidopsis*. *Science* **85**:1256-1258
- Apse MP, Blumwald E (2002) Engineering salt tolerance in plants. *Current Opinion Biotech.* **13**: 146-150
- Barro F, Rooke L, Bekes F, Gras P, Tatham AS, Fido R, Lazzeri PA, Shewry PR, Barcelo P (1997) Transformation of wheat with high molecular weight subunit genes results in improved functional properties. *Nature Biotech.* **15**: 1295-1299
- Berthomieu P, Conéjéro G, Nublat A, Brackenbury WJ, Lambert C, Savio C, Uozumi N, Oiki S, Yamada K, Cellier F (2003) Functional analysis of *AtHKT1* in *Arabidopsis* shows that Na<sup>+</sup> recirculation by the phloem is crucial for salt tolerance. *EMBO J* **22**: 2004-2014
- Bohnert HJ, Su H, Shen B (1999) Molecular mechanisms of salinity tolerance. In: Shinozaki K, Editor, *Cold, Drought, Heat, and Salt Stress: Molecular Responses in Higher Plants*, Landes RG, Austin. 29-60
- Bonnett DG, Rebetzke GJ, Spielmeyer W (2005) Strategies for efficient implementation of molecular markers in wheat breeding. *Mol. Breed.* **15**:75-85
- Burton RA, Shirley NJ, King BJ, Harvey AJ, Fincher GB (2004) The CesA gene family of barley. Quantitative analysis of transcripts reveals two groups of co-expressed genes. *Plant Physiol.* **134**:224-236
- Buschmann PH, Vaidyanathan R, Gassmann W, Schroeder JI (2000) Enhancement of Na<sup>+</sup> uptake currents, time-dependent inward-rectifying K<sup>+</sup> channel currents, and K<sup>+</sup> channel transcripts by K<sup>+</sup> starvation in wheat root cells. *Plant Physiol.* **122**: 1387-1397
- Byrt CS, Platten D, Spielmeyer W, James RA, Lagudah ES, Dennis ES, Tester M, Munns R (2007) HKT1;5-like cation transporters linked to Na<sup>+</sup> exclusion loci in wheat, *Nax2* and *Kna1*. *Plant Physiol.* **143**:1918-1928
- Byrt CS, Munns R (2008) Living with salinity. *New Phytol.* **179**:903-905
- Chinnusamy V, Jagendorf A, Zhu J-K (2005) Understanding and Improving Salt Tolerance in Plants, *Crop Sci.* **45**:437-448

- Christensen AH, Quail P (1996) Ubiquitin promoter-based vectors for high-level expression of selectable and/or screenable marker genes in monocotyledonous plants. *Transgenic Res.* **5**:13-18
- Colmer TD, Munns R, Flowers TJ (2005) Improving salt tolerance of wheat and barley: future prospects. *Aust. J. Exp. Agric.* **45**:1425-1443
- Colmer TJ, Flowers TJ, Munns R (2006) Use of wild relatives to improve salt tolerance in wheat. *J. Exp. Bot.* **57**:1059-1078
- Davenport RJ, Tester M (2000) A weakly voltage-dependent, nonselective cation channel mediates toxic sodium influx in wheat. *Plant Physiol.* **122**:823-834
- Davenport RJ, James RA, Zakrisson-Plogander A, Tester M, Munns R (2005) Control of sodium transport in durum wheat. *Plant Physiol.* **137**: 807-818
- Davenport RJ, Munoz-Mayer A, Jha D, Essah PA, Rus A, Tester M (2007) The Na<sup>+</sup> transporter AtHKT1;1 controls retrieval of Na<sup>+</sup> from the xylem in *Arabidopsis*. *Plant, Cell Environ.* **30**: 497-507
- Davenport RJ, Reid RJ, Smith FA (1997) Sodium-calcium interactions in two wheat species differing in salinity tolerance. *Physiol. Plant.* **99**:323-327
- Delhaize E, Ryan PR, Hebb DM, Yamamoto Y, Sasaki T, Matsumoto H (2004) Engineering high-level aluminum tolerance in barley with the *ALMT1* gene, *Proc. Nat. Acad. Sci. USA.* **42**:15249-15254
- Demidchick V, Davenport RJ, Tester M (2002) Nonselective cation channels in plants. *Annu. Rev. Plant Biol.* **53**:67-107
- Devos KM, Dubcovsky J, Dvořák J, Chinoy CN, Gale MD (1995) Structural evolution of wheat chromosomes 4A, 5A, and 7B and its impact on recombination. *Theor. Appl. Genet.* **91**:282-288
- Dubcovsky J, Galvez AF, Dvořák J (1994) Comparison of the genetic organization of the early salt-stress-responsive gene system in salt-tolerant *Lophopyrum elongatum* and salt-sensitive wheat. *Theor. Appl. Genet.* **87**: 957-964
- Dubcovsky J, Luo MC, Dvořák J (1995) Differentiation between homoeologous chromosomes 1A of wheat and 1A<sup>m</sup> of *Triticum monococcum* and its recognition by the wheat *Ph1* locus. *Proc. Natl. Acad. Sci. USA* **92**: 6645-6649
- Dubcovsky J, María GS, Epstein E, Luo MC, Dvořák J (1996) Mapping of the K<sup>+</sup>/Na<sup>+</sup> discrimination locus *Kna1* in wheat. *Theor. Appl. Genet* **92**: 448-454
- Dvořák J, Gorham J (1992) Methodology of gene-transfer by homoeologous recombination into *Triticum-turgidum* - transfer of K<sup>+</sup>/Na<sup>+</sup> discrimination from *Triticum-aestivum*. *Genome* **35**: 639-646

- Dvořák J, Zhang HB (1990) Variation in repeated nucleotide sequences shed light on the phylogeny of the wheat B and G genomes. *Proc. Natl. Acad. Sci. USA* **87**:9640-9644
- Dvořák J, Luo MC, Yang ZL, Zhang HB (1998) The structure of the *Aegilops tauschii* gene pool and the evolution of hexaploid wheat. *Theor. Appl. Genet.* **67**: 657-670
- Dvořák J, McGuire PE, Cassidy B (1988) Apparent sources of the A genomes of wheats inferred from polymorphism in abundance and restriction fragment length of repeated nucleotide sequences. *Genome* **30**: 680-689
- Dvořák J, Noaman MM, Goyal S, Gorham J (1994) Enhancement of the salt tolerance of *Triticum turgidum* L. by the *Kna1* locus transferred from the *Triticum aestivum* L. chromosome 4D by homoeologous recombination. *Theor. Appl. Genet.* **87**:872-877
- Dvořák J, Di Terlizzi P, Zhang HB, Resta P (1993) The evolution of polyploid wheats: identification of the A genome donor species. *Genome* **36**: 21-31
- Endo T, Gill B (1996) The deletion stocks of common wheat. *J. Hered.* **87**: 295-307
- Essah PA, Davenport RJ, Tester M (2003) Sodium influx and accumulation in *Arabidopsis*. *Plant Physiol.* **133**: 307-318
- Evans LT (1998) *Feeding the Ten Billion; Plants and Population Growth*, Cambridge University Press, ISBN 0521646855
- FAO (2008) Food and Agriculture Organization of the United Nations <http://www.fao.org/>
- Flowers TJ, Colmer TD (2008) Salinity tolerance in halophytes. *New Phytol.* **179**:945-963
- Fu D, Uauy C, Blechl A, Dubcovsky J (2007) RNA interference for wheat functional gene analysis. *Transgenic Res.* **16**:689-701
- Fukuda A, Chiba K, Maeda M, Nakamura A, Maeshima M, Tanaka Y (2004) Effect of salt and osmotic stress on the expression of genes for the vacuolar H<sup>+</sup>-pyrophosphatase, H<sup>+</sup>-ATPase subunit A, and Na<sup>+</sup>/H<sup>+</sup> antiporter from barley. *J. Exp. Bot.* **55**: 585-594
- Gao MJ, Dvořák J, Travis RL (2001) Expression of the extrinsic 23-kDa protein of photosystem II in response to salt stress is associated with the K<sup>+</sup>/Na<sup>+</sup> discrimination locus *Kna1* in wheat. *Plant Cell Rep.* **20**:774-778
- Garcia A, Rizzo Ca, Ud-din J, Bartos SL, Senadhira D, Flowers TJ, Yeo AR (1997) Sodium and potassium transport to the xylem are inherited independently in rice, and the mechanism of sodium:potassium selectivity differs between rice and wheat. *Plant, Cell Environ.* **20**: 1167-1174
- Garciadeblas B, Senn ME, Banuelos MA, Rodriguez-Navarro A (2003) Sodium transport and HKT transporters: the rice model. *Plant J* **34**: 788-801
- Garthwaite AJ, von Bothmer R, Colmer TD (2005) Salt tolerance in wild *Hordeum* species is associated with restricted entry of Na<sup>+</sup> and Cl<sup>-</sup> into the shoots. *J. Exp. Bot.* **56**:2365-2378

- Gassmann W, Rubio F, Schroeder J (1996) Alkali cation selectivity of the wheat root high-affinity potassium transporter HKT1. *Plant J.* **10**: 869-882
- Gaxiola RA, Rao R, Sherman A, Grisafi P, Alper SL, Fink GR (1999) The *Arabidopsis thaliana* proton transporters, AtNhx1 and Avp1, can function in cation detoxification in yeast. *Proc. Nat. Acad. Sci. USA* **96**: 1480-1485
- Gaymard F, Pilot G, Lancombe B, Bouchez D, Bruneau D, Boucherez J, Michauz-Ferriere N, Thibaud JB, Sentenac H (1998) Identification and disruption of a plant shaker-like outward channel involved in the K<sup>+</sup> release into the xylem sap. *Cell* **94**:647-655
- Genc Y, McDonald GK, Tester M (2007) Re-assessment of tissue Na<sup>+</sup> concentration as a criterion for salinity tolerance in bread wheat. *Plant, Cell and Environ.* **30**:1486-1498
- Golldack D, Su H, Quigley F, Kamasani UR, Munoz-Garay C, Balderas E, Popova OV, Bennett J, Bohnert HJ, Pantoja O (2002) Characterization of a HKT-type transporter in rice as a general alkali cation transporter. *Plant J.* **31**: 529-542
- Gorham J, Bridges J, Dubcovsky J, Dvorak J, Hollington PA, Luo M-C, Khan JA (1997) Genetic analysis and physiology of a trait for enhanced K<sup>+</sup>/Na<sup>+</sup> discrimination in wheat. *New Phytol.* **137**: 109-116
- Gorham J, Hardy C, Wyn Jones RG, Joppa LR, Law CN (1987) Chromosomal location of a K/Na discrimination character in the D genome of wheat. *Theor. Appl. Genet.* **74**:584-588
- Gorham J, Wyn Jones RG, Bristol A (1990) Partial characterisation of the trait for enhanced K<sup>+</sup>-Na<sup>+</sup> discrimination in the D genome of wheat. *Planta* **180**:590-597
- Greenway H, Munns R (1980) Mechanisms of salt tolerance in nonhalophytes. *Ann. Rev. Plant Physiol.* **31**:149-190
- Grewal HS, Cornish P and Norrish S (2004) Differential response of wheat cultivars to subsoil salinity/sodicity. In “*New directions for a diverse planet: Proceedings of the 4<sup>th</sup> International Crop Science Congress*”, Brisbane, Australia.
- Gustafsson JP (2003) Modelling molybdate and tungstate adsorption to ferrihydrite. *Chemical Geology* **200**:105-115
- Hamilton AJ, Baulcombe DC (1999) A species of small antisense RNA in posttranslational gene silencing in plants. *Science* **286**:950-952
- Hamilton AJ, Voinnet O, Chappell L, Baulcombe DC (2002) Two classes of short interfering RNA in RNA silencing. *EMBO J.* **21**:4671-4679
- Haro R, Banuelos MA, Senn ME, Barrero-Gil J, Rodriguez-Navarro A (2005) HKT1 mediates sodium uniport in roots. Pitfalls in the expression of HKT1 in yeast. *Plant Physiol.* **139**: 1495-1506

- Hartje S, Zimmermann S, Klonus D, Mueller-Roeber B (2000) Functional characterisation of LKT1, a K<sup>+</sup> uptake channel from tomato root hairs, and comparison with the closely related potato inwardly rectifying K<sup>+</sup> channel SKT1 after expression in *Xenopus* oocytes. *Planta* **210**:723-731
- Hirai S, Oka S-I, Adachi E, Kodama H (2007) The effects of spacer sequences on silencing efficiency of plant RNAi vectors. *Plant Cell Rep.* **26**:651-659
- Horie T, Costa A, Kim TH, Han MJ, Horie R, Lueng HY, Miyao A, Hirochika H, An G, Schroeder JI (2007) Rice OsHKT2;1 transporter mediates large Na<sup>+</sup> influx component into K<sup>+</sup>-starved roots for growth. *EMBO J.* **16**: 3003-3014
- Horie T, Yoshida K, Nakayama H, Yamada K, Oiki S, Shinmyo A (2001) Two types of HKT transporters with different properties of Na<sup>+</sup> and K<sup>+</sup> transport in *Oryza sativa*. *Plant J.* **27**: 129-138
- Huang S, Spielmeyer W, Lagudah ES, James RA, Platten JD, Dennis ES, Munns R (2006) A sodium transporter (HKT7) is a candidate for Nax1, a gene for salt tolerance in durum wheat. *Plant Physiol.* **142**:1718-1727
- Huang S, Spielmeyer W, Lagudah ES, Munns R (2008) Comparative mapping of *HKT* genes in wheat, barley and rice, key determinants of Na<sup>+</sup> transport, and salt tolerance. *J. Exp. Bot.* **59**: 927-937
- Huen M, Schafer-Pregl R, Klawan D, Castagna R, Accerbi M, Borghi B, Salamini F (1997) Sike of Einkorn Wheat Domestication Identified by DNA Fingerprinting, *Science* **278**:1312-1314
- Husain S, von Caemmerer S, Munns R (2004) Control of salt transport from roots to shoots of wheat in saline soil. *Funct. Plant Biol.* **31**:1115-1126
- James RA, Davenport RJ, Munns R (2006a) Physiological characterisation of two genes for Na<sup>+</sup> exclusion in durum wheat: *Nax1* and *Nax2*. *Plant Physiol.* **142**: 1537-1547
- James RA, Munns R, von Caemmerer S, Trejo C, Miller C, Condon AG (2006b) Photosynthetic capacity is related to the cellular and subcellular partitioning of Na<sup>+</sup>, K<sup>+</sup> and Cl<sup>-</sup> in salt-affected barley and durum wheat. *Plant Cell Environ.* **29**:2185-2197
- Jeschke WD, Pate JS (1991) Cation and chloride partitioning through xylem and phloem within the whole plant of *Ricinus communis* L. under conditions of salt stress. *J. Exp. Bot.* **42**: 1105-1116
- Joppa LR (1987) Aneuploid analysis in tetraploid wheat. In: Heyne EG (ed) *Wheat and wheat improvement*. Monograph 13, Am Soc Agron, Madison, Wis, pp 151-166
- Jin C, Lan H, Attie AD, Churchill GA, Bulutuglo D, Yandell BS (2004) Selective phenotyping for increased efficiency in genetic mapping studies. *Genetics* **168**: 2285-2293
- Jones HD, Doherty A, Wu H (2005) Review of methodologies and a protocol for the *Agrobacterium*-mediated transformation of wheat. *Plant Methods* **1**:5

- Karley AJ, Leigh RA, Sanders D (2000) Differential ion accumulation and ion fluxes in the mesophyll and epidermis of barley. *Plant Physiol.* **122**:835-844
- Kowdley GC, Ackerman SJ, John JE, Jones LR, Moorman JR (1994) Hyperpolarization-activated chloride currents in *Xenopus* oocytes. *J. Gen. Physiol.* **103**: 217-230
- Lagudah ES, Appels R, Brown A, McNeil D (1991) The molecular-genetic analysis of *Triticum tauschii*, the D-genome donor to hexaploid wheat. *Genome* **34**:375-386
- Laurie S, Feeney KA, Maathuis FJM, Heard PJ, Brown SJ, Leigh RA (2002) A role for HKT1 in sodium uptake by wheat roots. *Plant J.* **32**: 139-149
- Li JR, Zhao W, Li QZ, Ye XG, An BY, Li X, Zhang XS (2005) RNA silencing of *Waxy* gene results in low levels of amylase in the seeds of transgenic wheat (*Triticum aestivum* L.). *Acta Genet. Sin.* **32**:846-854
- Lijavetzky D, Muzzi G, Wicker T, Keller B, Wing R, Dubcovsky J (1999) Construction and characterization of a bacterial artificial chromosome (BAC) library for the A genome of wheat. *Genome* **42**:1176-1182
- Lin HX, Zhu MZ, Yano M, Gao JP, Liang ZW, Su WA, Hu ZH, Ren ZH, Chao DY (2004) QTLs for Na<sup>+</sup> and K<sup>+</sup> uptake of the shoots and roots controlling rice salt tolerance. *Theor. Appl. Genet.* **108**:253-260
- Lindsay MP, Lagudah ES, Hare RA, Munns R (2004) A locus for sodium exclusion (*Nax1*), a trait for salt tolerance, mapped in durum wheat. *Funct. Plant Biol.* **31**:1105-1114
- Liu CJ, Atkinson MD, Chinoy CN, Devos KM, Gale MD (1992) Nonhomoeologous translocations between group 4, 5 and 7 chromosomes within wheat and rye. *Theor. Appl. Genet.* **83**: 305-312
- Luo MC, Dubcovsky J, Goyal S, Dvorak J (1996) Engineering of interstitial foreign chromosome segments containing the K<sup>+</sup>/Na<sup>+</sup> selectivity gene *Kna1* by sequential homoeologous recombination in durum wheat. *Theor. Appl. Genet.* **93**: 1432-2242
- Loukoianov A, Yan L, Blechl A, Sanchez A, Dubcovsky J (2005) Regulation of VRN-1 vernalization genes in normal and transgenic polyploidy wheat. *Plant Physiol.* **138**:22364-2373
- Maathuis FJM, Amtmann A (1999) K<sup>+</sup> nutrition and Na<sup>+</sup> toxicity: the basis of cellular K<sup>+</sup>/Na<sup>+</sup> ratios. *Annals Bot.* **84**:123-133
- Mäser P, Gierth M, Schroeder JI (2002a) Molecular mechanisms of potassium and sodium uptake in plants. *Plant* **247**: 43-54
- Mäser P, Hosoo Y, Goshima S, Horie T, Eckelman B, Yamada K, Yoshida K, Bakker EP, Shinmyo A, Oiki S, Schroeder JI, Uozumi N (2002b) Glycine residues in potassium channel-like selectivity filters determine potassium selectivity in four-loop-per-subunit HKT transporters from plants. *Proc. Nat. Acad. Sci. USA* **99**: 6428-6433



- Mouillet O, Zhang H-B, Lagudah ES (1999) Construction and characterization of a large DNA insert library from the D genome of wheat. *Theor. Appl. Genet.* **99**:305-313
- Munns R (1985) Na<sup>+</sup>, K<sup>+</sup> and Cl<sup>-</sup> in xylem sap flowing to shoots of NaCl-treated barley. *J. Exp. Bot.* **36**:1032-1042
- Munns R (1993) Physiological processes limiting plant growth in saline soils: some dogmas and hypotheses. *Plant, Cell Environ.* **16**:15-24
- Munns R (2002) Comparative physiology of salt and water stress. *Plant, Cell Environ.* **25**:239-250
- Munns R (2005) Genes and salt tolerance: bringing them together. *New Phytol.* **167**: 645-663
- Munns R and James RA (2003) Screening methods for salinity tolerance: a case study with tetraploid wheat. *Plant Soil* **253**:201-218
- Munns R and Sharp RE (1993) Involvement of abscisic acid in controlling plant growth in soil of low water potential. *Aust. J. Plant Physiol.* **20**: 425-437
- Munns R and Tester M (2008) Mechanisms of salinity tolerance. *Annu. Rev. Plant Biol.* **59**:651-681
- Munns R, Hare RA, James RA, Rebetzke GJ (2000) Genetic variation for improving the salt tolerance of durum wheat. *Aust. J. Agric. Res.* **51**: 69-74
- Munns R, Husain S, Rivelli AR, James RA, Condon AG, Lindsay MP, Lagudah ES, Schachtman DP, Hare RA (2002) Avenues for increasing salt tolerance of crops, and the role of physiologically based selection traits. *Plant Soil* **247**:93-105
- Munns R, James RA, Läuchli, A (2006) Approaches to increasing the salt tolerance of wheat and other cereals. *J. Exp. Bot.* **57**: 1025-1043
- Munns R, James RA, Islam AKMR, Malik AL, Colmer TD (2008) Sodium excluding genes from durum wheat and sea barleygrass improve sodium exclusion of bread wheat. In "Salinity, water and society: global issue, local action. Proceedings of 2<sup>nd</sup> International Salinity Forum, Adelaide, March 2008. Published by the Future Farm Industries CRC.
- Munns R, Rebetzke GJ, Husain S, James RA, Hare RA (2003) Genetic control of sodium exclusion in durum wheat. *Aust. J. Agric. Res.* **54**: 627-635
- Murashige T and Skoog F (1962) A revised medium for rapid growth and bioassays with tobacco tissue cultures, *Physiol. Plant* **15**:473-497
- Nelson JC, Sorrells ME, Van-Deynze AE, Lu YH, Atkinson M, Bernard M, Leroy P, Faris JD, Anderson JA, (1995) Molecular mapping of wheat: major genes and rearrangements in homoeologous groups 4, 5, and 7. *Genetics* **141**: 721-731

NLWRA (2007) Australian Dryland Salinity Assessment 2000 Fast Facts 21. *Dryland Salinity in Australia – key findings*

[http://www.anra.gov.au/topics/publications/fast\\_facts/pubs/21-fastfact.pdf](http://www.anra.gov.au/topics/publications/fast_facts/pubs/21-fastfact.pdf)

Pellegrineschi A, Noguera LM, Skovmand B, Brito RM, Velazquez L, Salgado MM, Hernandez R, Warburton M, Hoisington D (2002) Identification of highly transformable wheat genotypes for mass production of fertile transgenic plants, *Genome* **45**: 421-430

Platten JD, Cotsaftis O, Berthomieu P, Bohnert H, Davenport RJ, Fairbairn DJ, Horie T, Leigh RA, Lin HX, Luan S (2006) Nomenclature for HKT transporters, key determinants of plant salinity tolerance. *Trends Plant Sci.* **11**:372-374

Pritchard J, Wyn Jones RG, Tomos AD (1991) Turgor, Growth and Rheological Gradients of Wheat Roots Following Osmotic Stress. *J. Exp. Bot.* **42**:1043-1049

Qiu QS, Guo Y, Quintero FJ, Pardo JM, Shumaker KS, Zhu JK (2004) Regulation of a vacuolar Na<sup>+</sup>/H<sup>+</sup> exchanger in *Arabidopsis thaliana* by the Salt-Overly-Sensitive (SOS) pathway. *J. Biol. Chem.* **279**: 207-215

Ramplung LR, Harker N, Shariflou MR, Morell MK (2001) Detection and analysis systems for microsatellite markers in wheat. *Aust. J. Agric. Res.* **52**:1131-1141

Ren ZH, Gao JP, Li LG, Cai XL, Huang W, Chao DY, Zhu MZ, Wang ZY, Luan S, Lin HX (2005) A rice quantitative trait locus for salt tolerance encodes a sodium transporter. *Nature Genet.* **37**: 1141-1146

Rengasamy P (2002) Transient salinity and subsoil constraints to dryland farming in Australian sodic soils: an overview. *Aust. J. Exp. Agric.* **42**:351-361

Rengasamy P (2006) World salinization with emphasis on Australia. *J. Exp. Bot.* **57**: 1017-1023

Roberts SK, Tester M (1995) Inward and outward K<sup>+</sup>-selective currents in the plasma membrane of protoplasts from maize root cortex and stele. *Plant J.* **8**:811-826

Roder MS, Korzun V, Wendehake K, Plaschke J, Tixier M-H, Leroy P, Ganal MW (1998) A microsatellite map of wheat. *Genetics* **149**: 2007-2023

Rodriguez-Navarro A, Rubio F (2006) High-affinity potassium and sodium transport systems in plants. *J. Exp. Bot.* **57**: 1149-1160

Rooke L, Byrne D, Salgueiro S (2000) Marker gene expression driven by the maize ubiquitin promoter in transgenic wheat. *Ann. Appl. Biol.* **136**:167-172

Rubio F, Gassmann W, Schroeder JI (1995) Sodium-driven potassium uptake by the plant potassium transporter HKT1 and mutations conferring salt tolerance. *Science* **270**: 1660-1663

Rus A, Baxter I, Muthukumar B, Gustin J, Lahner B, Yakubova E, Salt DE, (2006) Natural Variants of *AtHKT1* enhance Na<sup>+</sup> accumulation in two wild population of *Arabidopsis*. *PLoS Genetics* **2**: 1964-1973

- Rus A, Lee B-h, Munoz-Mayor A, Sharkhuu A, Miura K, Zhu J-K, Bressan RA, Hasegawa PM (2004) *AtHKT1* facilitates Na<sup>+</sup> homeostasis and K<sup>+</sup> nutrition in planta. *Plant Physiol.* **136**: 2500-2511
- Rus A, Yokoi S, Sharkhuu A, Reddy M, Lee B, Matsumoto TK, Koiwa H, Zhu JK, Bressan RA, Hasegawa PM (2001) *AtHKT1* is a salt tolerance determinant that controls Na<sup>+</sup> entry into plant roots. *Proc. Nat. Acad. Sci. USA* **98**:14150-14155
- Salamini F, Özkan H, Brandolini A, Schäfer-Pregl R, Martin W (2002) Genetics and geography of wild cereal domestication in the near east. *Nature Rev. Genet.* **3**: 429-441
- Sambrook J, Fritsch EF, Maniatis T (1989) *Molecular cloning a laboratory manual, Ed second edition*. Cold Spring Harbor Laboratory Press, Cold Spring Harbor
- Sanford JC, Klein TM, Wolf ED, Allen N (1987) Delivery of substances into cells and tissues using a particle bombardment process. *Particulate Sci. Tech.* **5**:27-37
- Santa-Maria GE, Rubio F, Dubcovsky J, Rodriguez-Navarro A (1997) The HAK1 gene of barley is a member of a large gene family and encodes a high-affinity potassium transporter. *Plant Cell* **9**: 2281-2289
- Schachtman DP, Schroeder JI (1994) Structure and transport mechanism of a high-affinity potassium uptake transporter from higher-plants. *Nature* **370**: 655-658
- Schachtman DP, Munns R, Whitecross MI (1991) Variation in sodium exclusion and salt tolerance in *Triticum tauschii*. *Crop Sci.* **31**(4):992-997
- Schachtman DP, Schroeder JI, Lucas WJ, Anderson JA, Gaber RF (1992) Expression of an inward-rectifying potassium channel by the *Arabidopsis KAT1* cDNA. *Science* **258**: 1654-1658
- Schenborn ET, Mierendorf RC (1985) A novel transcription property of SP6 and T7 RNA polymerases: dependence on template structure. *Nucleic Acids Res.* **13**: 6223-6236
- Sears ER (1954) The aneuploids of common wheat. *Mod. Agric. Exp. Stand. Res. Bull.* **572**:59
- Sears RG and Deckard EL (1982) Tissue culture variability in wheat: callus induction and plant regeneration. *Crop Sci.* **22**:546-550
- Shavrukov Y, Bowne J, Langridge P, Tester M (2006) Screening for sodium exclusion in wheat and barley. *Proceedings of 13<sup>th</sup> Australian Agronomy Conference*, 10-14 September 2006, Perth, Western Australia. *Australian Society of Agronomy*
- Shewry PR, Jones HD (2005) Transgenic wheat: where do we stand after the first 12 years? *Annals Appl. Biol.* **147**:1-14
- Shi H, Quintero FJ, Pardo JM, Zhu JK (2002) The putative plasma membrane Na<sup>+</sup>/H<sup>+</sup> antiporter SOS1 controls long-distance Na<sup>+</sup> transport in plants. *Plant Cell* **14**:465-477

- Smith NA, Singh SP, Wang MB, Stoutjesdijk PA, Green AG, Waterhouse PM (2000) Gene expression: Total silencing by intron-spliced hairpin RNAs. *Nature* **407**:319-320
- Somers D, Isaac P, Edwards K (2004) A high-density microsatellite consensus map for bread wheat (*Triticum aestivum* L.). *Theor. Appl. Genet.* **109**: 1105-1114
- Sorrells ME, La Rota M, Bermudez-Kandianis CE, Greene RA, Kantety R, Munkvold JD, Miftahudin, Mahmoud A, Ma X, Gustafson PJ (2003) Comparative DNA sequence Analysis of Wheat and Rice Genomes. *Genome Res.* **13**: 1818-1827
- Sunarpi, Horie T, Motoda J, Kubo M, Yang H, Yoda K, Horie R, Chan WY, Leung HY, Hattori K (2005) Enhanced salt tolerance mediated by AtHKT1 transporter-induced Na<sup>+</sup> unloading from xylem vessels to xylem parenchyma cells. *Plant J.* **44**: 928-938
- Tester M, Davenport RJ (2003) Na<sup>+</sup> tolerance and Na<sup>+</sup> transport in higher plants. *Annals Bot.* **91**: 503-527
- The TT (1973) *Transfer of resistance to stem rust from Triticum monococcum L. to hexaploid wheat*. PhD thesis. University of Sydney, Sydney.
- Theodoulou FL, Miller AJ (1995) *Xenopus* oocytes as a heterologous expression system for plant proteins. *Mol. Biot.* **3**: 101-115
- Till BJ, Reynolds SH, Greene EA, Codomo CA, Enns LC, Johnson JE, Burtner C, Odden AR, Young K<sup>+</sup>, Taylor NE, Henikoff JG, Comai L, Henikoff S (2003) Large-scale discovery of induced point mutations with high-throughput tilling. *Genome Res.* **13**:524-530
- Travella S, Klimm TE, Keller B (2006) RNA interference-based gene silencing as an efficient tool for functional genomics in hexaploid bread wheat. *Plant Physiol.* **142**:6-20
- Trevaskis B, Tadege M, Hemming MN, Peacock WJ, Dennis ES, Sheldon C (2007) *Short Vegetative Phase-Like MADS-Box* genes inhibit floral meristem identity in barley. *Plant Physiol.* **143**:225-235
- Uozumi N, Kim EJ, Rubio F, Yamaguchi T, Muto S, Tsuboi A, Bakker EP, Nakamura T, Schroeder JI (2000) The *Arabidopsis HKT1* gene homolog mediates inward Na<sup>+</sup> currents in *Xenopus laevis* oocytes and Na<sup>+</sup> uptake in *Saccharomyces cerevisiae*. *Plant Physiol.* **122**: 1249-1259
- USSL (2008) *Criteria for diagnosing saline and sodic soils*. Online accessed Feb 2005 (<http://www.usssl.ars.usda.gov> now <http://www.ars.usda.gov/Research/docs.htm?docid=10492>)
- Van Houdt H, Bleys A, Depicker A (2003) RNA target sequences promote spreading of RNA silencing. *Plant Physiol.* **131**: 245-253
- Véry AA, Gaymard F, Bosseux C, Sentenac H, Thibaud JB (1995) Expression of a cloned plant K<sup>+</sup> channel in *Xenopus* oocytes: analysis of macroscopic currents. *Plant J.* **7**: 321-332


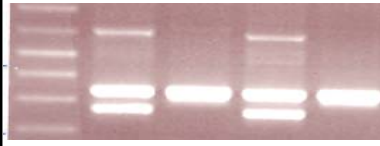


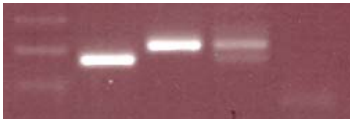
- Vincor B, Altman A (2005) Recent advances in engineering plant tolerance to abiotic stress: achievements and limitations. *Current Opinion Biotech.* **16**:123-132
- Walker NA, Sanders D, Maathuis FJM (1996) High-affinity potassium uptake in plants. *Science* **273**:977-978
- Wang TB, Gassmann W, Rubio F, Schroeder JI, Glass ADM (1998) Rapid up-regulation of *HKT1*, a high-affinity potassium transporter gene, in roots of barley and wheat following withdrawal of potassium. *Plant Physiol.* **118**: 651-659
- Wang W, Vincur B, Altman A (2003) Plant responses to drought, salinity and extreme temperatures: towards genetic engineering for stress tolerance. *Planta* **218**: 1-14
- Wesley SA, Helliwell CS, Smith NA<sup>+</sup>, Wang M, Rouse DT, Liu Q, Gooding PS, Singh SP, Abbot D, Stoutjesdijk PA, Robinson SP, Gleave AP, Green AG, Waterhouse PM (2001) Construct design for efficient, effective and high-throughput gene silencing in plants. *Plant J.* **27**:581-590
- Westgate ME, Passioura JB, Munns R (1996) Water status and ABA content of floral organs in drought-stressed wheat. *Aust. J. Plant. Physiol.* **23**: 763-772
- White PJ, Bowen HC, Demidchik V, Nichols C, Davies JM (2002) Genes for calcium-permeable channels in the plasma membrane of plant root cells. *Biochim. Biophys. Acta* **1564**: 299-309
- Yan L, Loukoianov A, Blechl A, Tranquilli G, Ramakrishna W, SanMiguel P, Bennetzen JL, Echenique V, Dubcovsky J (2004) The wheat *VRN2* gene is a flowering repressor down-regulated by vernalisation. *Science* **303**:1640-1644
- Zhou Y, Setz N, Niemiets C, Qu H, Offler CE, Tyerman SD, Patrick JW (2007) Aquaporins and unloading of phloem-imported water in coats of developing bean seeds. *Plant, Cell Environ.* **30**: 1566-1577

## Appendix

### Appendix Table 2.1: Agarose gel electrophoresis results from PCR with microsatellite markers on chromosome 5AL

Dominant markers linked to *Nax2* include *gwm291*, *gwm410* and *gpw2181*. The *gwm126* marker is one of four markers identified as being proximal to *Nax2*. *Vrn2* (BM1) is a co-dominant marker linked to *Nax2*, this marker can be used to distinguish lines that are heterozygous for *Nax2*. bp, base pairs; M, 1Kb<sup>+</sup> DNA ladder; Tam, Tamaroi; L149, Line 149; H, BC<sub>5</sub>F<sub>2:3</sub> line with high leaf Na<sup>+</sup>; L, BC<sub>5</sub>F<sub>2:3</sub> line with low leaf Na<sup>+</sup>; NTC, no template control; LB, bulked DNA from eight BC<sub>5</sub>F<sub>2:3</sub> lines with low leaf Na<sup>+</sup>; Het, BC<sub>5</sub>F<sub>2:3</sub> line heterozygous for *Nax2* with intermediate leaf Na<sup>+</sup>. Primer sequences:

*gwm291*; 5'-CATCCCTACGCCACTCTGC-3', 5'-AATGGTATCTATTCCGACCCG-3'  
*gwm410*; 5'-GCTTGAGACCGGCACAGT-3', 5'-CGAGACCTTGAGGGTCTAGA-3'  
*gpw2181*; 5'-CAAATTACAAACGCACAGCC-3', 5'-TTTGTGCCATTGTGTGTGTG-3'  
*gwm126*; 5'-CACACGCTCCACCATGAC-3', 5'-GTTGAGTTGATGCGGGAGG-3'  
*Vrn2* (BM1); 5'-TCTCCATCATTCAACATCAATCG-3', 5'-  
TGTAGCTCGTCGGGGTGTGTTGC-3'

		Gel electrophoresis data					
Marker	Ladder fragment size	M	Tam	L149	H	L	NTC
<i>gwm291</i>	200 bp →						
<i>gwm410</i>	200 bp →						
<i>gpw2181</i>	200 bp →						
			Tam	L149	LB	LB	
<i>gwm126</i>	200 bp →						
		M	Tam	L149	Het	NTC	
<i>Vrn2 (BM1)</i>	200 bp →						

**Appendix Table 3.1: Accession numbers of diploid wheat material**

<i>T. monococcum</i> ssp. <i>monococcum</i>	<i>T. monococcum</i> ssp. <i>boeoticum</i>			<i>Triticum urartu</i>		
44852	44811	44941	116134	44827	45462	116193
44891	44813	44948	116138	44831	45470	116194
44913	44818	44949	116139	44911	45471	116196
44914	44819	44953	116146	44942	45472	116197
44915	44820	44955	116153	44943	45475	116198
44916	44821	45103	126305	45111	45476	116199
44918	44822	109080	131176	45212	45477	116200
44931	44832	109081	131180	45213	45484	116201
44932	44833	109086	135341	45218	45485	116202
45085	44847	110749	137335	45219	45489	116203
45086	44855	110789	137341	45260	46395	116204
45092	44856	110820	137391	45261	46536	116206
45093	44857	110826	137409	45262	109084	117886
45110	44858	113254	137477	45263	109087	117911
45231	44861	113258	139313	45278	110748	119439
45232	44866	113260	140980	45281	110753	135343
45234	44868	113261		45282	110766	139150
45235	44870	113264		45283	110784	139173
45255	44878	113266		45284	110830	139175
45256	44887	113273		45285	110834	139317
45257	44890	113275		45286	110835	139317
45258	44895	113277		45287	110840	139969
45259	44899	113280		45288	110844	139973
45461	44900	113282		45290	115813	140058
132841	44904	113283		45291	115814	140061
132864	44906	113284		45292	115815	
132869	44907	113286		45293	116156	
132870	44919	113288		45298	116160	
132873	44921	113291		45299	116190	
139090	44936	113309		45300	116191	
141291	44937	113311		45301	116192	

**Appendix Table 3.2: Key to *HKT1;5 B* gene members from wheat**

The sequence data are available through the National Centre for Biotechnology Information ([www.ncbi.nlm.nih.gov/](http://www.ncbi.nlm.nih.gov/)). These sequences were isolated in collaboration with Dr. Damien Platten (CSIRO Plant Industry, Australia).

Gene	NCBI accession number
<i>HKT1;5-B1</i>	DQ646340
<i>HKT1;5-B2</i>	DQ646341



CATCACCGTCGAGGTTATCAGTGCGTACGGAAACGTGGGGTTCAGCACCGGGTAC  
AGCTGTGGCCGGCAGGTGACGCCCCGACGGCGGCTGCAGGGACACGTGGGGTTGGC  
TTCTCTGGGAAGTGGAGTTGGCAAGGGAAGCTGGCTCTCATTGCTGTCATGTTCT  
ACGGCAGGCTCAAGAAGTTCAGCATGCATGGTGGCGAGGCATGGAGGATAGTAT  
AACCTAGTAGCAGACTGCATATTTCTCAATGATCTCTCTTCAGACAGAGACTAGC  
TACATCTCGCTCTAGCCTAAAACCATCTGAACATATTTCCATTATGCCGAGTACCT  
CA

**Appendix Figure 2.1: Wheat *HKT1;5* RFLP probe sequence (331 bp)**

**5' UTR**

AGAACAGGCCAAGAAGTCTCTACACA ACTTACAGTAGAA

(start codon)

ATGGGTTCTTTGCATGTCTCCTCGAGTGCCACTCAACATAGCAAGCTTGAGAGGG  
CTTACCAACTCCTGGTTTTCCATGTGCACCCGTTCTGGCTCCAGCTCTTGTACTTTG  
TATCCATCTCCTTCTTCGGTTTTGGTGATCCTCAAAGCCCTCCCATGAAGACCAGC  
ACGGTCCCAGAGGCCCATGGATTTGGACCTGATCTTCACGTTCGGTCTCGGCGACCA  
CGGTGTTCGAGCATGGTGGCCGTGGAGATGGAGTCCTTCTCCAACCCCCAGCTCCT  
ACTCCTGACCCTCCTCATGCTCCTCGGCGGCGAGGTGTTACACGAGCATGCTTGGC  
CTGCACTTACCTACGTCAAGTCCAAGAAGAAAGAAGCACAAGCACCCACGAC  
CATGACGATGGTGACAAAGGCAAACCAGCACCATCATCTAGCCTAGAGCTCGCT  
GTTACCACCGGCATGGATGACGTCGATCGTGTGGAGCAAGGGTTTAAGGACCAG  
CCCCGTTACGATCGCGCCTTCTCACCAGGTTGCTTCTGTTTCATAGTGCTGGGCTA  
TCACGTGGTGGTGCACCTCGCCGGCTACTCCTTGATGCTGGTCTACCTGAGCGTG  
GTCTCCGGCGCGAGGGCTGTGCTCACCGGCAAGGGGATCAGCCTGCACACCTTCT  
CCGTCTTACCGTCGTCTCGACGTTCCGCAACTGCGGCTTCGTCCCGAACAAACGA  
AGGGATGATCGCCTTCCGGTCTTCCCGGGCCTCCTGCTCCTAGTCATGCCGCACG  
TCTCCTCGGCAACACACTCTTCCCCGTCTTCTCAGGCTGGCCATCTGGGCTCTC  
CGGAGAGTCACCAGGAGGCCCGAGCTCGGTGAGCTGAGGAGCATCGGCTACGAC  
CACCTGCTGACGAGCCGGCACACGTGGTTCCTGGCTTTCACCGTGGCGGGCTTCG  
TGCTAGCGCAGCTGTGCTCTTCTGCGCCATGGAGTGGGGCTCCAACGGGCTGCG  
CGGGCTCACCGCCGTGCAGAAGCTCGTTGCGGGACTGTTTCATGTTCGGTCAACTCC  
AGGCACACCGGTGAGATGGTGGTGGACCTTTCACCGTGTGCTCGGCCCTCGTGG  
TGCTCTATGTGGTCATGATGTGAGTACTTCTCAAGTCCATTTTACTCCGCATATA  
AAGTTTGTCTGAAGTCGAACTTTATAAAAATTTAACTAATTTTGTA AAAAGAAACAT  
CACCATTACACAGTACGAAATCATAACCATTAGATGCGTCATGAATTAATTTTC  
ATATCATATATTTTTAGTTTTGCAGATGTTGATATTTTTTTCATATAAATATGTGGTT  
AAACTTTCTGAACTTTTTTCCCTCCACTCCATATACATTTTATATACAGAGTGAAA  
ATGACCGGAGGGAGTACGTTACATACTCCACTCGATCGATTCAGATAGTGATAA  
CCATAAACTCTCTCATATCATGCTCGTGCCTATACTACGAACAGGTACCTACC  
ACCTTACACTACATTTCTACCAGTGGAAGACGACAGTGACCAACAAGTGGGAGC  
AGATCAGCGCGACCAGAAAAGGATAACAAGCATGTGGCGGAAGCTGCTCATGTC  
GCCGCTCTCGTGCTTGGCCATCTTCATCGCCGTGGTGTGCATCACGGAGCGGCGG  
CAGATCTCCGATGACCCCTCAACTTCAACGTCCTCAACATCACCGTTCGAGGTTA  
TCAGGTAATCCACTACTTAAACAAAACGTATAAGCACATGATCAATTGCAATATTC  
TTACCATGCATGATCGATACCATTATACACAAAACCTTACTTACCCAAATTGCAA  
ATTCAATCAGCATA CATATAGCTATTGCGACCACTATAACGTGTGGCATTGTGTG  
AACTGTGCTTGCAGTGCGTACGGAAACGTGGGGTTCAGCACCGGGTACAGCTGTG  
GCCGGCAGGTGACGCCGACGGCGGCTGCAGGGACACGTGGGTTGGCTTCTCTG  
GGAAGTGGAGTTGGCAAGGGAAGCTGGCTCTCATTGCTGTCATGTTCTACGGCAG  
GCTCAAGAAGTTCAGCATGCATGGTGGCGAGGCATGGAGGATAGTATAA (stop

codon)

**3' UTR**

CCTAGTAGCAGACTGCATATTTCTCAATGATCTCTCTTCAGACAGAGACTAGCTA  
CATCTCGCTCTAGCCTAAAACCATCTGAACATATTTCCATTATGCCGAGTACCTCA  
ATCACTGCATGCATATCAATATAATGAAACAAAAGTCATCCAAAAAAAAAAAAA  
AAAAA

**Predicted amino acid sequence**

MGSLHVSSSATQHSKLERAYQLLVFHVHPFWLQLLYFVSISFFGLVILKALPMKTSTV  
PRPMDLDLIFTSVSATTVSSMVAVEMESFSNPQLLLLTLMLLGGGEVFTSMLGLHFTY

VKSKKKEAQAPHDHDDGDKGKPAPSSSLELA VTTGMDDVDRVEQGFKDQPRYDRA  
FLTRLLLFIVLGYHVVVHLAGYSLMLVYLSVVSGARAVLTGKGISLHTFSVFTVVSTF  
ANCGFVPNNEGMIAFRSFPGLLLLVMPHVLLGNTLFPVFLRLAIWALRRVTRRPELGE  
LRSIGYDHL LTSRHTWFLAFTVAAFVLAQLSLFCAMEWGSNGLRGLTAVQKLVAGL  
FMSVNSRHTGEMVVDLSTVSSALVVLVVM MYLPPYTTFLPVEDDSDQQVGADQR  
DQKRITSMWRKLLMSPLSCLAIFIAVVCITERRQISDDPLNFNVLNITVEVISAYGNVG  
FSTGYSCGRQVTPDGGCRDTWVGFSGKWSWQGKLALIAVMFYGRLKKFSMHGGEA  
WRIV

**Appendix Figure 2.2: Wheat *TaHKT1;5-D* full length genomic sequence showing introns (shaded) and exons (GenBank accession DQ646342) and predicted amino acid sequence**

5' UTR

AGAACAGGCCAAGAAGTCTCTACACAACCTTACAGTAGAA

**(start codon)**

ATGGGTTCTTTGCATGTCTCCTCGAATGCCACTCAACATAGCAAGCTTGAGAGGG  
CTTACCAACTCCTGGTTTTCCATGTGCACCCGTTCTGGCTCCAGCTCTTGTACTTTG  
TATCCATCTCCTTCTTCGGTTTCGTGATCCTCAAAGCCCTCCCATGAAGACCAGC  
ACGGTCCCAGGCCCATGGATTTGGACCTGATCTTCATGTTCGGTGTTCGGCGACGA  
CGGTGTTCGAGCATGGTGGCCGTGGAGATGGAGTCCTTCTCCAACCCCCAACTCCT  
CCTCCTGACCCTCCTCATGCTCCTCGGTGGCGAGGTGTTACGAGCATGCTTGGGC  
TGC ACTTCACCTACGTCAAGTCCAAGAAGAAAGAAGCACAAGCACCCACGACC  
ATGACGATGGTGACAAAGGCAAACCAGCACCATCATGTAGCCTAAAGCTCGCTG  
CTACCACCTGCATGGATGACGTCGATCGTGTGGAGCAAGGGTTTAAGGACCAGCC  
CCGTTACGATCGCGCCTTCCCTCACCAGGTTGCTTCTGTTTCATAGTGCTGGGCTATC  
ACGTGGTGGTGCACCTCGCCGGCTACTCCCTGATGCTGGTCTACCTGAGCGTGGT  
CTCCGGCGCGGGGGCTGTGCTCACCGGCAAGGGGATCAGCCTGCACACCTTCTCC  
GTCTTACCCTGCTCCTCGACGTTTGCCAACTGCGGCTTCGTCCC GAACAACGAAG  
GGATGGTTCGCTTCCGGTCTTCCCGGGCCTCCTGCTCCTCGTCATGCCGCACGTC  
CTCCTCGGCAACACGCTCTTCCCCGTCTTCTCAGGCTGGCCATCTGGGCTCTCCG  
GAGGGTCACGAGGAGGCCCGAGCTCGGTGAGCTGCGGAGCACCGGGTACGACCA  
CCTGCTGACAAGCCGGCACACGTGGTTCTTGGCTTTCACCGTGGCCGCGTTCATG  
CTAGCTCAGCTGTCGCTCTTCTGCGCCATGGAGTGGGGCTCCGACGGGCTGAACG  
GGCTCACCGCCGCGCAGAAGCTCGTCGCGGCACTGTTTCATGTTCGGTCAACTCAAG  
GCACACCGGTGAGATGGTCGTGGACATTTCCACTGTGTCGTCAGCCGTCGTGGTG  
CTCTACGTGGTCATGATGTAAGTAGTCCTTCAGTCCATTTTACTCCGCGTATAAGA  
TTTGTCAATTTTATAGAAAAAAATCTAACCATTACACTACAGAATCAATCTAA  
CCATTACACTACAGAATCAATATCATTAGATGTGTTATTATTTAATTATCATATT  
TTATACTTTAATATTGCAGATGTTGATTTTTTGTTCATATAAATATGGTCAAATAA  
ATAAACCTTTATAATGTTTGACTTCAGACAATCTTACACTCCTTCGATTCTAGATA  
GTGATAACCATCAACTCTCTCATATCATGCTCTTGCCACACACTACGAGCAGGT  
ACCTACCACCTTACACTACATTTCTACCAGTGGAAAGACGACAGTGACCAACAAGT  
GGGAGCAGATCAGCACGACCACAAAAGGATAACAAGCATATGCCACAAGCTGCT  
CATGTCGCCGCTCTCGTGCCTGGCCATCTTCATCGCCGTTGTGTGCATCACCGAGC  
GCCGGCAGATCTCCGATGACCCCTCAACTTCAACGTCCTCAACATCACTGTCGA  
AGTTATCAGGTAATCAACTAGTAGTAATTAACAAAATGTAGAAGCACATGATCAA  
TTGCAATTTTTTTACCATGCATGATAGGTAGATACCATTATATACAAAATCTGACT  
TAGCTAAATTGCAAATTCAGTAACTTATATATAGGTATTGCGACCACTATAACG  
TGTGTCAATTGTGTGAGCTGTGCTTGCAGTGCGTACGGAAACGTGGGGTTTAGCAC  
CGGGTACAGCTGCGGCCGAGGTGACGCCTGACGACGGCGACTGCAGGGACAC  
GTGGGTTGGCTTCTCTGGGAAGTGGAGCTGGCAAGGGAAGCTGGCTCTCATTGCT  
GTCATGTTCTACGGCAGGCTCAAGAAGTTCAGCATTTCATGGCGGCCAGGCATGGA  
GGATAATATAA **(stop codon)**

**3'UTR**

CCTAGCAGACTACATATTTCTCAATGATCTCTCTTCAGACAGAGAGTAGCTACAT  
CTCGCTCTAGCCTAAAACCACCTGAACATATTTTCATTATGCCGAGTACCTCAA

**Predicted amino acid sequence**

MGSLHVSSNATQHSKLERAYQLLVFHVHPFWLQLLYFVSISFFGFVILKALPMKTSTV  
PRPMDLDLIFMSVSATTVSSMVAVEMESFSNPQLLLL TLLMLLGGEVFTSMLGLHFT  
YVSKSKKEAQAPHDHDGDKGKPAPSCSLKLAATTCMDDVDRVEQGFKDQPRYDR  
AFLTRLLL FIVLGYHV VVHLAGYSLMLVYLSVVS GAGAVLTGKGISLHTFSVFTVVST  
FANCGFVPNNEGMVAFRSFPGLLLL VMPHVLLGNTLFPVFLRLAIWALRRVTRRPEL

GELRSTGYDHLLTSRHTWFLAFTVAAFMLAQLSLFCAMEWGS DGLNGLTAAQKLV  
AALFMSVNSRHTGEMVVDISTVSSAVVVL YVVM MYLPPYTTFLPVEDDSDQQVGAD  
QHDHKRITSICHKLLMSPLSCLAIFIAVVCITERRQISDDPLNFNVLNITVEVISAYGNV  
GFSTGYSCGRQVTPDDGDCRDTWVGFS GKWSWQGKLALIAVMFYGRLKKFSIHGG  
QAWRII

**Appendix Figure 2.3: Wheat *TmHKT1;5-A* full length genomic sequence showing introns (shaded) and exons (GenBank accession DQ646339) and predicted amino acid sequence**





```

D 2008 TGGCTCTCATTGCTGTCATGTTCTACGGCAGGCTCAAGAAGTTCAGCATGCATGGTGGCG 2067
      |||
A 1975 TGGCTCTCATTGCTGTCATGTTCTACGGCAGGCTCAAGAAGTTCAGCATTTCATGGCGGCC 2034

D 2068 AGGCATGGAGGATAGTATAA 2087
      |||
A 2035 AGGCATGGAGGATAATATAA 2054

```

**Appendix Figure 2.4: Alignment of *TmHKT1;5-A* and *TaHKT1;5-D* genomic sequences**



A1 MGSLHVSSNATQHSKLERAYQLLVFHVHPFWLQLLYFVVISFFGFVILKALPMKTSTVPR 60  
MGSLHVSS+ATQHSKLERAYQLLVFHVHPFWLQLLYFVVISFFG VILKALPMKTSTVPR  
D1 MGSLHVSSSATQHSKLERAYQLLVFHVHPFWLQLLYFVVISFFGLVILKALPMKTSTVPR 60  
  
A61 PMDLDLIFMSVSATTVSSMVAVEMESFSNPQLLLLLTLLMLLGGEVFTSMLGLHFTYVKSK 120  
PMDLDLIF SVSATTVSSMVAVEMESFSNPQLLLLLTLLMLLGGEVFTSMLGLHFTYVKSK  
D61 PMDLDLIFTVSATTVSSMVAVEMESFSNPQLLLLLTLLMLLGGEVFTSMLGLHFTYVKSK 120  
  
A121 KKEAQAPHDHDDGDKGKPAPSCSLKLAATTCMDDVDRVEQGFKDQPRYDRAFLTRLLFI 180  
KKEAQAPHDHDDGDKGKPAPS SL+LA TT MDDVDRVEQGFKDQPRYDRAFLTRLLFI  
D121 KKEAQAPHDHDDGDKGKPAPSSSLELAVTTGMDDVDRVEQGFKDQPRYDRAFLTRLLFI 180  
  
A181 VLGYPVVHLAGYSLMLVYLSVVSAGAVLTGKGISLHTFSVFTVVSTFANCGFVPNEG 240  
VLGYPVVHLAGYSLMLVYLSVSGA AVLTGKGISLHTFSVFTVVSTFANCGFVPNEG  
D181 VLGYPVVHLAGYSLMLVYLSVSGARAVLTGKGISLHTFSVFTVVSTFANCGFVPNEG 240  
  
A241 MVAFRSFPGLLLLLVMPHVLLGNTLFPVFLRLAIWALRRVTRRPELGELRSTGYDHLTSR 300  
M+AFRSFPGLLLLLVMPHVLLGNTLFPVFLRLAIWALRRVTRRPELGELRS GYDHLTSR  
D241 MIAFRSFPGLLLLLVMPHVLLGNTLFPVFLRLAIWALRRVTRRPELGELRSIGYDHLTSR 300  
  
A301 HTWFLAFTVAAFMLAQLSLFCAMEWGS DGLNGLTAAQKLVAALFMSVNSRHTGEMVVDIS 360  
HTWFLAFTVAAF+LAQLSLFCAMEWGS+GL GLTA QKLVA LFMSVNSRHTGEMVVD+S  
D301 HTWFLAFTVAAFVLAQLSLFCAMEWGSNGLRGLTAVQKLVAAGLFMSVNSRHTGEMVVDLS 360  
  
A361 TVSSAVVLYVVMYLPPTYTFLPVEDSDQQVGADQHDHKRITSICHKLLMSPLSCLAI 420  
TVSSA+VLYVVMYLPPTYTFLPVEDSDQQVGADQ D KRITS+ KLLMSPLSCLAI  
D361 TVSSALVLYVVMYLPPTYTFLPVEDSDQQVGADQRDQKRITSMWRKLLMSPLSCLAI 420  
  
A421 FIAVVCITERRQISDDPLNFNVLNITVEVISAYGNVGFSTGYSCGRQVTPDDGDCRDTWV 480  
FIAVVCITERRQISDDPLNFNVLNITVEVISAYGNVGFSTGYSCGRQVTP DG CRDTWV  
D421 FIAVVCITERRQISDDPLNFNVLNITVEVISAYGNVGFSTGYSCGRQVTP-DGGCRDTWV 479  
  
A481 GFSGKWSWQKGLALIAVMFYGRLKKFSIHGGQAWRII 517  
GFSGKWSWQKGLALIAVMFYGRLKKFS+HGG+AWRI+  
D480 GFSGKWSWQKGLALIAVMFYGRLKKFSMHGGEAWRIV 516

**Appendix Figure 2.5: Alignment of predicted amino acid sequences for *TmHKT1;5-A* and *TaHKT1;5-D***



CAAGGCGGAGTCGCATGCTCCGGCCGCCATGGCGGCCGCGGGAATTCGATTGCA  
GATGTTTCGCATACACTCAACCCTAAGAATGCCTGCACACACACACACACACACAC  
ACACACACACACACACACACACACACTCCTACTAAAGGCACATCGCCGAAAGGC  
CTGAAATGAATGCAAGAAAACACGACCATCAATGTCAAGTCTAGAACTTGAATC  
CTGGTGGGTTATTTCCATCACAAACAAAGAAACCATTTGAGTTACCCTCAGTTCC  
CTATGCCAACATTAATTAACAATAGCAAACCTTGTTTCATTATATTTGTCATAATAT  
AATTTCTAAATATATAGTCAAATAAATTTCAAATATTTATGAACCAAGGGAGCAC  
CGTGCTACGGTAACATACATGCATTACTTTGGAGGAGCTAGTTGTAGGTAGCTCT  
AAACATGTATTTTCATAGTTTATAATTTTCGGCATGTATTTTCTATCTTCTATGTGT  
ATATCTTTTTTCAGGATTCTGTGTGTATATGTGTATATGTACTTTTTCGTTGCACTTAG  
TACAACACAAGTCAGGTGGTTGCCCTGAGCTCCTTCTCTTCACGATGCCACGCTC  
ACACCCTACGATCCATATCCAATGGAGCAAGGCATCGCACCCCGGTGGGCACCAA  
CCGACTCTTGTTTCGTTACGGGTGATATGGACGTGGAACCTTATCACTCACACGCAA  
AAGAAAAAAACTTATCACTCGATTCCATTTTTTCTTCCACAAGTCTGCTCTTCTG  
GGAGTACCTAATTTTCGTTCATATGATATGCCTCGCAAAAAAGATATGCCTCCAC  
GAGCTCCCATTGTGCGCTAGCTTTTGCGATTAGATTCAGTAATTAAGACACTATA  
ATGTCGTTACAGGGAGTAAAGCAACATCAACGGACAAATTTTACAGACCTCACG  
GGATGGGCTGTCGTAGCAGATCTATTTGGATAAAGAATTCAGATATTTCTTGTAG  
TCCGTCGTCTGTCTAGCATTTTGCGTCACCCCCCTTTTGGGTATAATAATCCAGT  
AGTTTCGATGCTCCAACAGAACAGCAGAAGTCTTTACACAACACTACAGTAGAAATG

**Appendix Figure 2.7: *TmHKT1;5-A* promoter**

Sequence from the neighbouring gene (GenBank accession CA673223) is highlighted in pink.  
The start codon for *HKT1;5-A* is underlined.

CATCCACGCGTTGGGAGCTCTCCCATATGGTTCGACCTGCAGGGCGGCCGCGAATTC  
ACTAGTGAATTGCAGATGTTTCGCATACACTCAACCATAAGAATGCATGCACACACA  
CACTCCTACTAAATGCACATCGCCGAAAGGCCTGAAATGAATGCAAGAAAATGC  
GACCACCAGTGTCAAGTCTAGAACTTGAACCCTGGTGGGTTATTTCCATCACAAG  
CAACCTAACCATTTGAGTTACCCTCAGCTCGCTATGCCAACATTAATTAACAATA  
GCAAACCTGTTTCACTATATTTATCATAATATAATTTCTAGATATATAGTCAAAAT  
AATTTCAAATATTTATGAATGAAGGGAGCACCATGCTATGGTAATATAGATGCAT  
TACTTTGGAGGAGCTAGTTGTAGGTAGCTCTAAACATGTATTTTCATAGTTTCTAA  
TTTTTGGCATGTATTTTCTATCTTCTATGTGTATATCTTTTTTCGGGATTCTGTATGT  
ATATGTGTATATGTACTTTTCGTTGCACTTAGTACAACACAAGTCAGGTGGTTGCC  
CTGAGCTCCTTCTCTTCATGATGCCACGCTCACACCCTACGATACATATCCAACGG  
AGCGGGGCATCGCACCCGGTGGGCACCAACTGACTCTTGTTTCGTTACCGGTGATA  
CGGACGTGGAACCTTATCACTCACCCGCAAAAAAAAAAAGTTATCACTCGATTCCAT  
TGTTTCTTCCACAAGTCTGCTCTCTTGTAGGAGTACCTAATTTTCGTCATATGATA  
TGCCTCGCAAAAAAGATATGCCTCCCACGAGCTCCCATTGTGCGCTAGCTTTTGC  
GATTAGATTCAGTAATTAAGACACTATAATGTCGTTGCAGGGAGTAAAGCAACAT  
CAACGGACAAATTTTACAGACCTCACGGGATGGGCTGTCGTAGCAGATCTATTT  
GGAAAAAGAAATTAGAGATTTTCTTTGTAGTCCGTCGGTTTGTCTAGCATTTTGC  
GTCCACCCCTTTTTTGGGTATAATAATCCATTAGTCTCTGATTGCCTCCAACAA  
AACAGACCAAGAAGTCTCTACACAACCTTACAGTAGAAATG

**Appendix Figure 2.8: *TaHKT1;5-D* promoter**

Sequence from the neighbouring gene (GenBank accession EL774258) is highlighted in pink.  
The start codon for *HKT1;5-D* is underlined.

**Appendix Table 4.1: Replicates of oocytes used in various experiments**

Solution	Number of replicates						
	Water	AtHKT1;1	OsHKT1;5 (Ni)	OsHKT1;5 (Pk)	OsHKT2;2	TaHKT1;5	TmHKT1;5
100 CsCl	4		4		4	7	
100 LiOH	4		4		4	12	
100 RbCl	6		4		4	7	
100 TRIS	4	6	4		6	7	
0 Na	20	12	4	2	4	17	12
1 Na	18	9	4	2	4	18	9
10 Na	19	8	4	2	4	20	8
30 Na	8	4	6		6	13	1
100 Na	21	10	16	2	12	24	10
1 K	4	2	1	1	2	5	3
10 K	13	5	1		2	10	6
30 K	4	2	3		3	8	
100 K	9	4		2		9	5
1Na1K	22	12	6	2	7	17	9
1Na10K	19	6	4	2	5	17	7
1Na30K	8	1	5	2	5	10	
30Na1K	6	6	4		5	10	2
10Na1K	4	1	3		3	7	
10Na10K	2	1	3		3	8	
10Na pH5.5	4		2		2	10	
10Na pH6.5	19		4		4	20	
10Na pH7.5	4		2		2	10	
10 Na 2Ca	19		4		4	20	
10 Na 5Ca	4		2			10	
10 Na 10Ca	4		2			10	
10 Na Gad	1		2		2	5	
10 Na Fluf	1		2		2	5	

Concentrations are in mM; Na is Na<sup>+</sup> glutamate; K is K<sup>+</sup> glutamate; Ni is Nipponbare; Pk is Pokkali